T.C.
HASAN KALYONCU UNIVERSITY
GRADUATE EDUCATION INSTITUTE
DEPARTMENT OF ELECTRICAL AND ELECTRONICS ENGINEERING

INVESTIGATION OF TRANSPOSITION MODELS, OPTIMIZATION OF TILT ANGLES, AND SOLAR RADIATION INTENSITY FOR FIXED AND TRACKED SOUTH-FACING SOLAR PHOTOVOLTAIC SURFACES IN PROVINCES OF TÜRKİYE

Batur Alp AKGÜL

Ph.D. THESIS

IN

ELECTRICAL AND ELECTRONICS ENGINEERING

GAZİANTEP- 2024

GRADUATE EDUCATION INSTITUTE
DOCTORAL THESIS ACCEPTANCE AND APPROVAL FORM

Electrical and Electronics Engineering Department, student of the Doctorate of Electrical and Electronics Engineering program Batur Alp AKGÜL prepared and submitted the thesis titled "Investigation Of Transposition Models, Optimization Of Tilt Angles, And Solar Radiation Intensity For Fixed And Tracked South-Facing Solar Photovoltaic Surfaces In Provinces Of Türkiye" and defended successfully at the date of 11/06/2024 and accepted by the jury as a Ph.D. thesis.

Position	Title, Name and Surname	Department/University	Signature
Supervisor	Prof. Dr. M. Sadettin ÖZYAZICI	EEE / Hasan Kalyoncu Uni.	
Jury Member	Prof. Dr. Arif NACAROĞLU	EEE / Gaziantep Uni.	
Jury Member	Prof. Dr. M. Fatih HASOĞLU	AE / Hasan Kalyoncu Uni.	
Jury Member	Assoc. Prof. Dr. Bülent HAZNEDAR	COMPE / Gaziantep Uni.	
Jury Member	Dr. K. Sercan BAYRAM	EEE / Hasan Kalyoncu Uni.	

This thesis is accepted by the jury members selected by institute management board and approved by institute management board.

Doç. Dr. Ufuk AKBAŞ
Director

DECLARATION PAGE

I hereby declare that all information in this document has been obtained and presented in accordance with academic rules and ethical conduct. I also declare that, as required by these rules and conduct, I have fully cited and referenced all material and results that are not original to this work.

Batur Alp AKGUL

11/06/2024

HASAN KALYONCU UNIVERSITY
GRADUATE EDUCATION INSTITUTE
ELECTRICAL AND ELECTRONICS ENGINEERING

INVESTIGATION OF TRANSPOSITION MODELS, OPTIMIZATION OF TILT ANGLES, AND SOLAR RADIATION INTENSITY FOR FIXED AND TRACKED SOUTH-FACING SOLAR PHOTOVOLTAIC SURFACES IN PROVINCES OF TÜRKİYE

Batur Alp AKGUL

Ph.D. THESIS

Advisor
Prof. Dr. Mustafa Sadettin ÖZYAZICI

ABSTRACT

Solar energy has become increasingly important in today's world and has become a viable primary energy source in the last decade. Therefore, this thesis is focused on a reliable estimation and quantitative analysis of OPTA values and TSR intensities for SFS and STS power plants by applying transposition models in 81 provinces and 7 geographical regions of Turkey. Annual OPTA values for south-facing PV surfaces are predicted between 28º to 36º throughout the year by applying an isotropic transposition model. It is revealed that the loss in annual TSR does not surpass 0.5% due to the 5° offset of the tilt angle from the OPTA of SFSs. It turns out that the correlation between solar deflection and energy gain is inverse in both actual and predicted data. Very small discrepancies were found between theoretical predictions and actual energy production. In the study conducted with real data, it was determined that the accuracy of NASA-SSE monthly GSR data was quite high. Additionally, it has been understood that METEONORM prediction values are always higher than NASA-SSE prediction values. Single-axis horizontal STS produced 22.34% more annual PV electricity than SFS. It was observed that the deviation rates between actual and predicted productions were 0.98% on average in SFS and 4.46% on average in STS. The annual energy loss for uniaxial STS and SFS was estimated to be 14% on average. It was found that the increase in TSR intensity in uniaxial horizontal STS was 0.63% if the rotation continued from ±60° to ±90° (±30°). The increase in net PV electricity production was 1.36%. It has been revealed that solar anisotropy parameters included in transposition models significantly affect the quality of prediction results. It has been found that the accuracy of model outputs largely depends on the density and quality of the solar input data sets. Actual production results confirm the trends of transposition models in solar energy production forecasts.

Keywords: Türkiye, PV, GSR, TSR, OPTA, STS, Solar energy.

HASAN KALYONCU ÜNİVERSİTESİ
LİSANSÜSTÜ EĞİTİM ENSTİTÜSÜ
ELEKTRİK-ELEKTRONİK MÜHENDİSLİĞİ ANABİLİM DALI

TRANSPOZİSYON MODELLERİNİN İNCELENMESİ, TÜRKİYE İLLERİNDE SABİT VE GÜNEŞ TAKİPLİ GÜNEYE BAKAN FOTOVOLTAİK YÜZEYLER İÇİN EĞİM AÇILARININ VE GÜNEŞ RADYASYON YOĞUNLUĞUNUN OPTİMİZASYONU

Batur Alp AKGÜL

DOKTORA TEZİ

Danışman
Prof. Dr. Mustafa Sadettin ÖZYAZICI

ÖZET

Güneş enerjisi günümüz dünyasında giderek artan bir önem kazanmış ve son on yılda uygulanabilir bir birincil enerji kaynağı haline gelmiştir. Bu nedenle bu tez, Türkiye'nin 81 ilinde ve 7 coğrafi bölgesinde, aktarım modelleri uygulayarak, SFS ve STS santralları için OPTA değerleri ve TSR yoğunluklarının güvenilir bir tahmini ve niceliksel bir analizine odaklanmıştır. PV yüzeyleri için yıllık OPTA değerleri, yıl boyunca 28° ila 36° arasında tahmin edilmiştir. SFS'lerin OPTA'sından eğim açısının 5° kayması nedeniyle yıllık TSR'deki kaybın %0,5'i aşmadığı ortaya çıkmıştır. Güneş sapması ile enerji kazanımı arasındaki korelasyonun hem gerçek hem de tahmin edilen verilerde ters olduğu anlaşılmıştır. Teorik tahminler ile gerçek enerji üretimleri arasında oldukça küçük uyumsuzluklar bulunmuştur. Gerçek verilerle yapılan çalışmada, NASA-SSE aylık GSR verilerinin doğruluğunun oldukça yüksek olduğu belirlenmiştir. Ayrıca METEONORM tahmin değerlerinin her zaman NASA-SSE tahmin değerlerinden yüksek olduğu anlaşılmıştır. Tek eksenli yatay STS, SFS'den %22,34 daha fazla yıllık PV elektrik üretmiştir. Gerçekleşen ve tahmin edilen üretimler arasındaki sapma oranlarının SFS'de ortalama %0,98, STS'de ise ortalama %4,46 olduğu görülmüştür. Tek eksenli STS ve SFS için yıllık enerji kaybının ortalama %14,00 olduğu tahmin edilmiştir. Döndürmenin ±60°'den ±90°'ye (±30°) kadar devam etmesi durumunda tek eksenli yatay STS'de TSR yoğunluğundaki artışın %0,63 olduğu bulunmuştur. Net PV elektrik üretimindeki artış ise %1,36 olmuştur. Transpozisyon modellerinde yer alan güneş anizotropi parametrelerinin tahmin sonuçlarının kalitesini önemli ölçüde etkilediği ortaya koyulmuştur. Model çıktılarının doğruluğunun büyük ölçüde güneş enerjisi girdi veri setlerinin yoğunluğuna ve kalitesine bağlı olduğu anlaşılmıştır. Gerçek üretim sonuçları, güneş enerjisi üretim tahminlerinde aktarım modellerinin eğilimlerini doğrulamaktadır.

Anahtar Kelimeler: Türkiye, PV, GSR, TSR, OPTA, STS, Güneş enerjisi.

ACKNOWLEDGMENTS

Achieving success in life is seldom a solitary endeavor; it often requires the support and assistance of many. I am deeply thankful to the community of Hasan Kalyoncu University's Engineering Faculty for their unwavering support and guidance in helping me reach my goals. Without the patience, time, insight, and understanding generously provided by scholars and colleagues throughout this journey, I would not have made it this far.

I am immensely grateful to my dissertation committee: Prof. Dr. Mustafa Sadettin ÖZYAZICI, Prof. Dr. Arif NACAROĞLU, Prof. Dr. Muhammet Fatih HASOĞLU, Asst. Prof. Dr. Bülent HAZNEDAR, and Asst. Prof. Dr. Kadir Sercan BAYRAM. Their advice and feedback leading up to the dissertation were invaluable, and their encouragement and support throughout the process were truly priceless.

A special debt of gratitude is owed to Prof. Dr. Mustafa Sadettin ÖZYAZICI, my supervisor and dissertation chair. His countless hours of support, feedback, advice, and encouragement were indispensable to my success. His guidance in improving my research skills, writing, and theoretical understanding laid the groundwork for my achievements. He played a pivotal role in my exploration of solar energy engineering, and I am forever thankful for his introduction to a wide range of engineering theories and perspectives, as well as his invaluable life advice.

At Hasan Kalyoncu University's Engineering Faculty, I have been fortunate to work closely with numerous professors and develop strong relationships with many others. I particularly appreciate Prof. Dr. Muhammet Fatih HASOĞLU, whose passion, knowledge, experience, and support continue to inspire and challenge me to strive for excellence. His mentorship has provided me with valuable research opportunities, critical feedback, and guidance, for which I am deeply grateful.

I also extend my gratitude to Prof. Dr. Celal KORASLI, my department head, for pushing me to exceed my limits, providing invaluable feedback, and offering unwavering support. His expertise and guidance have significantly enhanced my research skills and confidence. Additionally, I am thankful for the support and guidance of Prof. Dr. İlhami YEĞİNGİL during the dissertation proposal stage, and for his enthusiastic interest in my research.

Batur Alp AKGÜL

Gaziantep 2024

CONTENTS

LIST OF TABLES

LIST OF FIGURES

ACRONYMS AND ABBREVIATIONS

AC	Alternating Current
ASDC	Atmospheric Science Data Center
DC	Direct Current
ECU	Electronic Control Unit
ES	Energy Storage
ECU	Electronic Control Unit
ESMAP	Energy Sector Management Assistance Program
EU PVGIS	Photovoltaic Geographical Information System of European Commission
DER	Distributed Energy Resources
GEPA	Solar Energy Potential Map of Türkiye
GFSK	Gaussian Frequency Shift Keying
GSM	Global System for Mobile Communications
GSR	Global Solar Radiation
GPS	Global Positioning System
HCPV	High-Concentration Photovoltaic
HDKR	Hay, Davies, Klucher and Reindl
IEA	International Energy Agency
IFC	International Finance Corporation
IRENA	International Renewable Energy Agency
ISO	International Standard of Organization
LCOE	Levelized Cost of Energy
LDR	Light Dependent Resistor
LOLP	Loss of Load Probability
MPPT	Maximum Power Point Tracking
NASA	National Aeronautics and Space Administration
NOCT	Nominal Operating Cell Temperature
NREL	National Renewable Energy Laboratory
OPTA	Optimal Tilt Angle
PV	Photovoltaic
SSE	Surface Meteorology and Solar Energy
SFS	Solar Fixed System
SPA	Solar Position Algorithm
STS	Solar Tracking System
TSE	Turkish Standards Institution
TSMS	Turkish State Meteorological Service
TSR	Total Solar Radiation

NOMENCLATURE

δ	Solar declination angle
n	Julian day
R_β	Rotation tilt angle of the surface about the axis
R_γ	Rotation azimuth angle of the surface about the axis
$\emptyset$	Latitude angle
$COS\omega_s$	Solar time
ω_s	Sunset hour angle
G_{sc}	Solar constant
I_h	Solar radiation on the horizontal surface
I_0	Extraterrestrial solar radiation on horizontal surface
K_T	Clearness index
R_t	The ratio of hourly to daily horizontal radiation
R_d	The ratio of hourly to daily diffuse radiation
I_d	Horizontal diffuse solar radiation
I_b	Horizontal beam solar radiation
R_b	Beam radiation tilt factor
ρ_g	Ground reflectivity-albedo
R_r	Ratio of ground-reflected radiation
β	Surface tilt angle
θ	Solar radiation incidence angle
I_T	Total solar radiation intensity on the tilted surface
A_i	Anisotropy index
F	Modulating function
ϵ	Atmospheric clearness parameter
Δ	Atmospheric brightness parameter
m	Optical air mass
α_s	Solar altitude angle
γ_s	Solar azimuth angle
α_e	Orientation of the surface
γ_e	Elevation of the surface
γ	Surface azimuth angle
γ_a	Tracking axis azimuth angle
β_a	Tracking axis tilt angle
θ_s	The solar incidence angle of beam radiation
θ_z	Solar zenith angle
PG_{opt}	Percentage gains in TSR intensity for SFS
$I_{T,\beta=opt}$	TSR intensity on the tilted surface
$I_{T,\beta=0}$	GSR intensity on the horizontal surface
η_{pv-avg}	Average PV surface efficiency
η_{pv}	PV surface efficiency
T_{pv-avg}	Average PV temperature
T_{ref}	Reference temperature
T_{amb}	Monthly ambient temperature
β_p	Temperature coefficient
K_{mt}	Monthly clearness index
$D_{DC,eqv}$	DC equivalent

D_{DC}	Total DC demand
D_{AC}	Total AC demand
η_{inv}	Inverter efficiency
D_m	Demand directly met by the PV
D_c	Demand that remains constant throughout the day
D_{es}	demand primarily met by the ES
P_{crt}	Critical PV absorption level
D_{cnt}	Energy met either directly by the PV or the ES
E_{cl}	The energy delivered to the continuous load
E_{ml}	The energy delivered to the matched load
E_{dl}	The energy delivered to the load and the ES
U_d	Daily utilizability
E_{pv}	The energy available from the PV
f_{pv}	Fraction of PV
PVL_r	PV/L ratio
ESL_r	ES/L ratio
E'_{pv}	The available output of the PV
L'	Part of the load not met directly by the PV
ES_{uc}	Usable ES capacity
L	Load
η_{cc}	Charge control efficiency
η_{es}	ES efficiency
E_{gen}	The energy delivered by the generator
Q_{gen}	Energy used by the generator
E_{es}	The energy delivered by the ES
η_{ch}	Efficiency of charger
η_{gen}	Generator efficiency
η_{es}	ES efficiency
ES_{nc}	Nominal capacity of ES
f_c	Usable fraction of capacity available
L_{DC}	Equivalent DC load
d_{dod}	Maximum depth of discharge
C_f	Correction factor
β_{opta}	Optimaltilt angle
β_{act}	Actual tilt angle
A_{pv}	Area of the PV plant
η_{pv}	PV plant efficiency
I_{td}	TSRonthe Pvplant
L_{pv}	Miscellaneous PV plant losses
L_c	Other power conditioning losses
η_{eff}	overall solar PV plant efficiency.
E_{avlb}	PV plant energy available to the load and battery
E_{grid}	PV energy available to the grid
E_{act}	PV energy actually delivered
η_{abs}	PV energy absorption rate

1. INTRODUCTION

In the twenty-first century, one of the biggest problems that the globe faces is energy provision. Due to global climate changes and energy crises, the world has accelerated the transition from fossil fuels to renewable energy sources. Increasing technology usage and population have been continuously increasing energy demand. Solar energy systems have become more applicable and attractive because the energy produced is essentially renewable as well as free from pollution and noise. In addition, solar PV plants have become a viable primary energy source in the past decade because their installation costs have decreased, and their performance has greatly improved. That is why, in the last two decades, solar energy has been considered an alternative way to reduce global dependency on fossil fuels and researchers are concentrating more on solar PV plants to meet the increasing energy demands of countries. So, transforming global solar radiation (GSR) falling on the earth's surface into energy may be the final solution to the growing worldwide energy demand. However, burning fossil fuels to generate electricity causes irreparable harm to the environment, such as air pollution, climate change, global warming, etc. (Dincer & Kaymil, 2017; Nassar et al., 2018). Therefore, research studies evaluating the performance of PV plants have increased significantly in recent years and the evaluation of solar energy potential and modeling of solar photovoltaic (PV) systems by utilizing technological systems is becoming increasingly essential. A crucial issue is being aware of GSR data in a specific region at a certain time. Due to the change in the sun's angle during the year, each region has its unique position in terms of GSR. Different solar PV plants are designed to maximize the solar energy generated in the region. So, while designing a system, the consideration of GSR for the region is highly significant. Total solar radiation (TSR) intensity for the region to be installed solar PV plants is the most crucial metric for determining energy production. Because of these reasons, researchers have been focusing on optimizing the TSR intensity on PV surfaces that can be harvested from incoming GSR. Additionally, studies on the determination of the optimal tilt angle (OPTA) values and maximization of TSR collected by solar fixed systems (SFS) are also receiving great attention worldwide. Another important point is that to improve the uptake of TSR intensity, solar tracking systems (STS) are utilized by taking into account such factors. Tilting and tracking of PV surfaces generally benefit increases with increasing latitude. Also, the appropriate placement of

STS can yield a significant improvement in the performance of the PV surfaces in terms of TSR efficiency even though these devices are sometimes economically costly.

Solar PV microgrids have started to become the alternative source of renewable electric power production for rural and remote areas in the last decade as PV and Energy Storage (ES) technologies have offered more efficient, movable, flexible, easy-to-install, and more accessible products. Microgrids offer a variety of technological options to integrate distributed energy sources with ES within a system, and feed into the loads in more systematic and functional ways (Sufyan et al., 2019). The increasing energy demand has led engineers and scientists to seek new technologies to provide energy being generated at near places of consumption. Off-grid PV microgrids can be used as a primary electricity supply without grid extension in a sustainable way (Faccio et al., 2018). It provides the necessary functionality to ensure power production, transmission, distribution, and continuity when supported on a platform (Stanton et al., 2017). Therefore, the field of energy storage, PV energy, and off-grid PV plants have been studied deeply in the last decade (Parhizi et al., 2015). Especially in recent years due to the reduction in PV surface prices and the increment in production capacity, microgrid systems have become possible to work off-grid (Caspary, 2009). In some cases, the off-grid (isolated) microgrids are strongly dependent on regional and meteorological circumstances to provide stable electrical power (Afgan & Carvalho, 2008). Correct design and development are essential factors for all microgrids with solar PV energy sources to operate satisfactorily and ensure sustainability. The most important criteria in the design of an isolated microgrid are the designed microgrid should be optimal in size, affordable cost, and sufficient in terms of power. It is also essential the design of the solar PV microgrid is carried out after gathering data such as daily energy use, autonomy time, operating voltage, daily load profile, depth of discharge of the battery, closed days, efficiencies of PV surface, and PV inverter. So, in this thesis, an off-grid isolated microgrid has also been designed by covering all these criteria.

The remainder of this thesis is structured as follows: In the rest of the first section, the contribution of solar energy potential to the energy mix of Türkiye, along with the motivation and objectives are described. Factors and parameters affecting TSR optimization, and the importance of transposition models are described. In the second section, the literature review and associated investigations are conducted. Literature review on transposition, regression, and correlation models. Related works on the estimation of OPTA and TSR intensity along with the performance of solar STSs are presented. The development and design of solar PV plants are investigated. Ultimately, the literature review of this field is concluded by focusing on associated studies conducted in Türkiye. In the third section, the adopted methodologies, such as the theoretical approaches of the selected transposition models and the utilized solar data collections are described, which specifically presents knowledge estimating on the OPTA values and TSR intensities with theoretical analysis, basic concepts, algorithm descriptions, and calculations. Numerical modeling of solar PV plants, percentage gains of TSR intensity, and LCOE calculations are presented. In the fourth section, case studies, applications, and experimental studies conducted for Turkish geography are presented. Estimation of OPTA values and TSR intensities for south-facing SFSs and STSs in Provinces of Türkiye, investigation of transposition models estimating TSR intensity on PV surfaces, and design of isolated PV power production for rural and remote areas are conducted. In the fifth section, relevant results obtained from the performed studies are presented for increasing the efficiency of solar PV plants. Actual (experimental) and predicted PV energy production calculations and discussions are presented specifically by focusing on OPTA and TSR values, percentage gains, performance analysis, and comparisons of SFSs and STSs are carried out. The results of the transposition models are analyzed comparatively for the study region along with the results of regional and technical simulations. Apart from this, validations of adopted transposition and correlation models, OPTA, and latitude relations, as well as comparisons with previous studies, are evaluated from a global perspective. In the last section, the contributions of this thesis and concluding remarks are highlighted for the geography of Türkiye and worldwide, where suggestions for improving the efficiency of solar PV plants are also presented.

1.1. Solar Energy Potential in the Energy Mix of Türkiye

Technologically developed countries have more energy infrastructure and use energy resources more efficiently. Supporting research on energy resources and establishing facilities that can operate energy resources efficiently are important in terms of sustainability and an indicator of energy independence. The International Energy Agency (IEA), of which Türkiye is a founding member, has reported that the transition to sustainable and manageable clean energy should be accelerated. Our country has risen to fifth place in Europe by increasing its share in clean energy resources with the strategies it has developed to ensure national energy supply security (Sümer & Güngör, 2023). Türkiye is located between 36-42º North parallels and 26-45° East meridians. The territory of Türkiye is divided into 7 geographical regions named Marmara, Aegean, Mediterranean, Central Anatolia, Black Sea, Eastern Anatolia, and Southeastern Anatolia, there are 81 provinces spread through these 7 regions with the scope of this study. Geographically, Türkiye is located between the temperate and subtropical climate zones. Türkiye is an energy importer because of its heavy dependence on fossil fuels and scarcity of indigenous energy supplies. That is, fossil fuels are currently Türkiye's primary energy source. By increasing the efficiency of PV plants, the cost of energy and reliance on fossil fuels may be lowered significantly. Although Türkiye is located in the sun belt, its potential cannot be used effectively and widely. Therefore, these days, PV plants are considered by most researchers as the current and future task to ensure the sustainability of solar PV plants in Türkiye. Solar energy potential in Türkiye is particularly abundant in comparison to European countries. In the last couple of decades, Türkiye has focused more on renewable energy to diversify its energy mix and decrease fossil fuel imports. It is anticipated that solar energy will be crucial to Türkiye's sustainable electricity production and energy transformation process in the future. The government supports solar energy investments to achieve a significant solar energy portion of the energy mix. Solar energy can also help to benefit from the environmental resources of Türkiye and contribute to the sustainability of the energy source (Bilen et al. 2008). In recent years, despite an increasing interest in solar energy, in Türkiye, solar energy still makes up a modest portion of the energy mix (Erdem, 2010; Topal et al., 2021). Therefore, solar energy appears to be among the most practical options for the unlimited, clean, and sustainable energy future of Türkiye, because it's positioned in the sunny belt between 36° N and 42° N latitudes. According to the Solar Energy Potential Map of Türkiye (2024) prepared by the Ministry of Energy and Natural Resources (Emikonel & Bilhan, 2022), Türkiye's annual total sunshine duration is 2,766.5 hours/year (7.58 hours/day), and annual TSR value is 1,521.7 kWh/m²-year (4,17 kWh/m²-day). The Southeastern Anatolia Region has the greatest potential to benefit from solar energy among Türkiye's regions. The annual sunshine duration is 2,993 hours/year, and the annual TSR value is 1,460 kWh/m²-year of this region (Kok, 2015). It is well understood that Türkiye is lucky compared to many countries in terms of its solar energy potential due to its geographical location. European countries, whose sunshine duration and solar energy potential are much lower than Türkiye, meet a significant part of their energy needs from the sun. It is predicted that the rate of utilizing solar energy will increase further in the coming years as investments in renewable energy resources and awareness increase in Türkiye.

1.2. Motivation and Objectives of the Study

Transposition models are commonly employed by researchers to analyze and compare the energy production of solar PV systems constructed with SFSs and STSs. These models are also used to calculate theoretical and achievable energy production for various regions or geographic coordinates by taking into account some solar climatic parameters. However, the literature still does not provide adequate, clear comparative studies between the various transposition models, especially for Türkiye. Thus, this thesis accomplishes multiple primary goals. This thesis aims to apply transposition models for accurately estimating the TSR intensity on an optimal SFS without the need for measured GSR data, which is intentionally selected to be representative of Turkish territories. This thesis aims to estimate the TSR intensity on a single-axis STS and a dual-axis STS for the studied geolocations by using empirical relations of the proposed transposition models. In addition, the thesis aims to present a comprehensive analysis of each model using predicted TSR values collected by PV surfaces to determine the effect of the transposition models on an estimation of energy production. Another aim is to show the effects of a few degrees of deviation from the OPTA of PV surfaces on energy production and investigate the relations between OPTA and latitude values. So, the main source of motivation behind this thesis is to create an OPTA map of Turkish provinces to be used in the design stage of possible large-scale solar PV plants.

Another important point is that performed case studies should be supported with experimental or implementation studies, and the practical implications of theoretical studies should be evaluated. Comparing predicted and actual solar energy production results will help to find the most accurate prediction models and process them into the literature, which will not only contribute to academic and scientific studies in this field but will also make a significant contribution to the pre-analysis and feasibility studies of solar PV plant installations. Therefore, an important source of motivation for this thesis is the presentation of data collection, analysis, and results of solar PV plants over a long-term period and the comparison of actual results with the predicted results obtained from anisotropic transposition models to provide useful solar data for PV industries and researchers.

Solar energy models that ignore optimal tilting for large-scale PV plants may significantly underestimate the solar potential available. In this regard, this thesis offers a broad perspective on the utilization of transposition models for the preliminary analysis of the efficiency of large-scale PV plants to be installed in Türkiye. It is explained in Section 1.1 that Türkiye does not benefit from the potential of solar energy at the expected level. It is also emphasized that research studies conducted in the majority of Türkiye's regions have not yet reached an adequate level. Identifying the most viable transposition and correlation model remains a significant unmet need for research studies, especially concerning Türkiye. Due to the limited studies for Türkiye provinces, a more in-depth study is required to assess the transposition models. To increase the precision of the existing ones, research studies are still being conducted. Therefore, one of the importance of this research is to contribute to the literature by providing reliable and useful solar energy data for Türkiye identifying the OPTA and TSR values of PV surfaces. The last, but not least aim of this thesis is to design an isolated microgrid for rural and remote areas in Türkiye in which electricity is produced from PV cells and stored in the ES to support microgrid loads. Performing application study to optimize ES and PV capacity of the microgrid to maintain energy flow regularly, make a stable energy balance, and ensure a stable energy supply by keeping operating costs at low and affordable levels. It is anticipated that this study will make a substantial contribution as a guideline before the implementation of large-scale PV plants in the interested geolocation.

1.3. Factors and Parameters Affecting TSR Optimization

The performance of any PV surface is not only related to the manufacturing features and the technology being used but also the TSR collected by SFSs, and STSs, and solar PV plants' performance depends on several factors such as tilt angle, azimuth angle, solar declination, incidence angle, orientation, load profile, optical and geometric properties, utilization time, location latitude, geographical position, climatic conditions, atmospheric factors, seasonal variations, etc. Especially, both parameters orientation and tilt angle relative to horizontal surfaces impact the quantity of the GSR intensity reaching the PV surfaces, so directly plays an important role in its performance (Gunerhan &

Hepbasli, 2007; Benghanem, 2011; Sudhakar et al., 2013). So, reliable estimations of TSR intensity on PV surfaces are vitally important for the proper design of a PV plant in the interested geolocation. Therefore, OPTA must be carefully determined to collect the maximum TSR at the design stage of a PV plant. The OPTA is dependent on latitude, solar declination, and the time and days in the year (Kaygusuz & Sarı, 2003; Gunerhan & Hepbasli, 2007; Ulgen, 2007). For this reason, the OPTAs of PV surfaces should be adjusted monthly, seasonal, or annual to obtain TSR intensity from PV surfaces.

1.4. Importance of Transposition Models

Through the year, the sun's position above the horizon changes, resulting in varying GSR values over different months. TSR data on horizontal surfaces obtained from ground and/or satellite stations can be utilized to compute the potential of solar energy in geographical regions of interest. On the other hand, the TSR data for tilted or tracked PV surfaces cannot be obtained from the meteorological stations and can be predicted by applying transposition models (Noorian et al. 2008). Sky conditions and anisotropy solar parameters have a considerable impact on GSR distribution as well. Thus, most of the TSR estimations and calculations on PV surfaces are accomplished by taking into consideration the solar geometry and solar parameters in the geolocation of interest as highlighted above section. For these reasons, a large number of isotropic and anisotropic transposition models have been developed to estimate the OPTA and to compute the TSR intensity on a PV surface depending on the geo-referenced conditions including the clearness index. These models demonstrate the complexity of calculating TSR intensity on a tilted and tracked PV surface (Evseev & Kudish, 2009).

2. LITERATURE REVIEW AND RELATED STUDIES

In literature, numerous studies have been conducted to estimate the performance of PV plants at various global locations and solar climatic conditions by considering transposition models, correlation and regression models, OPTA values, TSR intensities, solar geometry, and STSs. Various studies have been carried out on optimizing OPTA values and TSR intensities for Türkiye provinces. Investigating solar potential, performing TSR estimations by using machine learning algorithms, and the TSR efficiency of STSs have been a source of motivation in these studies. Therefore, in this section, the research and associated studies on this field carried out worldwide have been investigated and the key points are briefly indicated.

2.1. Literature Review on Radiation and Transposition Models

Many scientists have investigated the transposition models' accuracies by contrasting the predicted and measured quantities of TSR under various climatic circumstances with different experimental methods. Due to the significant solar variations worldwide, isotropic and anisotropic sky models have been utilized to predict the performance of solar PV plants (Lave & Kleissl, 2011; Lubitz, 2011; El-Borie et al., 2020; Manzoor & Singh, 2021; Okhaifoh et al., 2021; Tuama et al., 2021; Agbo et al., 2022; Windarta et al., 2022). The significance of transposition models lies in the reliable determination of the OPTA for PV surfaces, as well as in calculating the intensity of TSR on a tilted surface (Yasin et al., 2016). Lui and Jordan (1961) developed an isotropic transposition model, and it is still commonly used in many scientific research studies and data banks. Initially, the model was aimed at being used for specific surface orientations, but it was later extended so that it could apply to other surface orientations (Klein, 1977). In subsequent research, more advanced anisotropic models were introduced such as Hay-Davies (1978), Klucher (1979), Reindl (1990), HDKR (2006), and Perez (1987). The daily TSR intensity on a tilted PV surface was predicted using another model, which differs from the isotropic model concerning the beam radiation component determination Klein & Theilacker (1981), where the presented TSR yield results on tilted surfaces were agreed more closely with the integrated hourly calculations. Comparison of transposition models by using five years of recorded tilted TSR values emphasizes the significance of taking into consideration the sky radiance anisotropy in both cloudy and clear weather conditions was highlighted, and the input data produced with an acceptable accuracy (Skartveit & Olseth (1986). A comparison of 12 models' performances that are utilized to compute diffuse radiation on tilted PV surfaces showed that all of the models produced massive errors for the west-facing surface, and comparatively good accordance with solar data measurements especially for a south-facing surface (Emikonel & Bilhan, 2022). In another study (Chandel & Aggarwal, 2011), the TSR values on tilted PV surfaces were predicted and compared to the measured TSR values for testing the accuracy of the Chandel (2005) and Gueymard (2000) models where the predicted TSR values by using were found to be mostly in line with the measured TSR values. 54 transposition models in the clear sky were reviewed and tested by using ground and derived satellite data (Badescu et al. 2012). It was emphasized that the precision of the models strongly depends on the collection of input data. Also concluded that no model can be declared to be the best for every collection of input data; both extremely simple and more complex models can produce good results.

The study (Jakhrani, 2013) focused on the effectiveness of radiation models and revealed that there was a 7% discrepancy between the annual TSR data collected by satellites and ground stations. Also, it was found that the Klucher (1979) model produced little error while the Reindl (1990) model operated at maximum variance for the computation of TSR intensity on a tilted PV surface. The study (Yao et al., 2014) pointed out that while complicated models were unable to improve the estimation, the existing linear and polynomial models were able to accurately estimate TSR.13 models were tested to estimate the OPTA values for obtaining the maximum TSR in Fes of Morocco (Ihya et al. 2014). In that study, the comparison of the TSR predicted and measured values indicated that the Koronakis (1986) model yielded the highest accuracy than other models. To compute the daily TSR on tilted PV surfaces, six transposition models were employed (Shukla et al. 2015). It was understood that the Hays and Davis (1978) model gave the best estimates whereas the Badescu (2002) model gave the worst estimates among all models. Also, Liu and Jordan (1961) and Koronakis (1986) models gave similar results. Hofmann & Seckmeyer (2017) developed a model by utilizing a time series of TSR data as input for the computation of diffuse radiation. The model revealed that the obtained results have better agreement with measurement data and provide high-accuracy modeling of the diffuse radiation. The modeled radiation values by using four models were compared to measured solar data (Mubarak et al., 2017). It was found that the deviations in results obtained from Liu-Jordan (1961), Klucher (1979), and Perez (1987) models increase as the tilt angle increases. The optimal outcomes were revealed by the Hay-Davies (1978) and Reindl (1990) models. In a study (Li et al., 2017), seven models were assessed against measurement data at different sky conditions. Iwaga's (2004) and Muneer's (1990) models gave the best results under clear and intermediate sky conditions, while the Skartveit-Olseth model (1986) obtained the best results under overcast sky conditions. Four models were tested by using solar data spanning 22 years. Olomiyesan-Oyedum model was implied to be the best in terms of precision and suitable for estimating TSR intensity in Nigeria (Olomiyesan, 2017).

24 transposition models were compared by using several statistical methods and measured time-series TSR data to identify the most precise model for Palestinian cities (Nassar et al. 2020). The HDKR model (2006) outperforms the other models for estimating tilted TSR intensity. As for overall performances, the Skartveit-Olseth model (1986) performed better than the others, specifically with 3.4% better accuracy than the HDKR (2006) model. In a study (Matius, 2021), four isotropic transposition models were applied to optimize OPTA, and results indicated that the Tian model (2001) was found to be more suitable for approximating insulation. Various isotropic and anisotropic models were applied comparatively for five cities in Saudi Arabia (Mansour et al. 2021). On average, the results demonstrated that 5% more energy is gained by the anisotropic model than by the isotropic model. A statistical method was introduced to determine the most precise transposition model (Nassar et al., 2022). Results showed that the most suitable model was Hay (32%), HDKR (42%), and Perez (21%), and it strongly relies on the PV surface OPTA and the geolocation. The determination of the most accurate horizontal-to-tilted sky-diffuse transposition model is investigated. 22 models were assessed for Libyan cities by obtaining solar data from SolarGis to investigate the performance of the models (Nassar et al., 2022). It was found that the Bugler model (1977) was suggested for some specific regions, and the Lui-Jordan model (1961) was suggested for the southern region in terms of accuracy. In another study (Abdulwahab, 2023), 18 models were investigated by focusing on their accuracies and reliabilities. These models were analyzed to represent a diverse range of climatic and geographic conditions in 220 cities worldwide. It was expected that the results contribute literature significantly and support technological advancements in the field for future design of large-scale investments.

2.2. Literature Review on Regression and Correlation Models

Various empirical correlation and regression models have been developed to make realistic analyses and to investigate parameters that affect the performance of tilted PV surfaces (Shukla et al., 2015; Yang & Lu, 2017). The variation and fraction of the diffuse radiation on an hourly basis must be determined at the highest accuracy to estimate the tilted TSR intensity from horizontal TSR intensity. Therefore, many authors have developed or suggested linear, nonlinear, and polynomial regression models that relate the sunshine ratio and clarity index to the diffusion coefficient. Many authors have also focused on comparing and validating correlation models by utilizing statistical indicators and experimental data to investigate their applicability. Orgill & Hollands (1977) suggested a correlation model and compared it to earlier models. For the computer-based calculations, the hourly midpoint model was suggested for handling vast amounts of data and decreasing the computation time. A model that describes the long-term radiation intensity on PV surfaces in any direction was developed by Collares-Pereira & Rabl (1979). The results revealed %3 better accuracy than the long-term radiation intensity for PV plants. In a study (Skartveit et al., 1998), an improved correlation version was presented by integrating hourly solar elevation, clearness index, and surface albedo input parameters. Also, a test against 32 years of independent solar data demonstrated that the developed model outperforms the Maxwell (1987) and Perez (1992) correlation models. In another study, multiple transposition models were evaluated and validated by using solar data and statistical parameters (Notton et al. 2004). It was found that there was no model significantly better than others, whatever the statistical indicator was selected to identify the model's quality. It was indicated that the Erbs model (1982) has satisfactory performance on the correlation between diffuse and beam radiations. A model was developed and compared to seven other correlation models (Khosravi et al. 2020). The monthly optimal setting of the surfaces led to an increase in TSR of about 20%. Moreover, an annual OPTA was found to result in a 7% increase in TSR when compared to horizontal surfaces. In this study (Nassar et al., 2023), it was presented that a regression function can be used for PV surfaces to correct the OPTA by involving the radiation components. The model was generic to apply to different locations. The outcomes demonstrated the applicability of the developed regression function in Libya.

2.3. Literature Review on Estimation of Optimal Tilt Angles (OPTA)

In literature, numerous sophisticated methods have been developed to precisely identify OPTA values to optimize TSR intensity on tilted PV surfaces for specific geographic locations worldwide. Many research studies have been conducted to estimate the OPTA of PV surfaces over time theoretically based on solar geometry (Chang, 2009; Kamali et al., 2006; Talebizadeh et al., 2011; Yadav et al., 2013). Also, various methods are proposed via different research studies about the OPTA values and TSR intensity obtained by the tilted surfaces for different geolocations (Yadav & Chandel, 2013; Mansouri et al., 2016; Hafeza et al., 2017; Hailu & Fung, 2019; Khosravi et al., 2020; Zhu et al., 2020; Khan et al., 2022). Optimal tilt and track computation methods have been carried out regionally or globally by using satellite and ground GSR datasets for solar radiation analysis including a selection of solar farm installation geolocations (Brayer & Schmid, 2010; Breyer et al., 2017; Uyan & Doğmuş, 2023). Also, several studies have been performed on the magnitude of TSR gain collected by the tracked PV surfaces, and findings were compared to south-oriented SFSs (Abdallah & Nijmeh, 2004; Koussa et al., 2011; Bahrami et al., 2016; Hua et al., 2019). The determinations of OPTA studies have revealed that the OPTA of a PV surface has a significant impact on the intensity of collected TSR (El-Sebaii et al. 2010; Chandel & Aggarwal, 2011; Maatallah et al., 2011; Demain et al., 2013; Masili & Ventura, 2019; Miguel et al., 2021). Additionally, some researchers proposed setting two OPTAs that can be used during the summer and winter seasons, depending on the latitude of the specific location of interest (Elminir et al. 2006; Pavlović et al. 2010). The annual OPTA was determined to be close to the latitude of the site (Benghanem, 201). Besides, an experimental study was performed to measure the performance of different PV surfaces with different tilt angle values (Kaldellis & Zafirakis). An optimal tilt estimation method for urban applications was presented based on a modified sky model (Siraki & Pillay), and the results showed that OPTA depends on latitude, weather conditions, and surroundings' environmental conditions. Other research studies were carried out for the optimization of surface orientation, performance evaluation, and TSR intensity on STSs continuously positioning the surface towards the Sun (Ghosh et al., 2010; Hafez et al. 2018; Jacobson & Jadhav, 2018; Al-Rawahi & Al-Azri, 2019; Praliyev et al., 2020; mah et al., 2021). Studies were conducted on the maximization of TSR for a given period and annual rotations (Mehler et al. 2010; Moghadam et al. 2011). Numerical methods were used to find the OPTAs for each hour and season under a variety of climatic conditions in accordance with annual horizontal GSR (Runsheng & Tong, 2004). The amounts of TSR collected by the tilted surfaces were compared by using measurement, determination, and generated TSR values (Othman et al. 2018; Akgül et al., 2022).

In this context, a monthly setting of OPTA has resulted in a very little gain, approximately 3% compared to a tilted surface (Koronakis, 1986). Tang and Wu 2004) proposed a numerical approach to compute the OPTA. A comparison between predicted and actual diffuse radiation values showed that an accurate estimation of the OPTA is provided by this model, except for places where the clearness index is significantly lower. The OPTA for Galway in Ireland was found 44° by applying a technique to maximize the production of solar energy (Armstrong & Hurley, 2020). A model was presented to determine the OPTA for Roorkee province in India by using predicted and generated solar data (Kapoor & Garg, 2021). According to the actual and predicted data, the OPTA for Roorkee province is 20°, and the monthly and annual variations in solar potential are around 14% and 11%, respectively. The determination of OPTA to collect the maximal TSR intensity was investigated based on the measured TSR data (Benghanem, 2011). The outcomes showed that the annual OPTA is 23.5° which closely corresponds to the latitude of Madinah province. The study (Mansouri et al., 2016) employed an empirical model in which TSR intensity on the PV surface was computed equal to 29° at Shiraz in Iran. Different optimization techniques were applied to determine maximal energy gain and it was emphasized that each place on earth needs precisely determined OPTA (Yadav & Chandel, 2013). OPTA values were predicted by developing a mathematical model for 35 locations in various countries of the Mediterranean region (Darhmaoui & Lahjouji, 2013). The OPTA values of Bursa and Isparta cities in Türkiye were determined to be 36° and 37°, respectively. OPTA and TSR values were predicted for four locations by applying four transposition models (Calabrò, 2013). In which, estimation of the OPTA concerning latitude employing a linear regression was conducted and it was found that regression coefficients strongly depend on total horizontal TSR data. In a study (Jafarkazemi & Saadabadi, 2016), it was suggested that the OPTA should be changed at least twice a year and that the annual OPTA be set to 22° if OPTA adjustment is not possible at all for Abu Dhabi. In another study (Abdulsalam & Alibaba, 2019), OPTAs in North Cyprus should be set between 28° and 30° for SFS annually. In a study (Ihya et al. 2014), for Fes province in Morocco, the annual OPTA was determined to be 32°. A study (Matius et al., 2021) stated that surfaces should be positioned at 8.05° for Sabah in

Malaysia. In another study (Udoakah & Okpura, 2015), the annual maximum TSR intensity was obtained at the OPTA of about 60° for Enugu in Nigeria, which approximately corresponds to the geolocation's latitude.

In a study (Mansour et al., 2021), the annual OPTA values for the cities of interest were determined as 27° for Dhahran, 26° for Riyadh, 22° for Jeddah, and 33° for Arar. In a study (Zang et al., 2016), by utilizing the measured solar data from ground stations spanning 16 years, annual OPTAs were predicted to be 15°, 24°, 27°, 39° and 47° for Sanya, Shanghai, Zhengzhou, Harbin, and Mohe, respectively. This study showed that the annual OPTA is equal to the latitude of the locations. The OPTA values of some cities in various countries were calculated in a polynomial form and presented in a tabular form with the other sources for comparison purposes (Yasin et al., 2016). The annual OPTA for Craiova in Romania was determined to be 45°, close to the measured values (Alboteanu et al., 2015). OPTA values of PV surfaces for a few cities from all countries worldwide were determined (Jacobson & Jadhav, 2018) where the OPTA values for Ankara and Diyarbakır in Türkiye were found as 29° and 30°, respectively. In another study (Berisha et al., 2018), using the Liu-Jordan model (1961), the annual OPTA for Pristina, Kosovo, was determined to be 34.7° where annual solar energy gain was predicted to be 14.43%. The OPTA values for 20 Moroccan cities were calculated annually by applying the mathematical models and it was determined that the OPTA values vary between 28° and 32° (Nfaoui & Hami, 2018). The OPTA values were predicted annually by applying isotropic and anisotropic transposition models (Hailu & Fung, 2019). The OPTA values for four isotropic models varied and ranged from 37° to 44°. Conversely, the outcomes of the four anisotropic models exhibited comparatively higher consistency, specifically ranging between 46°-47°. The annual OPTA for the majority of Palestinian cities was determined at approximately 29° and when compared to a horizontal surface, the application of the predicted value results in an energy gain increase of about 10% (Abdallah et al., 2020). The TSR intensity and the OPTA values were calculated to optimize the performance of solar energy transformers by using 5 years of measured solar data for Qena province in Egypt (Kassem et al., 2020). Results indicated that the OPTA is 27° and the yield is 6.57% for annual SFSs. In a study (Kambezidis & Psiloglou, 2021), OPTA values in Greece were examined annually by using solar data for the corresponding locations. Maximum energy was observed to have been collected by surfaces adjusted at OPTAs of 28° for Larisa, 29° for Agrinio, and 29° for Serres. In a study (Nassar et al. 2022), the Klucher model (1979) is adopted to estimate

OPTA values for 19 locations by using SODA satellite-derived solar data. The outcomes validated the Klucher model's applicability and reliability. The annual OPTAs for Tripoli and Tehran were predicted as 29° and 32°, respectively. The TSR intensity and OPTA were predicted for different locations based on Hottel and Woertz (1986), Liu-Jordan (1961), and HDKR (2006) models from the simplest one to the complex one (Stanciu & Stanciu, 2014). It was found that the tilt OPTA value increased along with the latitude value. The collected TSR values at monthly and annual OPTAs in different latitudes were found to be less than 4% for all latitudes.

2.4. Literature Review on Design, Development, and Performance Analysis of Solar Tracking Systems (STS)

Numerous researchers have looked into the design, development, and efficiency of STS's mechanisms for particular global geographic areas to optimize solar energy produced by tracked PV surfaces. Various sources have been presented in the literature about trigonometric relationships of the incidence angle for STSs, and the determination of zenith and solar azimuth angles based on time and location by using various algorithms (Brownson, 2014). Similarly, several studies have focused on the feasibility and efficiency of STS by investigating solar energy potential (Eldin et al., 2016; Alkaff et al., 2019; Nassar & Alsadi, 2019; Safaraliev et al., 2020; Akgül et al., 2023). Efficiency comparison of STSs versus optimally tilted SFSs, tilt angle effects on the performance of PV surfaces, and experimental implementation and performance evaluation of STS approaches have been conducted (Khan et al., 2020; Tchakounté et al., 2021; Aghamohammadi et al., 2023). In this context, for both single-axis and dual-axis STSs, relationships between the TSR intensity and surface OPTA values were determined (Braun & Mitchell, 1983). Klucher (1979) and Perez (1987) models were tested in various climate conditions to estimate the TSR intensities and compared the outcomes with measured solar data in Dhaka (Ghosh et al.,2010). The outcomes revealed that the TSR gain collected by the annual SFS became about 15% for a whole year. The TSR gains throughout the year received by the single-axis and dual-axis trackers were predicted as 22% and 25%, respectively. The performance of PV surfaces was investigated by using a mathematical model as a function concerning STSs and findings were validated experimentally (Eldin et al., 2016). It was revealed that the yield in TSR intensity from

STS is roughly 39% for cold regions, whereas the yield in TSR does not exceed 8% for hot regions. Six locations at different latitudes were chosen to analyze the PV plant efficiency near and away from the equator in various countries (Alkaff et al., 2019). The findings indicate that an SFS yields approximately 19% less energy production than a single-axis STS, and a two-axis STS achieves around 4% more energy production than a one-axis STS. Perez's model (1987) was applied to estimate the OPTA values for optimization of TSR intensity (Mah et al., 2021). The findings indicated that a dual-axis STS collected 22.14% more TSR than an SFS, whereas monthly OPTA modification boosted yield by just 2.15%. A technique to calculate the energy gain of solar trackers was proposed based on iterative algorithms at a low computational cost (Miguel et al., 2021). Results showed that a single-axis STS has an annual gain of 42.1% whereas a dual-axis STS has a gain of 47.4% in comparison to the SFS. The feasibility of STSs in the sunbelt region was investigated (Soulayman et al., 2021) showing that sunbelt countries do not require an STS due to the overheating caused by prolonged solar radiation. The performance of dual-axis STS at high altitudes was investigated (Larico & Gutierrez, 2022). The STS performed 37.63% better monthly than the SFS, according to the results. Overcast and rainy days brought up a TSR yield of less than 14.38%.

In a study, a standalone low-cost and high-precision two-axis closed-loop STS using the SPA was developed. Results revealed that STS outperformed the SFS by 13.9% (Chowdhury et al. 2019). In a different study, the performance of one-axis STS based on schedule and light-dependent resistor (LDR) was compared considering various weather conditions for one year. The one-axis STS based on the schedule indicated better results in cloudy and rainy weather conditions (Kuttybay et al. 2020). Also, an efficient two-axis STS with a real-time clock was developed, and a self-cleaning system was integrated. The proposed STS was achieved with low power consumption, high accuracy, and low cost. Also, the proposed self-cleaning system improved the efficiency of the two-axis tracking system by 17.8% (Brisha, 2019). In a study, an intelligent Arduino-based STS using LDR, and servo-motor was designed. The results indicated that PV energy was approximately 26.8% gains compared to SFS (Hasan & Abubakar, 2020). Additionally, an STS for high-concentration photovoltaic (HCPV) in a wireless environment was designed. The hardware and control strategy were introduced (Hu et al. 2012). In another study, the GPS-based STS was designed. The average energy produced from the two-axis STS was 25% more than the SFS (Cuong & Ancheta, 2018). In a study, a multiple-axis servo-motor feedback-based STS was developed, and the MPPT algorithm was implemented. The results showed that the STS increased efficiency by 23.95% (Laseinde & Ramewre, 2018). A new architecture approach was adopted for two-axis STS. The results demonstrate more than 40% PV energy efficiency with the developed STS in comparison with SFS (Anoune et al. 2015). Moreover, a new STS design methodology was described and validated experimentally. Based on the results, this STS has increased its efficiency by 24% compared to a SFS (Ruelas et al., 2019). An STS control system was designed and tested along with numerical analysis and the Simulink model in Saudi Arabia. The obtained results indicated the simplicity, accuracy, and applicability of design in meeting different operational conditions (Balabel et al. 2013). It was designed and implemented as a two-axis STS using LDR sensors, DC motors, and a microcontroller for rural applications in Nigeria. Experimental results showed that the designed system was more cost-effective and produced 31.4% more energy than a two-axis STS and 67.9% more than an SFS (Amadi, 2018). In a study, a comparison of the 24-month production of PV energy by an SFS and a two-axis STS was presented. Increases in the production of PV energy by 35.6% and 44.7% were observed for the two-axis STS during the first and second measuring years, respectively (Frydrychowicz-Jastrzebska & Bugała, 2021). A two-axis smart STS was designed by utilizing two servo motors, and LDR sensors, which were placed in the four corners. Based on experimental results the designed STS produced 36.26% more energy compared to a SFS (El-Hammoumi et al. 2018). Other than these studies, a two-axis STS was developed by utilizing a PLC motor to control STS and LDRs to detect the sun's position in the sky. The results showed that the STS increased the output power by 39.27% compared to the SFS (Sinjari & Shareef, 2016). In a study, an STS was designed with two stepper motors to guide the motion and controlled by a programmable logic controller. It was observed that the surplus energy was obtained at 36% (Hoque et al. 2018). A two-axis STS was constructed successfully which includes IDR to sense the position of the sun, two stepper motors to motion the STS either horizontally or vertically, and an AT mega microcontroller for control strategy. Experimental results indicated that the designed STS outperforms 10.7% better than an SFS (Acakpovi et al. 2015). In a study, it was proposed a durable and reliable two-axis STS design that utilizes GPS for fixing the time, date, and location in terms of longitude and latitude. Astronomical equations were utilized to find the sun's locations in any chosen location on Earth (Al-Naima et al. 2013). Additionally, in a different study, it was proposed a design, construction, and performance test of a two-axis STS, which consists of two light sensors and an automated microcontroller to drive the motor and three batteries. It was observed that yielded more energy by the STS was 47.5% compared to SFS (Oumarou et al. 2015).

It is understood from the literature review that the contribution of experimental studies of STSs performed in various parts of the world and climates to energy efficiency is undeniable. It is seen that one-axis STSs provide a performance increase of up to 30% on average, and two-axis STSs provide a performance increase of up to 40% on average. For this reason, in terms of independent energy sustainability and energy security, it is inevitable for Türkiye to prioritize solar PV energy production and for national academicians to contribute to the literature, especially on the development of STS systems. Governmental support and encouragement are essential.

2.5. Literature Review on Development Solar PV Plants and Application Studies

Many studies focusing on the modeling of insulated PV plants are available in the literature. The development of PV plants has progressed rapidly over time with new research studies concentrating on the optimal performance of PV applications, case studies, cost analysis, design, and numerical modeling. In literature, there exist several studies related to our research interest which are presented below. Power management, performance analysis, and optimization for PV plant studies were conducted (Mengi & Altas, 2015; Suchitra et al., 2016; Gabbar et al., 2016; Aghajani & Ghadimi; 2017; Vera et al. 2019; Shayeghi et al., 2019; Arıkan et al., 2919). Techno-economic and cost analysis studies were performed (Öztürk et al., 2012; Sulukan, 2020). The feasibility of setting up a PV facility in a rural clinic was performed, and the optimum system cost and electricity cost were calculated ([Al-Karaghouli & Kazmerski, 2010). A solar PV plant was established with the solar tower model, and technical and cost analyses were made (Selbaş et al., 2013). Small (54.15kW) off-grid PV power production was proposed for communities. The environmental and energy analysis of the system with the life cycle emissions was the focus of the research (Akınyele, 2017). The technical and financial viability of 50kWp PV plants with 50kW of ES capacity was investigated with some indicators (Patil et al. 2017). In a different study, a solution was provided for solar PV power supply to small-scale industries at a cost-effective and feasible level in Nigeria (Raji et al. 2021). In another study, a one-year performance analysis was conducted on the PV plant. It was observed that the results obtained from the field measurements verify the theoretical models (Yan et al., 2013). To address the electrical energy demands of a residence, an isolated PV plant was created, and the microgrid was modeled and simulated using MATLAB/Simulink (Akgül et al., 2021). Besides, off-grid PV-powered small microgrids for humanitarian action in refugee camps were designed (Franceschi et al., 2014). Apart from these, other related works are also referred to in the relevant parts of this study. It can be seen that previous studies have not focused on transportable design, and the objectives and criteria defined in this study have not been addressed completely in other types of research topics previously. In addition, the previous studies have not sufficiently focused on a system design with the simulation environment presented in this study. Several studies have been focused on the calculation of the Levelized Cost of Energy (LCOE) of solar PV plants. It was seen that the financial parameters have the biggest impact on the LCOE, apart from the location (Vartiainen et al., 2019), and it was shown that both device and field lifetimes are critical for achieving a low LCOE for a solar power station (Ahangharnejhad et al., 2022). In a review study, solar energy optimization management, along with comparative analysis, constraints, solution approaches, and simulation tools for PV plants, were presented (Vera et al., 2019). The energy gain and LCOE resulting from SFSs, and STSs had been compared (Bahramia et al., 2017). The impact of the installation parameters of SFS and single-axis STS on the energy yield, the LCOE, and the bifacial gain has been investigated (Chudinzow et al., 2020). In the current study, LCOE-based solar installation and solar energy costs have been investigated and evaluated for approximate cost analysis of solar PV plants to be installed in Antalya province.

2.6. Literature Review Focusing on Türkiye

In Türkiye, several studies in the literature have been carried out by researchers for different purposes and regions about the optimization of tilt angle, the orientation of PV surfaces, and the calculation of TSR and GSR values. Some considerable studies have been carried out for the region within the last decade. Investigation and determination of OPTA values and TSR gains for PV surfaces in provinces of Türkiye (Akgul et al., 2024). Usability and system analysis of solar PV plants in the Central Anatolia region is carried out (Ozturk & Kayabasi, 2023). Measurements of TSR intensity in Ankara province are performed (Caglar et al., 2013). A comparison of the models for solar PV plant performance calculations for Central Anatolia is carried out (Ozden et al., 2020). Determination of PV surface OPTA for Ankara province and districts is performed (Kocer et al., 2016). The effect of OPTA on yield in PV surfaces is investigated (Dal, 2021). GSR with the artificial neural networks for the Sivas province is predicted (Gurlek & Sahin, 2018). To calculate the OPTA values, generic correlations were developed in Türkiye and their accuracies were analyzed by using statistical methods (Bakırcı, 2012). It was determined that throughout the year, the OPTA varies between 0° and 65°. The annual OPTA values were found to be 31°, 33°, 33°, 34° and 33° in Adana, Ankara, Diyarbakir, Erzurum and Istanbul cities, respectively. In a study (Öztürk et al., 2016), The STS was shown to harvest 35% more energy under the same conditions in Düzce. Similarly, a study (Senpinar & Cebeci, 2012) showed that the daily energy production of the STS was 13-15% greater compared to the SFS in Elazığ province. Six models were carried out to estimate TSR from the daily values for Çanakkale and results were evaluated via statistical methods (Ayvazoğluyüksel & Filik, 2017) where the findings indicated that the CPRG model (2000) performs the best accuracy. To investigate the solar energy potential of Mersin province by using meteorological data, a simple method to estimate GSR intensity was developed and compared with the other methods in the literature. Daily and monthly GSR data were predicted with 14.7% and 9.1% absolute mean percentage error, respectively (Arslan & Bayhan, 2016). Six models were investigated for the estimation of horizontal TSR values in Mersin and compared to the measured TSR values (Kulcu et al. 2017). Statistical analyses indicated that the accuracy of Model 6 developed specifically for Türkiye is higher than other models. In a study, an ANN method was applied to predict GSR distribution in given atmospheric parameters in Adana province. Levenberg-Marquardt learning algorithm and logistic sigmoid transfer function were used in the ANN network (Şenkal, 2016). Moreover, an evaluation of the sunbathing rate and the solar energy potential in Burdur province was made. The data obtained were compared with the GSR values of Türkiye (Kırbaş et al., 2013). GSR intensity for six provinces of the Mediterranean region was generated from the daily GSR data measured using the Finkelstein-Schafer statistical method, the obtained data was comparatively analyzed between provinces, and results were assessed (Bulut et al., 2009). Empirical models to estimate the monthly daily horizontal GSR on a horizontal surface were developed for Antalya. Statistical methods were utilized to evaluate the accuracy of the GSR estimations (Balli et al., 2007). Measured daily GSR data for Adana province was used to estimate horizontal GSR. Hourly global, diffuse, and beam radiations on a horizontal surface were determined in Adana province (Oğulata & Oğulata, 2002).

Most of the studies to determine the solar radiation potential of a certain location were focused on the determination of GSR on a horizontal surface using measured data (Kulcu et al., 2017; Ruşen, 2018; Tırmıkcı & Yavuz, 2018; Beyazıt et al., 2020). Several GSR calculation models are performed in the literature by using Artificial Neural Networks (Gurlek et al., 2018; Arslan et al., 2019) and Machine Learning (Alsafadi & Filik, 2020; Ağbulut et al., 2021). The studies carried out optimization of OPTAs and maximization of TSR intensity on the tilted surface for the different locations are contributed to Türkiye in this field (Koçer et al., 2016; Tırmıkcı & Yavuz, 2018; Yıldırım & Aktacir, 2019; Geliş et al., 2020; Dal, 2021). Besides, there are different studies in the literature to provide maximal TSR with STSs and compare TSR values with SFSs for Türkiye (Akkılıç et al., 2015; Yılmaz & Kentli, 2015; Öztürk et al., 2016; Filik & Filik, 2017).In a study (Kentli & Yilmaz, 2017), the outcomes implied that the performance of the dual-axis STS is 31.67% greater compared with the annual SFS in Diyarbakır. The performance of a satellite-based HELIOSAT (Cano et al., 1986) method and a hybrid method was investigated for Nevşehir (Rusen, 2018). In that study, it was indicated that the hybrid model based on both the ground and satellites produced superior results than the empirical and satellite-based models. In another study (Kallioğlu et al., 2019), several correlations were established concerning latitude and declination. The annual OPTAs for Antalya, Kayseri, and Trabzon were calculated, and the found of regions is approximately 32°. The annual productivities at this OPTA value were 10.11%, 9.39%, and 9.58%, respectively. In a study (Şevik et al., 2021), the annual OPTA was predicted to be 34° in Çorum. When the OPTA is adjusted each season, an enhancement in the efficiency is achieved by more than 5% compared to SFSs. Study (Kulcu & Ersan, 2021) stated that the best estimation of the actual value is obtained by the Kulcu model (2015) and the worst estimation is produced by the El-Metwally model (2005) for computing TSR intensity in Hatay. In a study (Akgül et al. 2022), the annual OPTA is found to be between 28° and 30° all year round in Antalya province. So, it was found that there was a ±1° or ±2° OPTA difference between the districts. Moreover, in comparison to horizontal surfaces, SFSs harvest between 8.23% and 10.63% greater TSR. Districts of Antalya see higher TSR harvesting rates from single-axis trackers (28.72% to 33.17%) and dual-axis trackers (32.19% to 37.49%) compared to SFSs. Additionally, although there are a few studies to determine the OPTA and to calculate the TSR intensity for Antalya province

(Balli et al., 2007; Koçer et al. 2015; Karakaya et al., 2020), the number of district-based studies is negligible. In a study, TSR estimation outputs were compared with real PV production data, and the HDKR model was found to be 3.22%, according to the real production data (Dirlik et al., 2023). Besides, in a study for the Mediterranean region of Türkiye (Akgül et al. 2024), the annual OPTA range is 29°-33°, and the SFS gain ranges from 9.33 to 12.90% compared to non-tilted PV surfaces. It is also found that a one-axis STS harvests between 28.48 and 33.09% of daily TSR, whereas a two-axis STS harvests between 32.41 and 37.12% of daily TSR intensity when compared to the SFS under the same conditions. Additionally, In another study (Akgül et al., 2024), a transposition model was proposed to estimate the daily TSR intensity on optimally tilted SFS and STS in 81 provinces. Annual OPTA values were found between 28° and 36°. An OPTA map was created, and STS gains were tabulated for all provinces in Türkiye.

The study (Kacira et al., 2004) stated that all year long, the tilt angle changes between 13° and 61° in Şanlıurfa. Daily of 29.3% gain in TSR with a dual-axis STS compared to a 14˚ SFS on a regular day in July. Estimation of hourly TSR intensity by using two ANN models is utilized (Solmaz & Ozgoren, 2012) where the findings revealed that Model II performs better than Model I. In a study (Şahin et al. 2013), it was found that tested ANN models have the potential to perform satisfactorily compared to the multiple linear regression model. Also, a satellite-based GSR map of Türkiye was generated for the estimation of TSR capacities, and it was found that more accurate results were obtained from satellite data compared to the results obtained from ground station data. In a study (Akkılıç et al. 2015), Şanlıurfa's annual solar energy potential was calculated as 1830 kWh/m² for a SFS, and 2410 kWh/m² for a dual-axis STS. The annual energy gain for a two-axis STS is calculated as 31.85% more than an SFS. In another study (Arslanoğlu, 2016), three empirical models were suggested to compute the daily horizontal TSR intensity. The optimal values of statistical parameters from the cubic regression model were discovered to be superior to the results derived from the quadratic regression model. In a study (Beyazit et al. 2017), it was identified that the Erbs model (1982) is the most suitable model, with the lowest statistical errors. Liu-Jordan model (1961) exhibited a large deviation from measurement data. In a study (Gümüş & Kılıç, 2018), the statistical parameters showed that the proposed EWMA time series method was pretty good at estimating TSR intensity. In another study (Er & Turna, 2018), compared to current models, it was observed that second-order polynomial correlations are more appropriate in general. Besides, the measured daily TSR for Mersin was modeled using ANN, and common models for estimating daily TSR in the literature were investigated (Arslan et al., 2019). GSR capacities were compared daily, monthly, and yearly for Istanbul and Adana provinces. It was found that less solar energy is produced annually in Istanbul province (Sarkın & Dindar, 2017). Two different empirical models were analyzed for the GSR on a horizontal surface, and a new empirical model was developed for Osmaniye province to estimate GSR capacity (Yanıktepe et al., 2017). Calculation methods for the GSR coming to the earth were developed. The methods for the prediction of GSR were evaluated using measured GSR data for Mersin province (Kulcu et al., 2017). The performance measurements of a two-axis STS were performed. It was calculated that 33.8% more PV electricity was observed in the two-axis STS compared to the SFS in Muğla province (Eke et al. 2010). A PLC-controlled two-axis STS was designed and implemented. Application results showed that the energy production of STS was more efficient than SFS up to 34% (Demirtas, 2008). A two-axis STS was improved for STS efficiency. The energy consumption of the designed STS was too low to be taken into consideration, total daily consumption was less than 3Wh /Yılmaz, 2017) in Batman province. Experimental results showed that the STS which uses a fuzzy logic controller increases the efficiency of energy production by up to 35% from the PV surface in Kırklareli province (Toylan, 2017). A single-axis simple and economical STS was designed. The STS was enabled 8.89% more efficiently on average, even if the direction of the light changed, compared to the SFS in Düzce province (Gündoğdu et al. 2016). A mathematical model of STS and its mechanical components was derived. The designed two-axis STS was compared with an SFS, and it was observed that 30 % more electrical energy was produced annually in Batman province (Kentli & Yılmaz, 2015). One-axis and two-axis STS devices were designed. Results showed that a two-axis axis TSR was the most efficient one of all with 40% more efficiency than SFSs whereas a one-axis STS has 20% (Tırmıkcı & Yavuz, 2015). A dual-axis STS was built without the need for sensors to enhance energy output. The resulting design, which eliminates the need for sensors in the STS, was innovative (Er & Balcı, 2018).

In a study (Yıldırım & Aktacir, 2019), the optimal tilt for surfaces was determined between 20° with an error of 1.5% for building roof energy models by applying isotropic models. In a study (Karakaya et al., 2019), polynomial models were determined as the most appropriate ones to be used for TSR intensity on a horizontal surface. Three diffuse models were proposed, and outcomes were compared versus the measurement data (Beyazıt et al., 2020) where it was found that Model 1 and Model 2 gave better outcomes concerning clarity index constraints. PV technologies were investigated for 30° tilted surfaces by using measured data (Aktacir et al. 2020). The highest energy production was obtained by Thin-film PV whereas the lowest was generated by Mono-Si PV. Evaluation of the efficiency of solar energy on the roof of public buildings was studied for mono-Si, p-Si ve CdTe PV technologies (Yıldırım & Aktacir, 2021). Different annual TSR values were found although they were located on similar buildings with the same orientation and tilt OPTAs. In a study (Yiğit & Arslanoğlu, 2021), the annual OPTA was determined by using instantaneous TSR values at 28° and by using daily TSR values determined at 33°. It was observed that a 4% improvement in energy production can be achieved with seasonal OPTA. In a study (Yiğit et al. 2021), OPTA values were calculated by using instantaneous GSR and daily GSR. It was found that there was a difference of 3º-5º. The OPTA values were found using instantaneous GSR values were 29º for Bursa, Izmir, Konya, and Elazığ. It was 28º for Şanlıurfa and 30º for Erzurum. Besides, PV surface OPTA values by month were determined for Antalya province. The capacity calculation was performed based on monthly, seasonal, and annual OPTA values and horizontal situations (Kallioğlu et al., 2020). In another study (Gönül et al. 2022), the annual OPTA was identified to be 28° and also stated that a difference of 1° to 2° does not considerably alter the amount of energy generated.

The annual OPTA for a SFS was determined to range between 29° and 30° in the Şanlıurfa districts by using NASA solar data (Akgül et al., 2022). It was predicted that compared to the SFS, the single-axis STS gathers approximately 31% more TSR, whereas the dual-axis STS gathers approximately 35% more TSR. The different study determined that the seasonal OPTA values were 51° in winter, 19° in spring, 4° in summer, 44° in autumn, and the annual OPTA is 29° for Adana province (Yilmaz & Şimşek, 2022). The OPTA values of an SFS were found to be 29º in Tekirdağ, Artvin, İzmir, Kırşehir, and Antalya provinces, and 28º for Şanlıurfa province (Gönül et al., 2022). An optimized model based on the ANN method and Angstrom-Prescott model for the estimation of daily TSR was investigated in the Eastern Mediterranean Region to ensure the most feasible solution for estimating GSR for the region (Yıldırım et al., 2018). A study was conducted on PV energy production using different methodologies on the performance indicators of PV plants. The experimental data obtained in determining the annual production were predicted, and it was found to have an accuracy rate of 94.33% (Özcan et al., 2018). In another study, the annual OPTA was predicted as 33° by using EU JRC PVGIS solar data considering the worst-case scenario for off-grid PV plants in Şanlıurfa province. (Akgül et al., 2023). It was observed that a maximum hourly electric power can be obtained in the winter Bingöl province at OPTA of 45°. Although the PV surface temperature increased up to 35 °C in the outdoor environment, no significant change in electric power was observed (Işık & Çulun, 2023). Estimation of Annual TSR on the Tilted Surface at OPTA in two provinces of Turkiye. OPTA values where TSR values reach maximum were determined as 25º for Tekirdağ and 30º for Konya (Önler & Kayışoğlu, 2023). The impact of tilt angle on the performance of the PV plants for different row spacing was investigated. It was found that the PV plant with a 3 m surface row spacing and OPTA value of 21° is the most proper one in Konya province (Aksoy et al., 2023). In a study, an STS integrated with a type of Stirling motor-operated system on a moving mechanism was implemented in Bitlis province. The results showed that it is 32% more efficient than SFS (Cengiz et al. 2016). A two-axis STS was designed, which consists of a mechanical system, a DC engine, and an electronic control circuit in Afyonkarahisar province. It was observed that the designed STS produces 25% more energy than an SFS. (Özer et al. 2018). In another study, fuzzy logic and PID-based controllers were used to control STS. It was observed that the energy obtained from the developed STS increases by 21.2% compared to an SFS. The results showed that the fuzzy logic-based controller STS was found to be 2.4% more efficient compared to systems with an STS not using a fuzzy logic-based controller (Kiyak & Göl, 2016). An STS was developed employing different approaches including Traditional, PID controller, and solar orientation based on location and time. It was found that the geographical coordinate system was the most effective method from a technical standpoint (Özerdem & Shahin, 2014). A technique utilizing a microcontroller was devised and evaluated for locating the peak solar radiation across all azimuth and tilt angles throughout the day. Additionally, monitoring software was created (Bingöl et al. 2006). A one-axis STS with PID control using a servo motor was implemented and tested. Experimentally obtained results indicated that designed STS %15.11 more energy produced than the SFS (Aksungur & Koca, 2018).

Some studies are presented in Table 2.1 that have been carried out on the OPTA determination of SFSs in Türkiye based on theoretical calculation methods. More recently, further similar studies have been extended to the TSR efficiency of STSs and presented in Table 2.2. It is well understood in the literature that the OPTA is an important parameter for obtaining maximal TSR efficiency. In the literature, there exist some studies that focused on the calculation of the TSR components to find the OPTA. As indicated from the Tables, for some regions of Türkiye no research has been performed, also studies carried out for different regions have not yet been reached sufficiently. Therefore, the current study intends to contribute to literature by presenting more data on this subject for all provinces and regions of Türkiye for completeness and sufficiency. It is emphasized that although STS optimization efforts are constantly continuing, on increasing solar energy efficiency in the Turkish geography the studies are still quite insufficient, and it is very important to expand them to the whole of Turkey to provide energy sustainability and security. Because of the above-mentioned observations, it is believed that this study will provide a significant contribution just in the case of the installation of large-scale solar PV plants in regions or provinces of Türkiye.

Table 2.1. Studies on obtaining maximal TSR intensity by determining OPTAs of PV Surfaces in Türkiye

Author(s)	Year	Location(s)	Key Findings
Aksoy et al.	2023	Konya, Türkiye	The impact of OPTA on the performance of the PV plants for different row spacing was investigated. It was found that the PV plant with a 3 m surface row spacing and OPTA value of 21° is the most proper one in Konya province.
Önler & Kayışoğlu	2023	2 provinces of Türkiye	Estimation of Annual TSR on the Tilted Surface at OPTA in two provinces of Turkiye. OPTA values where TSR values reach maximum were determined as 25º for Tekirdağ and 30º for Konya.
Işık & Çulun	2023	Bingöl, Türkiye	It was observed that a maximum hourly electric power can be obtained in the winter Bingöl province at OPTA of 45°. Although the PV surface temperature increased up to 35 °C in the outdoor environment, no significant change in electric power was observed.
Gönül et al.	2022	6 provinces of Türkiye	The OPTA values of an SFS were found to be 29º in Tekirdağ, Artvin, İzmir, Kırşehir and Antalya. The OPTA values were found to be 28º for Şanlıurfa.
Yilmaz & Şimşek	2022	Adana, Türkiye	It was determined that the seasonal OPTA values were 51° in winter, 19° in spring, 4° in summer, 44° in autumn, and the annual OPTA is 29° for Adana province.
Şevik et al.	2021	Çorum, Türkiye	Identifying the OPTA for the PV surfaces in Çorum province and assessing the province's solar potential had been conducted. The annual OPTA of the province was discovered to be 34º, and the OPTAs of PV surfaces during the year were found between 1º and 67º.
Dal	2021	Kayseri, Türkiye	The impact of OPTA on yield in solar energy was investigated for monthly and seasonal performances of the PV surfaces. It was determined that the efficiency of the PV OPTAs was increased by 4.11% monthly, 3.25% seasonally, and 2.99% semi-annually. It was understood that positioning with monthly OPTA (30º) provides a great advantage.
Yiğit et al.	2021	5 provinces of Türkiye	OPTA values were calculated by using instantaneous GSR and daily GSR. It was found that there was a

			difference of 3º-5º. The OPTA values were found using instantaneous GSR values were 29º for Bursa, Izmir, Konya, and Elazığ. It was 28º for Şanlıurfa and 30º for Erzurum.
Kallioğlu et al.	2020	Antalya, Türkiye	PV surface OPTA values by month were determined for Antalya province. The capacity calculation was performed based on monthly, seasonal, and annual OPTA values and horizontal situations.
Yağlı & Koç	2020	Gaziantep, Türkiye	It was determined that the amount of energy produced at a 30º OPTA was not significant compared to a 31º OPTA. It was found that the PV surfaces were placed at an OPTA of 30º for efficiency.
Geliş et al.	2020	Iğdır, Türkiye	The effect of PV OPTA on the characteristics of the PV surfaces has been investigated between the variation of the PV surface OPTAs (0º-20º-40º). It was found that energy production was decreased with increasing distance and angle between the light source and the PV surface.
Kaygusuz	2020	Trabzon, Türkiye	Applying measured data, GSR data on horizontal and tilted surfaces in Trabzon province was calculated. The outcomes of GSR data were calculated as well as pertinent parameters.
Yolcan et al.	2020	Kütahya, Türkiye	PV OPTAs were determined for districts of Kütahya province to be between 32º and 33º. Maximal TSR intensity capturing on the annual tilted SFS was determined.
Arslan et al.	2019	Mersin, Türkiye	The measured daily TSR for Mersin was modeled using ANN, and common models for estimating daily TSR in the literature were investigated.
Akyürek et al.	2019	7 provinces of Türkiye	Determining the OPTA of PV surfaces to decrease carbon footprint was studied for the western Mediterranean region. The case study was performed in the western Mediterranean region. The OPTAs in all three provinces (Antalya, Burdur, and Isparta) range from 33º to 34º.
Kallioğlu et al.	2019	3 provinces of Türkiye	OPTAs of PV surface by months were determined for Antalya, Kayseri, and Trabzon provinces. Monthly, seasonal, and yearly OPTA measurements, as well as the horizontal situation, were calculated to perform the analysis in 3 mentioned provinces.
Yıldırım & Aktacir	2019	Şanlıurfa, Türkiye	The TSR values on the tilted PV surface were calculated by using the isotropic method to find the maximal potential of PV surfaces. The annual energy gain of PV surfaces directed to the south at optimum tilt (33º) is 11,5 % compared to the horizontal PV surface for the Şanlıurfa.
Çağlar	2018	4 provinces of Türkiye	Two alternative approaches were preferred to calculate the differences between the OPTAs for Istanbul, Ankara, Erzurum, and Adana provinces. The biggest difference between the OPTAs was 19% in January and the lowest difference was 4% in July. The difference between the two methods was 12% for the 4 provinces
Tırmıkçı & Yavuz	2018	Sakarya, Türkiye	OPTAs of the PV surfaces for various times in Sakarya province were determined. The correlation between the OPTA and the output of a PV surface is modeled numerically, the results are compared. The yearly OPTA of a PV surface is determined to be 32º.
Bakırcı	2018	Gaziantep, Türkiye	OPTAs for PV surfaces were determined, and model equations to provide OPTAs were developed for the

& Kaltakkıran			Gaziantep. OPTAs were found in Jan 53°, Feb 45°, Mar 32°, Apr 16°, May 3°, in Jun 0°, in Jul 0°, in Aug 14°, in Sep 31°, in Oct 46°, in Nov 56°, and in Dec 55°.
Kallioğlu et al.	2018	Muğla, Türkiye	Monthly OPTAs for the Southern Aegean (Muğla) in Türkiye were determined, and three different correlations were created. The seasonal OPTAs in Muğla were 56° for winter, 21° for spring, 5° for summer, and 47° for fall. The annual surface OPTA was found 32°.
Yıldırım et al.	2018	4 provinces of Türkiye	An optimized model based on the ANN method and Angstrom-Prescott model for the estimation of daily TSR was investigated in the Eastern Mediterranean Region to ensure the most feasible solution for estimating GSR for the region.
Bakırcı	2017	All of Türkiye	The f-chart solar energy utilization method was preferred to estimate the OPTA for the PV surface, and annual and seasonal results were analyzed. Comparing the PV surfaces of the OPTAs and horizontal, the increment in the annual fractions was found 21% for all of Türkiye.
Bilgili & Dağtekin	2017	Adana, Türkiye	The energy produced by PV surfaces a”t different tilts during different periods in a year was calculated. Energy yields were compared monthly at various tilts. The influence of the OPTA (31°) on the quantity of energy was determined as about % 7-10 energy loss in the first 4 and last 4 months.
Kallioğlu et al.	2017	Gaziantep, Türkiye	The OPTA of PV surfaces was predicted monthly and annually in Gaziantep province using the horizontal GSR values. PV OPTAs were determined as 55°, 44°, 35°, 19°, 4°, 0°, 0°, 14°, 30°, 47°, 55° and 57°. The annual OPTA is determined to be 30°. It was stated the OPTAs of PV surfaces must be set monthly or seasonally.
Ayaz et al.	2017	Burdur, Türkiye	The finding of OPTA considering the surrounding variables, and seasonal and annual TSR intensity on a PV surface was studied for Burdur province. The tilt angle at the obtained maximum GSR was considered the OPTA for PV surfaces.
Sarkın & Dindar	2017	Adana, Türkiye	GSR capacities were compared daily, monthly, and yearly for Istanbul and Adana provinces. It was found that less solar energy is produced annually in Istanbul province.
Yanıktepe et al.	2017	Osmaniye, Türkiye	Two different empirical models were analyzed for the GSR on a horizontal surface, and a new empirical model was developed for Osmaniye to estimate GSR capacity.
Kulcu et al.	2017	Mersin, Türkiye	Calculation methods for the GSR coming to the earth were developed. The methods for the prediction of GSR were evaluated using measured GSR data for Mersin.
Özbay et al.	2017	Bilecik, Türkiye	Monthly, seasonal, and yearly OPTA was monitored by Raspberry microcomputer for Bilecik province. OPTA value is the maximal energy generated from the PV surfaces that were investigated. According to the results, the OPTA of PV surfaces should be 20° or 40°, the power difference between the best and the worst angle was 0.9%.

Arslanoğlu	**2016**	**Bursa, Türkiye**	The OPTA to collect the maximal TSR on the PV surfaces was investigated in Bursa province using a theoretical model. For particular periods, GSR on PV surfaces at the OPTA was calculated, and the annual OPTA was obtained to be 31°. It was observed that OPTAs in spring should be 19.6°, in summer 5.6°, in autumn 44.3°, and in winter 55°.
Arslan & Bayhan	2016	Mersin, Türkiye	The solar energy potential of Mersin province was investigated by using meteorological data. A simple method to estimate GSR intensity was developed and compared with the other methods in the literature. Daily and monthly GSR data were predicted with 14% and 9% absolute mean percentage error, respectively.
Yılmaz et al.	2016	Batman, Türkiye	The OPTA values for designing a PV plant in Batman province were investigated. The yearly OPTA was predicted to be 33°, in summer is 4°, and in winter is 61°.
Şenkal	2016	Adana, Türkiye	ANN method was applied to predict GSR distribution in given atmospheric parameters in Adana province. Levenberg-Marquardt learning algorithm and logistic sigmoid transfer function were used in the ANN network.
Koçer et al.	2016	Ankara, Türkiye	OPTA values for Ankara province and its districts were calculated and compared to those found in other research. The annual OPTA was calculated as 34°.
Bawazir et al.	2016	İzmir, Türkiye	To determine the OPTA (33°), empirical formulas were established, and solar TSR efficiency was analyzed on PV surfaces by using software in İzmir province. The findings were collected per month, season, and annually, and compared between a representative day of each month.
Karafil et al.	2015	Bilecik, Türkiye	The OPTA of PV surfaces was predicted (40°) based on solar angles in Bilecik. The conclusions of the analysis were compared to those of experimental research. The findings showed that the OPTA of PV surfaces should be 10° during the summer for high efficiency.
Yanıktepe & Genç	2015	Osmaniye, Türkiye	Horizontal GSR models were investigated, and a new Horizontal GSR model for Osmaniye province was developed. Instantaneous GSR values on the horizontal surface were calculated.
Gebremed	2014	9 provinces of Türkiye	It was discovered that by simply adjusting PV surfaces weekly, up to 6.9% more TSR may be gathered. OPTAs for the cities located in Türkiye's different regions were found to be between 13° to 18° less than the latitude of the areas.
Kırbaş et al.	2013	Burdur, Türkiye	An evaluation of the sunbathing rate and the solar energy potential in Burdur province was made. The data obtained were compared with the GSR values of Türkiye.
Bakırcı	2012	All of Türkiye	The OPTA values were optimized using data from GSR measurements. The yearly OPTAs for a south-facing solar collector were 31°, 33°, 33°, 34°, 33°, 33, and 33° in Adana, Ankara, Diyarbakir, Erzurum, Istanbul, Izmir, Samsun, and Trabzon, respectively.
Kaçan & Ulgen	2012	İzmir, Türkiye	The effect of PV surface tilt and orientation on solar energy utilization was investigated for Izmir. The tilt angles were calculated between 0° and 61° based on the period of the year. The OPTA value was obtained as 30° yearly for PV surfaces.
Bulut et al.	2009	6 provinces of Türkiye	GSR intensity for six provinces of the Mediterranean region was generated from the daily GSR data measured using the Finkelstein-Schafer statistical method, the obtained data was comparatively analyzed between provinces, and results are assessed.
Ertekin et al.	2008	Whole of Türkiye	Depending on monthly TSR on a horizontal surface throughout Türkiye, OPTA values for PV surfaces were predicted. The PV surfaces were seen to be set by high OPTAs in the autumn and winter seasons, and low OPTAs in the summer season. Annual OPTA values for SFS ranged from 16° to 29° over Türkiye.

Günerhan & Hepbaşlı	2007	İzmir, Türkiye	Using experimental data collected in Izmir, the OPTA of PV surfaces for building implementations was investigated. The OPTA was found (36º) by searching for the maximal TSR on the tilted PV surfaces for a particular day or a specific period.
Balli et al.	2007	Antalya, Türkiye	Empirical models to estimate the monthly daily horizontal GSR on a horizontal surface were developed for Antalya. Statistical methods were utilized to evaluate the accuracy of the GSR estimations.
Ülgen	2007	İzmir, Türkiye	In Izmir, a numerical method was utilized to calculate TSR intensity on a tilted PV surface and estimate the OPTA. It was observed the OPTA varies between 0º and 61º over the year. In winter the tilt should be 55º, in spring 18º, in summer 4º, and in autumn 43º. The annual value was discovered to be 30º.
Çelik	2006	Ankara, Türkiye	The provided data with the distribution of clear and cloudy days was used to develop and analyze distributional GSR characteristics. Yearly and monthly OPTAs of PV surfaces were found for Ankara. The annual OPTA was 39.40º, the smallest OPTA was 7º in June, and the largest OPTA was 65º in November.
Bakırcı	2006	Erzurum, Türkiye	Daily TSR values on 0-90° tilted PV surfaces were predicted for Erzurum province. OPTAs for months were determined 66º, 58º, 44º, 25º, 8º, 0º, 3º, 18º, 37º, 54º, 64º and 68º using the Hottel calculation method. The annual OPTA was found to be 37º.
Oğulata & Oğulata	2002	Adana, Türkiye	Measured daily GSR data for Adana province was used to estimate horizontal GSR. Hourly global, diffuse, and direct solar radiations on a horizontal surface were determined in Adana province.

Table 2.2 Studies on design, development, and TSR efficiency of STSs for Türkiye.

Authors	Year	Location(s)	Key Findings
Akgül et al.	2024	8 provinces of Türkiye	The annual OPTA range was 29°-33°, and the SFS gain ranges from 9% to 12% compared to horizontal PV surfaces in the Mediterranean region of Türkiye. It was also found that a one-axis STS harvests between 28% and 33% of daily TSR, whereas a two-axis STS harvests between 32% and 37% of daily TSR when compared to the SFS.
Akgül et al.	2024	Whole of Türkiye	A transposition model was proposed to estimate the daily TSR intensity on optimally tilted and tracked PV surfaces in 81 provinces. Annual OPTA values were found between 28° and 36°. An OPTA map was created, and STS gains were tabulated for all provinces in Türkiye.
Akgül et al.	2022	Şanlıurfa, Türkiye	The annual OPTA for Şanlıurfa was calculated to be 29º-30º. It was seen that one-axis STS harvests about 31% higher TSR intensity than SFS. It was also seen that two-axis STS harvest about 35% higher TSR intensity than SFS systems.
Akgül et al.	2022	Antalya, Türkiye	The annual OPTA is found to be between 28° and 30°. It was found that there was a ±1° or ±2° difference between the districts, and SFSs harvested between 8% and 10% greater TSR compared to horizontal surfaces. Districts see higher TSR harvesting rates from one-axis STS (28% to 33%) and two-axis STS (32% to 37%) compared to SFSs.
Beyazıt et al.	2020	Şanlıurfa, Türkiye	Data from GSR measurement devices on the STS was used to calculate the TSR gain of the Şanlıurfa province. The findings were compared to the

			measurement data using 15 different diffuse radiation calculation methods found in the literature.
Aydemir & Toslak	2019	Kırşehir, Türkiye	TSR values collected by the computer-controlled biaxial STS were compared to the TSR values collected from the SFS in the Kırşehir province. It was observed that the one-axis STS was highly efficient than the SFS, 12% of the daily yield was collected.
Aksungur & Koca	2018	Malatya, Türkiye	An one-axis STS with PID control using a servo motor was implemented and tested. Experimentally obtained results indicated that designed STS %15.11 more energy produced than the SFS.
Er & Balcı	2018	İstanbul, Türkiye	A dual-axis STS was built without the need for sensors to enhance energy output. The resulting design, which eliminates the need for sensors in the STS, was innovative.
Özer et al.	2018	Afyon, Türkiye	A two-axis STS was designed, which consists of a mechanical system, a DC engine, and an electronic control circuit in Afyonkarahisar province. It was observed that the designed STS produces 25% more energy than an SFS.
Yılmaz & Kentli	2017	Diyarbakır, Türkiye	Improving STS efficiency and electrical energy production methods of two-axis STSs were examined for Diyarbakır. SFS and two-axis STS were compared to each other by performing annual measurements. It was computed yearly as a higher TSR intensity of 31%, 70% in winter, and 11% in summer based on the effectiveness of two-axis STS.
Filik & Filik	2017	Eskişehir, Türkiye	The STS's performance was investigated in Eskişehir province. The STS was found to provide around 33% more TSR intensity than the SFS. Instantaneous real solar power productions were used to figure out the ratio of sunny and cloudy days.
Yılmaz	2017	Batman, Türkiye	A two-axis STS was improved for STS efficiency. The energy consumption of the designed STS was too low to be taken into consideration (total daily consumption was less than 3Wh).
Toylan	2017	Kırklareli, Türkiye	Experimental results showed that the STS which uses a fuzzy logic controller increases the efficiency of energy production by up to 35% from the PV surface in Kırklareli.
Cengiz et al.	2016	Bitlis, Türkiye	An STS integrated with a type of Stirling motor-operated system on a moving mechanism was implemented in Bitlis. The results showed that it is 32% more efficient than a SFS.
Gündoğdu et al.	2016	Düzce, Türkiye	A two-axis economical STS was designed. The STS was enabled 8.89% more efficiently on average, even if the direction of the light changed, compared to the SFS.
Kıyak & Göl	2016	Eskişehir, Türkiye	Fuzzy logic and PID-based controllers were used to control STS. It was observed that the energy obtained from the developed STS increases by 21.2% compared to an SFS. The results showed that the fuzzy logic-based controller STS was found to be 2.4% more efficient compared to systems with an STS not using a fuzzy logic-based controller.
Öztürk et al.	2016	Düzce, Türkiye	For Düzce province, a tentative efficiency comparison of a two-axis STS with an SFS is carried out. It was found that the STS harvested 35% higher

			energy compared to the SFS, a SFS was amortized itself in 16 years.
Üçgül & Şenol	2016	Isparta, Türkiye	A simple STS was used to collect data related to the TSR capturing on the PV surfaces for Isparta province. In comparison to an SFS, the daily TSR intensity on the PV surfaces of the STS was collected by more than 28%.
Yılmaz & Kentli	2015	Diyarbakır, Türkiye	Over a year, it was discovered that the two-axis STS outperformed the SFS by 31%. During the winter months, this efficiency was up to 70%, while during the summer months, it was up to 11% for Diyarbakır province.
Kentli & Yılmaz	2015	Batman, Türkiye	A two-axis STS is designed based on a derived numerical model with LDR and its mechanical components. Designed STS is compared to SFS and it is observed that 30 % more PV energy was produced annually in Batman province.
Akkılıç et al.	2015	9 provinces of Türkiye	The solar energy potential and the methods of using this potential to produce energy were analyzed for 9 provinces. It was seen the two-axis STS with %30 more efficiencies observed than the SFS for the Southeastern Anatolia provinces.
Tırmıkcı & Yavuz	2015	Sakarya, Türkiye	One-axis and two-axis STS devices were designed. Results showed that a two-axis axis TSR was the most efficient one of all with 40% more efficiency than SFSs whereas a one-axis STS has 20%.
Özerdem & Shahin	2014	Mersin, Türkiye	An STS was developed employing different approaches including Traditional, PID controller, and solar orientation based on location and time. It was found that the geographical coordinate system was the most effective method from a technical standpoint.
Şenpınar & Cebeci	2012	All of Türkiye	The performance of the SFS and two-axis STS was compared in terms of the received TSR intensity on the PV surfaces. It was observed the daily TSR of the STS was 13%-15% more than the SFS for the whole of Türkiye.
Eke & Şentürk	2012	Muğla, Türkiye	Measurements of the efficiency of STSs were carried out. The discrepancy between the simulated and calculated values was determined to be less than 5%, and when compared to the SFS, the two-axis STS produced 30% more TSR intensity for Muğla province.
Kıvrak et al.	2012	Denizli, Türkiye	Two-axis STS was designed, and its performance was analyzed for the climatic condition of Denizli province. When comparing the STS to the SFS, it was discovered that the STS captured 64% more TSR intensity.
Eke et al.	2010	Muğla, Türkiye	The performance measurements of a one-axis STS were performed. It was calculated that 33% more PV electricity was observed in the two-axis STS compared to the SFS in Muğla province.
Rustemli et al.	2010	Van, Türkiye	The STS was developed, and an experimental setup was carried out in Van province. When compared to an SFS, it was discovered that the STS gathered 29% more TSR intensity for Van province.
Eke et al	2011	Muğla, Türkiye	The biggest two-axis STS in Türkiye with one electronic control and one photo sensor was described and installed in Mugla province. It was

			seen that the dual-axis STS produced 33% more energy compared to the SFS.
Sungur	2009	All of Türkiye	Measurements of the sun STS's performance was performed for one year in the whole of Türkiye. When comparing the two-axis STS to the SFS, it was discovered that the two-axis STS captured 42% more TSR intensity.
Demirtaş	2009	Ankara, Türkiye	A PLC-controlled two-axis STS was designed and implemented. Application results showed that the energy production of STS was more efficient than SFS up to 34%.
Bingöl et al.	2006	Ankara, Türkiye	A technique utilizing a microcontroller was devised and evaluated for locating the peak solar radiation across all azimuth and tilt angles throughout the day. Additionally, monitoring software was created.
Kaçıra et al.	2004	Şanlıurfa, Türkiye	A numerical method was used to determine the TSR intensity and OPTAs for PV surfaces in Şanlıurfa province. It was found that the TSR capturing was increased by 34% for the STS than the SFS at a 14° tilt angle.

3. MATERIALS AND METHODS

OPTA and TSR computation can be related to various empirical optimization techniques. Applying a variety of transposition models is an essential step before the implementation of various solar PV plants. A variety of transposition models can be employed to estimate reliable and accurate TSR distribution in the sky. The horizontal GSR data of the regions can be computationally exploited in these models to calculate the intensity of TSR on tilted and tracked PV surfaces. The proposed transposition models provide more advanced approaches that include factors such as atmospheric scattering, the impact of air pollution, climatic conditions, as well as direct sunlight. So, this section is devoted to the introduction of the transposition models with solar geometry parameters and other components. In this section, the adopted methodologies, such as the theoretical approaches of the selected transposition models and the utilized solar data collections are described, Theoretical background, basic concepts, algorithm descriptions, solar geometry, and solar radiation parameters are presented. Numerical modeling of solar PV plants, percentage gains of TSR intensity, and levelized cost of energy (LCOE) calculations are presented.

3.1. Solar Geometry, Radiation Parameters, and Corresponding Cartesian Coordinates

OPTA and TSR computation methods are based on solar geometry and solar radiation parameters to maximize the solar radiation collected by a tilted surface. The graphical drawing of the geometric relationships that fall within the scope of solar geometry and are used in case, application, and experimental studies in this thesis is as follows: Solar radiation parameters and the corresponding cartesian coordinates based on solar geometry for facing south SFS are shown in Figure 3.1. Solar geometry for STS is given in Figure 3.2. Representations of south-axis-oriented SFS, one-axis STS, and two-axis STS are illustrated in Fig. 3.2 a), Fig. 3.2 b), and Fig. 3.2 c), respectively. Additionally, Figure 3.3 shows the schematic representation of the solar incidence angle on a tilted surface.

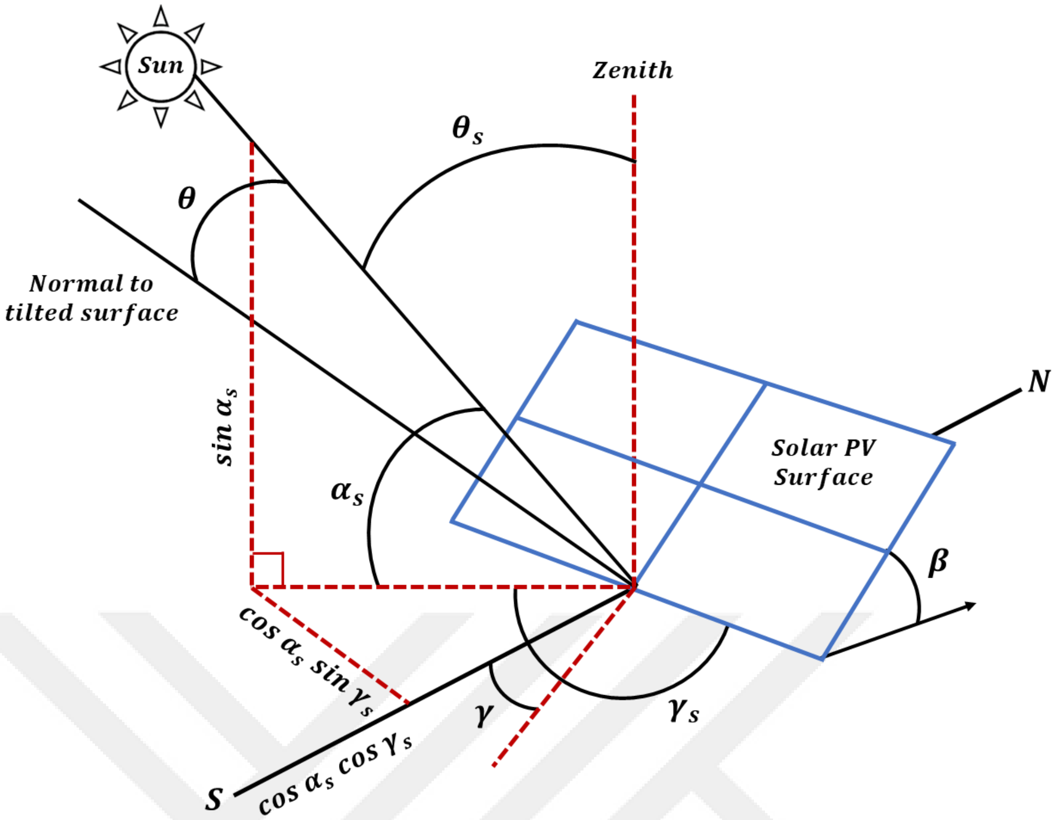

Figure 3.1. Solar radiation parameters and corresponding cartesian coordinates.

where θ is the incidence angle of the beam radiation on the PV surface [º], θ_s is the solar incidence angle of beam radiation, [°] α_s is the altitude of the sun [º], Y is the solar surface azimuth [º], γ_s is the solar azimuth [º], and β is the solar PV surface tilt [º].

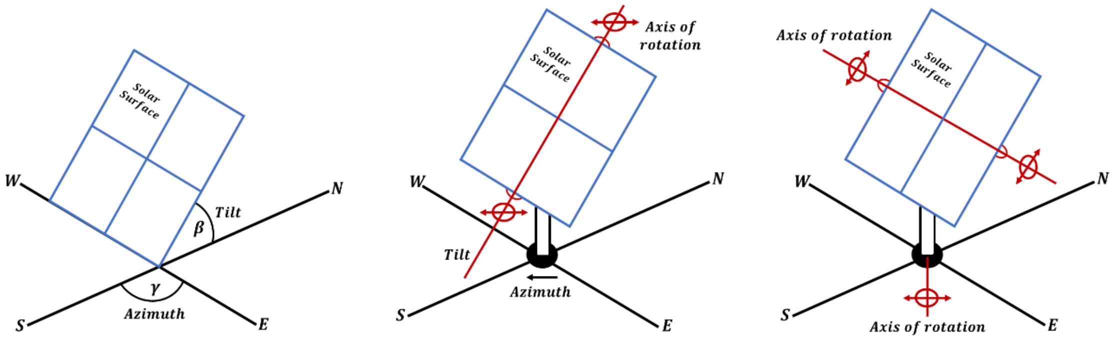

a) b) c)

Figure 3.2. a) Solar geometry for a SFS with south axis-oriented. b) Solar geometry for a one-axis STS. c) Solar geometry for a two-axis STS.

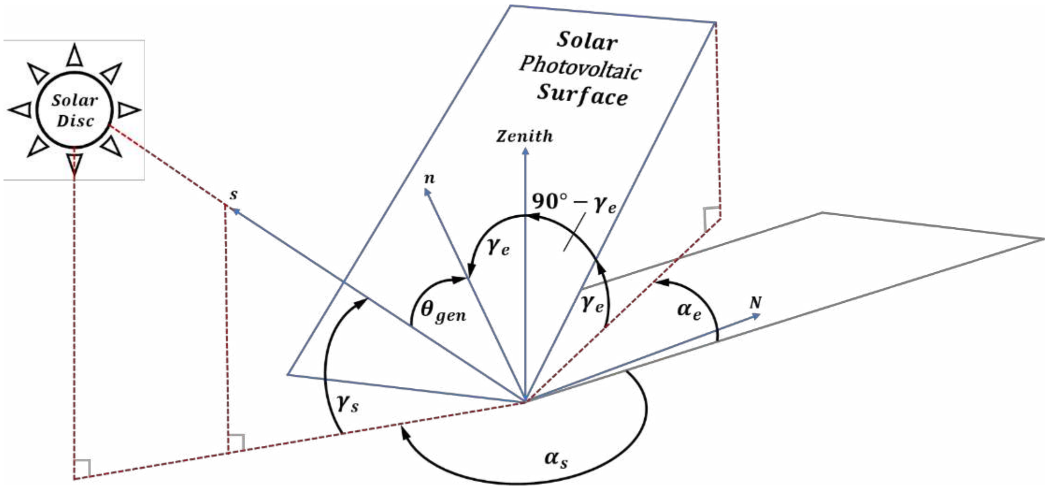

Figure 3.3. The schematic representation of the angle of solar incidence on a tilted surface.

where θ is the incidence angle of the radiation on the PV surfaces [º], α_s is the orientation of the sun [º], γ_s is the elevation of the sun [º], α_e is the orientation of the PV surface [º], and γ_e is the elevation of the PV surface [º].

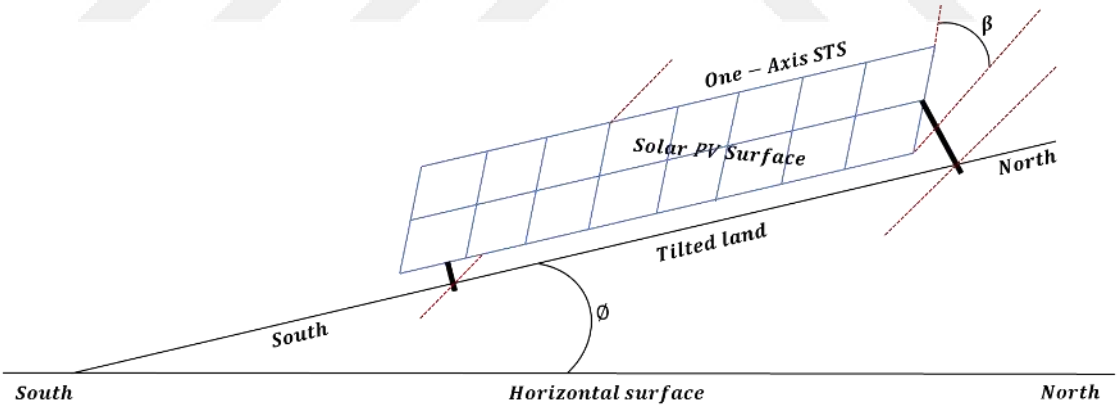

Figure 3.4. Schematic representation of one-axis N-S oriented horizontal STS.

where β is the solar PV surface tilt [º], and $\emptyset$ is the latitude of the geolocation [º].

3.2. Data Collection of Total Solar Radiation (TSR)

Türkiye is under the continental climatic region classified as 3B-Warm-Dry according to ASHRAE Thermal Climate Zones (ANSI/ASHRAE, 2021; Alawadhi &

Phelan, 2022) and experiences year-round high levels of GSR. To estimate TSR collected on tilted and tracked PV surfaces, first of all, GSR on a horizontal plane which can be obtained from meteorological and satellite stations then the collective data of the horizontal surface is transformed to calculate the TSR collected by a PV surface. Since the GSR distribution varies according to the geolocation of the world, the horizontal GSR is the most important parameter to optimize TSR intensities and OPTA values. Therefore, the TSR values must be predicted at the specified location for the correct design of solar PV surfaces. In this thesis, as depicted in Section 4, map-based and geo-referenced climatic horizontal GSR datasets are provided from the National Aeronautics and Space Administration, Surface Meteorology and Solar Energy (NASA-SSE), Photovoltaic Geographical Information System of the European Commission (EU JRC PVGIS), Meteotest-METEONORM for the optimization of OPTA values and TSR on PV surfaces. Types of the GSR data utilized in the studies of this thesis are detailed in Section 4.

3.3. Introduction to Transposition Models

Transposition is the calculation of the incident TSR intensity on a tilted PV surface from the horizontal GSR data. Transposition models provide a strong capability to estimate TSR intensity on PV surfaces for the specified location (Sawyer et al., 2009; Lalita et al., 2013; Sharma et al., 2014). Two categories of transposition models exist anisotropic and isotropic models in general. Even though the isotropic models provide simple approaches, anisotropic models provide more advanced approaches that include factors such as atmospheric scattering, the impact of air pollution, climatic conditions, and direct sunlight. So, this section applies the proposed transposition models and other components. In isotropic models (Liu & Jordan, 1960; Liu & Jordan, 1961), the beam and diffuse fractions are the two components of GSR that are present on a tilted surface. The presumption is the diffuse radiation over the sky dome is only isotropic, whereas circumsolar and horizon brightening are taken as zero. In other words, isotropic sky radiance models present a reduction in complexity to TSR calculation by presuming sky GSR is isotropic. Over the years, these transposition models have served as the foundation for many investigations (Liu & Jordan, 1963). Nonetheless, recently conducted research indicates that anisotropic models yield significantly more precise estimations than isotropic models (Muneer, 2003). Thus, in this study, the most preferred anisotropic transposition models are utilized to calculate TSR intensity on tilted and tracked surfaces. The proposed modeling procedures utilized in this thesis can be broken down into two stages. The first stage is the modeling of how GSR is distributed, and the second stage is the modeling of the TSR on the tilted PV surface. The computation of GSR distribution is based on the Klein (1981), Erbs (1982), and Duffie (2006) models by applying an hourly timestep. The computation of TSR intensity on a tilted PV surface is based on Hay-Davies (1978), Klucher (1979), Reindl (1990), Perez (1987), and HDKR (2006), anisotropic models by applying an hourly timestep. The TSR intensity on a tilted surface for the desired region is predicted by utilizing the equations of the transposition models as presented in Section 3.4.

3.4. Total solar Radiation (TSR) Modeling on a Horizontal Surface

The solar declination angle (δ) is the angular distance of the sun's rays north (or south) of the equator, with the north declination designated as positive. So, the declination angle δ results from the 23.45º angle that because of the earth makes with its axis and orbital plane. It's the angle that the sun's rays make with the equatorial plane or the angle that the sun's rays make with the earth according to the months and seasons. The declination angle is mathematically modeled by Cooper (1969) and given in Equation (1).

$$\delta = 23.45 \sin\left(2\pi \frac{284+n}{365}\right) \quad (1)$$

where δ is the declination angle [º], and n is the Julian day.

The recommended "average Julian days" of months having the same daily GSR (beam & diffuse) as the monthly average on which extraterrestrial GSR equals the monthly mean value (Klein & Theilacker, 1981; Duffie & Beckman, 2006) are displayed in Table 3.1.

Table 3.1. Recommended "average Julian days" and declination angles for Months of a year.

MONTH	N FOR KTH DAY OF MONTH	FOR AVERAGE DAY OF MONTH		
		Date	**n**	[δ]
1	k	17	17	-20.9
2	31 + k	16	47	-13.0
3	59 + k	16	75	-2.4
4	90 + k	15	105	9.4
5	120 + k	15	135	18.8
6	151 + k	11	162	23.1
7	181 + k	17	198	21.2
8	212 + k	16	228	13.5
9	243 + k	15	258	2.2
10	273 + k	15	288	-9.6
11	304 + k	14	318	-18.9
12	334 + k	10	334.00	-23.00

Source: (Klein & Theilacker, 1981; Duffie & Beckman, 2013).

Solar time is a calculation of the passage of time based on the position of the sun in the sky. The time when the sun reaches its highest point in the sky is solar noon. The solar hour angle is expressed in the angular measurement of the sun east or west of the local meridian, in which mornings are negative and afternoons are positive. At solar noon, the solar hour angle becomes zero, and it varies by 15 degrees per hour in the afternoons. The cosine of the zenith angle is 0° when the sun is above the horizon during sunrise and sunset. The sunset hour angle, (ω_s) is the angle between the longitude of the sun's rays and the longitude of the place under consideration. It can be calculated concerning latitude and declination angles for the horizontal plane by setting the cosine of the zenith angle to 0°. The sunshine hour angle can be calculated concerning latitude and declination angles. The position of the sun in the sky is given by Equation (2) (Duffie & Backman, 2006; Solanki & Sangani, 2008).

$$cos\omega_s = cos^{-1}(-tan\emptyset\ tan\delta) \quad (2)$$

where $cos\omega_s$ is the sunshine hour angle [º].

GSR outside of the earth's atmosphere is expressed as extraterrestrial GSR. So, the daily extraterrestrial GSR on a horizontal surface (I_0) is the GSR intensity of the sun at the top of the Earth's atmosphere. The empirical connection expressed in Equation (3) (Iqbal, 1980) can be utilized to obtain the monthly average daily extraterrestrial GSR on a horizontal surface.

$$I_0 = G_{sc}\left(1 + 0.033\cos\frac{360n}{365}\right)(cos\emptyset\ cos\delta\ sin\omega_s + sin\emptyset\ sin\delta) \quad (3)$$

where I_0 is the daily extraterrestrial GSR on a horizontal surface $[\mathrm{W/m^2}]$, G_{sc} is the solar constant $[1{,}367\mathrm{W/m^2}]$, $\emptyset$ is the latitude angle [º].

The relationship between TSR on the earth's surface and extraterrestrial GSR gives a measure of atmospheric transparency and is called the clearness index. The clearness index is not only related to the physical path that GSR travels through the atmosphere but also to the gas composition and cloudiness of the atmosphere. It is used to accurately characterize the solar climate of a region. Therefore, due to the atmosphere, GSR is subject to scattering and absorption effects, so the daily clearness index (K_T) accounting for such effects can be calculated by Equation 3. This index is the ratio of daily GSR (I_h) to daily extraterrestrial GSR (I_0) on a horizontal surface. The clearness index is mainly employed to precisely describe a region's solar climate. Specifically, the index varies between 0.3 and 0.8 from the most overcast climates to the sunniest regions. So, the daily clearness index can be computed by applying Equation (3).

$$K_T = \frac{I_h}{I_0} \quad (4)$$

where K_T is the daily clearness index $[\mathrm{coeff.}]$, I_h is the daily incident GSR on a horizontal surface $[\mathrm{W/m^2}]$, and I_0 is the daily extraterrestrial GSR on a horizontal surface $[\mathrm{W/m^2}]$.

The beam and diffuse components are not only significant to calculate the TSR on the tilted surfaces but also essential to measure the performance of PV surfaces. So, the proposed algorithm requires the hourly GSR values of the beam and diffuse components over the GSR of an average Julian day. Daily diffuse radiation is obtained from daily GSR by using the correlation expressions given in Equations (5) and (6) (Erbs et al., 1982; Duffie & Beckman, 2006). Equation (5) is applied if the average day's sunshine hour angle is less than 81.4°; if not, Equation (6) is applied.

$$\frac{I_d}{I_h} = 1.391 - 3.560\bar{K}_T + 4.189\bar{K}_T^2 - 2.137\bar{K}_T^3 \quad (5)$$

$$\frac{I_d}{I_h} = 1.311 - 3.022\bar{K}_T + 3.427\bar{K}_T^2 - 1.821\bar{K}_T^3 \quad (6)$$

where $\bar{I}_d$ is the daily diffuse radiation $[W/m^2]$.

Equation (4) ratio is utilized to determine the daily clearness index. After that, to perform the ratio of hourly to daily GSR (R_t), the daily GSR is broken down into hourly values. Therefore, the hourly values of the daily GSR are decomposed by using Equation (7) (Collares-Pereira & Rabl, 1979).

$$R_t = \frac{\pi}{24}(a + b\ cos\omega)\frac{cos\omega - cos\,\omega_s}{sin\,\omega_s - \omega_s\ cos\omega_s} \quad (7)$$

$$a = 0.409 + 0.5016\sin(\omega_s - 60) \quad (8)$$

$$b = 0.6609 - 0.4767\sin(\omega_s - 60) \quad (9)$$

where R_t is the ratio of hourly total to daily GSR $[W/m^2]$.

The hourly to daily total ratio of diffuse radiation (R_d) is obtained by using Equation (10) (Liu & Jordan, 1960; Duffie & Beckman, 2006).

$$R_d = \frac{\pi}{24} \frac{cos\omega - cos\omega_s}{sin\omega_s - \omega_s\, cos\omega_s} \tag{10}$$

where R_d is the hourly to daily total ratio of diffuse radiation $[W/m^2]$.

For each hour of the "average Julian day", horizontal GSR (I_h), and its components diffuse radiation (I_d) and beam radiation (I_b) is calculated by Equations (11), (12), and (13).

$$I_h = R_t \bar{I}_h \tag{11}$$

$$I_d = R_d \bar{I}_d \tag{12}$$

$$I_b = I_h - I_d \tag{13}$$

where I_h is the hourly horizontal GSR of the "average Julian day" $[\mathrm{W/m^2}]$, I_d is the total horizontal diffuse radiation $[\mathrm{W/m^2}]$, and I_b is total horizontal beam radiation $[\mathrm{W/m^2}]$.

3.5. TSR (TSR) Modeling on a Tilted Surface

Transposition models are utilized to compute the tilted TSR intensity from horizontal GSR. The TSR intensity on a tilted PV surface consists of beam-tilted and diffuse-tilted TSR components. The atmospheric transmittance, which is made up of cloud cover, particulate matter concentration, and water vapor, determines the beam radiation tilt factor. So, the beam radiation tilt factor (R_b) is a function of atmospheric permeability based on solar climatic conditions the cloudiness index, water vapor, and atmospheric particle density. It is the ratio of daily beam radiation on a tilted surface to a horizontal surface. The value of the tilt factor is computed by using Equation (14) for tilted PV surfaces where the equation's left side represents the general form, while the right side represents south-facing surfaces.

$$R_b = \frac{cos\theta}{cos\theta_z} = \frac{sin\delta \sin(\emptyset - \beta) + cos\delta \cos(\emptyset - \beta)}{sin\delta sin\emptyset + cos\delta cos\emptyset cos\omega_s} \tag{14}$$

where R_b is the ratio of beam radiation on the tilted surface [W/m^2], θ is the beam incidence angle on the surface, θ_z is the solar zenith angle, β is the slope of the tilted surface [°].

Similarly, the value of ground-reflected radiation (R_r) is calculated by using Equation (15) (Alsadi & Nassar, 2007).

$$R_r = \rho_g \frac{1-cos\beta}{2} \quad (15)$$

where R_r is the ratio of ground-reflected radiation, and ρ_g is the ground reflectivity-albedo, it is usually treated with a constant value of 0.2.

The general transposition form of TSR intensity on a tilted surface (I_T) from a horizontal surface is expressed in Equation 16 (Nassar, 2006).

$$I_T = I_b R_b + I_d R_d + I_h R_r \quad (16)$$

where I_T is the TSR on a tilted surface in the general form [kWh/m^2].

3.5.1. Hay-Davies transposition model

The diffuse radiation is separated into isotropic and circumsolar components by the Hay-Davies (1978) model. According to the Hay-Davies (HD) model, the diffuse component that reaches from the sun is circumsolar, whereas the diffuse component that reaches through the remaining portion of the sky dome is isotropic. An anisotropy index is used to determine the weights of these components. Therefore, the TSR intensity on a tilted solar PV surface (I_T) is computed by Equation (17).

$$I_T = (I_b + I_d A_i) R_b + I_d (1 - A_i) \left(\frac{1+cos\beta}{2}\right) + I\rho_g \left(\frac{1-cos\beta}{2}\right) \quad (17)$$

$$A_i = \frac{I_b}{I_0} \quad (18)$$

where I_T is the daily TSR intensity, [kWh/m^2], and A_i is the anisotropy index which represents the transmittance of beam radiation via the atmosphere [coeff.].

3.5.2. Klucher transposition model

Klucher (1979) indicated that the Liu-Jordan (1961) isotropic model works better on cloudy skies whereas the Temps-Coulson model works better on clear skies conditions. Therefore, it is developed an anisotropic model by taking into account the horizon brightness and the circumsolar brightness components. A modulating function is integrated into the model by Klucher to demonstrate the sky varies from clear to cloudy conditions by multiplying the term of horizon brightening. The Klucher model for TSR (I_T) is presented in Equation (19).

$$I_T = I_b R_b + I_d \left(\frac{1+cos\beta}{2}\right)\left[1 + Fsin^3\left(\frac{\beta}{2}\right)\right][1 + Fcos^2\theta sin^3\theta_z] + I\rho_g \left(\frac{1-cos\beta}{2}\right)\Big] \quad (19)$$

$$F = 1 - \left(\frac{I_d}{I}\right)^2 \quad (20)$$

where F is the modulating function [coeff.]. Under cloudy sky conditions, F goes zero and the model reduces to the Liu-Jordan model.

3.5.3. Reindl transposition model

In the Reindl Model (1990), the horizon brightening component is applied to the isotropic component for modulation. Beam and reflected fractions of GSR are considered to be the same as in the Liu-Jordan (1961) model. The anisotropy index is defined as presented in the Hay-Davies model. The model for TSR (I_T) is presented in Equation 21.

$$I_T = (I_b + I_d A_i)R_b + I\rho_g \left(\frac{1-cos\beta}{2}\right) + I_d \left[(1 - A_i)\left(\frac{1+cos\beta}{2}\right)\left[1 + Fsin^3\left(\frac{\beta}{2}\right)\right] + A_i I_b\right] \quad (21)$$

$$F = \sqrt{\frac{I_b}{I}} \quad (22)$$

where under cloudy sky conditions, the F and the A_i go to zero, and the model converts to the Liu-Jordan model. Under partly cloudy sky conditions, both the F and A_i have non-zero values.

3.5.4. HDKR transposition model

HDKR's (2006) model is a combination of Hay, Davies, Klucher, and Reindl's models presented by Duffie and Beckman (2006). In this model, it is assumed that the diffuse radiation consists of three components. An isotropic component that is uniformly distributed over the sky, a circumsolar brightening component that spreads from the sun's direction, and a horizon brightening component that spreads from the horizon. The TSR intensity on a tilted surface (I_T) is computed via Equation (23).

$$I_T = (I_b + I_d A_i)R_b + I_d(1 - A_i)\left(\frac{1+cos\beta}{2}\right)\left[1 + Fsin^3\left(\frac{\beta}{2}\right)\right] + I\rho_g\left(\frac{1-cos\beta}{2}\right) \quad (23)$$

where the circumsolar part is calculated using A_i [coeff.], and A_i is obtained from Eq. (18). The Horizon brightening part is calculated by using [coeff.], which is mainly related to cloudiness given in Eq. (21).

3.5.5. Perez transposition model

A more in-depth examination of diffuse radiation is developed by Perez (1986). The model consists of three components: isotropic, circumsolar brightening, and horizon brightening. The total TSR intensity on a tilted PV surface (I_T) is obtained by applying Equation (24) (Perez et al., 1987; Perez et al., 1990).

$$I_T = I_T = I_b R_b + I_d\left[(1 - F_1)\left(\frac{1+cos\beta}{2}\right) + F_1\frac{a}{b} + F_2 sin\beta\right] + I\rho_g\left(\frac{1-cos\beta}{2}\right) \quad (24)$$

where F_1 and F_2 are the circumsolar and horizon brightness [coeff.], and a and b are solid angles related to the circumsolar part of a tilted surface [coeff.]. a and b coefficients are determined from the solar geometry described in Equations (25) and (26).

$$a = \max(0, cos\theta) \tag{25}$$

$$b = \max(cos85^{\circ}, cos\theta_z) \tag{26}$$

Atmospheric clearness and brightness parameters are obtained by using Equations (27) and (28).

$$\epsilon = \frac{\frac{I_d + I_b}{I_d} + 5.535X10^{-6}\theta_z^3}{1 + 5.535X10^{-6}\theta_z^3} \tag{27}$$

$$\Delta = m\frac{I_d}{I_0} \tag{28}$$

where ϵ is the atmospheric clearness parameter $[\text{coeff.}]$, Δ is the atmospheric brightness parameter $[\text{kWh/m}^2]$, and m is the optical air mass $[\text{coeff.}]$.

F_1 and F_2 are the functions of clarity, zenith angle, and brightness, and are expressed in Equations (29) and (30).

$$F_1 = \max[0, (f_{11} + f_{12}\Delta + \frac{\pi\theta_z}{180} f_{13}] \tag{29}$$

$$F_2 = f_{21} + f_{22}\Delta + \frac{\pi\theta_z}{180} f_{23} \tag{30}$$

where the f_{11}, f_{12}, f_{13}, f_{21}, f_{22} and f_{23} are derived from Perez's (1987) model coefficients of clearness ϵ index $[\text{coeff.}]$.

3.5.6. Liu-Jordan isotropic transposition model

Several isotropic transposition models are developed to determine hourly TSR intensity on the PV surface (I_T). In this study, Liu and Jordan's isotropic (1961) model is preferred to estimate TSR intensity on tilted south-faced PV surfaces specifically given by Equation (31) (Erbs et al., 1982; Gueymard, 2000; Abdulwahab et al., 2023).

$$I_t = I_b R_b + I_d \left(\frac{1+cos\beta}{2}\right) + \rho_g \left(\frac{1-cos\beta}{2}\right) \tag{31}$$

3.6. TSR Modelling for an STS

To be able to adapt the algorithm to circumstances when the position of the STSs varies during the day, the tilt angle (β) and the incidence angle θ for each hour are calculated by using solar geometry equations (Braun & Mitchell, 1983). After calculating the TSR intensity for every hour of the day, the daily TSR intensity (I_T) is determined simply by adding up the values of every hour of the day. The PV surfaces' alignment and inclination angles vary during the computing process depending on the kind of STS. By using the PV surfaces' orientation and inclination angles and the sun's position, the incidence angle of the sun's rays is then computed for each time step. In this study, calculations are performed considering single-axis (east-west) and dual-axis STSs. The PV surfaces are oriented toward the equator, while the axis of rotation is on the east-west plane. This indicates that for single-axis east-west STSs, both tilt angle and alignment angle vary over the route of computation. The sun's tilt and orientation are tracked by the PV surfaces, and both angles vary over the route of computation for dual-axis STSs. Figure 3.3 shows the schematic representation of the solar incidence angle on a tilted surface. The incidence angle of the GSR on the PV surfaces can be represented from the solar geometric events by using Equation (32) (Quaschning, 1996; PVSOL, 2024).

$$\cos(\theta) = -cos\gamma_s sin\gamma_e \cos(\alpha_s - \alpha_e + \pi) + sin\gamma_s cos\gamma_e \tag{32}$$

where θ is the incidence angle of solar radiation on the PV surfaces [º], α_s is the orientation of the sun [º], γ_s is the elevation of the sun [º], α_e is the orientation of the PV surface [º], and γ_e is the elevation of the PV surface [º].

STSs typically are designed as one-axis and two-axis forms to optimize TSR on PV surfaces, and TSR intensity is maximized by changing the plane of incidence of PV surfaces. A realistic estimation of how much TSR intensity is being received from STSs facilitates more accurate optimal tilt analyses as well as the feasibility of solar PV plants. It is vital to establish a functional relationship between PV surface tilt (β) and PV surface azimuth γ while tracking surfaces. The tilt and/or azimuth angles are determined and set continuously to provide the maximum amount of beam radiation (I_b) all the time. In the case of the one-axis STS rotating around a vertical axis with a fixed tilt and variable azimuth, the amount of beam radiation is maximized by using Equation (33). It yields ($\gamma = \gamma_s$) condition for the azimuth angle.

$$\frac{d(cos\theta)}{d_\gamma} = -sin\theta_z\, sin\beta \sin(\gamma_s - \gamma) = 0 \tag{33}$$

where γ is the solar surface azimuth [º], and γ_s is the solar azimuth [º].

In the case of a PV surface rotating (R_β) around a one-axis that is all the time parallel to the surface, the amount of beam radiation is maximized by using Equations (34), and (35) when the axis is horizontal.

$$\frac{d(cos\theta)}{d\beta} = sin\theta_z \cos(\gamma_s - \gamma)\, \beta - cos\theta_z\, sin\beta = 0 \tag{34}$$

$$tan\beta = tan\theta_z \cos(\gamma - \gamma_s) \tag{35}$$

where θ_z is the Solar zenith angle [º].

The PV surface tilt (β) is defined between 0º and 180º. So, a general expression for PV surface tilt and its components are given in Equations (36), (37), and (38).

$$\beta = \beta_0 + R_\beta(180º) \tag{36}$$

$$\beta_0 = tan^{-1}(tan\theta_z \cos(\gamma - \gamma_s)) \tag{37}$$

$$R_\beta = 0 \ if \ \beta_0 \geq 0, otherwise \ 1 \quad (38)$$

where R_β is the tilt rotation angle of the solar surface about the axis, [º].

The surface azimuth is expressed in terms of axis azimuth by using Equations (39) and (40).

$$\gamma = \gamma_a + 90° \ if \ \gamma_s - \gamma_a \geq 0º \quad (39)$$

$$\gamma = \gamma_a - 90° \ if \ \gamma_s - \gamma_a < 0º \quad (40)$$

where γ_a is the tracking axis azimuth, [º].

The amount of beam radiation is maximized all the time when the sun lies in the plane vertical to the PV surface and contains the tracking axis. If a PV surface is tracked parallel to the surface but is not vertical or horizontal, both the azimuth and tilt angles of the PV surface change over time. In this case, the relationship between the PV surface tilt and azimuth is expressed by Equations 41 and 42.

$$tan\beta = \frac{tan\beta_a}{\cos(\gamma - \gamma_a)} \quad (41)$$

$$\tan(\gamma - \gamma_a) = \frac{sin\theta_z \sin(\gamma_s - \gamma_a)}{cos\theta_a sin\beta_a} \quad (42)$$

Good to point out that the sign $(\gamma - \gamma_{a)}$ is always the same as the sign of $(\gamma_s - \gamma_a)$, therefore, the PV surface azimuth is expressed in Equation (43), the components of this equation are given in Equations (44), (45), and (46).

$$\gamma = \gamma_0 + (R_{\gamma 1})(R_{\gamma 2})(180º) \quad (43)$$

$$\gamma_0 = \gamma_a + tan^{-1} = [\frac{sin\theta_z \sin(\gamma_s - \gamma_a)}{cos\theta_a sin\beta_a}] \quad (44)$$

$$R_{\gamma 1} = 0 \; if \; (\gamma_0 - \gamma_a)(\gamma_s - \gamma_a) \geq 0, \; otherwise \; 1 \quad (45)$$

$$R_{\gamma 2} = 1 \; if \; (\gamma_s - \gamma_a) \geq 0, otherwise \; -1 \quad (46)$$

where R_γ is the azimuth rotation angle of the solar surface about the axis, [º].

Because the PV surface tilt is always between 0° and 180°, (β) is expressed by Equation (47), the terms of the equation are given in Equations (48) and (49).

$$\beta = \beta_{a0} + R_\beta(180º) \quad (47)$$

$$\beta_{a0} = tan^{-1}[\frac{tan\beta_a}{\cos(\gamma - \gamma_a)}] \quad (48)$$

$$R_\beta = 0 \; if \; \beta_{a0} \geq 0, otherwise \; 1 \quad (49)$$

The surface is set such that the sun is all the time at normal incidence to maximize the amount of beam radiation for a two-axis STS. Thus, the maximum amount of beam radiation is guaranteed by Equations (50) and (51). These equations are satisfied with $(\gamma = \gamma_s)$ and $(\beta = \theta_Z)$ conditions.

$$\frac{\partial(cos\theta)}{\partial\beta} = 0 \quad (50)$$

$$\frac{\partial(cos\theta)}{\partial\gamma} = 0 \quad (51)$$

3.7. Calculations of Gains for TSR on PV Surfaces

The percentage efficiency and percentage comparison of solar PV surfaces equipped with STS and SFS have been analyzed with the following equations (Jamroen et al. 2020).

Percentage gains (PG_{opt}) in the availability of TSR intensity on an annual SFS (I_T) are obtained by using Equation (52).

$$PG_{opt} = \left(\frac{I_{T,\beta=opt}}{I_{T,\beta=0}} - 1\right) X100 \quad (52)$$

where PG_{opt} is the percentage gain in TSR intensity for optimally tilted PV surfaces [%], $I_{T,\beta=opt}$ is the TSR intensity captured by tilted surfaces [$\mathrm{kWh/m^2}$], and $I_{T,\beta=0}$ is the GSR intensity on horizontal surfaces [$\mathrm{kWh/m^2}$].

Percentage gains for one-axis (PG_{single}) and two-axis (PG_{dual}) STSs in the availability of TSR intensity (I_T) are defined by Equations (53) and (54).

$$PG_{single} = \left(\frac{I_{T,1-axis}}{I_{T,\beta=OPT}} - 1\right) X100 \quad (53)$$

$$PG_{dual} = \left(\frac{I_{T,2-axis}}{I_{T,\beta=OPT}} - 1\right) X100 \quad (54)$$

where PG_{single} and PG_{dual} are the percentage gain in the availability of TSR intensity for single and dual-axis STS, respectively [%], and $I_{T,1-axis}$ and $I_{T,2-axis}$ are the TSR intensity collected by STSs, respectively [$\mathrm{kWh/m^2}$].

3.8. Calculations of Levelized Cost of Energy (LCOE)

A direct comparison of the costs of all energy systems is possible thanks to LCOE, which takes into account capital expenses, depreciation, operation, maintenance, and administration, among other factors. The economic potential of solar PV plants is determined in this study via an LCOE, which describes how much it would cost to produce a unit of energy taking generalized assumptions about the costs of construction and operation of a typical solar PV plant. It is expressed by Equation (55) (ESMAP-World Bank, 2020; IRENA, 2022).

$$LCOE = \frac{\sum_{t=1}^{n} \frac{I_t + M_t F_t}{(1+d)^t}}{\sum_{t=1}^{n} \frac{E_t}{(1+d)^t}} \tag{55}$$

where $LCOE$ is the average lifetime levelized cost of electricity production, I_t is investment expenditures in the year t, M_t is operations and maintenance expenditures in the year t, F_t is fuel expenditures in the year if any, E_t is energy production in the year t, d is the discount rate, and n is the lifetime of the solar PV plant in years.

3.9. Numerical Modeling of an Isolated (Off-Grid) Solar PV Plants

To minimize and balance the storage size by decreasing energy consumption. Photovoltaic (PV), energy storage (ES), generator sizing, energy flow, and breakdown calculations are numerically modeled for a solar PV microgrid design. The PV model is based on a simplified method for predicting PV output (Evans, 1981). The average efficiency of PV (η_{pv-avg}) is a function of the average PV temperature as expressed in Equation (56) and the average PV temperature (T_{pv-avg}) is expressed by Equation (57).

$$\eta_{pv-avg} = \eta_{pv}[1 - \beta_p(T_{pv-avg} - T_{ref})] \tag{56}$$

$$T_{pv-avg} - T_{amb} = (219 + 832K_{mt})\frac{NOCT-20}{800} \tag{57}$$

where η_{pv-avg} is the average PV surface efficiency, η_{pv} is the PV surface efficiency, T_{pv-avg} is the average PV temperature, T_{ref} is the reference temperature (25°C), T_{amb} is the monthly ambient temperature, β_p is the temperature coefficient, K_{mt} is the monthly clearness index, and The Nominal Operating Cell Temperature *(NOCT)* is the nominal operating PV cell temperature ($Mono - Si = 45$°C).

The total direct current (DC) energy demand, as well as the total alternating current (AC) energy demand of the microgrid load, are specified by the microgrid developer in kWh/d. AC energy demand is converted to a DC equivalent using the inverter efficiency; the total DC equivalent ($D_{DC,eqv}$) is expressed by Equation (58). The DC equivalent has three components and is expressed by Equation (59).

$$D_{DC,eqv} = D_{DC} + \frac{D_{AC}}{\eta_{inv}} \tag{58}$$

$$D_{DC,eqv} = D_m + D_c + D_{es} \tag{59}$$

where $D_{DC,eqv}$ is the total DC equivalent of the total microgrid AC energy demand, D_{DC} is the total DC demand, D_{AC} is the total AC demand, and η_{inv} is the inverter efficiency. D_m is the demand directly met by the PV, D_c is the demand that remains constant throughout the day, and D_{es} is the demand primarily met by the ES.

The critical PV absorption level (P_{crt}) is the load corresponding to the constant energy demand and is expressed by Equation (60).

$$P_{crt} = \frac{D_{cnt}}{24} \tag{60}$$

where P_{crt} is the critical PV absorption level and is expressed in W. D_{cnt} is met either directly by the PV during enough sunshine or through the ES during not enough sunshine is expressed in kWh.

The total energy demand of the continuous load can be met directly by the PV without being stored in the ES first. The energy delivered directly to the continuous load (E_{cl}) is expressed in Equation (61) by handling daily utilizability (Zlateva, 2020). Also, the energy delivered to the matched load (E_{ml}), the energy delivered directly to the load, and the energy delivered to the ES (E_{dl}) are expressed by Equations (62) and (63).

$$E_{cl} = (1 - U_d)E_{pv} \tag{61}$$

$$E_{ml} = \min(D_{m,}E_{pv-}E_{cl}) \tag{62}$$

$$E_{dl} = E_{cl} + E_{ml} \tag{63}$$

where E_{cl} is the energy delivered directly to the continuous load, U_d is the daily utilizability, E_{pv} is the energy available from the PV, E_{ml} is the energy delivered to the matched load, E_{dl} is the energy delivered directly to the load.

A fraction of the load for an off-grid PV plant is determined by two factors: the PV size and the ES size. The loss of load probability (LOLP) is the probability that the system has failed to meet the load. In the literature, there are some ways to calculate LOLP (Louis & Bucciarelli, 1986; Klein & Beckman, 1987; Khorramde et al., 2016; Modiri-Delshad et al., 2016). The monthly fraction of the load met by the PV based on the PV/L and the ES/L ratios (f_{pv}) are expressed by Equations (64) and (65). Also, the part of the load is not met directly by the PV (L'), as well as the available output of the PV decreased by the energy delivered directly to the load (E'_{pv}) are expressed by Equations (66) and (67).

$$f_{pv} = PVL_r = E'_{pv}/L' \tag{64}$$

$$f_{pv} = ESL_r = ES_{uc}/L' \tag{65}$$

$$L' = L - E_{dl} \tag{66}$$

$$E'_{pv} = (E_{pv} - E_{dl})\eta_{cc}\eta_{es} \tag{67}$$

where f_{pv} is the fraction of PV, PVL_r is the PV/L ratio, ESL_r is the ES/L ratio, E'_{pv} is the available output of the PV decreased by the energy delivered directly to the load, L' is the part of the load not met directly by the PV, ES_{uc} is the usable ES capacity, L is the load, η_{cc} is the charge control efficiency, and η_{es} is the ES efficiency.

The energy delivered by the generator (E_{gen}) is the differentiation between the load and what can be provided by the PV directly or through the ES and is expressed by Equation (68). Additionally, the energy used by the generator (Q_{gen}) is expressed by Equation (69).

$$E_{gen} = L - E_{dl} - E_{es} \tag{68}$$

$$Q_{gen} = \frac{E_{gen}}{\eta_{ch}\eta_{gen}\eta_{es}} \tag{69}$$

where E_{gen} is the Energy delivered by the generator, E_{es} is the energy delivered by the ES, Q_{gen} is the energy used by the generator, η_{ch} is the efficiency of the charger which is the energy to charge the ES in 8 hours, η_{gen} is the generator's efficiency, and η_{es} is the ES efficiency.

The desired number of days is used to size the ES. The usable ES capacity (ES_{uc}) is expressed by Equations (70) and (71). Then the nominal capacity (ES_{nc}), that means the design ES capacity, is expressed by Equation (72). Lastly, the generator capacity (C_{gen}) is considered as the maximum of the AC demand, and it is expressed by Equation (73).

$$ES_{uc} = ES_{nc} f_c \tag{70}$$

$$ES_{uc} = \frac{L_{DC} n}{d_{dod} \eta_{es}} \tag{71}$$

$$ES_{nc} = \frac{ES_{uc}}{f_c} \tag{72}$$

$$C_{gen} = \frac{1}{8} = \frac{ES_{nc}}{\eta_{ch}} \tag{73}$$

where ES_{uc} is the usable ES capacity, ES_{nc} is the nominal capacity, f_c is the usable fraction of capacity available, depends on ES temperature and discharge rate, L_{DC} is the equivalent DC load, n is the number of days, d_{dod} is the maximum depth of discharge, and C_{gen} is the generator capacity.

3.10. Numerical Modeling of an On-Grid Solar PV Plants

The most basic model of the system is the on-grid PV plant. The PV modeling is presented based on Evans (1981) and is common to all types of PV applications. The average efficiency of PV is a function of the characteristics of the utilized PV module for standard technologies such as average PV temperature, which was expressed in Equation (56) and the average PV temperature was expressed in Equation (57). Please see Section 3.9. It is noted that Equation (57) is valid in the case of the tilt angle of the PV surface is adjusted to OPTA. If the PV surface angle differs from OPTA, the right side of Equation (57) needs to be revised by multiplying it by a correction factor (C_f) is defined by Equation (74).

$$C_f = 1 - 1.17x10^{-4}(\beta_{opta} - \beta_{act}) \tag{74}$$

where C_f is the correction factor, β_{opta} is the optimal tilt angle of the PV surface [º], and β is the actual tilt angle of the PV surface [º].

The produced PV energy delivered by the solar PV plant (E_{pv}) can be expressed simply in Equation (75).

$$E_{pv} = A_{pv}\eta_{pv}I_{td} \tag{75}$$

where E_{pv} is the produced PV energy delivered by the solar PV plant, A_{pv} is the area of the PV plant, η_{pv} is the PV plant efficiency, and I_{td} is the TSR on the PV plant.

Miscellaneous PV plant losses (L_{pv}) and other power conditioning losses (L_c) have to be reduced. The mentioned losses can be expressed in Equation (76).

$$E_{avlb} = E_{pv}(1 - L_{pv})(1 - L_c) \quad (76)$$

where E_{avlb} is the PV plant energy available to the load and battery, L_{pv} is the miscellaneous PV array losses, and L_c is the other power conditioning loss.

Ultimately, The overall solar PV plant efficiency (η_{eff}) A is defined in Equation (77).

$$\eta_{eff} = \frac{E_{avlb}}{A_{pv} I_{td}} \quad (77)$$

where η_{eff} is the overall solar PV plant efficiency.

Specifically, neither a recommended PV module size nor a specified load is mentioned in on-grid solar PV plants. The nominal PV power is simply equal to the recommended inverter capacity. After deducting inverter losses, the energy produced by the PV plant becomes available to the grid. The nominal PV power is simply equal to the recommended inverter capacity. After deducting inverter losses, the energy produced by the PV plant becomes available to the grid (E_{grid}) is given by Equation (78).

$$E_{grid} = E_{avlb} \eta_{inv} \quad (78)$$

where E_{grid} is PV energy available to the grid, and η_{inv} is the inverter efficiency.

Based on the grid configuration, it is possible that the grid won't absorb all of this electricity. Therefore, the PV energy actually delivered (E_{act}) is expressed in Equation (79).

$$E_{act} = E_{grid} \eta_{abs} \quad (79)$$

where E_{act} is the PV energy actually delivered, and η_{abs} is the PV energy absorption rate.

3.11. Descriptions of the Optimization and Computation Methodologies

The solar PV plant optimization and computation methodologies usually handle the following issues: Maximize the output power of the PV plant, minimize the operating costs of the PV plant, maximize the lifetime of ES, and minimize the environmental costs (Vera et al. 2019). In this context, descriptions of the calculation algorithms, flowcharts, working diagrams, and simple representations for the estimation of TSR on optimization of solar PV plant design have been depicted in this section. In Section 3.10 can be concluded that the proposed methodologies can be applied to any place of interest to generate precise estimates with lower computational expense because tilting and tracking are important impacts that increase incident solar energy at all latitudes. The algorithms and optimizations can be also used to assess the solar potential of a certain location in Türkiye and in the world for installation of solar PV plants to prevent energy yield losses and needlessly equipment cost because it can be easily applied by researchers and engineers in the field. The proposed optimization handling of the solar PV plants and microgrids is described. So, to summarize: The algorithms, flowcharts, and numerical relationships used in case, application, and experimental studies have been presented. Energy management, and optimization objectives along with the solution approaches and numerical tools have been handled in this section.

3.11.1. Description of the computation algorithm for TSR intensity on PV Surfaces

Because the GSR distribution varies according to the latitudes and places on the earth. The horizontal GSR is the most important parameter to optimize the OPTA values and TSR intensity on PV surfaces. Therefore, daily and hourly TSR values on SFS and STS can be obtained for the target geolocations with the proposed algorithm presented in Sections 3.4 and 3.5. The independent variables of the algorithm are the latitude, longitude, and elevation of the analyzed geolocation. The OPTA is determined by looking for values at which the TSR on the PV surface is maximal for a certain period. The calculation is done in one-hour increments for all 365 days of the year. The calculation algorithm is an improved form of the previous methodologies given by some researchers in the literature (Liu & Jordan, 1962; Jakhrani, 2013). The algorithm uses an approach similar to Klein & Theilacker's (1981) algorithm described by Duffie & Beckman (2006) for fixed (tilted) PV surfaces. On the other hand, the algorithm is extended to STSs to investigate TSR on the one-axis, and two-axis constructed PV surfaces as described by Braun & Mitchell (1983). The calculation steps of the algorithm can be broken down into 2 phases. Phase 1 consists of OPTA optimization by maximizing TSR for SFSs. Phase 2 consists of an extension of the algorithm to one-axis and two-axis STS and solar geometry optimization with the well-known solar geometry equations. So, the algorithm starts with the initial computation of the GSR (horizontal beam and diffuse components) intensity for each hour by using the recommended average Julian day of the month. Then, the TSR (tilted) for each hour of an average Julian day is computed. Lastly, the summation of the hourly values is considered to compute the daily TSR intensity on the tilted PV surfaces. In short, computations start with values on a horizontal surface, and horizontal values are subsequently transposed on a tilted surface by utilizing transposition models. In this context, solar declination values and recommended average days of months for calculation of the average Julian day of the months are depicted in Table 3.1. The simple representation of the algorithm is presented in Figure 3.5. The advanced flow chart of the proposed calculation algorithm is illustrated in Figure 3.6. The illustrative summary of the phases of the proposed algorithm is presented in Table 3.2 and Table 3.3.

Table 3.2. Summary of the proposed algorithm to estimate TSR intensity on PV surfaces.

Parameters & Descriptions	**Calculation Method**
Recommended "Average Julian Days" for Months	Table 3.1.
Declination angle ($\boldsymbol{\delta}$)	Eq. (1)
Solar time ($\boldsymbol{COS\omega_s}$)	Eq. (2)
Daily extraterrestrial GSR on the horizontal surface ($\boldsymbol{I_0}$)	Eq. (3)
Daily clearness index ($\boldsymbol{\overline{K}_T}$)	Eq. (4)
Daily diffuse radiation ($\boldsymbol{I_d}$)	Eqs. (5) & (6)
The ratio of hourly to daily GSR ($\boldsymbol{R_t}$)	Eqs. (7), (8) & (9)
The ratio of hourly to daily diffuse radiation ($\boldsymbol{R_d}$)	Eq. (10)
Horizontal GSR for each hour of "average Julian day" ($\boldsymbol{I_h}$), ($\boldsymbol{I_d}$), ($\boldsymbol{I_b}$)	Eqs. (11), (12) & (13)

Beam radiation tilt factor $(\boldsymbol{R_b})$	Eq. (14)
The ratio of ground-reflected GSR $(\boldsymbol{R_r})$	Eq. (15)
Hourly TSR intensity on PV surface $(\boldsymbol{I_t})$	Eq. (16)
Tilt angle and incidence angle for each hour $(\boldsymbol{\beta})$, $(\boldsymbol{\theta})$	solar geometry equations
Daily TSR $(\boldsymbol{I_{td}})$	by summing individual hours

Table 3.3. Extension of the algorithm for one-axis and two-axis STSs (solar geometry Equations).

Parameters & Descriptions	**Calculation Method**
The vertical axis, fixed-tilt, surface azimuth satisfied with $(\boldsymbol{\gamma} = \boldsymbol{\gamma_s})$	Eq. (33)
The horizontal axis, a surface parallel to the axis, surface azimuth $(\boldsymbol{\gamma})$	Eqs. (34) & (35)
The horizontal axis, a surface parallel to the axis, surface tilt $(\boldsymbol{\beta})$	Eqs. (36), (37) & (38)
Expressing the surface azimuth as the axis azimuth $(\boldsymbol{\gamma_a})$	Eqs. (39) & (40)
Relationship between the PV surface tilt and azimuth $(\boldsymbol{tan\beta}), \mathbf{tan}(\boldsymbol{\gamma} - \boldsymbol{\gamma_a})$	Eqs. (41) & (42)
Tilted axis, a surface parallel to the axis, and surface azimuth $(\boldsymbol{\gamma})$	Eqs. (43), (44), (45) & (46)
Tilted axis, a surface parallel to the axis, and surface tilt $(\boldsymbol{\beta})$	Eqs. (47), (48) & (49)
Two-axis STS satisfied with $(\boldsymbol{\gamma} = \boldsymbol{\gamma_s})$, $(\boldsymbol{\beta} = \boldsymbol{\theta_z})$	Eqs. (50) & (51)

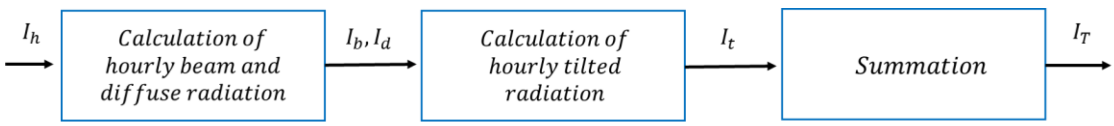

Figure 3.5. Simple representation of the computation algorithm.

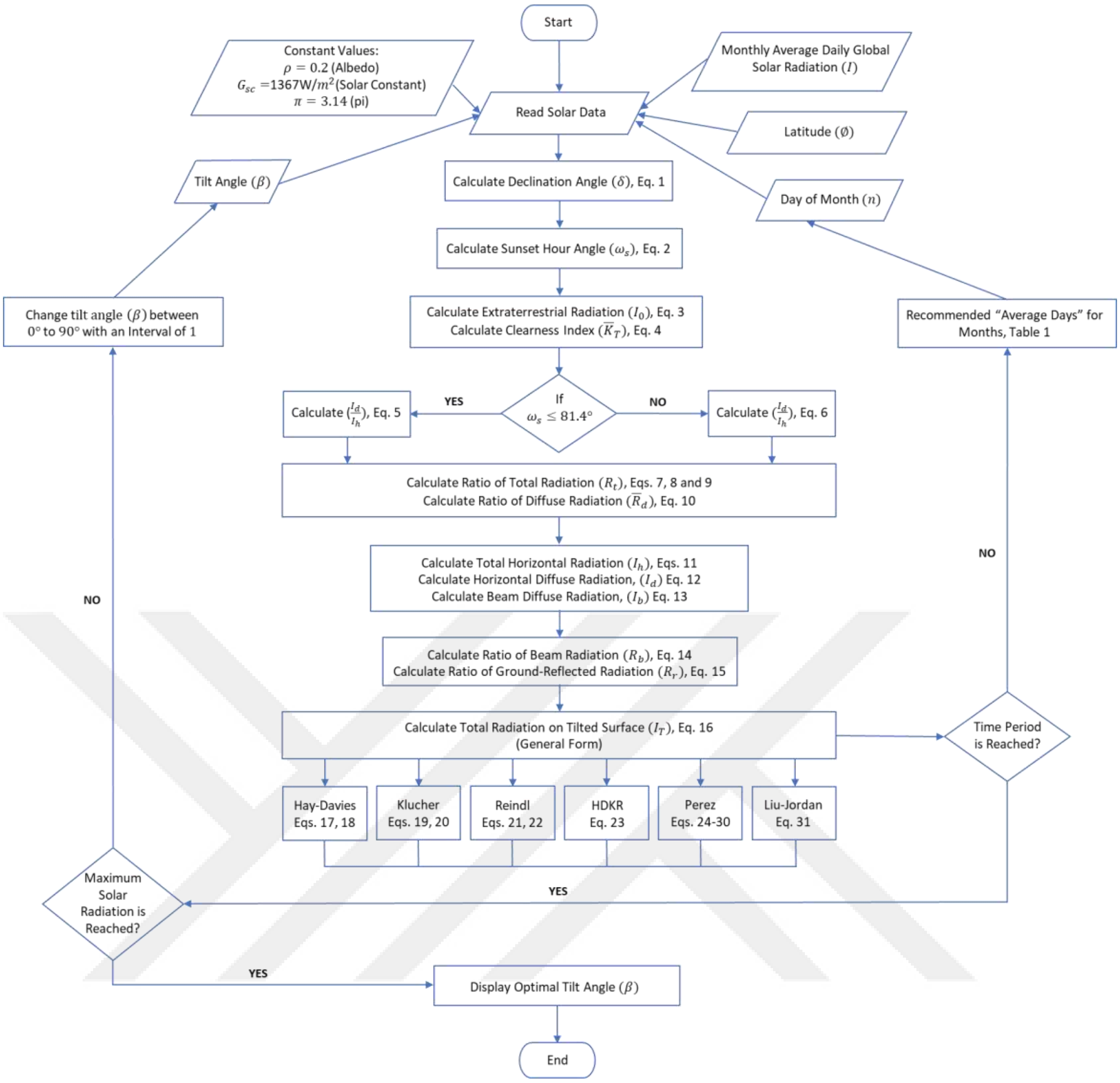

Figure 3.6. The advanced flowchart of the computation algorithm for OPTA and TSR intensity.

3.11.2. Description of the computations for TSR gains on PV surfaces and LCOE

LCOE serves as a metric for evaluating and comparing various methods of energy production consistently. It aids in analyzing different cost-performance trade-offs and formulating investment strategies. LCOE represents the average cost of energy generated over the lifespan of different energy-producing assets. It can be seen as the mean electricity price necessary for a specific generation method to break even. In the context of solar PV plants, LCOE is linked to the cost of producing a single unit of electricity throughout the plant's lifetime. Another important note is that to provide a reliable assessment and reliable performance estimation of solar potential in any desired geolocation, a percentage of solar energy gains on PV surfaces for an SFS, one-axis STS, and two-axis STS must be calculated, and results must be indicated. In line with Sections 3.7 and 3.8, a summary of the proposed calculations of TSR Gains and LCOE is tabulated in Table 3.4.

Table 3.4. Summary of the proposed calculations of TSR Gains and LCOE

Parameters & Descriptions	Calculation Method
Percentage gain in TSR for an optimally tilted PV surface ($\boldsymbol{PG_{opt}}$)	Eq. (52)
Percentage gain in TSR intensity for a one-axis STS ($\boldsymbol{PG_{single}}$)	Eq. (53)
Percentage gain in TSR intensity for a two-axis STS ($\boldsymbol{PG_{dual}}$)	Eq. (54)
Average lifetime levelized cost of electricity production ($\boldsymbol{LCOE}$)	Eq. (55)

3.11.3. Description of the PV power optimization of the isolated microgrid

A stand-alone microgrid, also known as an isolated microgrid, functions independently from the wider electric power system and cannot be connected to it. Typically, they are tailored for geographical islands or rural areas lacking access to centralized electricity. Isolated microgrids offer a viable solution for rural electrification by generating solar energy and operating autonomously, disconnected from the main grid. However, supplying electrical energy in remote and rural areas is constrained by technical barriers such as long-distance transmission, rugged terrain, a highly dispersed population, etc. In this context, one of the main issues of this thesis is to minimize and balance the storage size by decreasing energy consumption for solar PV-powered microgrids. So, in this section, PV, ES generator sizing, and energy flow and breakdown calculations are carried out to take into account the load capacity planned to be used in the microgrid. A summary of the proposed optimization modeling of a solar PV microgrid is depicted in Table 3.5. Also, the optimization and working diagram of the off-grid model with the fuel generator designed in this study is shown in Figure 3.7 following numerical modeling in Section 3.9.

Table 3.5. Summary of the proposed optimization modeling of a solar PV microgrid

Parameters & Descriptions	**Calculation Method**
Average PV efficiency (η_{pv-avg})	Eq. (56)
Average PV temperature (T_{ref})	Eq. (57)
Total DC equivalent of a total microgrid AC energy demand $(\mathbf{D}_{\mathbf{DC,eqv}})$	Eqs. (58) & (59)
Critical PV absorption level (P_{crt})	Eq. (60)
The energy delivered to the continuous load (E_{cl})	Eq. (61)
The energy delivered to the matched load (E_{ml})	Eq. (62)
The energy delivered directly to the load (E_{dl})	Eq. (63)
Fraction of a PV surface (f_{pv})	Eqs. (64) & (65)
Part of the load not met directly by a PV surface (L')	Eq. (66)
The available output of a PV surface is decreased by the energy delivered directly to the load (E'_{pv})	Eq. (67)
The energy delivered by a generator (E_{gen})	Eq. (68)
Energy used by a generator (Q_{gen})	Eq. (69)
Usable ES capacity of a microgrid (ES_{uc})	Eqs. (70) & (71)
Nominal ES capacity of a microgrid (ES_{nc})	Eq. (72)
The generator capacity of a microgrid (C_{gen})	Eq. (73)

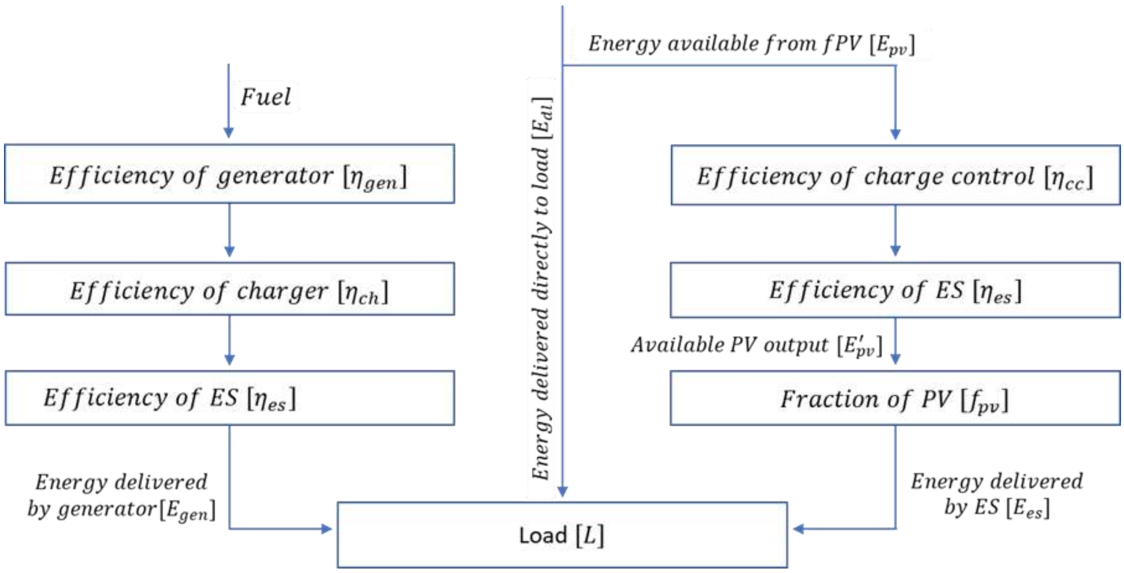

Figure 3.7. Optimization & working diagram for off-grid microgrid with fuel generator.

3.11.4. Description of modeling of the on-grid solar PV plant

The on-grid solar PV plant model is one of the simplest PV plant models. However, the electricity production of an on-grid solar PV plant is influenced by a range of factors, including the components of the photovoltaic system, configuration, geographical location, weather conditions, operational issues, and more. Numerous research works delve into the PV energy efficiency, financial evaluations, and ecological footprint of various on-grid PV plants. This study aims to conduct numerical and logical modeling of an on-grid solar PV plant as one of its objectives. In this context, the summary of the proposed modeling of an on-grid solar PV plant and average efficiency is depicted in Table 3.6 following numerical modeling in Section 3.10. The basis flowchart for the average efficiency of the PV plant is presented in Figure 3.8. The basis flowchart for the on-grid PV plant model is presented in Figure 3.9.

Table 3.6. Summary of the proposed modeling of an on-grid solar PV plant and average efficiency.

Parameters & Descriptions	Calculation Method
Average PV efficiency (η_{pv-avg})	Eq. (56)
Average PV temperature (T_{ref})	Eq. (57)
Correction factor (C_f)	Eq. (74)
Produced PV energy delivered by the solar PV plant (E_{pv})	Eq. (75)
PV plant energy available to the load and battery (E_{avlb})	Eq. (76)
Overall solar PV plant efficiency (η_{eff})	Eq. (77)
PV energy available to the grid (E_{grid})	Eq. (78)
PV energy actually delivered (E_{dl})	Eq. (79)

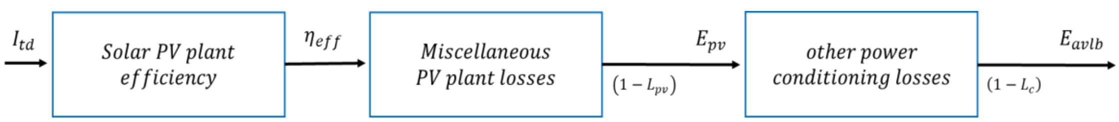

Figure 3.8. The basis flowchart for average efficiency of PV plant.

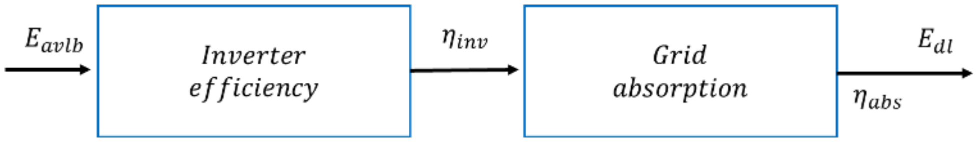

Figure 3.9. The basis flowchart for the on-grid PV plant model.

3.11.5. Description of the ECU Development for STS

The comprehensive review of existing literature indicates that incorporating STSs can enhance the effectiveness of PV modules by as much as 40%. one-axis systems boost efficiency by 25% to 30%, whereas two-axis trackers offer an additional 5% to 10%, resulting in increased PV energy production. Nonetheless, to realize such energy gains, it's imperative to optimize STS mechanisms alongside mechanical, electronic, and software components, as well as ensure the high-quality and sufficient capacity of PV modules. Therefore, one of the aims of this thesis is the design, development, and programming of ECUs for STSs to achieve optimal sun tracking and maximal TSR intensity. The uncertainties in calculating the solar position have decreased with the continuous advancements in GSR applications. There have been many published articles describing solar position algorithms for GSR and TSR applications (Michalsky, 1988; Blanco-Muriel et al., 2001). Further, NREL (2008) has developed a C source code for the Solar Position Algorithm (SPA). So, in this context, an STS electronic control unit (ECU) has been developed with the scope of this thesis in which the SPA is embedded. It is noted that an improved version of the SPA offered by NREL (2008) has been utilized in the programming of the STS electronic controller. The flowchart of the ECU unit embedded into SPS is presented in Figure 3.10.

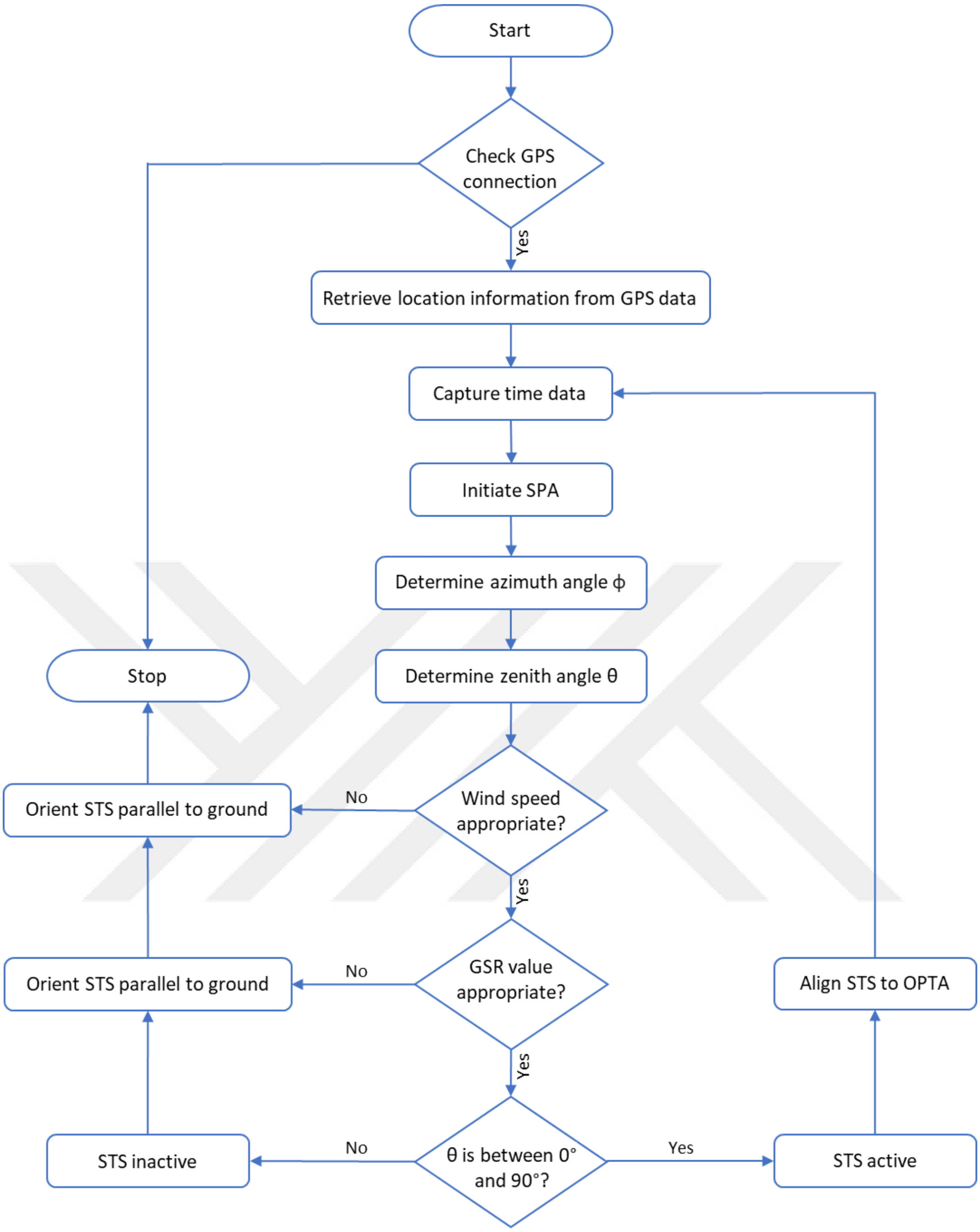

Figure 3.10. The flowchart of the developed ECU for STS.

4. CASE AND EXPERIMENTAL STUDIES

In this section, case studies, applications, and experimental studies conducted for Turkish geography are presented. Estimation of OPTA values and TSR intensities for south-facing SFS and STS in the Provinces of Türkiye have been carried out. Investigation of transposition models estimating TSR intensity on PV surfaces has been performed. Design of isolated PV power production for rural and remote areas has been conducted.

4.1. Case Study (1): Investigation of OPTA and TSR Intensity for Solar PV Surfaces in Türkiye Provinces

Türkiye is located between 36-42° North parallels and 26-45° East meridians. The territory of Türkiye is divided into 7 geographical regions named Marmara, Aegean, Mediterranean, Central Anatolia, Black Sea, Eastern Anatolia, and Southeastern Anatolia, there are 81 provinces spread through these 7 regions with the scope of this study. Türkiye is an energy importer because of its heavy dependence on fossil fuels and scarcity of indigenous energy supplies. Geographically, Türkiye is located between the temperate and subtropical climate zones. In Türkiye's Solar Energy Potential Atlas (GEPA), the average annual total sunshine duration is determined as 2,640 hours, and the annual GSR intensity is determined as 1,311 kWh/m². Although Türkiye is located in the sun belt, its potential cannot be used effectively and widely. Therefore, in this section, A solar energy potential investigation has been conducted covering the whole of Türkiye. The case study results and conclusions have been presented in Sections 5 and 6.

4.1.1. GSR data utilized in this case study

Many locations have GSR data on the horizontal surface, but TSR data on a tilted surface is generally unavailable or insufficient. GSR data on a horizontal surface is essential to estimate TSR on tilted surfaces and is an essential parameter for modeling, designing, and efficiency analysis of PV plants. TSR on the tilted PV surface is the summation of direct and diffuse horizontal GSR. In this case study, solar datasets provided by the National Aeronautics and Space Administration’s Atmospheric Science Data Center (NASA-ASDC, 2024) have been utilized. The long-term (1999-2018) yearly

GSR on the horizontal surface in Türkiye is given in Figure 4.1. Türkiye's GSR and sunshine duration values are presented as daily and monthly average values in Table 4.1. As can be deduced from the provided solar climatic data, Türkiye has the advantage of receiving GSR due to its geographic location.

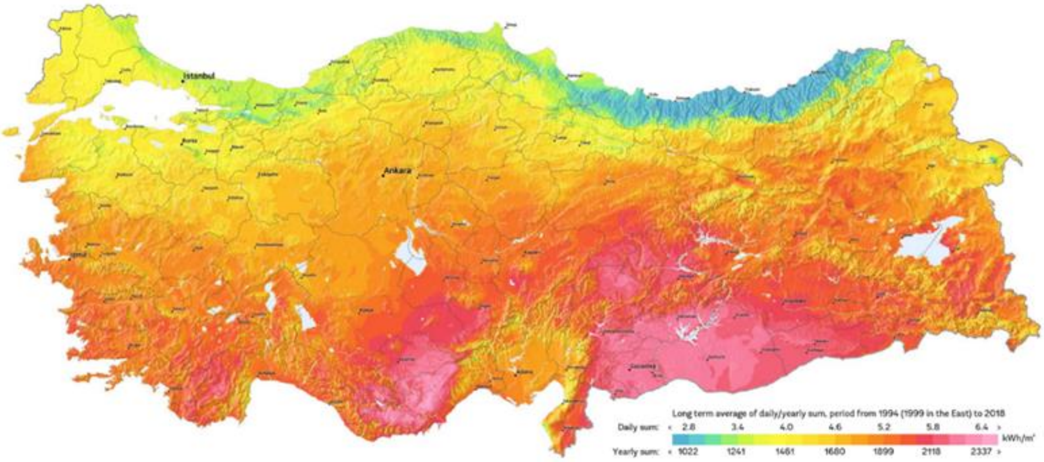

Figure 4.1. The annual GSR on the horizontal surface in Türkiye.
(https://globalsolaratlas.info/)

Table 4.1. GSR and sunshine duration values of Türkiye.

Month	**GSR Values**		**Sunshine Duration Values**	
	[kWh/m²-d]	[kWh/m²-m]	[hour/d]	[hour/m]
1	1.79	55.49	4.11	127.41
2	2.50	70.00	5.22	146.16
3	3.87	119.97	6.27	194.37
4	4.93	147.90	7.46	223.80
5	6.14	190.34	9.10	282.10
6	6.57	197.10	10.81	324.30
7	6.50	201.50	11.31	350.61
8	5.81	180.11	10.70	331.70
9	4.81	144.30	9.23	276.90
10	3.46	107.26	6.87	212.97
11	2.14	64.20	5.15	154.10
12	1.59	49.29	3.75	116.25
AVG	4.18	127.29	7.50	228.39

Source: (Kamil et al., 2006; Taşkın & Korucu, 2014; GEPA, 2022).

4.1.2. TSR estimation model utilized in this case study

RETScreen estimation model provides a map-based solar resource and efficiency analysis, it is quite useful for the analysis of the PV plants and describing solar PV plants' performance under given conditions by using GSR values and climatic data provided by the NASA-ASDC, (2024). By inputting the required data of the region, it is possible to reach the TSR ratios on the tilted PV surfaces for the desired region. The model is proposed due to its simplicity and strong capability to estimate daily TSR on tilted PV surfaces for the specified location (Sawyer et al., 2009; Lalita et al., 2013; Sharma et al., 2014). The estimation model applies an isotropic transposition clear sky approach for TSR intensity calculations of SFS and STS. The diffuse radiation calculations in RETScreen are based on a similar method to the Klein and Theilacker model with modeling hourly time steps (Liu & Jordan, 1961; Duffie & Beckman 1991). For this study, daily TSR on a tilted PV surface is investigated using the measured GSR data on the horizontal surface. Map-based and geo-referenced datasets of daily TSR on a horizontal surface are obtained by combining both ground and satellite station data shown in Figure 4.2. This data has been used to calculate annual OPTAs to be used by SFSs and determine the maximal TSR intensity collected by STSs. Increasing the number of stations in calculations provides more optimistic results. Establishing stations in non-existent provinces contributes significantly to more efficient and realistic solar energy analysis. The proposed model can be applied to any place of interest to generate precise estimates with little extra computational expense because tilting and tracking are important impacts that increase incident solar energy at all latitudes. The model can be also used to assess the solar potential of a certain location in the world before installation of such a solar PV plant, prevent energy yield losses, and needlessly equipment cost because it can be easily applied by researchers and technicians in the field. The estimation of TSR intensity on a tilted surface for the respective geolocation is utilized by using the presented equations in Section 3.

Figure 4.2. Map-based and geo-referenced solar data sources by ground and satellite stations (RETScreen, 2024).

4.2. Case Study (2): Estimation of OPTA and TSR Intensity Collected by Solar PV Surfaces in the Provinces of Mediterranean Region, Türkiye

The second region in Türkiye that receives the most sun is the Mediterranean Region. According to the GEPA (2024), the annual GSR of the Mediterranean region is 1,390 kWh/m², and the annual sunshine duration is 2,956 hours. In this context, the Mediterranean region is in a unique position in terms of solar energy production. However, it is a known fact that this natural wealth is not utilized sufficiently. However, the studies carried out for the Mediterranean provinces on determining OPTAs investigating solar potential, performing the intensity of TSR estimations in geo-referenced conditions, and efficiency of STSs have not been yet at the desired level. A detailed case study is performed for the Mediterranean provinces (Adana, Antalya, Burdur, Hatay, Isparta, Kahramanmaraş, Mersin, and Osmaniye) due to its high potential to develop a solar PV plant, and the OPTAs are determined for provinces where solar PV plants are planned to be installed in the region to collect maximal TSR intensity. So, it is believed that this case study will contribute to the literature for the Mediterranean region in terms of these mentioned subjects. The case study results and conclusions have been presented in Sections 5 and 6.

4.2.1. GSR data utilized in mediterranean case study

GSR is an important energy source in the Mediterranean region because of its geographical position. For many locations, GSR distribution values on horizontal surfaces are available, whereas TSR values collected by tilted surfaces are mostly unavailable. The values of TSR on the horizontal surface can be utilized to calculate TSR collected by a tilted surface with the direction of the beam and diffuse radiation components. In this case study, horizontal GSR data have been obtained from ground and satellite stations in the region, thanks to NASA-SSE. The daily GSR values on a horizontal surface have been provided by NASA-SSE for the Mediterranean region. The GSR distribution map of the region provided by the Turkish State Meteorological Service (TSMS) is shown in Figure 4.3. Provinces of the region are located in the south of Türkiye, and the coordinates and daily GSR values of investigated provinces are presented in Table 4.2.

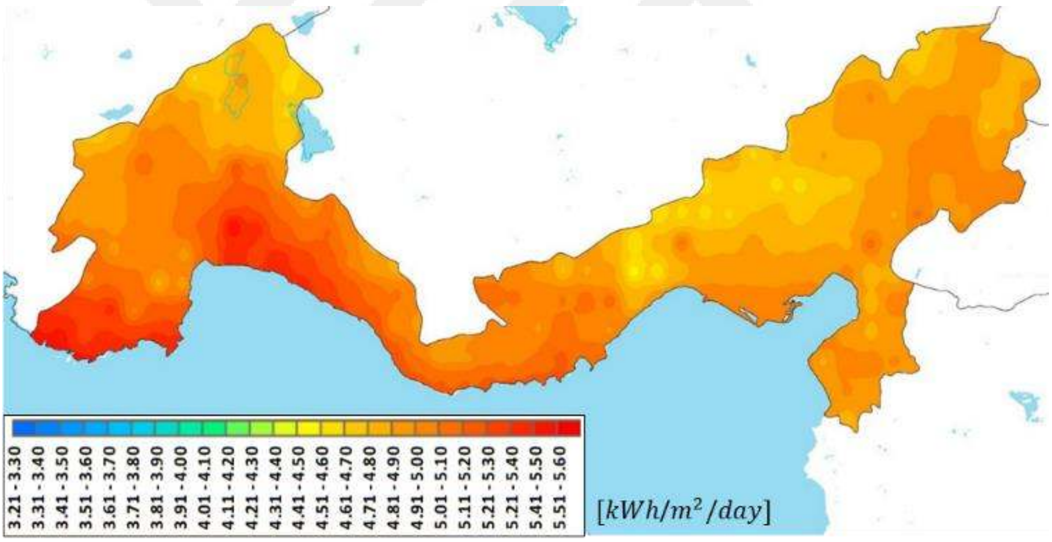

Figure 4.3. GSR distribution of the Mediterranean region (TSMS, 2024).

Table 4.2 Geographic coordinates of provinces in the Mediterranean region of Türkiye

Provinces	Daily GSR [kWh/m²]	Latitude [°]	Longitude [°]	Elevation [°]
Adana	5.05	37.1	35.4	21
Antalya	5.16	36.8	30.6	56
Burdur	4.88	37.8	30.4	919
Hatay	4.73	36.6	36.3	5

Isparta	4.59	37.7	30.5	998
K. Maraş	4.65	37.7	36.8	1,207
Mersin	4.82	36.9	34.5	391
Osmaniye	4.81	36.7	37.3	135

Source: (RETScreen & NASA, 2024).

4.2.2. TSR estimation model utilized in mediterranean case study

In this case study, the RETScreen (2024) analysis model developed by the Minister of Natural Resources Canada is applied to investigate the OPTAs of PV surfaces and to estimate TSR intensity collected by SFS and STS. RETScreen is well well-known solar energy tool due to its understandable structure. The optimization model for OPTAs and the TSR intensities is presented in RETScreen, which is a computer-based solar energy tool. It also presents geographical and meteorological data that allows for the use of the National Aeronautics and Space Administration's Surface Meteorology and Solar Energy (NASA-SSE) climatic database. It is also possible to manually enter climatic data into the system in case of need. It is easy to compare the predicted TSR rate depending on the region of interest, and it offers a rigorous, systematic validation approach. The RETScreen model applies an isotropic transposition clear sky approach to estimate OPTAs and TSR intensity for PV surfaces. The diffuse radiation calculations in RETScreen are based on a similar model to the Klein and Theilacker calculation model with modeling hourly time steps (Banguero et al., 2019; Diken & Kayişoğlu, 2022). The estimation of TSR intensity on a tilted surface for the respective geolocation is utilized by using the presented equations in Section 3.

4.3. Case Study (3): Investigation of Anisotropic Models in Estimating TSR Intensity on Solar PV Surfaces, A Case Study for the Southeastern of Türkiye

The region that receives the most sun in Türkiye is the Southeastern Anatolia Region. The region is the richest region of Türkiye in terms of solar energy. Şanlıurfa province is the most suitable geolocation to invest in producing solar PV plants, selling them to the region and neighboring countries, and providing after-sales technical services. The Southeastern Anatolia Region has the greatest potential to benefit from solar energy among Türkiye's regions. According to GEPA (2024), in Şanlıurfa, the annual total sunshine duration is 3,033 hours, and the annual GSR intensity is 1,586 kWh/m². Therefore, Şanlıurfa province (37.2º'N-38.8º'E) is chosen as it is significantly representative of the climate zone and territories in the Southeastern Anatolia Region. This region is under the continental climatic region classified as 3B-Warm-Dry according to ASHRAE Thermal Climate Zones (ANSI/ASHRAE, 2021; Alawadhi & Phelan, 2022) and experiences year-round high levels of GSR. Despite this province's great solar energy potential, research studies focusing on TSR intensity on PV surfaces are rarely available in the literature. For these reasons, it is expected that this case study will contribute data on TSR for Türkiye's southeastern region to the body of literature. The case study results and conclusions have been presented in Sections 5 and 6.

4.3.1. GSR data utilized in Şanlıurfa case study

GSR data is the most reliable source for efficiently implementing PV plants for specific regions. The TSR data on a tilted PV surface is required for assessing the performance of a solar PV plant. Generally, horizontal GSR data obtained from ground and satellite stations is available and can be utilized to estimate TSR intensity on PV surfaces by applying transposition models. Horizontal GSR data used in this case study have been collected based on the measurements for the period 1984-2005 from METEONORM (2024). METEONORM is a well-known producer for providing accurate historical time series data of GSR and for all relevant meteorological bodies of knowledge needed for planning PV plants in any place on Earth, such as typical years, monthly averages, and hourly time series. Figure 4.4. depicts Şanlıurfa's geolocation on the Türkiye Map and the GSR distribution on the horizontal surface (Ministry of Energy and Natural Resources, 2024). The monthly horizontal GSR values and clearness index ratios from METEONORM (2024) solar data are presented in Table 4.3. According to METEONORM, the annual GSR value is 1811.5 kWh/m². Since the most significant solar parameter is TSR intensity on a tilted PV surface, Table 4.3 reflects that Şanlıurfa province has highly advantageous productivity in terms of solar energy.

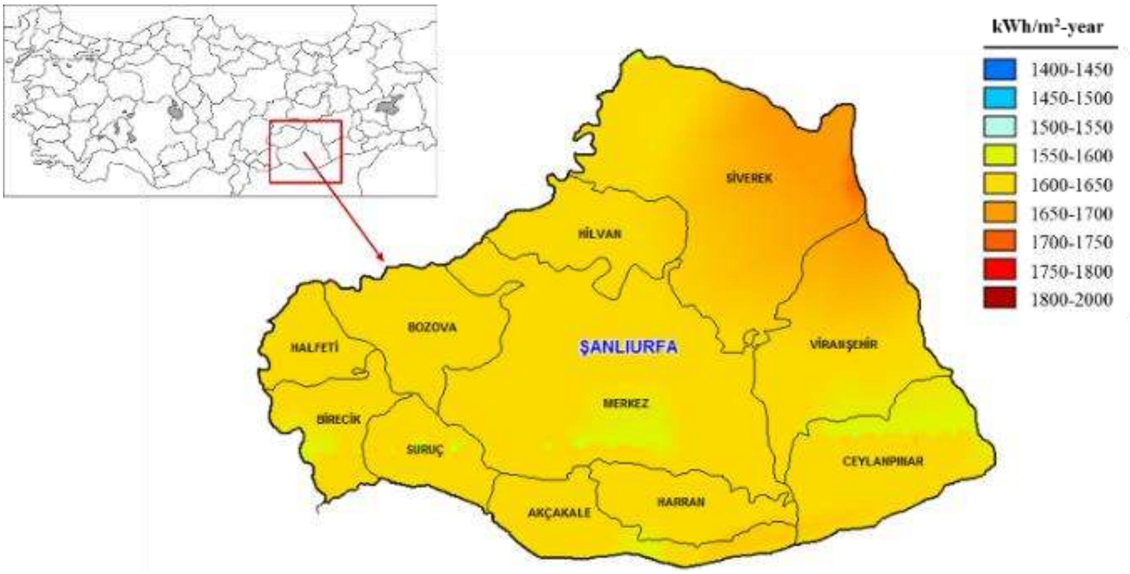

Figure 4.4. GSR distribution of the Şanlıurfa province (Ministry of Energy and Natural Resources, 2024).

Table 4.3. The monthly GSR values on a horizontal surface, and clearness index ratios.

Month	GSR [kWh/m²]	KT [ratio]
1	71	0.5
2	85	0.5
3	137	0.6
4	168	0.6
5	209	0.6
6	232	0.7
7	237	0.7
8	216	0.7
9	176	0.7
10	128	0.6
11	87	0.6
12	69	0.5

Source: (METEONORM, 2024).

4.3.2. Proposed transposition models for the case study of Sanliurfa

Isotropic transposition models have been the basis for numerous studies over the years (Liu & Jordan, 1963). However, recently conducted studies show that anisotropic transposition models yield significantly more precise estimations than isotropic transposition models (Muneer et al. 2003). Therefore, in this case study, globally accepted anisotropic transposition models have been utilized to optimize OPTA and TSR intensity on PV surfaces. The estimation model used in the case study can be divided into two phases. The first phase is the modeling of the diffuse radiation distribution, and the second phase is the modeling of the TSR on the tilted PV surface. The computation of diffuse radiation distribution is based on the Erbs, Klein & Duffie (1982) model. The computation of TSR intensity on a tilted PV surface is based on Hay-Davies (1978), Klucher (1979), Reindl (1990), HDKR (2006), and Perez (1987) anisotropic transposition models. The estimation of TSR intensity on a tilted surface for the respective geolocation is utilized by using the presented equations in Section 3.

4.4. Case Study (4): Maximization of TSR on Solar PV Surfaces in Antalya Province of Türkiye Based on LCOE

The fact that Antalya province, which is located in the southern part of Türkiye and has a high number of sunbathing days, has a high solar energy potential makes this case study even more valuable. According to GEPA (2024), in Antalya province, the annual total sunshine duration is 3,011 hours, and the annual average GSR intensity is 1,646 kWh/m². For this reason, a case study has been focused on the solar energy potential and PV electricity production scenarios based on districts of Antalya province. Solar PV energy investments in Antalya province have the potential to support Türkiye's sustainable energy development. Considering that districts of Antalya province’s biggest sector is summer tourism, investments in solar PV energy have become even more important. The study results and conclusions have been presented in Sections 5 and 6.

4.4.1. GSR data utilized in Antalya case study

Knowledge of GSR distribution is needed for the correct structure and size of solar PV plants. The annual GSR distribution (between 2004 and 2018) provided by the TSMS

(2024) for the Antalya province is illustrated in Figure 4.5. As depicted in Figure 4.5, Antalya has a high GSR distribution. Also, the geographical coordinates and elevations of Antalya districts are presented in Table 4.3. The districts of research interest in this study are established at altitudes very close to sea level except for Manavgat. In this case study, Satellite and ground station interactive meteorological GSR data provided by the NASA-SSE (2024) have been utilized. The daily GSR values on the horizontal surface for the districts of Antalya province are presented in Table 4.4.

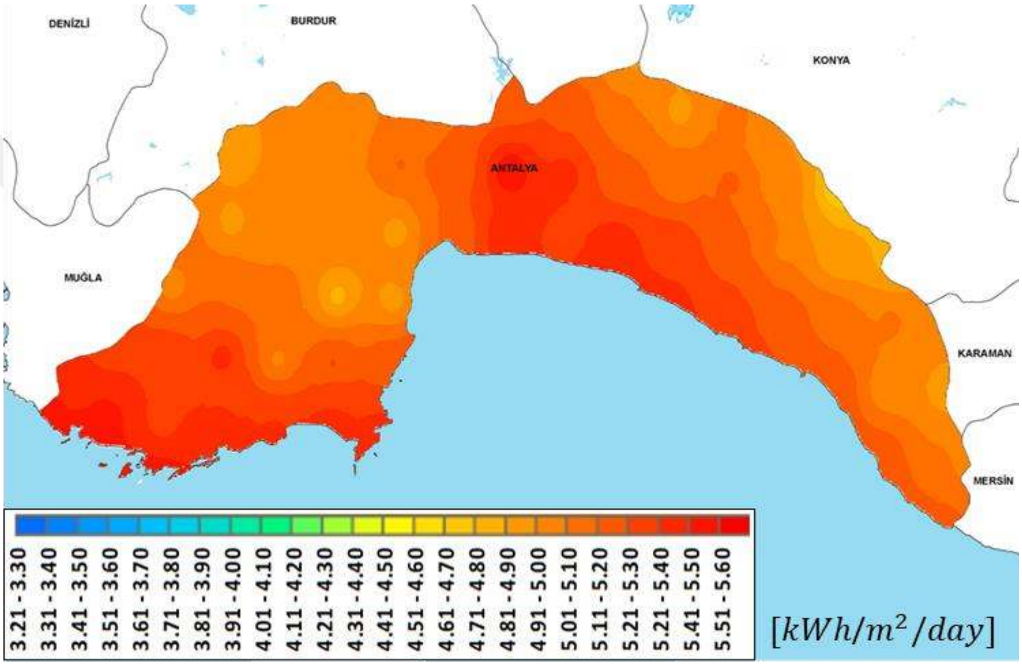

Figure 4.5. Annual average daily GSR distribution of Antalya Province.

Table 4.3. Geographical coordinates and elevations of Antalya districts.

Districts	Latitude [°N]	Longitude [°N]	Elevation [°]
Alanya	36.7	32.1	87
Kaş	36.3	29.7	18
Manavgat	36.7	31.6	271
Muratpaşa	36.8	30.8	46

Source: (RETScreen, 2024).

Table 4.4 Monthly average daily GSR on the horizontal surface [kWh/m²/d].

Month	Alanya	Kaş	Manavgat	Muratpaşa
1	2.17	2.49	2.47	2.08
2	2.89	3.31	3.37	2.89
3	4.01	4.62	4.74	4.11
4	5.05	5.69	5.77	5.13
5	6.37	6.95	7.02	6.12
6	7.46	8.05	8.05	7.18
7	7.43	7.94	7.99	7.17
8	6.62	7.09	7.20	6.33
9	5.43	5.91	6.01	5.29
10	3.85	4.21	4.24	3.80
11	2.49	2.78	2.79	2.57
12	1.86	2.12	2.12	1.86
Annual	4.64	5.11	5.16	4.55

Source: (NASA-SSE, 2024).

4.4.2. Sr estimation models utilized in the Antalya case study

Various estimation methods and simulation programs are used by researchers to determine OPTA and obtain maximal benefit from GSR. In this way, it has become easier to make realistic analyses. RETScreen (2024) is a clean energy management and simulation software developed by the Minister of Natural Resources Canada that calculates using satellite and ground station interactive meteorological data provided by the NASA-SSE (2024). It simulates the optimal hourly, daily, monthly, and annual solar TSR values in different options, depending on the desired geographical region and the clearness index (Uçkan, 2018). So, within the scope of the study, the RETScreen model is preferred to compute the amount of TSR on the tilted surfaces and to find OPTAs of the SFSs and STSs. To measure TSR on a tilted PV surface, GSR is initially measured on a horizontal surface, and collective data of the horizontal surface is used to calculate TSR on a tilted surface. Because the amount of GSR can be varied according to the geolocation, the daily values of GSR on a horizontal surface are the most essential parameter to optimize the OPTA and TSR for PV surfaces. The RETScreen (2024) model is applied based on Duffie and Beckman's (2006) model by utilizing a similar approach to the Klein and Theilacker (1981) algorithm. On the other hand, the algorithm has been extended to solar STSs by using Braun & Mitchell’s (1983) solar geometry equations to investigate maximal TSR.

4.4.3. Investigation of LCOE for solar PV plants

There are various cost and suitability analyses regarding the feasibility of solar energy potential. LCOE is defined as the total present value of a time series of cash flows that includes the initial cost of all system components, component replacement costs occurring throughout the project life, and maintenance cost, that is, the investment cost (Kondili, 2010). When determining energy policies, it is important to determine the benefits and costs of different energy sources and technologies accurately. For this reason, LCOE enables the comparison of production technologies with different energy sources, capacity factors, investment costs, and installed capacity, while also helping to make predictions about electricity prices. When the PV plant investment suitability across Türkiye is evaluated with other provinces, it is seen that Antalya has the lowest reduced LCOE. In this context, the LCOE components payback period (recovery of investment), solar PV energy cost, solar PV plant installation cost, and dependent cost factors have been discussed in this case study, and findings have been presented in Section 5.

4.5. Case Study (5): Estimation of TSR Intensity and OPTAs for PV Surfaces in the Central Anatolia Region of Türkiye by Applying Transposition Models

For maximum electricity production from solar energy, the installations must be performed in provinces with high GSR distribution, clarity index, number of sunny days, and sunshine duration. The fact that the Central Anatolia Region has GSR distribution above the average of some regions in Türkiye and the suitability of the geographical structure of the region creates an opportunity for solar energy investments and forms the basis of this study (Öztürk & Kayabaşı, 2023). The annual GSR intensity of the region is 1,314 kWh/m², and the annual sunshine time is 2,628 hours/year (GEPA, 2024). In this study, the solar energy potential of the provinces in the Central Anatolia Region (Ankara, Eskişehir, Konya, Niğde, Kayser, Sivas, Yozgat, Kırşehir), which is in the middle of Türkiye and a very advantageous position in terms of solar energy potential, was analyzed using isotropic and anisotropic transposition models accepted in the literature. The potential of the region has been comparatively brought to the literature and the case study results and conclusions have been presented in Sections 5 and 6.

4.5.1. GSR data utilized in the case study of the central Anatolia region

In general, GSR intensity on a horizontal surface is available and can be utilized to estimate TSR intensity by applying transposition models. TSR intensity on tilted and tracked PV surfaces is needed for prior analysis and the proper design of PV plants for specific regions. Figure 4.6 shows Central Anatolia's geographical location on the Türkiye Map and the GSR distribution on the horizontal surface within the scope of this case study. Table 4.5 presents geographical positions and annual GSR values on the horizontal surface of the investigated provinces in the Central Anatolia region. It is well understood from Figure 4.6 and Table 4.5 that this region receives a considerable intensity of GSR throughout the year. In this case study, the average measurements for the period from 1984 to 2005 from the METEONORM dataset have been used. METEONORM (2024) is well known for providing accurate historical time series data and all relevant meteorological bodies needed for planning solar PV plants in any place around the world.

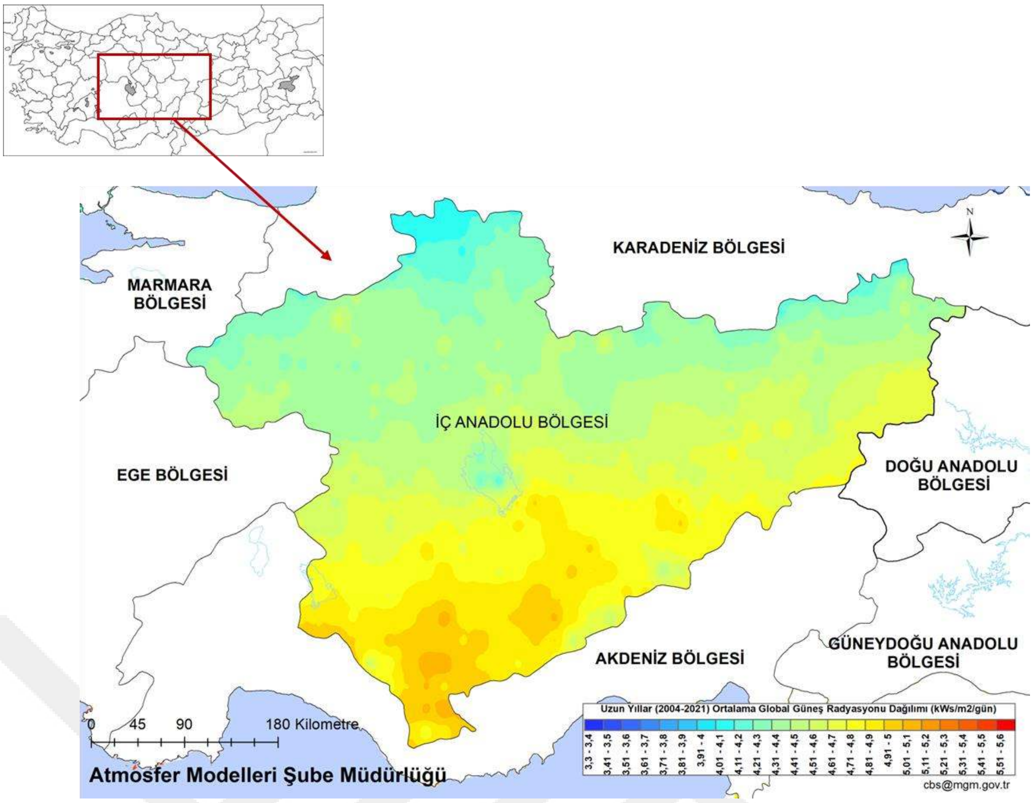

Figure 4.6. GSR distribution of the Central Anatolia region. Source: www.mgm.gov.tr (2024).

Table 4.5. Positions and annual GSR values of the investigated in Central Anatolia.

Province	Latitude [º]	Longitude [º]	Annual GSR [kWh/m²]	Annual Average Temperature [ºC]
Ankara	39.58º'N	32.53º'E	1423.7	11.4
Eskişehir	39.45º'N	30.35º'E	1546.5	11.3
Konya	37.57º'N	32.32º'E	1761.1	12.1
Niğde	37.57º'N	34.41º'E	1965.6	11.2
Kayseri	38.47º'N	35.29º'E	1745.3	10.7
Sivas	39.46º'N	37.02º'E	1536.7	9.7
Yozgat	39.49º'N	34.46º'E	1630.1	10.2
Kırşehir	39.09º'N	34.08º'E	1694.5	12.2

Source: (Nasa, 2024).

4.5.2. Proposed transposition models for the case study of the central Anatolia region

In general, transposition models are categorized into two main types: isotropic and anisotropic models. In this case study, the Liu-Jordan (1960) isotropic and Perez (1990) anisotropic transposition models have been preferred to estimate TSR intensity on PV surfaces. In the Liu-Jordan isotropic model, it is assumed that the diffuse radiation over the sky dome is only isotropic; circumsolar and horizon brightening are taken as zero. Liu-Jordan model has formed the basis of numerous studies over the years. On the other hand, recent studies show that anisotropic models yield significantly more accurate estimations than isotropic models. Thus, the Perez anisotropic model is also applied to the case study region. The OPTA is determined by looking for values at which the TSR on the PV surface is maximal for a certain period. The calculation is done in one-hour increments for all 365 days of the year. The proposed transposition models have also covered the maximization of TSR for STSs by using solar geometry equations presented in Section 3.

4.6. Application Study (1): Transportable Solar Power Production for Rural Electricity Supply: An Application Study of Şanlıurfa

The Southeastern Anatolia Region has the greatest potential to benefit from solar energy among Türkiye's regions. In Şanlıurfa, the annual total sunshine duration is 3,033 hours, and the annual GSR intensity is 1,586 kWh/m² (Kok, 2015; GEPA, 2024). Therefore, Şanlıurfa province (37.2º'N-38.8º'E) is selected as it is significantly representative of the climate zone and territories in the Southeastern Anatolia Region. Şanlıurfa province is one of the most suitable provinces to invest in producing solar energy. Despite this province's great solar energy potential, research studies focusing on solar energy production based on transportable isolated solar PV microgrid developments are rarely available in the literature. That is why, in this application study, the design of isolated PV power production for rural and remote areas with technical simulations has been conducted. For these reasons, it is expected that this case study will contribute data on solar energy production for rural areas in a transportable way. The case study results and conclusions have been presented in Sections 5 and 6.

The microgrid must be easily installed in place where needed. So, the physical dimensions of the microgrid also should be considered to be transportable. For off-grid (isolated) systems with transportable solutions, it is needed to calculate the amount of energy production, and consumption precisely, and the microgrid's load design accordingly. In this study, the emphasis is placed on application and design engineering. In this aspect, this application study offers a different approach and solution to these areas. In the region where an isolated microgrid is planned to be built (Şanlıurfa, Türkiye), the problems persist in rural areas regarding access to electricity. In this application study, priority is given to the production of the necessary energy for grid loads and to reduce dependence on external energy sources (fuel generator, on-grid electricity). Besides, humanitarian migration to the region due to the Syrian war further increased the need for electricity. To our knowledge, there is almost no existing study available in the literature for the off-grid systems in this region. So, a detailed cost-benefit analysis of the microgrid setup for this region has also been made. For all these reasons addressed above, it is planned to establish a transportable isolated microgrid in the region as depicted in Figure 4.7 that provides electricity to refugee camps or rural living areas.

Figure 4.7. 3D drawing of habitat and PV plant.

A simple diagram of an isolated (off-grid) microgrid is represented in Figure 4.8. As detailed in the following sections, a 60.75 kWp PV plant supported with a 16 kVA fuel generator and 105.98 kWh capacity energy storage to meet a 115-kWh load for 20 families is designed considering climate and regional conditions. It has been seen that designing the system by utilizing the findings in the light of technical simulations and setting the PV plant at an OPTA provides an annual energy production of 39.83 MWh. It is calculated that the surfaces adjusted at OPTA throughout the year contribute 10.18% more to the annual energy production, and the payback period of the system becomes 10.67 years. It is foreseen that this study can be used in the areas where refugees and migrants live in camps or rural areas to meet electricity needs.

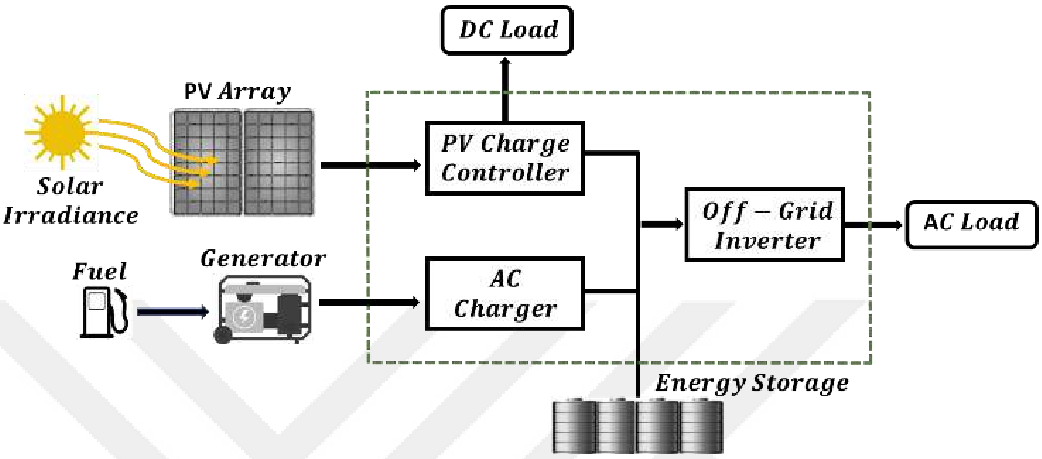

Figure 4.8. A simple diagram of the PV energy model.

4.6.1. Solar climatic conditions and GSR data of the region

PV energy production is influenced by environmental and regional conditions, aside from the technical structure of the microgrid. The horizontal GSR data and PV energy production results used in this part of the application study have been provided by the EU JRC PVGIS (2024) while other climatic parameters have been provided by NASA-SSE (2024). The summary of the climatic conditions of the application region is tabulated in Table 4.6.

Table 4.6. Climatic conditions of the application region.

AVG Temp	**18.2**	**AVG GSR [kWh/m²/day]**	**17.8**
MAX Temp. [°C]	46.6	AVG Soil Temp. [5CM, °C]	20.3
MIN Temp. [°C]	-12.3	AVG Relative Humidity [%]	50.1
AVG Open Days	176.1	AVG Sunny Days [h]	8.6
AVG Daily GSR [kWh/m²]	4.87	Annual GSR [kWh/m²]	1776.58

Source: (NASA, 2024 & EU JRC PVGIS, 2024).

4.6.2. Solar PV plant design

Choosing the correct location for a PV plant is very important to provide a strong impact on energy production. The choice of PV energy technology and storage depends on the balance of energy demand in the microgrid. It also depends on the environmental and meteorological conditions, microgrid structure, and usage purposes. In this section, microgrid design issues related to power and energy are handled with the climatic and radiation parameters of the target region. Also, the load capacity for the microgrid has been discussed and calculated according to needs. The PV electricity production model is shown in Figure 4.8.

4.6.3. Load capacity

The Şanlıurfa province of Southeastern Anatolia region where the microgrid will be installed is a partially rural area that has a dense immigrant and refugee population. Therefore, electricity production is required for humanitarian purposes to meet daily electricity needs as stable. Table 4.7 shows the weekly predicted electricity need of a family of 5 people, and considering the values taken from Table 4.7, the average daily electricity consumption is calculated as 5.75 kWh. In this study, the average daily electricity consumption is considered to be 115 kWh of 20 families, and the PV plant capacity is determined accordingly.

Table 4.7. The weekly electricity requirement of a family.

Appliance	(W)	(h)	Unit	(Wh)	Days	Weekly (Wh)
Refrigerator	44	24	1	1056	7	7392
49" LED TV	98	5	1	490	7	3430
Laptop PC	90	4	2	720	7	5040
Iron	2600	2	1	3200	1	3200
Oven	2500	1.5	1	3750	1	3750
Washer	303	3	1	909	3	2727
Dishwasher	510	2.5	1	1275	4	5100
Vac. Cln.	750	1	1	750	1	750

LEDs	12	5	6	360	7	2520
Toaster	2000	0.25	1	500	2	1000
Kettle	2200	0.2	1	440	7	3080
Microwave	800	0.1	1	80	4	320
Blow Dryer	2200	0.2	1	440	3	1320
FAN+Charger	320	1	1	320	2	640
Weekly predicted energy consumption: 40,269Wh						

4.6.4. PV module technology

PV modules work with chemical-electrical interaction between solar radiation and a semiconductor to collect DC electricity. The amount of electricity is produced directly depending on solar intensity, and the PV module produces PV electricity even in cloudy winter weather. The production rate varies according to the orientation and solar angle. For off-grid systems, it is necessary to make a design according to the worst-case scenario in which the average sunshine duration of the winter months in the region is taken into account for the continuity of the system. So, the climatic conditions must be carefully taken into consideration during the determination of the PV capacity and the PV power of the microgrid has been decided to be 60.75 kWp. The 450 W peak capacity ARCLK-144HC-450W PV surface (2022) is preferred in the model design due to the domestic production, transportable planning, capacity, and dimensions of the microgrid. The PV specs to be used in this study are listed in Table 4.8. When calculations are made including shading according to Table 4.8, it is quite possible to establish a 60.75 kWp off-grid PV plant on an area of 760m^2. Due to its physical dimensions and weight, the developed PV plant can be assembled, disassembled, and transferred to other locations. Array voltage sizing is configured by using a total of 135 PV surfaces in the form of 9 series and 15 strings.

Table 4.8. Specifications of the PV Module (ARCLK-144HC-450)

Electrical Data	
Nominal Power (Wp)	450 Wp
Power Tolerance (W)	+5 W
Open Circuit Voltage (Voc)	49.27 V
Short Circuit Current (Isc)	11.53 A
Module Efficiency (%)	20.7 %
Max Power Voltage (Vmax)	41.37 V
Max Current Voltage (Imax)	10.88 A
Max System Voltage (V)	1,500 V
Max Series Fuse (A)	20 A
Thermal and Mechanical Data	
Operating Temperature (°C)	(−40°C to +85°C)
Solar Cells	144, Monocrystalline
Junction Box	IP-68, MC4
Surface Dimension (H/W/D)	2,094x1,038x35 mm

Source: (Vestel A.Ş., 2022).

4.6.5. ES, CCU, battery type, and off-grid inverter

The ES (battery) specifications and the experience of the system designs are typically quite important, although each ES technology has advantages for certain solar and UPS applications. If the ES is sized suitably to deliver the expected design life considering the operating temperature range, it can provide excellent performance. The battery should be the size of shallower average depth of discharge and a higher cycle life rating should be chosen to maximize the service life of the ES. Lithium Iron Phosphate ($LiFePO_4$) battery for renewable energy technology is preferred owing to its high energy density, long cycle, standby life, low self-discharge, tolerance to heat during operation, and high efficiency (Torreglosa et al., 2014). ES capacity is configured by using 3.2V 230AH batteries in series. A total of 144 batteries are used and a capacity of 105.98kW is reached. In the storage of surplus energy produced by the PV, the charge control unit (CCU) protects the battery's efficiency and lifespan by preventing the batteries from overheating and overcharging. The technical specification of the all-in-one centralized Energy Management System (EMS) including the batteries, CCU, and off-grid solar inverter to be planned for use in the microgrid is introduced in Table 4.9 (Zhejiang Sandi Electric Ltd., 2022).

Table 4.9. Technical specifications of the ES and solar CCU.

Battery Parameters	
Cell type, rated capacity, cycles	LiFePO4, 105.98kWh, 5000
Battery Configuration	3.2V, 230Ah, 144Pcs in series
Nominal capacity, nominal voltage	230Ah, 460V
Charge voltage, charge current	504Vdc, 115A
Discharge voltage, discharge current	389Vdc, 115A
Charge and discharge temp range	1~45℃, -10~45℃
Solar Charge Controller Parameters	
Max input voltage and power of PV	<900Vdc, 50kW
Battery system voltage	460Vdc
Max charge current	80A
Charging and recovery voltage	511.2Vdc, 486.5Vdc
Overvoltage disconnect and reconnect	569.4Vdc, 525.6Vdc
Undervoltage recovery and disconnect	432Vdc, 374Vdc
Working temperature	-10~45℃
Inverter Parameters	
Rated Power and isolation mode	50kW, LFT
DC input rated voltage and current	360Vdc, 139A
DC Input voltage range	324~480V
AC output rated voltage and current	380V±3%, 76A
AC output voltage range	220-480VAC (optional)
Output frequency	50Hz / 60Hz
Inverter efficiency	>93%
Power factor and phases	0.99, 3 phases

Overload ability and cooling	150%,10s, FAN-cooled
Method of working	Working continuously
Working temperature	-20~+50℃

Source: (Zhejiang Sandi Electric Ltd., 2022).

A centralized EMS system has advantages in terms of control, maintenance, cost, and space-saving installation. From a technical point of view, EMS centrally manages charge and discharge, effectively controls the charge and discharge current within the cell usage conditions, protects the cell, and extends the service life. The ES (battery) autonomy is the time during which the load can be met with the ES alone without any solar inputs (Romana et al., 2018). It is a function of battery charge state, load size, and capacity. The ES should ensure the energy demand during the night; therefore, the ES autonomy has been calculated to average 10.5 hours. It is more cost-effective to combine an ES with a fuel generator. If the PV array cannot produce enough energy, ES and the fuel generator are capable of meeting the load during cloudy, rainy, or night periods in an autonomous system (Samadi & Singh, 2014). The number of autonomy days depends on the system, location, and total load. The system autonomy has been taken into account as 3 days for microgrid load.

4.6.6. Fuel generator

In stand-alone (isolated) PV microgrid systems, it is an inevitable necessity to have a fuel generator to prevent the energy continuity and fluctuations of the system. Therefore, a 16 kVA diesel engine is integrated into a designed microgrid to use a secondary power supply and provide fault tolerance. The diesel generator planned to be used in the developed microgrid is presented in Table 4.10 (KARJEN, 2022). The generator's fuel tank capacity of 143 liters, and the fuel consumption is 4.2 liters per hour under 100% load.

Table 4.10. Technical specifications of the diesel generator.

Stand-by and prime power [kVA-kW]	16-13, 14-11
Power factor [Cos φ] and frequency [Hz]	0.8, 50

Fuel Consumption 100%, and %50 loaded [Lt/h]	4.2, 2.1
Fuel tank capacity [Lt]	143
Alternator voltage [V]	231/400
Dimensions LxWxH [mm]	2000x900x1500

Source: (KARJEN Karadeniz Generator, 2022).

4.6.7. Energy losses of the PV plant

Various methods have been developed in the literature to calculate energy losses. Total miscellaneous losses such as cable, angle of incidence, and spectral effects are assumed for this analysis ~3% (Kumar & Sudhakar, 2015). The total system losses are assumed ~14%, and the PV losses due to temperature and irradiance effects are assumed ~8% (European Commission, 2021). In off-grid PV plants, transmission, and distribution losses (T&D losses) are expected to be <1% due to the small installation area and limited load capacity. The energy loss parameters used in the study are stated in Table 4.11.

Table 4.11. Estimation of energy losses.

System losses	~14%
Inverter losses	~2%
Miscellaneous losses	~3%
T&D losses	<1%

Source: (Kumar & Sudhakar, 2015 & European Commission, 2021).

4.6.8. Regional simulation

PV electricity production fluctuates during the days of the year and production capacity depends on solar climatic data of the region. The provided inputs and simulation outputs of the location are presented in Table 4.12. The developed microgrid is primarily intended to be used in the Şanlıurfa province. For this reason, the microgrid has been simulated under the target location conditions using the EU PVGIS application.

Table 4.12. Inputs and simulation outputs of the application region.

Inputs & Outputs	Values
Location [Lat/Lon]	37.029, 37.973
Database used, Horizon	PVGIS-SARAH, Calculated
PV installed [Wp]	60.750
Battery capacity [Wh]	105.980
Discharge cutoff limit [%]	10
Consumption per day [Wh]	115.000
Tilt and azimuth angles [°]	33 / 0
Percentage days with full battery [%]	86.47
Percentage days with empty battery [%]	15.95
Average energy not captured [Wh]	141,061.08
Average energy missing [Wh]	36,600.55

4.6.9. Matlab simulation of the designed microgrid

MATLAB Simulink is a good simulation technique to control power electronics components under some scenarios and test system architectures before implementation. In stand-alone microgrids, EMS aids in the efficient use of Distributed Energy Resources (DER). In this section, DER consists of energy storage, diesel engine, and PV energy versus the load of the microgrid is simulated based on technical constraints and solar climatic data by using a heuristic state machine strategy (Alberto & Simao, 2013), and the adaptive zero-crossing algorithm (Đurić & Đurišić, 2005). An overview of the designed microgrid model in MATLAB/Simulink is shown in Figure 4.9, and general parameters and values used in the simulation are presented in Table 4.13.

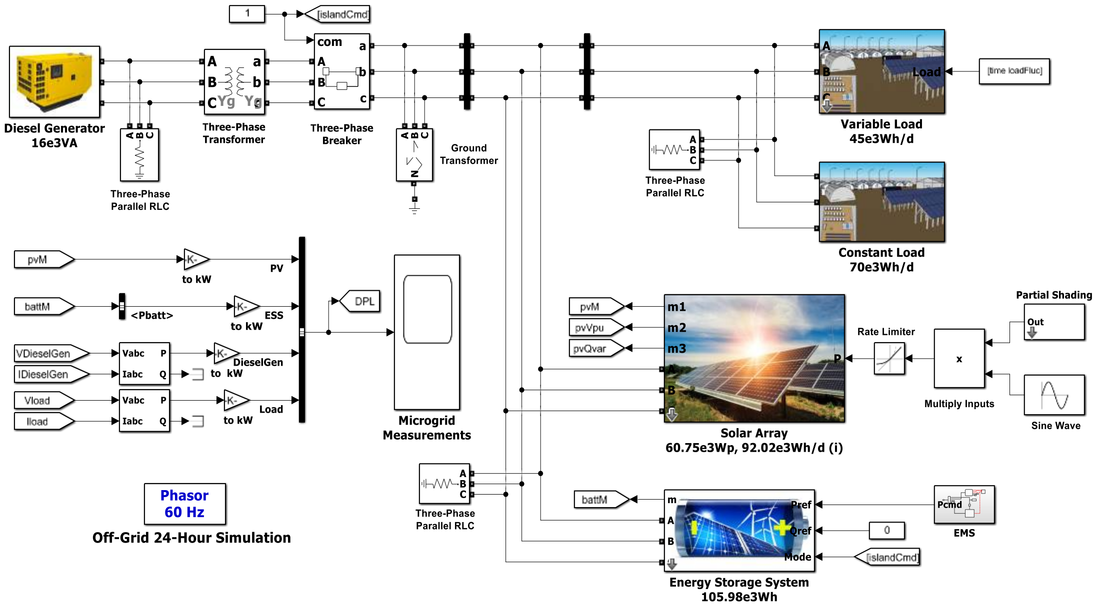

Figure 4.9. Overview of the simulation model in MATLAB.

Table 4.13. General parameters and values used in the simulation.

Total AVG daily load	**115kWh/d**
Solar array capacity	59.9kWp
AVG daily PV energy production in January	92.06kWh/d
Generator rated power	10kVA
Microgrid frequency	50Hz
ES rated capacity	105.98kWh
ES SOC to recharge	10%
ES recharge rate	50%
ES initial state-of-charge	50%
ES upper/lower charge limits	90-10%

4.6.10. Cost Parameters of the Designed Microgrid

One of the aims of this study is to serve humanitarian purposes such as refugee camps by providing stable electricity to rural areas where access to electricity is very difficult, very expensive, or not at all rather than economic benefit. The cost of a microgrid project is highly important. Although the off-grid PV plant increases the cost, its humanitarian benefits have helped non-commercial donors to be positive about the cost of the system. Besides, climatic data availability in simulations is also helpful in predicting system performance and microgrid lifespan. The total cost of the microgrid consists of power system components (PV, inverter, ES, CCU, etc.), diesel generator, feasibility studies, development, engineering, transmission, and periodic maintenance. Determination of a budget for operations and maintenance (O&M) is essential for an off-grid PV plant (Canada et al., 2005; Steffen et al., 2020). O&M cost consists of preventive and corrective activities such as structure, cable connection, inspection, cleaning, repairing, and replacing PV surfaces, inverters, batteries, etc. O&M cost of small PV plants is ~ 1-2% of the total initial cost (European Commission, 2021). The cost of the PV power system components and the total cost of the PV plant are given in Tables 4.14 and 4.15, respectively. The total cost is high mainly due to battery costs in the microgrid. Batteries need to be replaced depending on the battery's technical specifications. Since a 5000-cycle life is equivalent to 12-13 years of operation, just a one-time battery replacement is needed over the 25-year life of the microgrid (McKeon et al. 2014).

Table 4.14. Cost of the PV power components of the designed microgrid.

Product	**QTY**	**Unit Cost ($)**	**Total Cost ($)**
ARCLK-144HC-450W PV array	135	187	25,245
EMS (all in one) 50kW off-grid smart inverter, CCU, 105.98kWh LiFePO4 lithium battery	1	17,500	17,500
6mm solar cable	400	1.5	600
Galvanized steel construction	135	22	2,970
MC+ solar PV connectors	set	288	288
Battery connection (jump) cables	set	128	128
The total cost of the power system components (USD)			46,731

Table 4.15. The total cost of the isolated microgrid.

Initial Cost Items	Cost (USD)
Feasibility study	750
Development	1,250
Engineering	1,900
Transmission line	750
PV Power system components	46,731
Diesel Generator	5,750
Annual O&M cost	935

4.6.11. Payback period and lifespan estimation

The average time to gain back the total microgrid cost (payback period) is an indicator of how long is expected to return the initial investment of the microgrid. When evaluated in terms of cost-benefit analysis, the smaller the payback period is the more desirable for investors or donors (Sharma et al. 2015). It is seen from the studies; that the lifespan of PV modules is beyond 25 years and current ones can likely improve their lifespan further. It is expected to have a 30-year lifespan or more (Dunlop et al., 2005; Skoczek et al., 2009). It should not be ignored that PV plants continue to produce after 25 years. Also, it is possible to increase the lifespan of the PV plants with the O&M activities.

4.7. Experimental Study (1): Optimization of OPTA and TSR on PV Surfaces: An Experimental Study in Malatya Province of Türkiye

Case studies should be supported with experimental or implementation studies, and the practical implications of theoretical studies should be evaluated. Comparing predicted and actual solar energy production results will help to find the most accurate prediction models and process them into the literature will not only contribute to academic and scientific studies in this field but will also make a significant contribution to the pre-analysis and feasibility studies of solar PV plant installations. Eastern Anatolia region is one of the richest regions of Türkiye in terms of solar energy production. Malatya is one of the most suitable provinces in the Eastern Anatolia region to invest in producing solar PV plants. According to GEPA (2024), in Malatya, the sunshine duration is 2,873 hours, and the annual GSR intensity is 1,599 kWh/m². Thus, Malatya province (38.4°'N-38.1°'E) is chosen as it is significantly representative of the climate zone and territories in Eastern Anatolia. Despite this province having considerable solar energy potential, research studies focusing on TSR intensity on PV surfaces are rarely available in the literature. It can even be said that this implementation study provides a study that is absent in the literature: The results of the actual implementation data have been carried out on an N-S-oriented one-axis STS at the solar climatic conditions of Malatya province. For these reasons, it is expected that this application (experimental) study will contribute data on TSR for Eastern Anatolia and Malatya province to the body of literature.

Grid-connected PV plants have become the best alternatives to solar energy on a large scale. Performance analysis of solar PV systems could provide essential data in the design and operation of new solar PV systems. To optimize the GSR, PV surfaces are generally equipped with an STS. In this section, the field performance of an 11.8 kWp PV system integrated with horizontal one-axis N-S aligned STS and an 11.8 kWp PV system integrated with annual SFS have been designed and studied in the solar climatic conditions in Malatya province of Türkiye since PV energy is being considered as a feasible option for distributed energy production. This implementation study results and conclusions have been presented in Sections 5 and 6. So, it is expected that this experimental application study will not only provide invaluable information and tools for Turkish PV industries and researchers but also offer helpful prediction methodologies for PV implementations in other countries. It can be summarized that this implementation study investigates solar PV plant performances in Malatya Turkey, by using yearlong recorded production data from the PV plant geolocation. Actual implementation images taken from the field are presented in Figure 4.10.

Figure 4.10. a) Images taken from the implementation field (Malatya, 2024).

Figure 4.10. b) Images taken from the implementation field (Malatya, 2024).

4.7.1. Geolocation and GSR data utilized in Malatya implementation study

Choosing the correct location for a solar PV plant is very important to provide a strong impact on energy production, and location selection needs to assess some characteristics for the installation of solar PV plants. Temperature effects, GSR intensity, economic aspects, and land use are important ones. GSR intensity is an essential key for productivity. PV modules are temperature sensitive; the PV module efficiency is higher at low temperatures. The land cost in the non-agricultural and mountainous regions is usually cheaper. As introduced in earlier sections, the GSR data on the horizontal surface is the most reliable source for efficiently implementing PV plants for specific regions. The TSR data on a tilted PV surface is required for assessing the performance of a solar PV plant. In general, horizontal GSR data obtained from ground and satellite stations is available and can be utilized to estimate TSR intensity on PV surfaces by applying transposition models. In this implementation study, the horizontal GSR data on the horizontal surface have been obtained from ground and satellite stations in the region, thanks to NASA-SSE (2024). The daily GSR values on a horizontal surface are provided by NASA-SSE for the implementation site of the Malatya province. The long-term (1999-2018) yearly GSR on the horizontal surface in Malatya province is given in Figure 4.11. The monthly horizontal GSR values and clearness index ratios from NASA-SSE (2024) solar data are presented in Figure 4.12 in graphical form.

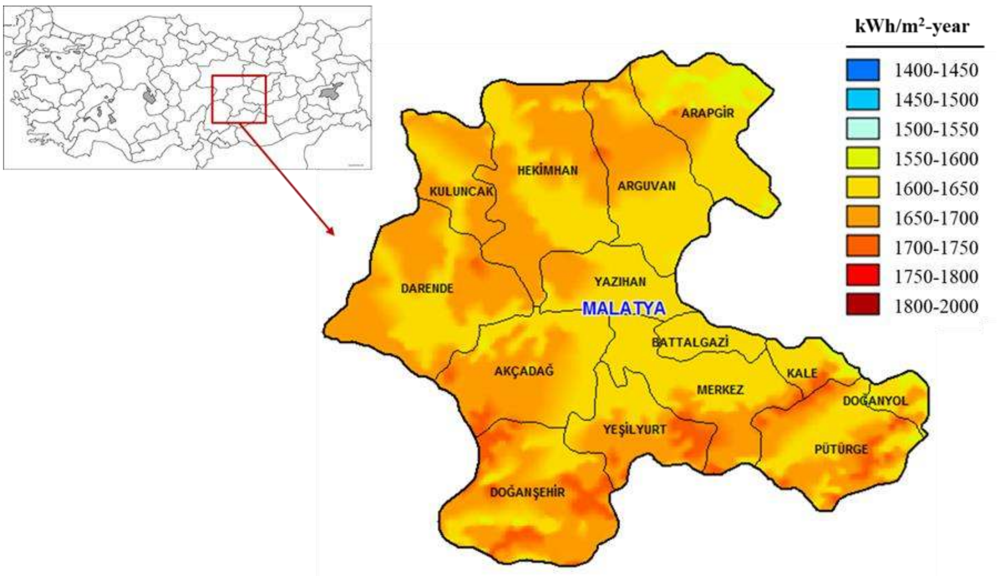

Figure 4.11. The long-term yearly average of GSR on horizontal surfaces in Malatya. (GEPA, 2024).

Experimental (actual) PV electricity production data has been produced under the conditions of Malatya province daily and monthly periods during the years 2022 and 2023 of total 24 full months. The research and process were carried out at the Hasan Kalyoncu University of Gaziantep, Türkiye. The performance of both annual tilted SFS and one-axis horizontal STS in the Malatya province of Turkey has been investigated by using yearlong recorded actual energy production data from the PV both PV systems.

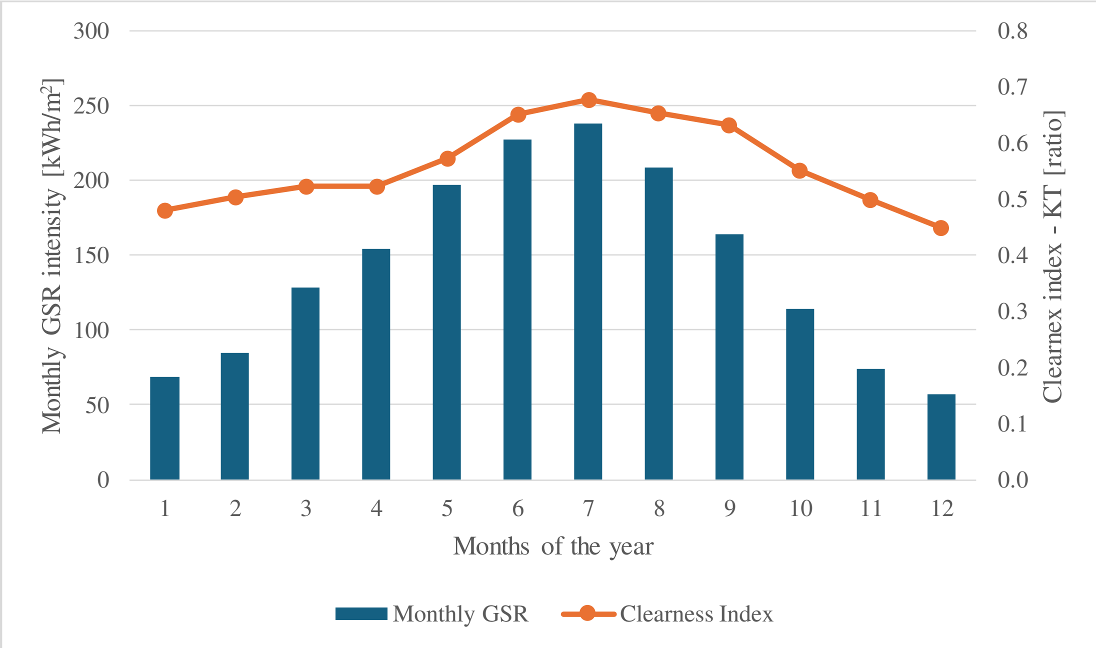

Figure 4.12. Monthly horizontal GSR values and clearness index ratios for Malatya (NASA-SSE, 2024).

4.7.2. Transposition models for the implementation study

In this implementation study, the Hay-Davies (1978) and Perez (1990) anisotropic transposition models have been proposed to estimate TSR intensity on PV surfaces. In the isotropic models, it is assumed that the diffuse radiation over the sky dome is only isotropic; circumsolar and horizon brightening are taken as zero. The isotropic models model has formed the basis of numerous scientific studies for many years. However, recent studies show that anisotropic models yield significantly more accurate estimations than isotropic models. Therefore, the Hay-Davies and Perez anisotropic models have been applied to the implementation study region. The OPTA is determined by looking for values at which the TSR on the PV surface is maximal for a certain period. The calculation is done in one-hour increments for all 365 days of the year. The proposed anisotropic transposition models have also covered the maximization of TSR for STSs by using solar geometry equations presented in Section 3.

Transposition is the calculation of the incident TSR on a tilted PV surface from the horizontal GSR data. The Hay-Davies model is a classic model, and the Perez model is a more sophisticated model requiring well-measured horizontal GSR data. A transposition model is separately calculated for each solar radiation component. The beam component involves a purely geometrical transformation that doesn't involve any physical assumptions. These two models differ in the diffuse component transformation. In the Hay-Davies model, the diffuse radiation is divided into an isotropic part and a circumsolar part, which is proportional to the beam component. Through transposition, the isotropic part is reduced according to the solid angle seen by the PV surface. The circumsolar part is transposed geometrically as the beam component. In the Hay-Davies model, the circumsolar fraction is identified, which is chosen as the clearness index of the beam component. The Perez model introduces the horizon band as a third diffuse component. It divides the sky into sectors and parametrizes the transformations of the circumsolar and horizon bands according to correlations established based on serial data. The albedo component is evaluated in the same manner in both models, as a given fraction of the global, weighted between the horizontal and the tilted plane extension. The Perez model is more complex and especially sensitive to a realistic determination of diffuse radiation when measured GSR data is available. The Perez model usually gives yearly averages higher than the Hay model, of the order of 0% to 2%, depending on the climate and the plane orientation (Pvsyst, 2024).

4.7.3. Design strategies and general specifications

Grid-connected solar PV plants are the most effective production way of PV electricity as there are no ES losses. The grid-connected PV plants are designed to supply the excess PV electricity beyond consumption to the public grid. Recent studies show that maximum power point tracking (MPPT) with a regulator or STS (Oclon et al., 2020) is integrated into the PV plants to improve the TSR intensity. Moreover, the performance of STSs can be improved by utilizing MPPT-based solar inverters (Kumar et al., 2020). STSs allow the capture of more TSR intensity by maintaining the PV surface approximately perpendicular to the source for a longer period (Seme et al., 2017). These strategies help to increase the performance of the solar PV plant (Xiaoqiang et al., 2021). STSs maximize energy production and increase the intensity of TSR between 15% and 45% compared to other SFS of equal power (Soulayman et al., 2021). Currently, one-axis STSs have a greater yield in electricity production because they follow the orbit of the sun in synchronized movement across the horizontal axes with control algorithms (Motahhir et al., 2020). One of the important aspects of one-axis STS is that they can follow the orbit of the sun horizontally employing motors or actuators, making their operation more precise (Sidek et al., 2017). Wind loads are a significant issue for any type of solar PV plant in some locations. The STSs are more sensitive to wind loads, and this is a major disadvantage (Shingleton, 2008).

The N-S-oriented one-axis STS has a higher ground coverage rate than the two-axis STS, and the one-axis STS is much less complex to install than the two-axis STS, which reduces the overall cost of implementation. The control unit of the one-axis STS is less sophisticated than the two-axis STS, which also reduces the cost of development. Although wind loads can be an issue for any type of solar PV plant, the high installation of the two-axis STS compared to the one-axis STS causes it to be more affected by wind loads. For these reasons, the use of one-axis STSs is much more widespread than two-axis STSs. So, in this section, an N-S-oriented one-axis horizontal STS is implemented to take advantage of this kind of STS as presented in a schematic representation in Figure 3.4. The SFS and STS PV systems are structured cost-effectively and reliably. During nights, because there will be no PV energy production due to a lack of GSR, the energy is taken back from the grid for internal requirements. To control the STSs, several control strategies are used, such as ON-OFF, PI, PLC, PID, etc. In this implementation study, a mathematical control algorithm is used as the tracking method that calculates the instantaneous angle of the sun. The control strategy is implemented in C++ programming language by using an advanced solar position algorithm (SPA). This control strategy is organized the search for the maximum GSR of the PV modules on the one-axis STS to find the point of maximum power. Ultimately, the geolocation systems have been implemented side by side with the same type of components such as PV modules, inverter control parts, and so on. So most factors are the same such as GSR, ambient temperature, and climatic density. The general features of the developed PV systems are listed as follows.

- The STS follows the sun on a single axis.
- The mathematical method that calculates the instantaneous angle of the sun is used as the tracking method.
- There is no light sensor, timed sun tracking device, or similar equipment on the STS.
- The implementations comprise an 11.8 kWp structural SFS and an 11.8 kWp one-axis STS.
- 18 units of 330 W solar PV surfaces and a 10-kW on-grid inverter are used for each PV plant.
- The sun tracking angle range of the system is 60º in each direction, up to 120º in total.
- The accuracy of instant tracking of the sun's position is below 1º.
- The STS ECU communicates wirelessly with the central unit.
- The STS is machined to be resistant to wind and rain.
- Reducer and DC engines are used on the STS.
- Push mechanisms containing linear motors, actuators, pneumatic, hydraulic, or piston elements are not used.
- A dedicated server is available for control and data collection. Actual production data are taken every 20 seconds.
- The system can withstand wind speeds of 100 km per hour following the TS498 standard.

4.7.4. Solar PV system designs

The Malatya province's mentioned geolocation is selected for the proposed solar PV systems. The performance of solar PV plants is not only related to depends on the environmental and meteorological conditions, but also depends on the PV manufacturing features, design factors, and the technology being used in the PV plant technical structure. In this section, solar PV system design issues related to power and energy are handled with the climatic and radiation parameters of the target geolocation. In this context, two different grid-connected PV systems, which are SFS and STS, have been designed to perform comparisons and analyze the actual results. The 11.8 kWp PV system equipped with horizontal one-axis NS-oriented STS and the 11.8 kWp PV system equipped with annual tilted SFS have been designed in the meteorological conditions in Malatya province of Türkiye. The PV modules are mounted on the SFS at OPTA of 33º, facing south. The orientation angle is 0◦. It is also noted that OPTA cannot be adjusted for security and protection reasons for the horizontal one-axis STSs designed on a large scale as in this study. So, adjusting the OPTA constant at 0º is a result of physical construction. The SFS-constructed PV energy production model is shown in Figure 4.13. Moreover, the one-axis STS-constructed PV energy production model is shown in Figure 4.14.

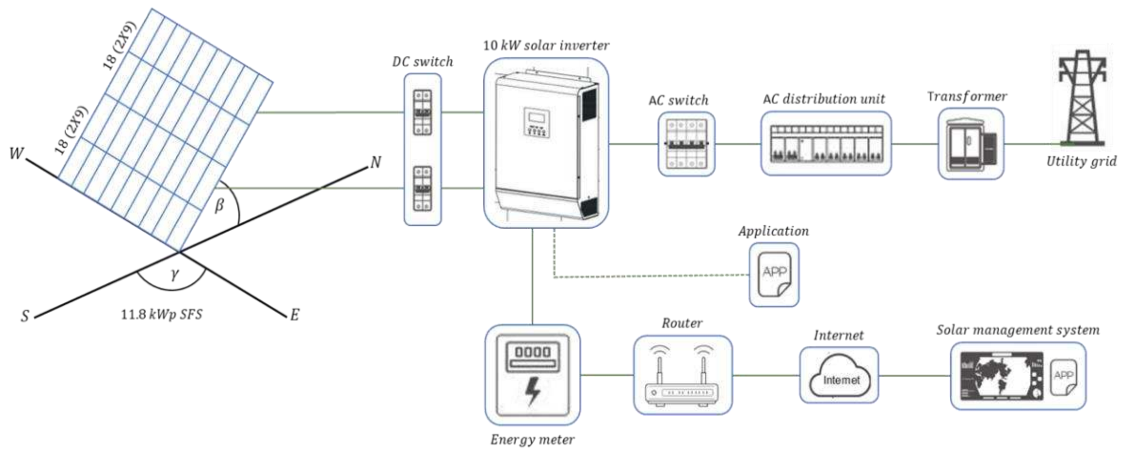

Figure 4.13. SFS constructed a PV electricity production model.

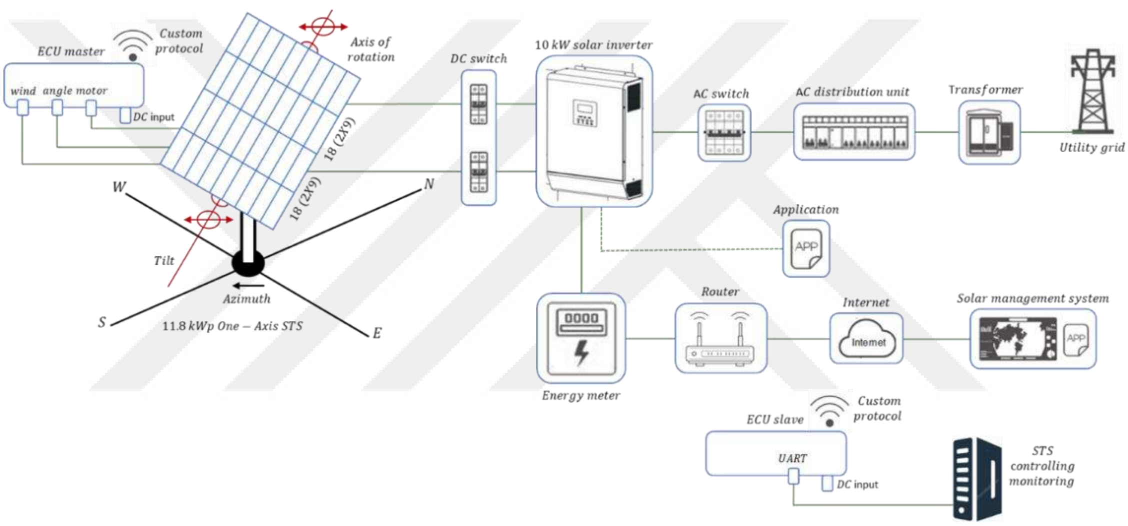

Figure 4.14. One-axis STS constructed a PV electricity production model.

4.7.5. PV module technology integrated in PV plant design

PV modules work with chemical-electrical interaction between solar radiation and a semiconductor to collect DC electricity. The electricity is produced directly depending on GSR, and a PV module produces PV electricity even in all seasons like cloudy winter weather. The energy production rate varies according to environmental, climatic, and technical parameters. For easy transportation and effective utilization, the PV power of PV systems has been decided to be 11.8 kWp. The 72-cell polycrystalline 330 Wp capacity (Alfa Solar Energy A3S72P, 2021) modules have been utilized in the PV plant design due to the domestic production, cost-effectiveness, and high efficiency. The technical specifications of the PV module used in these solar PV plants are tabulated in

Table X.X. Solar PV systems' voltage and capacity sizing are configured by using a total of 36 PV modules using two-unit Maximum power point tracking (MPPT) sockets. So, there are 18 PV modules in each MPPT. That is, each of the proposed PV systems consists of 36 PV modules. The number of modules in a string is 18. The number of strings in the PV array is 2. Polycrystalline solar modules are a good fit for the proposed PV systems. The PV modules with a 330-watt power rating manufactured in Turkey are chosen because of their easy availability and reduced cost. The energy efficiency for the proposed solar PV system is an average of 16.92%. The specifications of the utilized PV Module are presented in Table 4.16.

Table 4.16. Specifications of the PV Module (A3S72P).

Electrical Data	
Nominal Power (Wp)	330
Power Tolerance (W)	
Open Circuit Voltage (Voc)	46.60
Short Circuit Current (Isc)	9.12
Module Efficiency (%)	16.92
Max Power Voltage (Vmax)	38.38
Max Power Current (Imax)	8.60
Max System Voltage (V)	DC 1000/1500
Series Fuse Rating (A)	15
Thermal and Mechanical Data	
Nominal Operating Cell Temperature (°C)	(44°C ± 2°C)
Solar Cells	72, Polycrystalline, Type 6
Junction Box	Tyco, IP-68, MC4
Surface Dimension (mm) (L/W/D)	1957x997x42

Source: (Alfa Solar Energy, 2021).

4.7.6. On-grid inverter used in implementation study

Central inverter provides high reliability, and simplicity in implementation. A centralized on-grid inverter has advantages in terms of control, maintenance, cost, and space-saving installation. From a technical point of view, the inverter centrally manages current within the cell usage conditions, protects the cell, and extends the service life of the PV system. Central inverters of 10 kWp nominal ratings are chosen for each solar PV system. The energy produced from the PV systems of the location is converted to AC output using the on-grid inverter. The number of inverters needed for the proposed solar PV plants is 2. For implemented PV systems smart, efficient, safe, and reliable inverter type is chosen (SUN2000-10KTL). The technical specifications of the selected inverter are given in Table 4.17.

Table 4.17. The technical specifications of the implemented SUN2000-10KTL on-grid inverter.

Efficiency	
Max. Efficiency	98.6%
European efficiency	98.1%
Input	
Max. input voltage	1,100 V
Max. current per MPPT	13.5 A
Max short circuit current per MPPT	19.5 A
MPPT operating voltage range	140 V ~ 980 V
Number of inputs & MPPT trackers	2, 1
Output	
Max-rated AC active power & apparent power	10000 W, 11000 VA
Max. AC active power (cos φ=1)	66000 W
Rated output voltage	220 V AC/380 V AC, 230 V AC/400 V AC
Rated AC grid frequency	50 Hz / 60 Hz
Max. output current	16.9 A
Adjustable power factor range	0.8 leading... 0.8 lagging
Max. total harmonic distortion	≤3%

Protection & Communication	
Display	LED Indicators; WLAN + Fusion Solar app
RS485, USB, WLAN/Ethernet	Yes
Monitoring BUS (MBUS)	Yes
General Specification	
Dimensions (W x H x D)	525mm x 470mm x 146.5mm
Operating temperature range	(-25°C ~ 60°C, -13°F ~ 140°F)
DC & AC connectors	Amphenol Helios H4, Waterproof PG terminal
Protection degree & topology	IP65, Transformerless
Nighttime power consumption	< 5.5 W

4.7.7. Implementation of the STS movement mechanism

The STS consists of a transmission system, a reducer, a DC engine and drivers, and an ECU. It uses a single engine, which rotates the PV modules from East to West on a horizontal axis, following the daily motion of the Sun. Its rotation range is ±60° concerning the horizontal (0°). There is no light sensor, timed device, or similar equipment on the STS. The STS is moved around the central shaft of the carrier system mounted on STS steel legs, utilizing a high-power engine and reducer. The amount of mechanical power produced in the engine is increased on the reducer and transferred to the main rotation shaft. This process is achieved by reducing the engine speed by the amount of the reducer gear ratio and simultaneously increasing the output torque value. The operating voltage of the DC engine is 24 volts. When this voltage is applied to the motor, the motor starts to move. The gear structure inside the engine has a ratio of 580:1. Thanks to this ratio, the torque value produced at the engine output is increased by 580 times, while the number of revolutions is reduced by 580 times. These values are increased by 62 times thanks to the additional reducer ratio of 62:1 connected to the output of the engine's gear block. Ultimately, a power of 3,000 Nm tilt moment torque is achieved at the main output of the worm gear, rotating at a speed of 0.048 RPM. Thanks to this power, the main shaft and the solar panels on it can be moved easily by applying very little electrical energy (24V x 1.2A = 28.8W) to the engine. Slewing drive performance data and planetary reducer performance data are tabulated in Table 4.18.

Table 4.18. Slewing drive performance data and planetary reducer performance data.

Slewing Drive Performance Data		
Rated Output Speed	0.048 rpm	
Rated Output Torque	600 N.m	443 1bf.ft
Tilting Moment Torque (Max)	3000 N.m	2212.5 1bf.ft
Holding Torque	5500 N.m	4056.25 1bf.ft
Axial Load (Max)	45 kN	10116 1bf
Radial Load (Max)	22 kN	4945.6 1bf
The ratio of Wprm Gear	62:01:00	
Tracking Precision	≤0.2	
Planetary Reducer Performance Data		
Rated Voltage	24 VDC	
Rated Current	<1.2 A	
Gear Ratio	580: !	
Noises	≤60 dB	
IP Class	IP54	
Temperature	-40 & +80 C	

4.7.8. Development of control and communication mechanism

To develop a useful STS, the electrical control unit must give an accurate control signal to the mechanical system, it must be reliable, and it must have low power consumption. The one-axis STS requires sophisticated software development for the ECU to adjust the position of the PV modules throughout the day. The ECU of the STS is developed by using the STM32 microcontroller. The C++ programming language is implemented by utilizing the advanced solar position algorithm (SPA) to organize the search for the maximum GSR of the PV modules on the one-axis STS to find the point of maximum power. The flowchart of the developed ECU for STS is shown in Figure 3.10. The initial position of the STS is approximately perpendicular to the ground and facing east, following the sun during the day, finally ending with an almost perpendicular position facing west and it returns to its initial position. East-West rotation range limit is up to ±60° because of security reasons. This function of tracking the maximum point of

GSR is performed as a function of time programming following the orbit of the sun every 15 minutes within specified hours thanks to the SPA. Control of STS movement is performed with the developed ECU. The angle of the PV surfaces on the STS is measured with information received from the angle sensor with a precision of 0.01° degrees. The STS angle is measured approximately 10 times per second. According to the sun angles calculated in the ECU, the OPTA that the STS should have (the steepest angle they can make with the sun) is compared with the current angle of the STS. According to this comparison result, the relevant movement of the STS via the engine is provided. The STS can be moved in the desired direction and to the desired angle with the ECU. In this way, cleaning, maintenance, repair, or similar needs can be easily performed. After these needs are met, the system automatically returns to its normal operating state. All of these operations can also be performed by making a remote connection via the server. The components of the developed ECU have been presented in Figure 4.15.

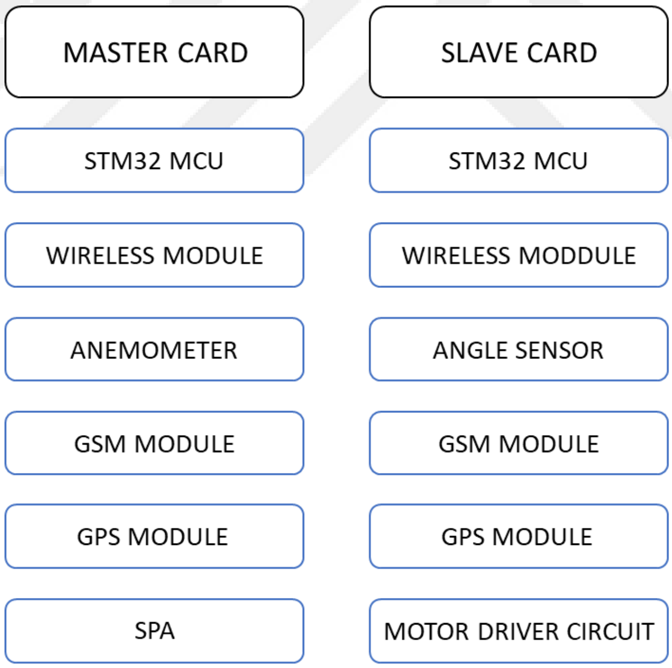

Figure 4.15. The components of the developed ECU.

The wireless communication module is utilized in the wireless communication infrastructure of the ECU circuit. Apart from this, there is no communication equipment in the electronic circuits. This module broadcasts in the 2.4 GHz ISM band with Gaussian frequency shift keying (GFSK) modulation and low data packet sizes. Therefore, it cannot connect to, send data to, or receive data from any existing Bluetooth, wireless fidelity (Wi-Fi), global positioning system (GSM), or other network. So, the ECU circuit can exchange data only with a specific communication protocol specific to the determined. Remote monitoring and control of the STS is carried out via the wireless communication interface of the ECU. Utilizing mutual communication with this interface, data is exchanged from the computer server to the ECU and from the ECU to the computer server. A dedicated server is used for control and data collection (cloud-based or local). Actual production data are taken every 20 seconds. This communication is handled following a specially developed software protocol. The data that can be transferred between devices with this protocol is shown in Table 4.19 below. Data such as STS angle, wind speed, sun angle in the sky, sunrise time, sunset time, some topocentric parameters, solar transit time, and so on are instantly transmitted to the remote monitoring system. A user connected to the remote monitoring system can see this data instantly and can change the STS angles to the desired position. It should be noted that the GSM module is optional to access a cloud-based data working environment, it is not required for local networks.

Table 4.19. Data is carried between devices via a communication protocol.

Data Package	**Length [Byte]**	**Examples**
Time information	6	160315
Angle value	4	973
Wind speed	2	28
Auto / Man	1	1
Sunrise time	6	21878
Sunrise time	6	168968
Observer hour angle	4	686
Sun equatorial horizontal parallax	4	2403
Topocentric right ascension	4	900
Topocentric local hour angle	4	686
Topocentric elevation angle	4	7517
Atmospheric refraction correction	4	4262
Topocentric elevation angle corrected	4	7518
Topocentric zenith angle	4	1481

Topocentric azimuth angle astro	4	2537
Topocentric azimuth angle	4	2053
Sun transit	6	954237
CRC	3	93

4.7.9. Advanced spa algorithm utilized in ECU

NREL has developed a C source code for the solar position algorithm (SPA). In the present studies of this thesis, an improved version of the SPA offered by NREL (2003, updated in 2008) has been utilized in the programming of the ECU. No light sensor or predefined time information is used in the system, and no data is received by connecting to a server. The position of the sun is calculated completely within the ECU. This calculation is performed using the SPA published by the NREL. Using the SPA, zenith, and azimuth angles, which indicate the angle of the sun in the sky, can be calculated with an accuracy of 0.0003 degrees up to the year 6,000.

Instant date and location information is obtained with the GPS module integrated into the ECU. Using GPS information, the instantaneous position of the sun in the sky is calculated. While performing these calculations, information such as sunrise time, sunset time, the time when it is at its peak at noon, instantaneous sun angles, etc. is also obtained for the day in question. Using the provided data, the optimal angle value for the STS is found. By comparing this angle value with the instantaneous angle values read from the STS' angle sensor, the difference is calculated. If this difference is below ±0.5 degrees, no action is taken; if it is above this value, the relevant movement is performed by controlling the STS engine. Location and time data from GPS satellites is extracted with the GPS sensor located on the ECU. This data is used as the input for the SPA. At function entry, current time and location information is precisely assigned to function variables. SPA calculations are performed using these variables. At the function output, if the instantaneous angle of the sun in the sky is above the horizon line (during the day), the angle of the sun is calculated, and the tracking angle to be used to control the tripod is calculated.

4.7.10. Mechanical Structure and Security

The mechanical part of the PV systems (SFS and STS) is designed in this study to help resist deformation and damage caused by wind forces. So, it can be emphasized that the STS is machined to be resistant to wind and rain. The PV systems (SFS and STS) are mounted on cold galvanized dipped steel legs. All other metal materials are also coated with cold-dip galvanization. Anchor piles for the piers were driven and a concrete platform was built on the ground for each pillar. When the GSR value is determined below the defined limit on cloudy days (400W/m^2) and wind speed is above the defined limit on windy days (40km/h), the STS is blocked to prevent performing a search. When the wind speed exceeds 40 km per hour, the panels are placed in a horizontal position to keep the system safe against the wind. When cleaning or maintenance is to be carried out on the site, the angle of the power plant can be changed as desired throughout the operations through the developed software. The engine and reducer used are capable of working in outdoor environments, comply with IP54 standards, are dust, waterproof, and can withstand high temperatures. The STS is designed to withstand high wind speeds. The STS is designed according to the TS498 (Turkish Standards Institution, 1987) and ISO9194 (International Standard of Organization, 1987) standards. In addition, using instant data from the wind speed measurement sensor (an anemometer) integrated into the STS, the solar surfaces on the STS are turned 1° horizontally and put into protection mode before dangerous wind speeds are reached. By giving a low angle in this way, dirt and debris that may accumulate on the STS are thrown out of the panel thanks to the slope.

4.7.11. Losses of PV electricity production

Energy losses can occur in electronic components for grid-connected PV plants under real operating conditions. Losses of PV electricity production in the DC include PV module mismatch, heat losses in power cables and PV modules, interconnections, and losses due to dirt, snow, icing, soiling, etc. Losses of energy in the AC include inverter, AC cable, grid, etc. Various studies have been conducted in the literature to estimate PV energy losses. Total miscellaneous losses such as cable, angle of incidence, and spectral effects are assumed for this analysis ~3% (Kumar & Sudhakar, 2015). The PV losses due to temperature and irradiance effects are assumed ~8% (European Commission, 2024).

Highly efficient inverters with total harmonic distortion of less than 3% reduce energy losses and assure power quality. The efficiency of the inverter utilized in this study is 98.6%, so, the expected loss is very low (1.4%). The detailed ratio of loss estimation for SFS and STS systems is tabulated in Section 5.7.

5. RESULTS AND DISCUSSIONS

In this section of the thesis, relevant results obtained from the performed studies have been presented for increasing the efficiency of solar PV plants. Calculations and discussions are presented specifically by focusing on OPTA and TSR values, percentage gains, performance analysis, and comparisons of SFSs and STSs have been carried out. The results of the transposition models have been analyzed comparatively for the study region along with the results of regional and technical simulations. Apart from this, validations of adopted transposition and correlation models, OPTA, and latitude relations, as well as comparisons with previous studies have been evaluated from a global perspective.

5.1. Results of Case Study (1): Investigation of OPTA and TSR Intensity for Solar PV Surfaces in Türkiye Provinces

In this section, results, and discussion on the efficiency analysis of one-axis and two-axis STSs and SFSs have been presented for all geographical regions of Türkiye. Annual OPTAs and TSR gains have been predicted for the provinces of Türkiye by using the proposed Liu-Jordan (1960) isotropic transposition model. In addition, the maximum TSR that can be generated has been calculated in the case of fixed-tilt PV surfaces and optimally tracked one and two-axis surfaces in the provinces of Türkiye. OPTA and TSR values have been tabulated in Table 5.1 and Table 5.2. The horizontal GSR data provided from ground and satellite stations (presented in Figure 4.2) have been used closest to provinces.

5.1.1. GSR values on the horizontal surfaces

The daily GSR values on solar PV surfaces for the provinces of Türkiye are presented in Table 5.1. It is observed that the horizontal GSR quantity varies from 3.62 kWh/m² to 5.29 kWh/m² over Türkiye. Since the most important solar parameter is horizontal GSR distribution; the Mediterranean, Aegean, South Anatolia regions, and Muğla, Antalya, and Aydın provinces have more advantageous PV energy productivity than other provinces in line with the data received from Table 5.1, Table 5.2 and Table 5.3.

Table 5.1. Daily average GSR and daily average TSR intensity on PV surfaces for the Türkiye provinces [kWh/m²-day].

Region & Province		GSR-TSR Intensity [kWh/m²-day]				Region & Province		GSR-TSR Intensity [kWh/m²-day]			
		H	Fixed	One-Axis	Two-Axis			H	Fixed	One-Axis	Two-Axis
Aegean	Afyon	4.51	5.01	6.47	6.64	Central Anatolia	Aksaray	4.57	5.06	6.53	6.75
	Aydın	5.12	5.67	7.55	7.78		Ankara	4.41	4.93	6.38	6.58
	Denizli	4.77	5.28	6.84	7.08		Çankırı	4.18	4.68	5.98	6.16
	İzmir	5.10	5.64	7.56	7.78		Eskişehir	4.28	4.73	6.05	6.22
	Kütahya	4.35	4.80	6.18	6.35		Karaman	4.65	5.08	6.57	6.76
	Manisa	4.70	5.20	6.79	6.98		Kayseri	4.55	5.08	6.58	6.78
	Muğla	5.29	5.85	7.85	8.09		Kırıkkale	4.41	4.93	6.37	6.57
	Uşak	4.61	5.12	6.67	6.85		Kırşehir	4.44	4.94	6.41	6.58
Black Sea	Amasya	4.66	5.19	6.83	7.06		Konya	4.66	5.17	6.68	6.88
	Artvin	3.62	3.97	4.90	5.03		Nevşehir	4.57	5.07	6.57	6.77
	Bartın	4.01	4.40	5.61	5.75		Niğde	4.52	4.93	6.34	6.52
	Bayburt	4.61	5.26	6.89	7.16		Sivas	4.51	5.11	6.62	6.84
	Bolu	4.09	4.53	5.77	5.93		Yozgat	4.47	5.01	6.49	6.69
	Çorum	4.28	4.78	6.16	6.35	Mediterranean	Adana	5.06	5.62	7.42	7.65
	Düzce	4.08	4.53	5.77	5.93		Antalya	5.17	5.72	7.61	7.84
	Giresun	3.85	4.32	5.37	5.56		Burdur	4.87	5.50	7.16	7.42
	Gümüşhane	3.78	4.23	5.24	5.45		Hatay	4.72	5.16	6.71	6.91
	Karabük	4.01	4.36	5.55	5.71		Isparta	4.58	5.10	6.55	6.75
	Kastamonu	3.83	4.22	5.30	5.44		K. Maraş	4.64	5.15	6.69	6.92
	Ordu	4.18	4.58	5.88	6.06		Mersin	4.83	5.28	6.89	7.09
	Rize	3.97	4.40	5.57	5.74		Osmaniye	4.81	5.40	7.04	7.27
	Samsun	3.81	4.22	5.28	5.44	Marmara	Balıkesir	4.21	4.58	5.84	5.99
	Sinop	4.16	4.58	5.97	6.12		Bilecik	4.27	4.76	6.09	6.28
	Tokat	4.05	4.52	5.72	5.88		Bursa	4.04	4.40	5.57	5.71
	Trabzon	4.08	4.48	5.73	5.89		Çanakkale	4.21	4.61	5.91	6.08
	Zonguldak	4.23	4.63	5.98	6.16		Edirne	3.92	4.35	5.49	5.65
Eastern Anatolia	Ağrı	4.51	5.12	6.63	6.87		İstanbul	4.19	4.56	5.89	6.03
	Ardahan	3.74	4.21	5.24	5.41		Kırklareli	3.92	4.36	5.52	5.66
	Bingöl	4.77	5.30	6.99	7.22		Kocaeli	4.03	4.42	5.63	5.77
	Bitlis	4.72	5.23	6.85	7.08		Sakarya	3.98	4.37	5.52	5.67
	Elazığ	4.81	5.35	7.04	7.26		Tekirdağ	4.17	4.61	5.91	6.06
	Erzincan	4.53	5.07	6.59	6.79		Yalova	4.02	4.40	5.61	5.74
	Erzurum	4.57	5.20	6.81	7.07	Southeast Anatolia	Adıyaman	4.71	5.18	6.72	6.92
	Hakkari	4.76	5.26	6.92	7.17		Batman	4.78	5.30	6.92	7.13
	Iğdır	4.41	4.98	6.43	6.63		Diyarbakır	4.78	5.29	6.89	7.11
	Kars	4.36	5.02	6.46	6.73		Gaziantep	4.83	5.29	6.94	7.15
	Malatya	4.71	5.22	6.83	7.02		Kilis	4.84	5.27	6.91	7.11
	Muş	4.66	5.16	6.77	7.02		Mardin	4.79	5.28	6.89	7.11
	Şırnak	4.79	5.29	6.93	7.15		Siirt	4.78	5.31	6.91	7.13
	Tunceli	4.51	5.01	6.51	6.72		Şanlıurfa	4.96	5.46	7.16	7.39
	Van	4.66	5.22	6.80	7.03						

5.1.2. Annual OPTA findings for SFSs

To achieve maximal TSR intensity, the SFSs should be set at OPTAs. The daily GSR is predicted by using the NASA-SSE solar data on the horizontal surface for the south-facing PV surfaces (azimuth angle is 0º) whose tilt angle is changed in steps of 1 from 0º to 90º. Annual OPTAs are predicted as a function of latitude across Türkiye by using the geo-referenced datasets and presented in Table 5.2. Türkiye's map indicating the OPTA values of its provinces is shown in Figure 5.1. It is found that the annual OPTAs for a south-faced (azimuth angle value is fixed to 0º) PV surfaces varied from 28º to 36º throughout Türkiye. It has also been found that the OPTAs for all provinces and regions of Türkiye are below the latitude values. If the OPTAs of the surfaces are not possible to set monthly or seasonally, the OPTAs of the PV surfaces should be set as an annual-SFS. As depicted in the map presented in Figure 5.1, the existence of different OPTAs in close latitude values is due to the effect of solar climatic parameters, geographical locations, weather conditions, and seasonal variations. For instance, the fact that the OPTAs of Adana located at 37.01Nº latitude, Artvin located at 41.18Nº latitude, and Edirne located at 41.68Nº are found to be 31°. Average OPTAs and TSR gains on tilted surfaces in regions of Türkiye are tabulated in Table 5.4. As inferred from Table 5.4 the annual OPTAs of the geographical regions change between 30.0º and 32.6º.

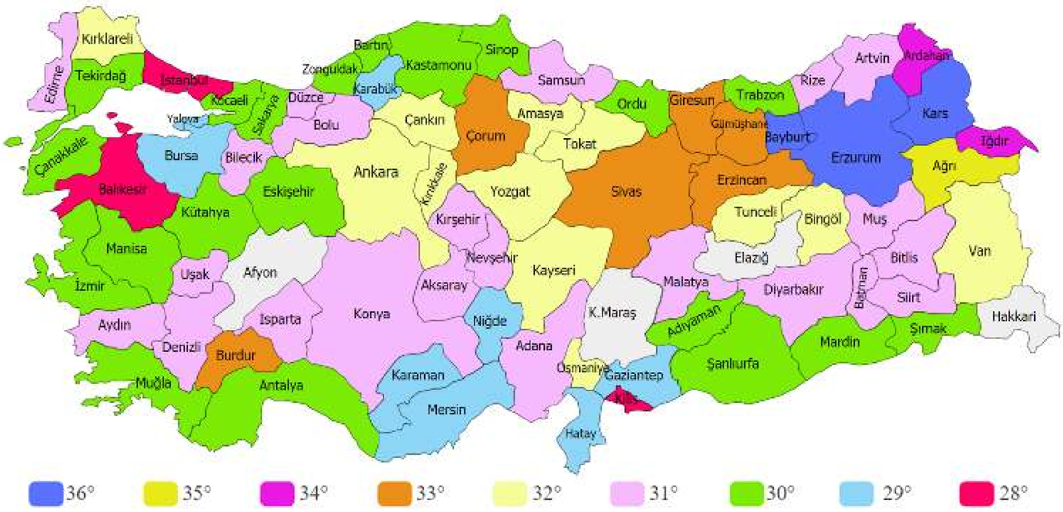

Figure 5.1. Türkiye map showing the OPTA values of its provinces.

Table 5.2. OPTA values [°] and TSR gains [%] on PV surfaces for the provinces of Türkiye.

Region & Province		OPT [°]	TSR Gain [%] Fixed	One-Axis	Two-Axis	Region & Province		OPT [°]	TSR Gain [%] Fixed	One-Axis	Two-Axis
Aegean	Afyon	31	11.12	29.21	33.02	Central Anatolia	Aksaray	31	10.75	29.51	33.45
	Aydın	31	11.16	32.73	36.78		Ankara	32	12.27	28.95	32.98
	Denizli	31	10.72	29.97	34.16		Çankırı	32	11.99	27.84	31.68
	İzmir	30	10.61	34.11	38.02		Eskişehir	30	10.54	27.97	31.57
	Kütahya	30	10.37	28.82	32.36		Karaman	29	9.27	29.57	33.34
	Manisa	30	10.67	30.64	34.67		Kayseri	32	11.43	29.58	33.73
	Muğla	30	10.61	34.25	38.36		Kırıkkale	32	12.02	29.13	33.18
	Uşak	31	11.29	30.08	33.97		Kırşehir	31	11.24	29.28	33.14
Black Sea	Amasya	32	11.14	31.41	35.84		Konya	31	10.96	29.25	33.14
	Artvin	31	10.23	23.12	26.37		Nevşehir	31	10.97	29.63	33.58
	Bartın	30	9.76	27.57	30.76		Niğde	29	9.098	28.85	32.53
	Bayburt	35	14.14	31.24	36.18		Sivas	33	12.84	29.98	34.32
	Bolu	31	10.77	27.44	30.98		Yozgat	32	12.11	29.62	33.61
	Çorum	33	12.16	28.38	32.36	Mediterranean	Adana	31	11.08	32.07	36.17
	Düzce	31	11.03	27.36	30.91		Antalya	30	10.66	33.08	37.13
	Giresun	33	12.24	24.88	28.54		Burdur	33	12.91	30.13	34.47
	Gümüşhane	33	11.88	24.28	28.78		Hatay	29	9.30	29.58	33.47
	Karabük	29	9.26	27.24	30.44		Isparta	31	10.88	28.47	32.42
	Kastamonu	30	10.16	25.55	28.85		K. Maraş	31	10.97	29.85	33.92
	Ordu	30	10.08	28.33	31.81		Mersin	29	9.32	30.54	34.35
	Rize	31	10.81	26.54	30.16		Osmaniye	32	12.25	30.17	34.45
	Samsun	31	10.77	25.12	28.66	Marmara	Balıkesir	28	8.82	27.787	31.08
	Sinop	30	10.10	30.35	33.63		Bilecik	31	11.25	28.22	31.98
	Tokat	32	11.36	26.61	30.58		Bursa	29	8.94	26.66	29.85
	Trabzon	30	10.32	27.38	30.96		Çanakkale	30	9.75	28.18	31.66
	Zonguldak	30	9.72	29.36	32.83		Edirne	31	10.98	26.48	29.96
Eastern Anatolia	Ağrı	35	13.56	29.73	34.64		İstanbul	28	8.58	29.24	32.31
	Ardahan	34	12.28	24.51	28.81		Kırklareli	32	10.98	26.73	30.18
	Bingöl	32	11.35	31.68	36.04		Kocaeli	30	9.66	27.15	30.55
	Bitlis	31	10.83	31.04	35.45		Sakarya	30	9.83	26.38	29.82
	Elazığ	31	11.25	31.63	35.77		Tekirdağ	30	10.05	28.68	31.95
	Erzincan	33	11.95	30.04	34.17		Yalova	29	9.43	26.97	30.16
	Erzurum	36	13.74	30.91	35.88	Southeast Anatolia	Adıyaman	30	9.98	29.77	33.65
	Hakkari	31	10.47	31.48	36.25		Batman	31	10.86	30.38	34.34
	Iğdır	34	13.16	28.92	33.14		Diyarbakır	31	10.91	30.25	34.22
	Kars	36	14.66	29.13	34.13		Gaziantep	29	9.32	31.24	35.23
	Malatya	31	10.86	30.72	34.55		Kilis	28	8.90	31.16	34.97
	Muş	31	10.71	31.13	35.58		Mardin	30	10.26	30.56	34.54
	Şırnak	30	10.40	30.93	34.91		Siirt	31	11.09	30.14	34.26
	Tunceli	32	11.05	29.87	34.06		Şanlıurfa	30	10.10	31.56	35.58
	Van	32	11.98	30.22	34.60						

5.1.3. TSR Gain Collected by SFSs

The annual TSR intensity on PV surfaces oriented with an azimuth angle of 0º is calculated by using the GSR values on the horizontal surface obtained from NASA-SSE for the SFSs. As presented in Table 5.1, the TSR values to be obtained in the provinces of Türkiye are predicted as a minimum of 3.97 kWh/m² in Artvin and a maximum of 5.85 kWh/m² in Muğla in the case of using annual OPTAs for SFSs The differences in the intensity of TSR as a result of the effect of OPTA are presented in Table 5.2. An increase of between 8.58% (İstanbul) and 14.66% (Kars) daily TSR intensity is achieved when the annual OPTA is set to SFS.

Table 5.3. Predicted average daily GSR and TSR intensities on PV surfaces of geographical regions, Türkiye.

Regions	Horizontal [kWh/m²-day]	Fixed [kWh/m²-day]	One-Axis [kWh/m²-day]	Two-Axis [kWh/m²-day]
Aegean	4.81	5.33	6.98	7.19
Black Sea	4.08	4.52	5.76	5.93
Central Anatolia	4.48	4.98	6.43	6.63
Eastern Anatolia	4.58	5.12	6.66	6.88
Marmara	4.09	4.49	5.73	5.87
Mediterranean	4.85	5.38	7.02	7.23
Southeast Anatolia	4.81	5.29	6.92	7.13

Table 5.4. Average OPTAs and daily TSR gains on tilted surfaces in regions of Türkiye.

Regions	AVG OPT [º]	Fixed [%]	One-Axis [%]	Two-Axis [%]
Aegean	30.51	10.82	31.35	35.31
Black Sea	31.23	10.91	27.46	31.18
Central Anatolia	31.14	11.16	29.18	33.12
Eastern Anatolia	32.59	11.86	30.23	34.63
Marmara	29.82	9.84	27.53	30.87
Mediterranean	30.76	10.94	30.55	34.58
Southeast Anatolia	30.00	10.16	30.65	34.61

Figure 5.2 shows the annual TSR values of optimally tilted PV surfaces compared to horizontal surfaces of the regions. It is clear from the graph that the Mediterranean region has the best efficiency considering the TSR values (1,958.23 kWh/m²) and is followed by the Aegean region (1,939.98 kWh/m²) for annual optimally tilted PV (solar) surfaces. The annual OPTA can be set for the setup of SFSs throughout Türkiye in the absence of an STS. Especially for large-capacity solar PV plants, this difference will have a significant impact quantitatively. Therefore, it is extremely important to position the PV surfaces in the south-faced and at an OPTA to obtain the best TSR efficiency.

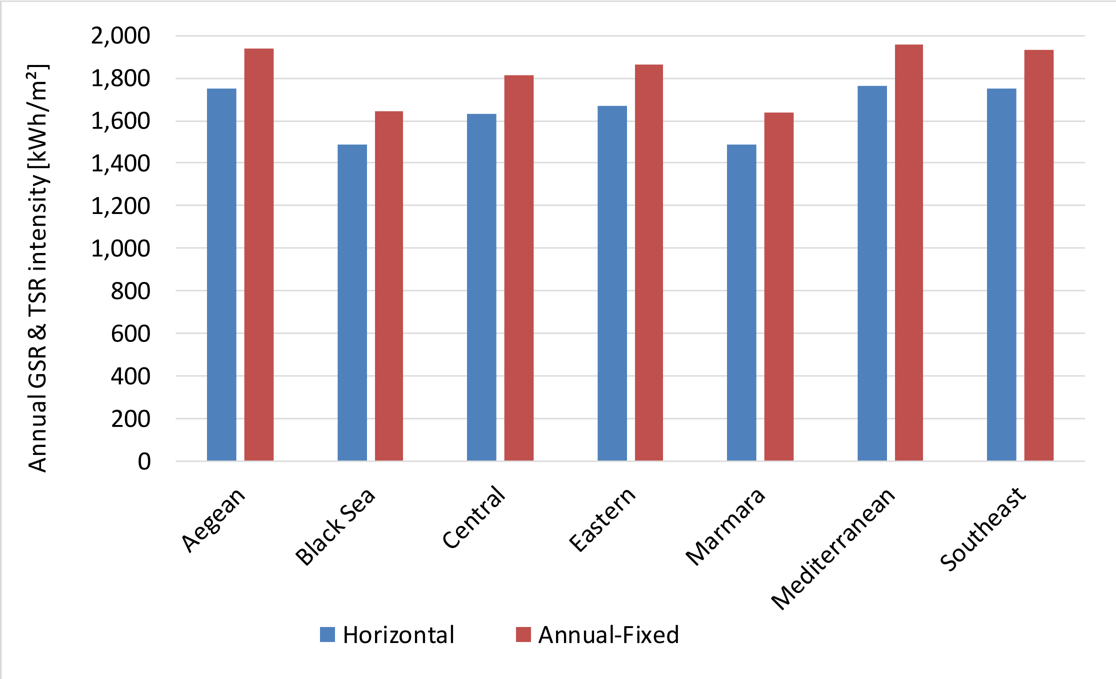

Figure 5.2. Annual average TSR gains for SFSs compared to horizontal surfaces in the regions of Türkiye.

5.1.4. TSR gains collected by the solar tracking (STS)

STSs are costly to operate and maintain and aren't always feasible because of the lack of free space. It should be noted here that the installation area and the equipment costs are not fixed and vary in time depending on supply and demand. For this reason, before the installation of one-axis and two-axis STS in the regions where the solar plant will be installed, benefit and cost analysis should be performed carefully and precisely as much as possible. The obtained TSR values for one-axis and two-axis STSs are compared to an annual SFS for evaluating the existing solar potential in Türkiye. It is overall understood from Table 5.1 and Table 5.2 that daily collected TSR is calculated to be between 23.12% in Artvin and 34.25% in Muğla has higher TSR efficiency by a PV surface with a one-axis STS compared to an SFS. It is also observed that the daily collected TSR of the two-axis STS is calculated as 26.37% in Artvin and 38.36% in Muğla provinces higher than the SFSs for other provinces of Türkiye. The TSR collection of the STSs is always superior compared to the SFS, as seen by the findings, but the efficiency ratio is changed following solar climatic conditions as expected. In the case of using one-axis STS in solar plants to be established in Türkiye, the daily TSR values to be obtained are predicted as a minimum of 4.90 $kWhm^2$ and a maximum of 7.85 $kWhm^2$. As for the two axes STS, the daily TSR values are found to be slightly increased at a minimum of 5.03 $kWhm^2$ and a maximum of 8.09 $kWhm^2$. Predicted daily TSR values and trends of the daily TSR values on tilted surfaces for geographical regions of Türkiye are presented in Table 5.3 and Figure 5.3 respectively. The findings show that the regions where energy production with the highest efficiencies are the Mediterranean and Aegean regions in the case of structuring STSs in solar plants. The daily TSR values are predicted to be 7.02 kWh/m^2 and 7.23 kWh/m^2 in the Mediterranean region in the case of using one-axis and two-axis STSs, respectively. Likewise, the daily TSR values are predicted at 6.98 kWh/m^2 and 7.19 kWh/m^2 in the Aegean region for one-axis and two-axis STSs, respectively.

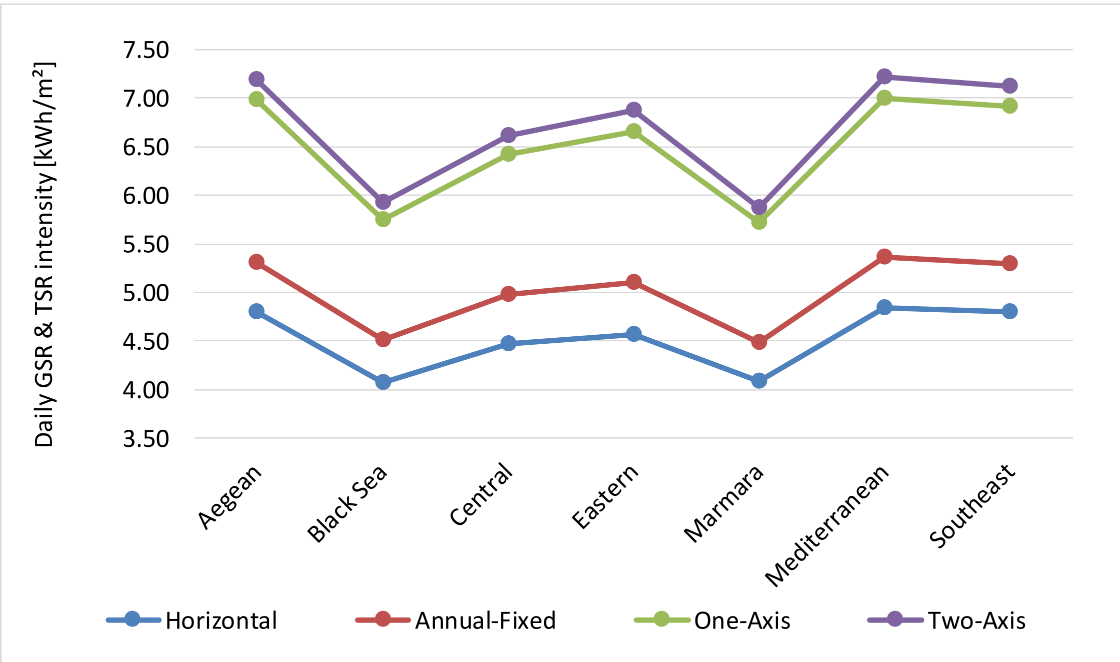

Figure 5.3. Trends of the average daily TSR values on PV surfaces in the regions.

Predicted daily TSR gains on tilted surfaces and percentage values for the geographical regions of Türkiye are also presented in Table 5.2. As inferred from Table 5.2 the Aegean region benefits the most from STSs among other regions in Türkiye. The daily TSR gains are predicted at 31.35% and 35.31% for the Aegean region in the case of the setup of one-axis and two-axis STS respectively in solar plants. Annual TSR values for one-axis and two-axis tracked PV surfaces compared to SFSs are of the regions as shown in Figure 5.4.

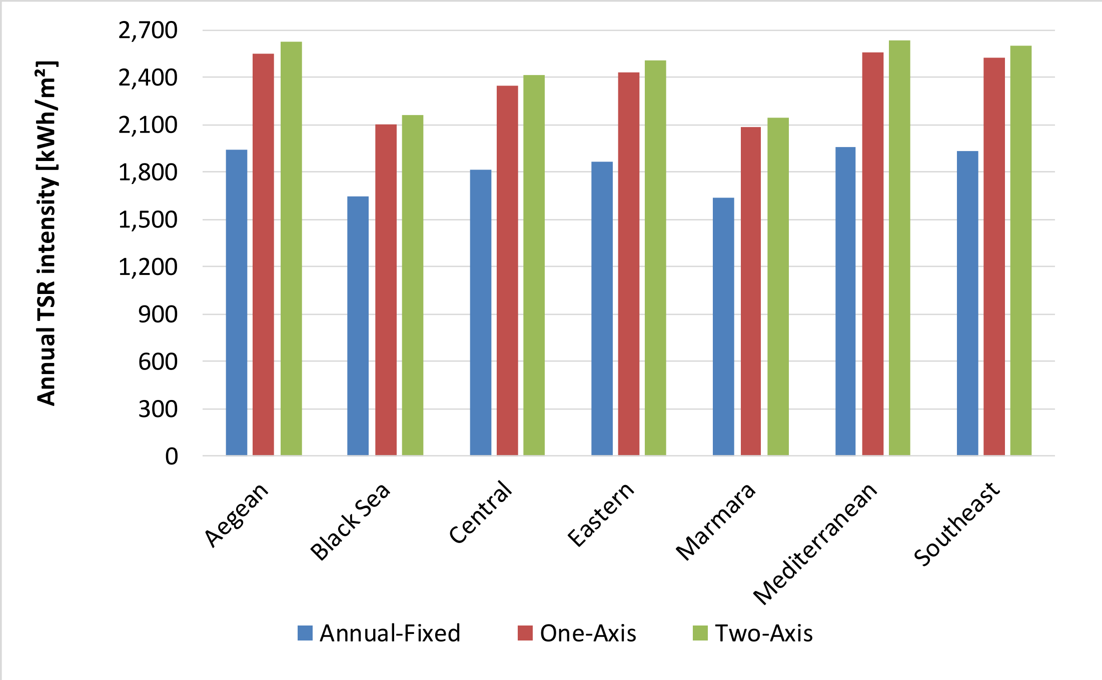

Figure 5.4. Annual TSR intensity for PV surfaces in the regions of Türkiye.

Multiple unique factors go into the cost of PV surface installations, STSs have constraints such as cost-budget, wastage of energy, and limitations due to the area of installation. The one-axis or two-axis STS can increase the area usage, capital, and operation costs. However, taking into account the findings of this study, it is strongly recommended to use one-axis STSs in the setup of large-scale solar PV plants in Türkiye. If it is applied to high-capacity solar PV plants in Türkiye, the contribution of solar energy to the economy will be great in the case of using STSs. It is depicted from the graph in Figure 5.4 that the Mediterranean region has the best energy production efficiency, and the second one is the Aegean Region considering the annual energy production capacity in the case of the use of STSs. in the case of using one-axis STSs, the annual TSR values are predicted at 1,958.23 kWh/m² and 1,939.98 kWh/m² for the Mediterranean and Aegean regions respectively.

5.1.5. Effect of OPTA on monthly average daily TSR intensity

It is known that components such as the diffuse fraction correlation model and sky-diffuse transposition model, along with the solar datasets used in the calculation algorithm, are also highly effective in determining OPTA values. The sensitivity of the OPTA determination analysis is performed based on an isotropic transposition model using the NASA-SSE dataset for all cities in Türkiye. The effect of different OPTAs on the TSR data for the Ankara province is presented in Table 5.5. As can be concluded from the table, the OPTA of Ankara is found to be 32º yielding a daily TSR of 4.932 kWh/m², while this estimation becomes 4.923 kWh/m² at 36º. This corresponds to a 0.18% fluctuation in the TSR value. Results reached for all other provinces yield similar conclusions made for Ankara province. Although this difference may be negligible in small-scale solar PV plants, it may create serious energy production variations in large-scale solar PV plants. One notable point is that this study and some other studies generally estimate the OPTAs below the latitude of the location as illustrated in Table 5.6.

Table 5.5. Monthly average daily TSR for different tilt angles in Ankara province.

Month	Monthly Average Daily TSR [kWhm2-day]				
	β=32º	β=33º	β=34º	β=35º	β=36º
1	3.281	3.306	3.332	3.357	3.381
2	3.955	3.975	3.993	4.011	4.028
3	4.875	4.883	4.889	4.894	4.898
4	5.082	5.072	5.060	5.047	5.033
5	5.811	5.785	5.757	5.728	5.698
6	6.363	6.325	6.287	6.247	6.206
7	6.727	6.691	6.653	6.614	6.573
8	6.364	6.345	6.324	6.301	6.277
9	5.847	5.850	5.851	5.850	5.849
10	4.548	4.566	4.582	4.598	4.612

11	3.582	3.609	3.635	3.660	3.684
12	2.749	2.772	2.795	2.817	2.838
Annual	4.932	4.931	4.930	4.927	4.923

5.1.6. Comparison of available OPTA studies for the provinces of Türkiye

A comparison of some OPTAs from previous studies for the provinces of Türkiye to the present study is tabulated in Table 5.6. For the studies on determining the OPTAs of solar PV plants for the provinces of Türkiye in the last ten years are reviewed, it is found that the results obtained from the present study are in good agreement and similar to the results of previous studies (see Table 5.6). As can be depicted from Table 5.6, the predicted discrepancy between the OPTA values fluctuates between ±1° and ±3° range for all provinces. This discrepancy is mainly caused by the differences in solar datasets, solar parameters, and calculation methods used in the studies. It is also well understood that an inadequate number of studies are conducted for Türkiye provinces manifesting the importance of the current study for contributions to literature.

Table 5.6. Comparison of OPTA values from previously conducted studies to present study for Türkiye provinces.

Province	**OPTAs [β°]**		**Authors**
	Present Study	**Previous Studies**	
Kayseri	32	30	Dal, 2021
Çorum	33	34	Şevik et al., 2021
Gaziantep	29	30	Yağlı & Koç, 2020
Kütahya	30	32	Yolcan et al., 2020
Antalya	30	33	Akyürek et al., 2019
Burdur	33	34	
Isparta	31	34	
Antalya	30	32	Kallioğlu et al., 2019
Kayseri	32	33	
Trabzon	30	33	
Şanlıurfa	30	33	Yıldırım et al., 2019
Gaziantep	29	29	Bakırcı et al., 2018

Muğla	30	32	Kallioğlu et al., 2018
Sakarya	30	32	Tırmıkcı et al., 2018
Erzurum	36	34	Bakırcı, 2017
Adana	31	34	Bilgili et al., 2017
Gaziantep	29	30	Kallioğlu et al. 2017
Bursa	29	31	Arslanoğlu, 2016
Batman	31	33	Yilmaz et al., 2016
Ankara	32	34	Koçer et al., 2016
Izmir	30	33	Bawazir et al., 2016
Adana	31	31	Bakırcı et al., 2012
Ankara	32	33	
Diyarbakır	31	33	
Erzurum	36	34	
İstanbul	28	33	
İzmir	30	33	
Samsun	31	33	
Trabzon	30	32	
Izmir	30	30	Kaçan et al., 2012

5.2. Results of Case Study (2): Estimation of OPTA and TSR Intensity Collected by Solar PV Surfaces in the Provinces of Mediterranean Region, Türkiye

In this section, the calculations of the Mediterranean region provinces are carried out by using the proposed algorithm between 0°-90° tilt angle values, and the OPTA values with the maximal energy production are determined based on the clearness index and the angle of declination for the specific period. It is assumed that the surface azimuth angle is fixed to 0° for directly facing the equator. Results are obtained by producing data via a graphical interface. In this respect, the calculations are performed for all days of the year on a south-facing PV surface.

5.2.1. Analyzing of GSR on horizontal surfaces

The monthly and annual values of GSR captured on average during one day on a horizontal surface in the provinces of the region are presented in Table 5.7. The most important solar energy production parameters are GSR values; therefore as depicted in Table 5.7, Antalya province has the highest GSR efficiency. The second-most productive province is Adana. It can be observed that the GSR values of the provinces established near the seaside are significantly better than those of the provinces in the inner regions. It is also understood, in the Mediterranean region, that the extension of the mountains parallel to the sea creates a shadowing effect on the inner regions and interrupts the GSR interaction. As seen from Table 5.7, the intensity of GSR on the horizontal surface significantly varies according to the time and the place.

Table 5.7. GSR intensity on the horizontal surface of provinces [kWh/m²-day].

M	Adana	Antalya	Burdur	Hatay	Isparta	Maraş	Mersin	Osmaniye
1	2.47	2.49	2.66	2.29	2.32	2.31	2.26	2.53
2	3.43	3.38	3.46	3.18	3.09	3.15	3.12	3.32
3	4.67	4.76	4.79	4.36	4.28	4.17	4.47	4.63
4	5.72	5.78	5.71	5.33	5.07	4.91	5.52	5.33
5	6.89	7.04	6.56	6.47	6.08	6.09	6.59	6.59
6	7.83	8.07	7.44	7.48	7.11	7.27	7.53	7.31
7	7.76	7.98	7.27	7.25	7.07	7.47	7.47	7.03
8	6.97	7.19	6.42	6.41	6.36	6.61	6.66	6.28
9	5.76	6.01	5.31	5.37	5.37	5.42	5.53	5.42
10	4.21	4.24	3.96	3.95	3.78	3.87	4.04	4.06
11	2.75	2.78	2.84	2.61	2.56	2.57	2.64	2.97
12	2.15	2.12	2.19	2.02	1.95	2.02	2.02	2.32
AVG	5.06	5.17	4.88	4.74	4.59	4.66	4.83	4.82

Source: (NASA-SSE, 2024).

5.2.2. TSR Analysis for SFSs

In this case study, the OPTAs are determined by spanning the tilt angle from 0° to 90° in increments of 1° steps in the proposed method. The OPTA is then determined based on the angle values at which the maximal TSR is collected. The percentage contributions of OPTAs to daily TSR efficiency are presented in Table 5.8. It is seen that provinces are in the OPTA range of 29°-33° for PV surfaces directly oriented south-facing to the equator (0°) across the Mediterranean region. This result is the optimal tilt throughout the year when using the proposed calculation method. As depicted from the results for the provinces in Table 6, PV surfaces adjusted at OPTA achieve approximately 10% more energy production (between 9.34% and 12.91%) daily compared to the surfaces that are not angled at all for the SFS. The energy percentage contribution in SFSs at OPTA is found to be the most significant in Burdur and Osmaniye provinces with percentages of 12.91% and 12.22%, respectively. Considering the 25-year life of the solar PV plants, that may correspond to a significant amount of energy depending on the size of the established system. Therefore, optimal tilting of the surfaces should be seriously taken into consideration in solar PV plant installations. On the other hand, it has been revealed that the geographical and climatic characteristics of the region are also important factors due to the differences in the OPTAs.

Table 5.8. Percent contributions of OPTAs to daily TSR efficiency [%].

Province	Fixed-Axis OPTA [β°]	Maximal TSR Gain [%]
Adana	31	11.69
Antalya	30	10.66
Burdur	33	12.91
Hatay	29	9.52
Isparta	31	10.90
K. Maraş	31	10.97
Mersin	30	9.34
Osmaniye	32	12.27

In theoretical calculations for provinces in the Mediterranean region regarding OPTAs, the results are approximately similar, but not the same. The main reason for the variations in the OPTAs is because the climatic parameters besides latitude are also taken into account in this calculation method. The annual OPTA for Hatay is quantified as 1°-4° lower than the other provinces of interest. One of the reasons for this difference is that the latitude value of Hatay province is lower than all the other provinces in the region. The fact that Hatay is closer to the equator causes it to benefit more from the sun's rays. As a consequence of having a lower latitude, the PV surface should be set at a tilt of 1°-4° less than other provinces for the maximal yield.

To achieve maximal benefit from GSR, PV surfaces need to be designed so that the OPTAs can be set effortlessly on a monthly or seasonal basis. A comparison of daily TSR values on SFSs at different tilt angles is presented in Table 5.9. To determine how much more energy is generated throughout the year, starting from the tilt angle of 0° with an increment of 5° steps. It is observed that the energy generated increases until the OPTA and then decreases gradually. So, it is seen that tilting the surface significantly increases energy production. For this reason, it is extremely important to align the PV surfaces at an OPTA in the south direction to get maximal efficiency.

The variation of daily TSR values according to the annual OPTA is shown in Fig. 5.5. As depicted from the graph in Fig. 5.5, the variation of solar radiation values according to the annual OPTA difference and the high TSR rates of Antalya province compared to other provinces contribute significantly to energy production. The reason why Antalya province is preferred especially for the establishment of large-capacity solar PV plants is because of its high potential and significant yield in energy production.

Table 5.9. Average daily TSR on SFSs at different tilt angles 0° to 50° [kWh/m²-day].

Tilt β [°]	Adana	Antalya	Burdur	Hatay	Isparta	K. Maraş	Mersin	Osmaniye
0°	5.06	5.167	4.87	4.72	4.58	4.66	4.83	4.80
5°	5.23	5.33	5.05	4.86	4.75	4.82	4.96	4.97
10°	5.34	5.47	5.20	4.97	4.87	4.94	5.07	5.11
15°	5.47	5.58	5.31	5.06	4.97	5.04	5.16	5.23
20°	5.55	5.65	5.40	5.12	5.04	5.11	5.22	5.31
25°	5.60	5.70	5.46	5.15	5.08	5.15	5.26	5.37
30°	5.59	5.69	5.51	5.18	5.08	5.14	5.26	5.41
35°	5.58	5.67	5.51	5.16	5.07	5.14	5.24	5.41
40°	5.53	5.62	5.48	5.10	5.03	5.11	5.18	5.37
45°	5.45	5.53	5.41	5.02	4.96	5.02	5.11	5.30
50°	5.34	5.41	5.31	4.91	4.86	4.92	4.98	5.21

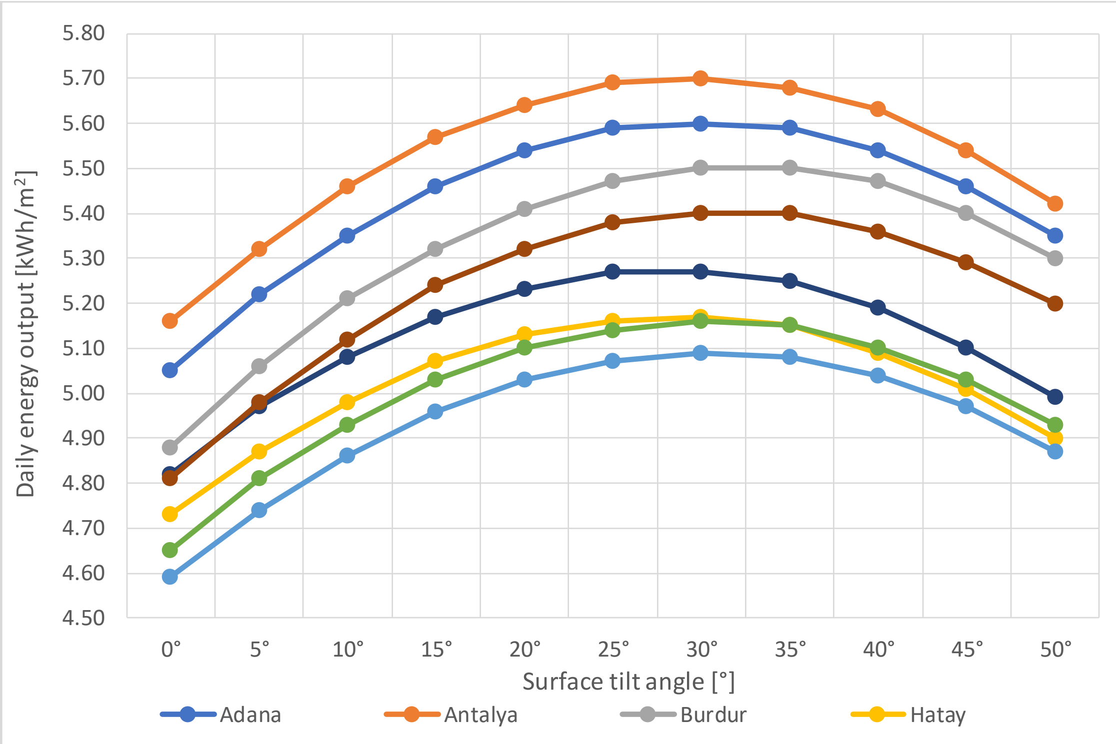

Figure 5.5. Comparison of average daily TSR on SFSs at different tilt angles.

Operation and maintenance costs of STSs are not always applicable because of the lack of free space therefore, it is more convenient to set the PV surface at an OPTA over time. In cases where it is not applicable to alter the tilt angles of the PV surfaces, the OPTA values presented in Table 5.9 can be used to obtain maximal yield in the provinces of the Mediterranean region. If large-capacity solar PV plants are to be established, this production difference becomes even more important and taken into consideration seriously. These results indicate that the yearly positioning of the PV surfaces at the OPTA provides significant TSR efficiency gains, the intensity of TSR obtained by the PV surface varied according to the location, and the influence of climatic characteristics on the OPTA.

5.2.3. TSR Analysis for STSs

STSs are effective tools to be used in solar PV plants when higher TSR efficiency is required. The provinces of the Mediterranean region are analyzed in terms of the TSR collected and the TSR efficiency of the STS in comparison to the SFS. The daily TSR on south-faced PV surfaces is presented in Table 5.10 including a horizontal surface, a fixed-axis tilted, and one-axis and two-axis STSs for provinces of the Mediterranean region of Türkiye. The daily TSR values for a fixed-axis system vary from 5.10 kW/m^2 and 5.72 kW/m^2 whereas for a one-axis system vary from 6.55 kW/m^2 and 7.61 kW/m^2, finally for a two-axis system found to be between 6.75 kW/m^2 and 7.84 kW/m^2 across the Mediterranean region. It is found that the obtained TSR values are the highest for Antalya, and the lowest for Isparta.

Table 5.10. Average daily GSR and TSR intensity on PV surfaces [kWh/m^2-day].

Province	Horizontal	Fixed-Axis	One-Axis	Two-Axis
Adana	5.06	5.65	7.48	7.72
Antalya	5.17	5.72	7.61	7.84
Burdur	4.89	5.52	7.18	7.42
Hatay	4.74	5.19	6.72	6.93
Isparta	4.60	5.10	6.55	6.75
Kahramanmaraş	4.66	5.17	6.71	6.92
Mersin	4.83	5.28	6.88	7.08
Osmaniye	4.82	5.41	7.04	7.27

Table 5.11 presents the daily TSR gain for STSs compared to the SFSs. Overall, it is found that daily collected TSR is between 28.49% and 33.09% higher for a PV surface with a one-axis STS than by an annual tilted SFS. The efficiency increment of a two-axis STS is calculated between 32.42% and 37.13% more. Based on the values presented in Table 5.11, the gain of STSs to TSR efficiency is the highest in Antalya province. Especially for large-capacity solar PV plants, this difference may have a significant impact on the yield of the installed system.

Table 5.11. Average daily TSR gain of STSs Mediterranean provinces [%].

Province	One-Axis TSR Gain [%]	Two-Axis TSR Gain [%]
Adana	32.45	36.71
Antalya	33.10	37.13
Burdur	30.13	34.49
Hatay	29.54	33.60
Isparta	28.49	32.42
K. Maraş	29.85	33.92
Mersin	30.37	34.16
Osmaniye	30.19	34.45

Table 5.12 summarizes the obtained results for the TSR efficiency in the Mediterranean provinces. It is seen that the intensity of TSR collected by the STSs is always higher than the SFSs. SFSs contribute to the Antalya province approximately 2.09 MW/m^2 per year by applying the OPTAs, whereas one-axis and two-axis STSs contribute 2.78 MW/m^2 and 2.87 MW/m^2, respectively. Similarly, for the Adana province, the contribution of the SFS is 2.06 MW/m^2 whereas one-axis and two-axis contributions are 2.72 MW/m^2 and 2.78 MW/m^2, respectively. For this reason, it is strongly recommended that investors prefer Antalya and Adana provinces in the installation of solar PV plants for higher percent contribution to the economy of the Mediterranean region of Türkiye.

Table 5.12. Annual TSR values of the Mediterranean provinces [MWh/m^2-year].

Province	Fixed-Axis	One-Axis	Two-Axis
Adana	2.06	2.72	2.80
Antalya	2.09	2.78	2.87
Burdur	2.02	2.63	2.71
Hatay	1.90	2.46	2.54
Isparta	1.87	2.40	2.47
Kahramanmaraş	1.89	2.45	2.53
Mersin	1.93	2.52	2.59
Osmaniye	1.98	2.58	2.66

The annual collected TSR values for one-axis and two-axis STSs are compared to an annual tilted SFS in Figure 5.6 to evaluate the existing solar potential in Mediterranean region provinces. It is seen that especially for large-capacity solar PV plants, a two-axis STS brings out a notable impact on efficiency and makes a great contribution to the business economy. However, to utilize a two-axis STS, first of all, cost and benefit analysis should be done carefully because two-axis systems are quite costly. In this context, it is strongly advised to utilize a one-axis STS in solar PV plants. In solar PV plants without STSs or changing the tilt angles as desired, PV surfaces should be set to OPTAs throughout the year for Mediterranean provinces.

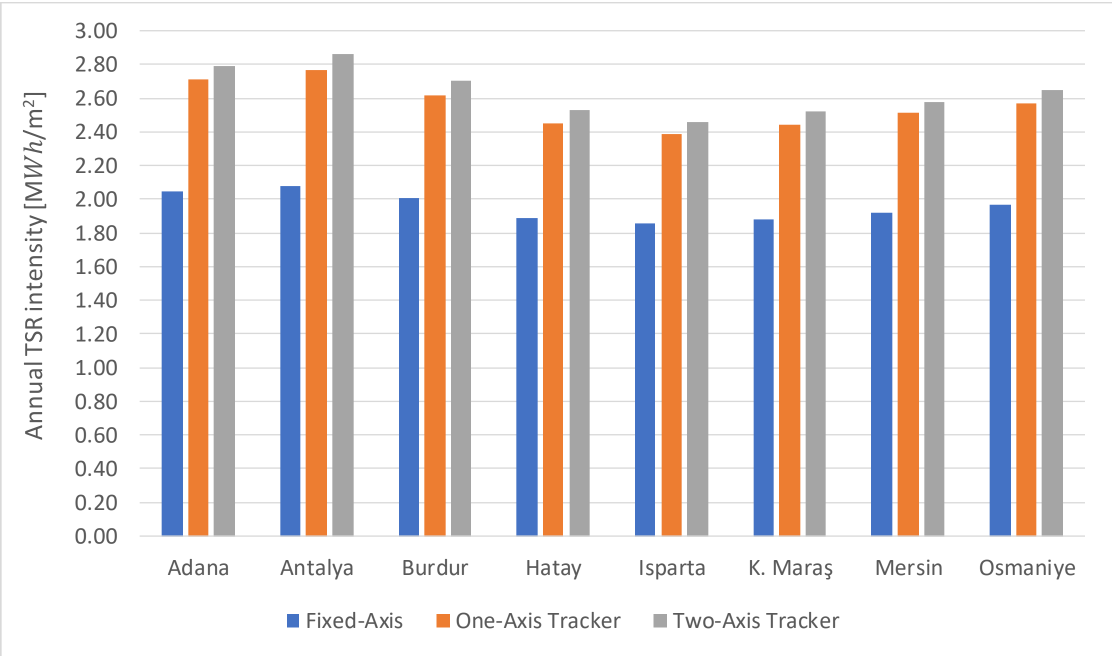

Figure 5.6. Comparison of TSR intensity collected by a tilted surface for the provinces of the Mediterranean region.

5.2.4. Analysis of TSR efficiency and OPTA in terms of latitude

The further the region is from the equator, the greater the effect of optimally tilted surfaces on the TSR efficiency of solar PV plants. That is because, as moving away from the equator, tilting provides a more positive effect. Another important point is that as moving away from the equator, the optimal tilt degree moves away from the latitude value. OPTA calculations based on latitude values may only provide an approximate optimization and do not always give the correct result. Table 5.13 gives the OPTAs at some latitudes, confirming this inference statement. Therefore, optimization techniques should be based on a mathematical method to maximize the TSR collected on a tilted surface in the selected location along with the solar climatic conditions. Another point is that at greater latitudes, greater variation occurs in the incidence angle of TSR, which reduces the collection of TSR. In terms of collected solar TSR as a function of latitude, as the latitude value gets larger, the farther the location is from the equator, the importance of solar trackers increases, and more annual energy yield is gained by increasing the number of solar trackers.

Table 5.13. PV OPTAs at some latitudes.

Location	Latitude N [°]	OPTA β [°]
Oslo	59.91	44
Berlin	52.52	39
Madrid	40.43	32
Cairo	30.14	24

5.3. Results of Case Study (3): Investigation of Anisotropic Models in Estimating TSR Intensity on Solar PV Surfaces, A Case Study for the Southeastern of Türkiye

In this section, there are multiple comprehensive as well as comparative analyses of TSR intensity on tilted and tracked PV surfaces for specific periods in Şanlıurfa province are performed by applying anisotropic transposition models. The estimation procedures are based on Hay-Davies, Klucher, Reindl, HDKR, and Perez's anisotropic transposition models described in Section 3. An annual OPTA has been suggested, and the TSR gains of annual tilted SFS and STS have been predicted by using each model for the study region. So, the section evaluates the performance of anisotropic models for the Şanlıurfa province of Türkiye. It is noted that the current investigation does not aim to identify the best anisotropic model, but in a relative cross-comparison, it points out the high variability of outputs and disagreements between models used for the optimization of PV plants.

5.3.1. GSR (GSR) intensity on the Horizontal Surface

The horizontal GSR values and clearness index ratios from METEONORM (2024) solar data are presented in Figure 5.7. As shown in Figure 5.7, the summer season receives a significantly large amount of horizontal GSR in this region while receiving the least GSR throughout the winter. The maximal monthly GSR value is predicted in July (237.9 kWh/m²), and the minimal GSR value is predicted in December (68.4 kWh/m²). The annual GSR value is 1811.6 kWh/m². Since the most significant solar parameter is GSR intensity on the horizontal surface, Şanlıurfa province has highly advantageous productivity in terms of solar energy.

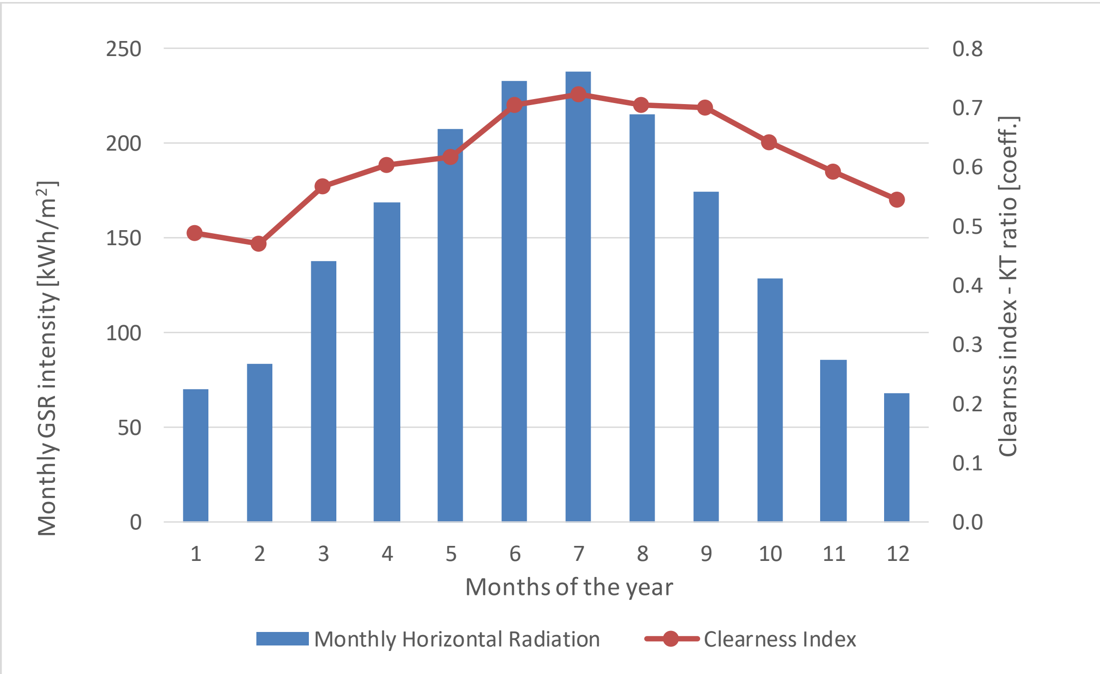

Figure 5.7. The TSR values on a horizontal surface, and clearness index ratios.

5.3.2. Determination of OPTAs (OPTA) for Sanliurfa

Solar components and their parameters used in calculation algorithms such as diffuse fraction correlation models, tilted surface transposition models, and solar datasets greatly affect the results of OPTA values in the desired location. Monthly OPTA values are set 12 times a year and predicted monthly OPTAs for Şanlıurfa province determined by using the anisotropic transposition models are presented in Table 5.14 and Figure 5.8.

Table 5.14. Monthly OPTA values for Şanlıurfa determined by the anisotropic models.

Month	Hay-Davies	Klucher	Reindl	HDKR	Perez
1	57	58	59	61	60
2	49	49	50	51	51
3	37	36	38	39	37
4	23	24	23	22	25
5	8	9	10	8	12
6	4	3	4	3	5
7	6	7	6	5	8
8	19	18	18	16	19
9	33	32	33	34	34
10	48	46	47	48	47
11	59	57	59	58	58
12	64	61	63	63	61

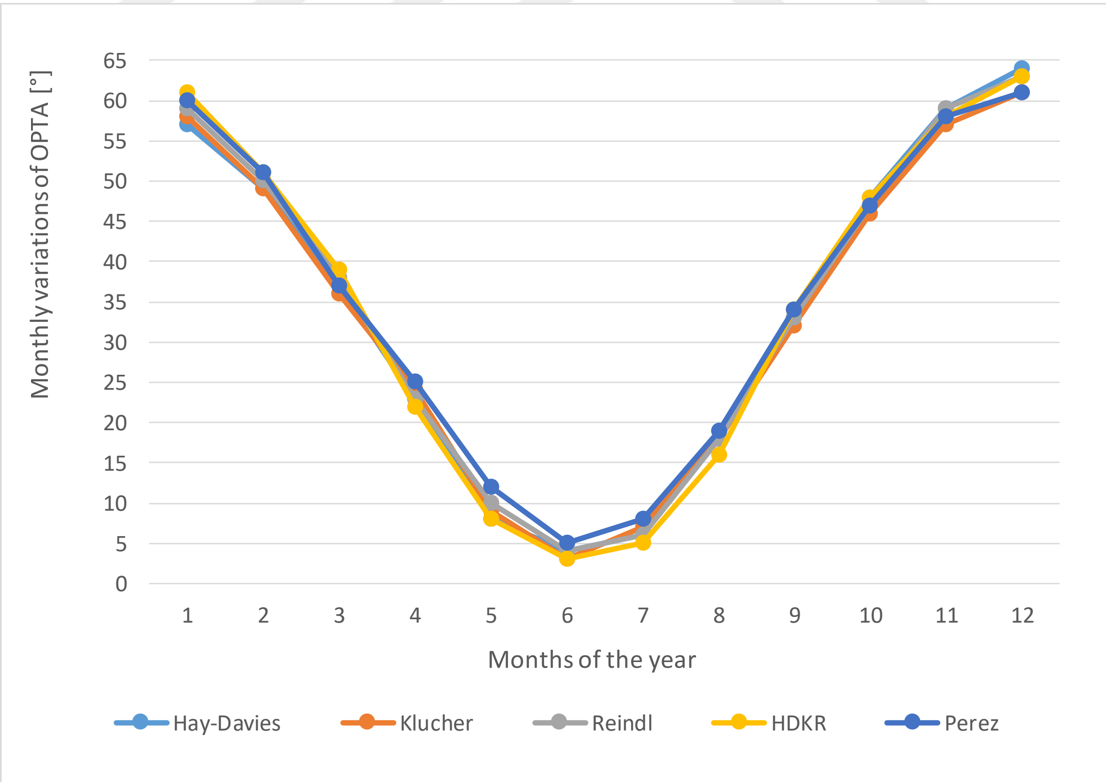

Figure 5.8. Monthly variations of OPTA values.

The monthly OPTA values range from 3° in July to 64° in December for the entire year. Seasonal OPTA values for the case study region are also illustrated in Table 5.15. The seasonal OPTA values are between the lowest value of 8° in summer and the highest value of 59° in winter for the entire year. It is understood from Table 3 that the OPTA values are lower compared to latitude values in the spring and summer seasons, whereas they become higher in autumn and winter. As depicted in Tables 5.14 and 5.15, monthly OPTA values become higher compared to latitude values from October to February. In March, the OPTA value remains equal to the latitude value. The values between April and October are below the latitude value. Upon investigation of the OPTA and latitude relationship, the above conclusions have been obtained. The annual average OPTA value is computed by considering an average of the monthly or seasonal OPTA values determined in Tables 5.14 and 5.15. The annual average OPTA values obtained from anisotropic models are found to be between 33° and 35°. It is seen that the annual OPTA and the annual average OPTA differ by 3° to 4°. This deviation is expected to be higher once moved from the equator to the poles with greater latitudes due to the fluctuations in the sun's incidence angle being larger and more frequent. This means the annual average OPTA does not indicate the annual OPTA; it is an approximate estimation of the tilt angle. The OPTA must be determined based on the maximum TSR intensity captured by the tilted surface.

Table 5.15. Seasonal OPTA values for Şanlıurfa determined by anisotropic models.

Season		Hay-Davies	Klucher	Reindl	HDKR	Perez
Winter	Dec	57	56	58	59	58
	Jan					
	Feb					
Spring	Mar	23	22	23	22	25
	Apr					
	May					
Summer	Jun	9	9	9	8	11
	Jul					
	Aug					
Autu mn	Sept	44	46	45	48	45

Oct	
Nov	

In Table 5.16, the OPTA and corresponding daily TSR values obtained by applying presented anisotropic models are shown, the annual OPTA for Şanlıurfa province is identified to be 30°-31°, which is close to the latitude as expected but below the latitude (6°-7°) of the region in interest. The applied models yielded the daily TSR values on tilted surfaces in the range of 5.27 to 5.38 kWhm^2. While calculating the OPTA, it has been assumed that the diffuse radiation fraction is the same for all transposition models by using the Erbs correlation model.

Table 5.16. OPTA values [and corresponding daily TSR values determined by the anisotropic transposition models.

Anisotropic Model	**Correlation Model**	**OPTA [β=OPT°]**	**Daily TSR [kWhm2-day]**
H-D	Erbs et al.	30°	5.262
Klucher	Erbs et al.	30°	5.355
Reindl	Erbs et al.	31°	5.276
HDKR	Erbs et al.	30°	5.358
Perez	Erbs et al.	31°	5.375

Also, previously predicted OPTA values for Şanlıurfa are tabulated in 5.17. As inferred from 5.17, the models used in the present study yield OPTA values in good accordance with earlier research findings in the literature.

Table 5.17. Literature comparison of annual OPTA results for Şanlıurfa Province.

Province	Annual OPTAs [β°]		Authors
	Present	Literature	
Şanlıurfa	30°-31°	33°	Akgul et al., 2023
		30°	Akgul et al., 2022
		28°	Gonul et al., 2022

33º	Yigit & Arslanoglu
30º	Aktacir et al., 2020
31º	Yildirim & Aktacir, 2019
37º	Kacira et al., 2004

The connection between the annual OPTA and the obtained TSR outcomes is shown in 5.9. It is inferred that the collected TSR by PV surfaces is considerably affected when the tilt angle changes between 5° and 70°. At these tilt angles, the lowest and highest values of annual TSR are predicted at 1524.8 kWh/m² (Hay-Davies) and 1968.2 kWh/m² (HDKR), respectively. This means that tilt angle changes of 0°-70° can yield a gain in energy production of up to 29.09%.

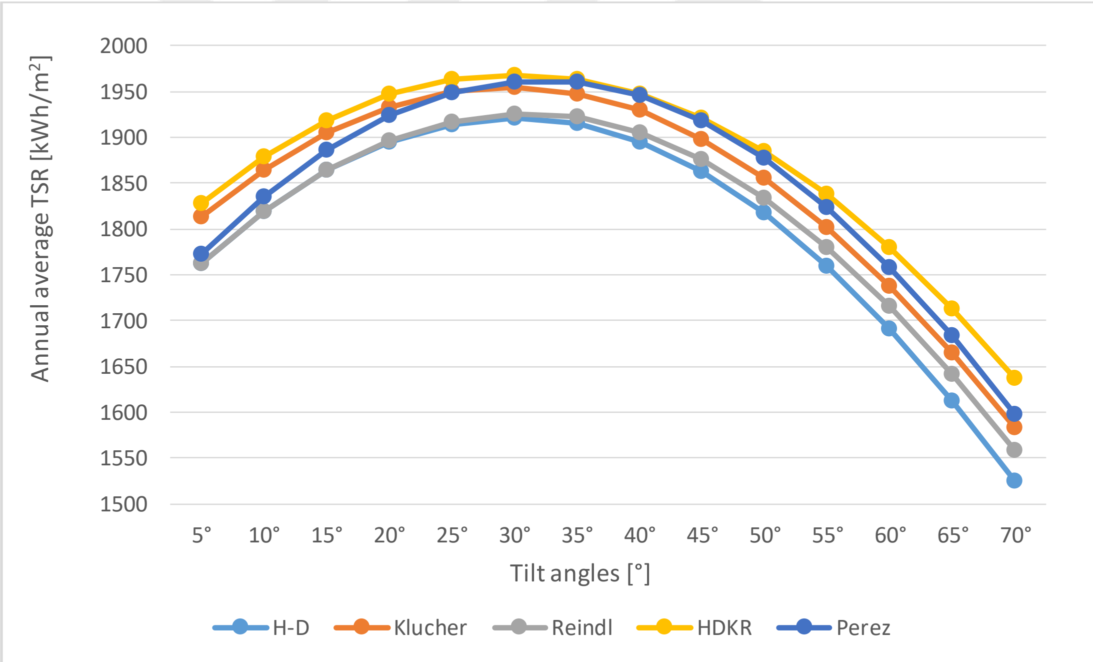

Figure 5.9. The relation between the annual tilt angle and the yielded TSR.

5.3.3. TSR intensity on SFSs

By applying the anisotropic transposition models presented in Section 3.5, TSR values corresponding to the monthly and seasonal OPTAs of PV surfaces by utilizing different models have been tabulated in Tables 5.18 and 5.19, respectively. As depicted in Tables 5.17 and 5.18, the monthly OPTA values generated from the models show a peak in July (HDKR, 246.8 kWh/m²) and a dip in December (HDKR, 111.3 kWh/m²). The lowest and highest TSR values at a seasonal OPTA occur in winter (up to 354.9 kWm^2) and summer (up to 701.5 kWh/m²), respectively.

Table 5.18. Predicted TSR intensity by utilizing monthly OPTA values.

Month	**Hay-Davies**	**Klucher**	**Reindl**	**HDKR**	**Perez**
1	114.1	112.4	115.4	121.3	116.7
2	110.9	111.8	112.1	123.2	114.8
3	156.9	159.6	157.6	156.9	161.2
4	172.1	175.8	172.4	165.7	175.3
5	199.6	204.3	199.7	206.7	201.3
6	222.7	227.4	222.7	235.8	223.4
7	227.7	232.6	227.8	246.8	229.1
8	212.8	217.4	212.9	223.1	215.8
9	193.2	195.6	193.5	200.7	197.3
10	166.1	167.4	167.2	163.4	170.8
11	137.2	136.2	138.7	131.1	140.5
12	116.2	114.4	118.1	111.3	119.6

Table 5.19. Predicted TSR intensity by utilizing seasonal OPTA values.

Season		**Hay Davies**	**Klucher**	**Reindl**	**HDKR**	**Perez**
Winter	Dec	340.2	337.6	344.4	354.9	350.2
	Jan					
	Feb					
Spring	Mar	519.7	531.7	520.5	519.6	529.3
	Apr					
	May					
Summer	Jun	660.5	674.7	660.6	701.5	665.2
	Jul					

	Aug					
	Sept	489.2	492.2	491.9	488.8	501.8
	Oct					
Autumn	Nov					

The predicted monthly TSR values on a tilted surface (30°) are presented in Table 5.20 for comparison purposes along with the monthly horizontal GSR values (0º). As tabulated in Table 5.20, some solar parameters involved in anisotropic models significantly affect the estimation results. For the case study region, minimum and maximum values of monthly TSR at the annual OPTA are predicted at 100.3 kWh/m² (December) and 237.8 kWh/m² (July), respectively. In other words, it may be assumed that the monthly TSR varies between these values throughout the year. It is understood that from the analysis of Table 5.19, setting a PV surface at an annual OPTA contributes significantly to the TSR efficiency in the winter season. Despite all this, setting a PV surface at its annual OPTA cannot contribute sufficiently to TSR efficiency in the summer season. That is because the angulation to OPTA has a negative effect in the summer months in the Şanlıurfa province.

Table 5.20. Comparison of monthly TSR values for anisotropic transposition models.

M	H-0°	H-D	Klucher	Reindl	HDKR	Perez
1	70.3	100.5	100.4	100.9	106.2	102.2
2	83.6	105.1	106.8	105.4	115.5	107.8
3	137.9	155.8	158.8	156.2	155.1	159.4
4	169.2	171.3	174.8	171.7	164.4	175.1
5	207.9	189.2	194.1	189.7	196.6	193.1
6	233.2	203.2	208.9	203.7	213.2	207.3
7	237.8	211.6	217.2	212.1	229.2	216.1
8	215.2	209.1	213.3	209.3	218.3	213.3
9	174.5	192.9	195.5	193.2	200.2	196.5
10	128.6	160.1	162.3	160.3	156.4	163.4
11	85.8	122.2	122.9	122.6	117.2	124.4
12	68.4	100.4	100.3	100.8	95.9	102.6

Estimations of solar energy potential differences with the monthly variation in Şanlıurfa province for a tilted PV surface are drawn in Figure 5.10. The data in Figure 5.10 demonstrates that installing an optimal SFS for the whole year is not appropriate for achieving maximum energy efficiency. The TSR values on an optimally tilted PV surface (annual, seasonal, and monthly) by applying anisotropic models in comparison with the solar horizontal TSR values are graphically presented in Figure 5.11. The drawn curves reflect the solar power potential in the Şanlıurfa province separately for each transposition model. It is found that the annual TSR values at the annual OPTA are predicted between 1,921.3 kWh/m² (HD) and 1,968.2 kWh/m² (HDKR) by applying anisotropic models for the region under investigation. In other words, these values can be considered as the minimum and maximum TSR values. It is implied from Table 5.14, Figure 5.10, and Figure 5.11 that the TSR intensity on a PV surface is a function of tilt angle. It is clear that for the investigated geolocation, the PV surface orientation must be set to the south (surface azimuth angle is 0°). There is no doubt that the proper installation of PV surfaces can have a substantial effect on the production of solar energy. It is therefore recommended that the OPTA be adjusted to an annual for an SFS if it is not possible to set it monthly.

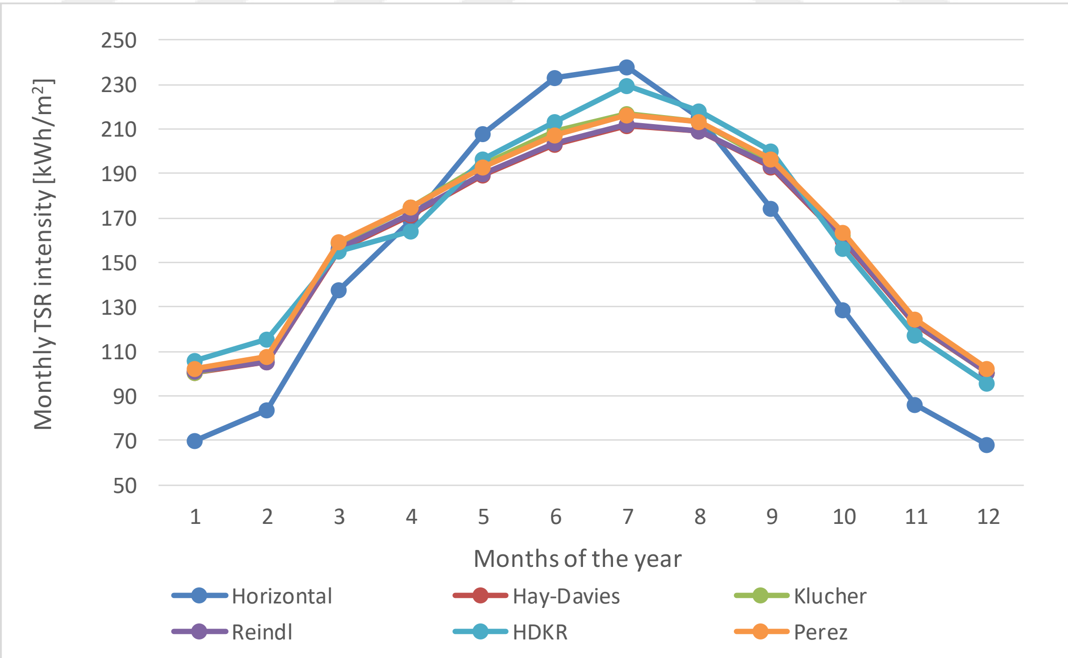

Figure 5.10. Estimations of solar energy potential with the monthly variation.

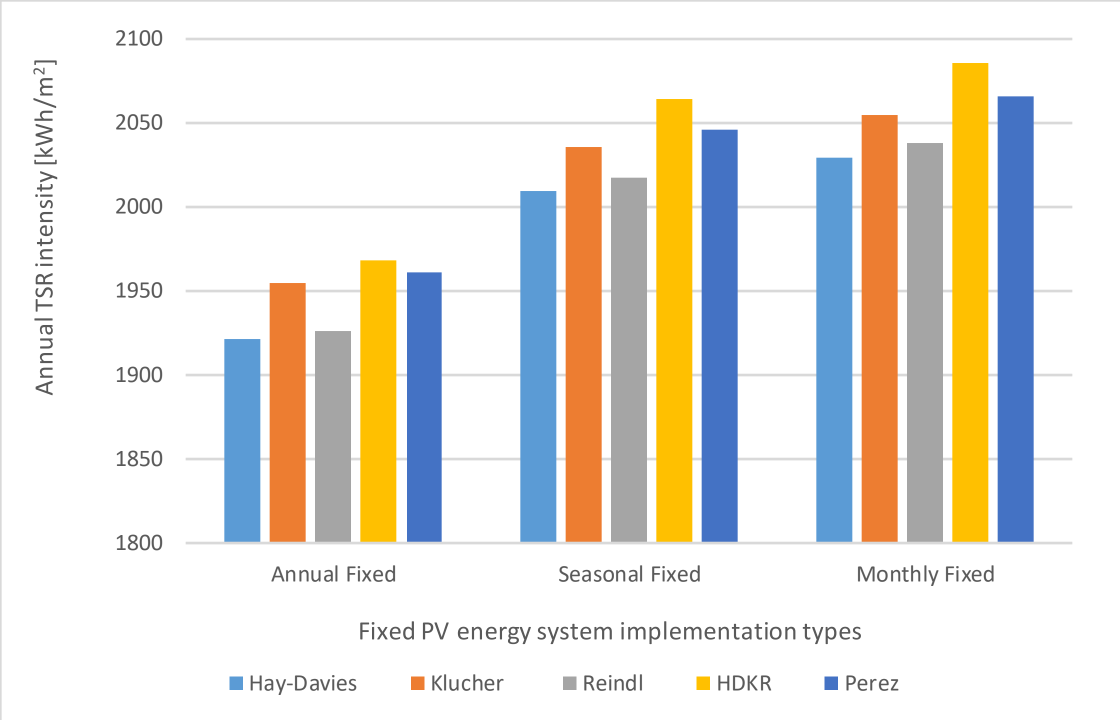

Figure 5.11. Comparison of TSR values on annual, seasonal, and monthly tilted surfaces in Sanliurfa.

5.3.4. TSR Intensity on STSs

No general rule has been standardized to evaluate the technical and financial efficiencies of STSs. However, it is well understood that solar energy production capacity can be significantly increased by utilizing STS technologies, especially at high latitudes. Most of the PV plant implementations have not been done with the STSs in Türkiye territories so far. Keeping that point in mind, this section discusses the benefits of STSs by theoretically analyzing the possible PV plant implementations for the future in Şanlıurfa as an example. The predicted monthly TSR values on single-axis and dual-axis STSs are tabulated in Table 5.21 comparatively. It is seen that the maximum TSR values are calculated in July of the summer season, whereas the minimum TSR values are calculated in January of the winter season for both the single-axis and dual-axis STSs in Şanlıurfa province. Monthly TSR values are predicted between 118.4 kWh/m² and 317.7 kWh/m² for a single-axis STS, between 129.2 kWh/m² and 337.2 kWh/m² for a dual-axis STS.

Table 5.21. Monthly TSR values [kWh/m²] on an STS by applying anisotropic models for the study region.

Month	Hay-Davies		Klucher		Reindl		HDKR		Perez	
	1-Axis	2-Axis	1-Axis	2-Axis	1-Axis	2-Axis	1-Axis	2-Axis	1-Axis	2-Axis
1	120.9	132.3	118.4	129.2	121.3	133.9	116.3	134.4	122.8	134.8
2	124.2	129.6	124.7	129.3	125.2	131.2	128.8	139.6	127.8	134.3
3	190.9	196.8	191.8	196.7	191.9	198.5	183.5	199.8	196.2	203.2
4	212.7	222.5	213.4	222.3	213.8	223.8	204.3	215.3	218.4	228.8
5	238.9	268.5	239.7	266.8	239.9	269.6	261.6	278.3	245.2	274.5
6	261.3	302.3	261.9	299.8	262.3	303.2	304.8	321.9	267.2	307.2
7	273.7	315.9	273.9	312.6	274.5	316.7	317.7	337.2	279.5	320.6
8	267.9	294.9	267.8	291.8	268.8	295.8	291.5	314.5	273.7	300.8
9	249.8	260.5	248.2	257.5	250.6	261.6	245.8	268.6	253.6	264.4
10	196.8	203.9	196.9	202.7	197.8	205.7	177.3	200.3	200.9	209.3
11	148.6	162.2	147.2	158.9	149.6	163.9	130.2	150.4	150.9	165.3
12	121.3	133.9	118.9	130.4	121.8	135.9	117.9	139.2	123.7	137.4

It is also possible to visualize monthly predicted TSR values by applying anisotropic models when it comes to setting up STSs in the geolocation of interest. Accordingly, estimations of solar energy potential differences with the monthly variation in Şanlıurfa province regarding a single-axis and a dual-axis PV surface have been plotted in Figure 5.12 and Figure 5.13. As can be deduced from the comparative analysis of the plotted figures, installing STSs generates more solar energy than an annual SFS. So, it can be expressed that STSs may compensate for the cost of initial investment rapidly or over certain years. In conclusion, implementing an STS is highly suggested to boost system output and the yields of the PV plant to be installed in Şanlıurfa province. The results confirm the region's significant potential for solar energy.

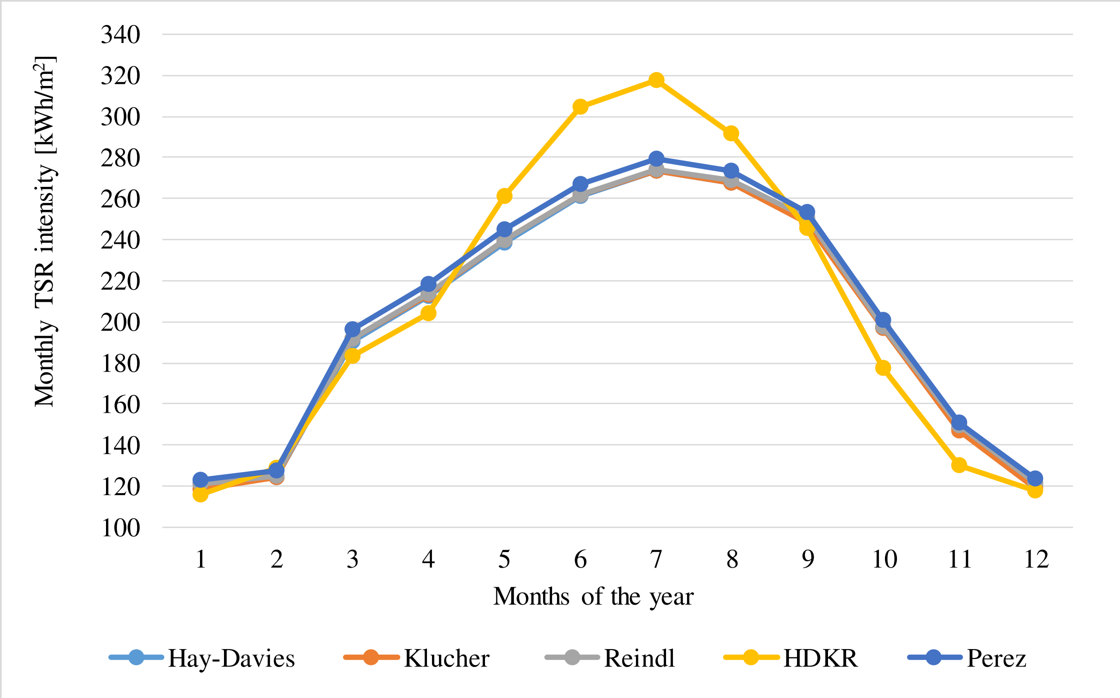

Figure 5.12. Estimations of solar energy potential with the monthly variation on a single-axis STS in Şanlıurfa.

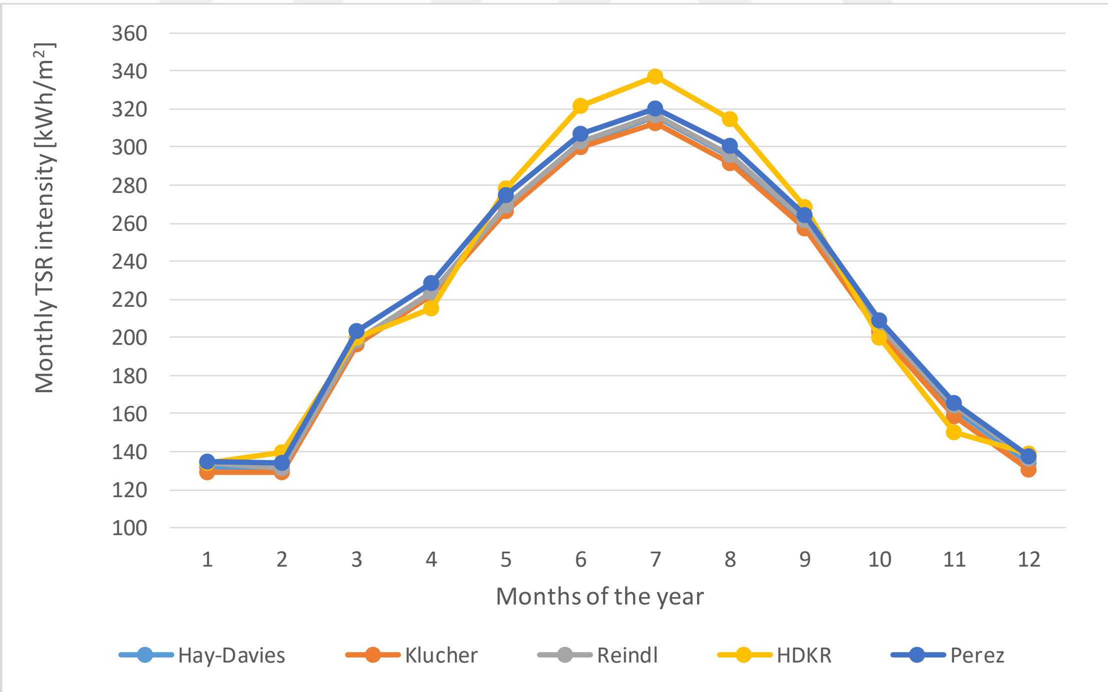

Figure 5.13. Predicted solar energy potential with the monthly variation on a dual-axis STS in Sanliurfa.

The predicted annual TSR values on a single-axis and a dual-axis STSs versus annual TSR values on an SFS are presented in Figure 5.14 for each anisotropic model. The lowest and highest annual TSR values are predicted for a single-axis tracker 2,401.8 kWh/m² (Klucher) and 2,478.9 kWh/m² (HDKR), for a dual-axis tracker 2,596.7 kWh/m² (Klucher) and 2,698.6 kWh/m² (HDKR), respectively. That is, the predicted TSR varies between these values throughout the year. Figure 5.14 infers that since the sun travels from east to west, SFSs are not sufficient to generate a maximal amount of energy. So, there is an absolute need for an STS that will be able to track the sun all through the day to optimize the PV energy.

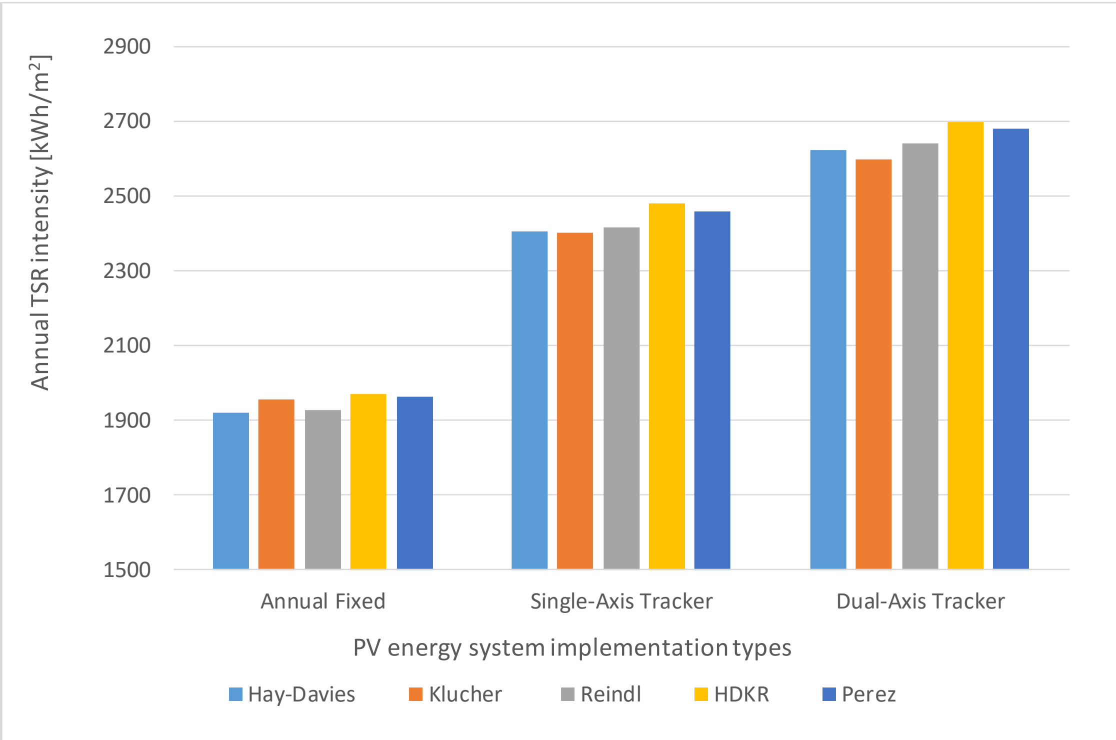

Figure 5.14. Predicted annual TSR intensity [kWh/m²] on STSs compared to an SFS [β=30º].

5.3.5. Percentage Gain for SFSs

A comparison of monthly TSR gains as a percentage on a tilted PV surface for anisotropic models is presented in Table 5.22. The circumsolar and horizontal-brightening components in the anisotropic models have more significant effects in the winter season when the sky is overcast, implying that adjusting PV surfaces at an OPTA in winter has the maximum impact on energy efficiency. As depicted in Table 5.16, the highest productivity is reached by adjusting OPTAs in the winter season. For example, the maximum TSR gain in January is predicted at 51.29% (HDKR) for an annual SFS. It is also seen from Table 5.22 that optimal annual angulation has a negative effect in the summer season because an annual OPTA of the PV surface cannot collect all the horizontal GSR.

Table 5.22. Monthly TSR gains [%] on adjusted at OPTA of PV surface for each anisotropic model.

Month	Hay-Davies	Klucher	Reindl	HDKR	Perez
1	43.17+	42.86+	43.73+	51.29+	45.58+
2	25.87+	27.77+	26.22+	38.32+	29.10+
3	12.99+	15.16+	13.27+	12.47+	15.59+
4	1.37+	3.44+	1.59+	5.43-	3.55+
5	8.98-	6.67-	8.75-	5.48-	7.11-
6	12.77-	10.34-	12.57-	8.11-	11.02-
7	11.02-	8.74-	10.84-	3.61-	9.11-
8	2.78-	0.83-	2.64-	1.53+	0.79-
9	10.55+	12.04+	10.71+	14.73+	12.61+
10	24.52+	26.31+	24.74+	21.64+	27.09+
11	42.26+	43.08+	42.72+	36.43+	44.70+
12	46.98+	46.86+	47.58+	40.41+	50.21+

Comparisons of annual TSR gains as a percentage value on a tilted Surface by applying the presented anisotropic transposition models are presented in Figure 5.15. The gain in annual TSR for an annual OPTA (30º) compared to a horizontal surface (0º) is predicted at 6.05% (HD), 7.91 (Klucher), 6.32% (Reindl), 8.62% (HDKR), and 8.24% (Perez). It is understood that setting the OPTA of a PV surface can provide a gain in the amount of TSR from 6.05% to 8.24% under solar climatic conditions of the case study region. It is also found that the HDKR model calculates more TSR gain than other models. Acceptable and tolerable disagreements have been detected between the presented models in the estimation of TSR for an optimally tilted PV surface, which may be due to the different insight calculations of correlation factors such as circumsolar brightening and horizon brightening, and unique features of the case study region.

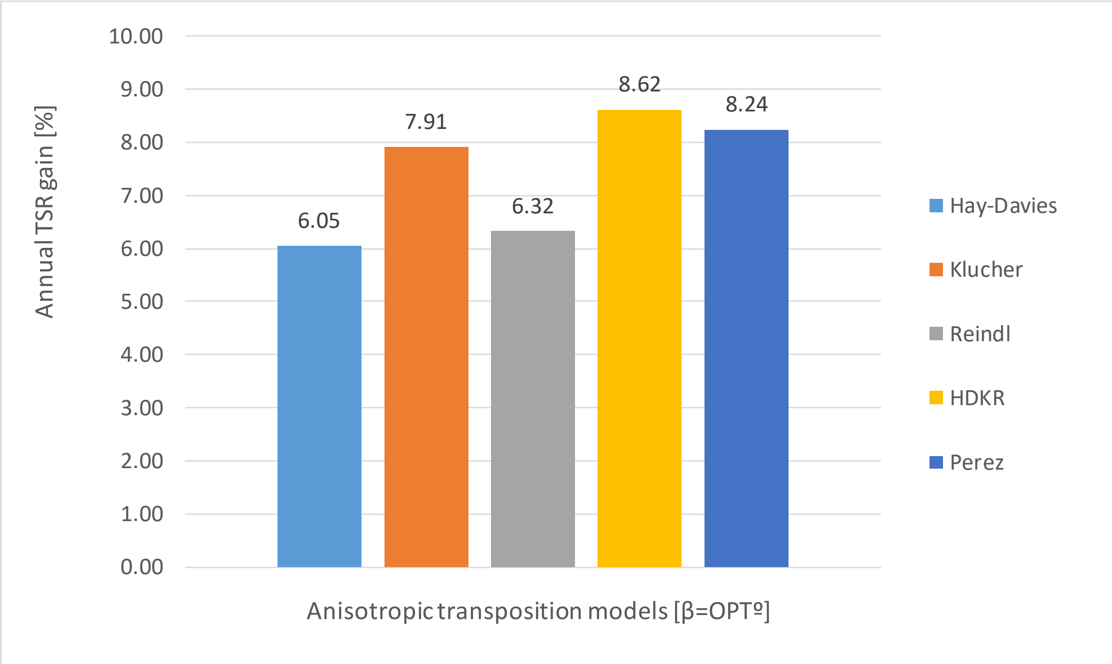

Figure 5.15. Comparison of annual TSR gains [kWh/m²] on a tilted Surface [β=30º] for anisotropic transposition models.

5.3.6. Percentage Gain for STSs

A comparison of monthly TSR gains compared to annual SFSs as a percentage [%] on STSs for anisotropic models is illustrated in Table 5.23. It is depicted in Table 5.23 that the impact of STSs on energy efficiency is at its maximum in the summer season. For example, the maximum TSR gain is predicted in June at 43.03% (HDKR) for a single-axis tracker and 51.05% (HDKR) for a dual-axis tracker. The minimum TSR gain is predicted in Jan at 9.41% (HDKR) for a single-axis tracker and in February at 20.79% (Klucher) for a dual-axis tracker. The results indicate that the amount of TSR on a tilted surface can be particularly improved by setting the tilt of a PV surface. Therefore, the annual OPTA should be adjusted for SFS where varying the OPTA is not possible monthly or seasonally. Such adjusting at OPTA of SFSs helps reduce the time of recovery and assess the profitability associated with an investment.

Table 5.23. Monthly TSR gains compared to annual SFSs as a percentage [%] on STS.

Month	HD Model		Klucher Model		Reindl Model		HDKR Model		Perez Model	
	1-Axis	2-Axis	1-Axis	2-Axis	1-Axis	2-Axis	1-Axis	2-Axis	1-Axis	2-Axis
Jan	20.20	31.55	18.55	28.62	20.62	32.71	9.42	26.46	20.16	31.90
Feb	18.08	23.22	16.78	20.80	18.60	24.39	11.43	20.88	18.56	24.49
Mar	22.47	26.26	20.72	23.81	22.86	27.02	18.25	28.76	23.03	27.36
Apr	24.11	29.84	22.03	27.12	24.47	30.29	24.21	30.91	24.80	30.75
May	26.22	41.87	23.51	37.48	26.47	42.07	33.02	41.51	26.88	42.16
Jun	28.55	48.73	25.33	43.47	28.67	48.75	43.04	51.06	28.85	48.15
Jul	29.31	49.30	26.18	44.01	29.44	49.34	38.57	47.08	29.34	48.36
Aug	27.76	41.06	25.57	36.82	28.43	41.33	33.49	44.07	28.32	41.03
Sep	29.45	34.99	26.91	31.67	29.66	35.36	22.73	34.12	29.02	34.51
Oct	22.94	27.44	21.26	24.84	23.33	28.26	13.38	28.09	23.03	28.12
Nov	21.53	32.66	19.70	29.22	21.95	33.69	11.02	28.25	21.40	32.92
Dec	19.73	33.27	17.95	29.92	20.24	34.73	22.95	45.05	19.79	33.83

Figure 5.16 illustrates the comparison of the annual TSR gain differences and variations on optimally tilted, single-axis, and dual-axis tracked surfaces by using anisotropic sky transposition models for Şanlıurfa province. As can be depicted from Figure 5.17, the gain in annual TSR on a single-axis tracker in comparison to an annual SFS is predicted between 22.04% (Klucher) and 25.95% (HDKR). In addition, the gain in annual TSR on a dual-axis tracker in comparison to an annual SFS is predicted between 31.50% (Klucher) and 37.12% (HDKR).

From a broad perspective, Figure 5.16 indicate that PV surfaces must be equipped with solar trackers to optimize PV plants and enhance TSR intensity on the PV surface. In other words, considering the findings obtained by these models, it is recommended that, when possible, the PV surface be configured with trackers for better utilization of solar energy in the case study region. However, trackers need periodic maintenance, input energy, etc. Therefore, these options are not always economical. Another strategy, rather than installing trackers, is to optimize the OPTA of PV surfaces. Moreover, it is seen that anisotropic transposition models involve some solar parameters that impact the performance of these models and the quality and precision of the outcomes. The proposed anisotropic models can be utilized for estimating TSR intensity on tilted and tracked PV surfaces.

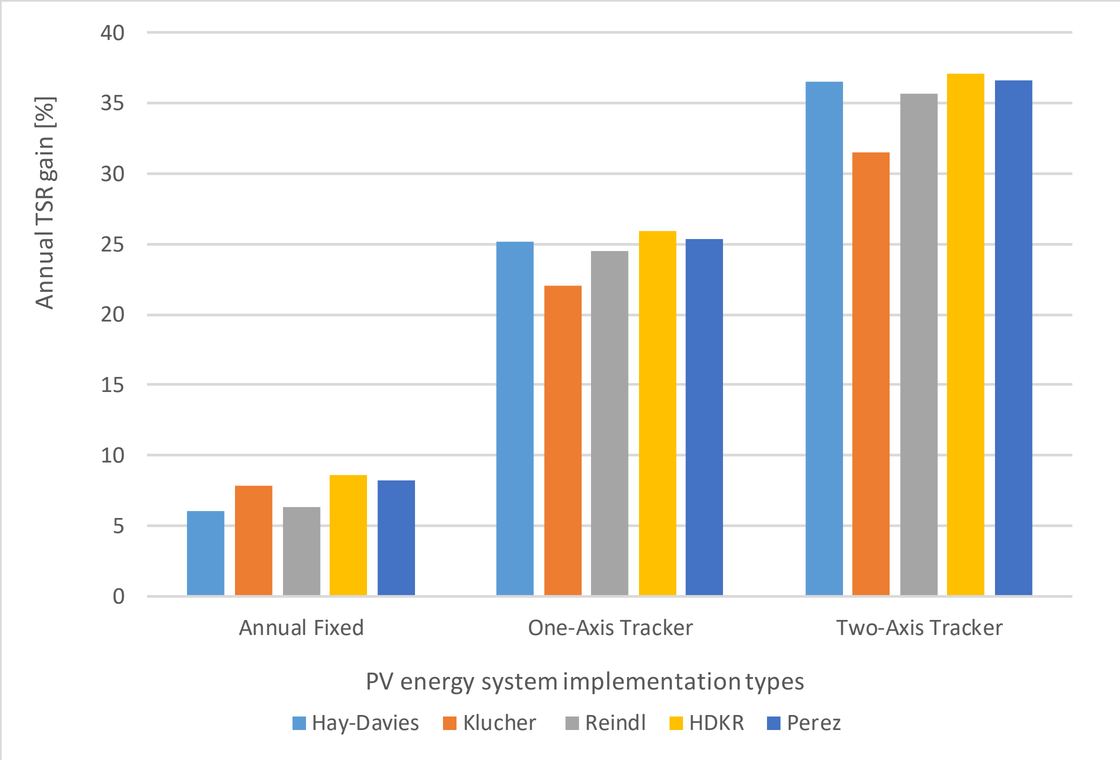

Figure 5.16. Comparison of the annual TSR gain in the case of implementing fixed and tracked systems.

5.3.7. Average of the results obtained from the investigated models

The averages of the annual TSR intensity outputs computed from the investigated anisotropic transposition models are illustrated in Figure 5.17. Considering the findings, annual, seasonal, and monthly adjustments of PV surfaces will generate approximately higher TSR of 7.44%, 12.32%, and 13.41%, respectively, than a horizontal surface in the Şanlıurfa province. On the other hand, monthly adjustments of the PV surfaces can generate an average of 6.36% more TSR, whereas seasonal adjustments can generate an average of 5.45% more TSR gain to the SFS adjusted with annual OPTA. Besides, there is a 0.97% loss in TSR on a seasonal optimal tilt surface compared to a monthly OPTA. That is to say, setting the OPTA monthly can cause an approximately 1% increment compared to seasonally set PV surfaces. Since it is costly to set the OPTAs of PV surfaces monthly or seasonally in PV plants, the tilt angles may be set to align with the annual OPTA in the absence of STSs. As can be concluded from Figure 5.17, compared to an SFS, single-axis and dual-axis trackers will generate approximately an average of 24.99% and 36.03% more TSR, respectively. It is inferred that a dual-axis STS could yield 8.84% more TSR than a single-axis tracker for the case study region.

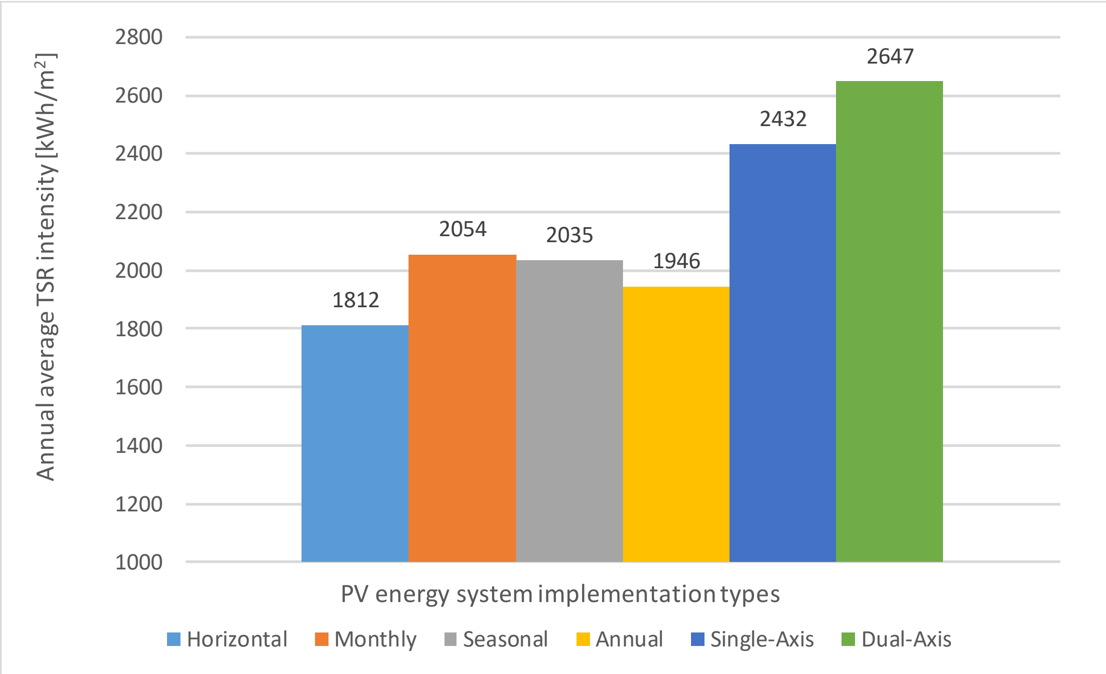

Figure 5.17. Average TSR intensity computed from the anisotropic transposition models in Şanlıurfa.

5.3.8. Effects of OPTA on TSR intensity collected by PV surfaces

The sensitivity of an OPTA within a deviation of 5° is analyzed based on anisotropic transposition models using the METEONORM dataset. The impact of OPTAs on the annual TSR values for the Şanlıurfa is tabulated in Table 5.24 based on findings of Table 5.24, considering the OPTA values and the TSR values corresponding to these angles, it is found that there is a reduction in TSR efficiency of between 0.11% and 0.34% at a deviation of 5°. The 5° tilt angle departure from the OPTA when using the anisotropic transposition models results in a reduction in annual TSR of no more than 0.5%. In small-scale PV plants, this discrepancy might not even be noticeable, but in the consideration of large-scale PV plants, it could correspond to significant energy losses.

Table 5.24. The impact of OPTAs [β] on the annual TSR intensity [kWh/m²].

[β]	Hay-Davies	Klucher	Reindl	HDKR	Perez
30º	1921.3	1954.7	1925.7	1968.1	1960.8
31º	1920.8	1954.6	1926.1	1968.5	1962.1
32º	1920.3	1953.7	1925.5	1967.9	1962.1
33º	1918.8	1952.4	1925.1	1966.5	1961.8
34º	1917.3	1950.3	1923.6	1965.1	1961.4
35º	1914.8	1948.2	1921.9	1962.8	1960.0
Loss %	0.32	0.34	0.21	0.25	0.11

5.3.9. OPTA and latitude relation

Optimization of OPTA considerably increases the TSR intensity for PV plants. Several researchers have investigated relations between OPTA and latitude to be used as general rules by solar PV plant designers for determining the OPTA values. In Table 5.25, OPTA relations concerning latitude are presented, where summer and winter seasons are denoted by a minus sign and a plus sign, respectively. These studies claim that the annual OPTA can be directly related to the latitude of a geolocation. Most probably, the annual OPTA value rises with increasing latitude, and the TSR intensity decreases with increasing tilt angle value, nevertheless, no general inference can be drawn about it because the TSR intensity varies significantly from location to location and even for locations with the same latitude. These general rules obtained by utilizing latitude relations only provide simple and approximate tilt angle values. Thus, precise determination of the OPTA for a particular location requires the use of transposition models with solar data on horizontal surfaces.

The latitude-based OPTA relations presented in Table 5.25 do not take into consideration the solar parameters that may significantly impact the TSR intensity, such as height above sea level, the patterns of cloud cover, etc. Therefore, the claimed general rules may not give precise results for cloudy regions, especially for high latitudes. It has been understood that the OPTA estimations in some studies in the literature seem not useful and efficient, depending on the case study. Improper OPTA analysis could lead to high system costs and undervaluing systems. This impact will be more noticeable, especially in large-scale PV plants, and lead to a loss of potential solar energy.

Table 5.25. OPTA values relative to latitude in previous research.

Author(s)	Date	Suggested OPTA
Stanciu & Stanciu	2014	∅ − δ
Uba & Sarsah	2013	∅+17º
Benghanem	2011	∅
Lave & Kleissl	2011	∅-(1º-10º)
Rowlands et al.	2011	∅
Gunerhan & Hepbasli	2007	∅±15º
Elminir et al.	2006	∅±15º
Tang & Wu	2004	∅+(4º→10º)
Shariah et al.	2002	∅-3º
Garg	1982	∅+15º
Duffie & Backman	1980	(∅+15º)±15º
Lunde	1980	∅±15º
Kern & Harris	1975	∅+10º
Yellot,	1973	∅+20º
Lof & Tybout	1973	∅+(10º→30º)
Heywood	1971	∅-10º
Chinnery	1967	∅+10º

5.3.10. Comparison with previous studies

Regardless of the statistical test used to identify the model's quality, none of the models are noticeably superior to the others, such statistical analysis yields similar results (Notton et al., 2004). Therefore, it would be a more reasonable approach to analyze the precision of the presented anisotropic models by comparing their consistency with existing results from previous studies in literature. Several studies available in the literature have been investigated to quantify and verify the presented transposition models' performance by comparing the determined OPTA to maximize TSR intensity on the tilted surfaces. A comparison of OPTA values found in other research and the current study is presented in Table 5.26.

It is known that a few degree differences in OPTA values may arise from the usage of different solar data (satellite-derived or measured) or depend on whether instantaneous TSR values or daily TSR values are taken in the different transposition models. Table 5.25 exhibits some fluctuations in the results, mainly due to these reasons. On average, tilt angle deviation is within 3°-4° between different calculations in this study and literature; such differences are within an engineering tolerable percentage since it has been shown that a 5° deviation of the annual OPTA does not exceed 0.5% in the yield of annual TSR (see Table 5.24). In light of these findings, it is understood that the anisotropic methods used in this study are applicable and are in agreement with the results of other research studies. As depicted in Table 5.26 the calculated operation of the OPTA yields similar results, so they should be considered before the effective design of the PV plants. The efficiency of a PV plant cannot be brought up to its maximum performance without considering the OPTA. Previous studies stated in Table 5.26 imply that different models can produce reliable outcomes.

Table 5.26. A comparison of previous studies and the current study in terms of predicted OPTA values [β=OPT°].

Country	**Cities**	**Latitude**	**Present Study [β=OPT°]**					**Previous Study**		
			H-D	Klucher	Reindl	HDKR	Perez	Research	Date	OPTA
Türkiye	Izmir	38.25	30	29	31	32	32	Akgul et al.	2023	30
Türkiye	Mersin	36.48	29	29	30	30	32	Akgul et al.	2023	30
Libya	Tripoli	32.53	28	28	29	25	30	Nassar et al.	2022	29
Iran	Tehran	35.43	30	30	31	29	32			32
Algeria	Alger	36.45	30	30	31	30	32	Obiwulu et al.	2022	30
Angola	Luanda	8.48	6	5	6	5	7			11
Malaysia	Sabah	5.25	3	3	3	2	5	Matius et al.	2021	8
Greece	Larissa	39.38	28	28	30	33	31	Kambezidis & Psiloglou	2021	25
S. Arabia	Riyadh	24.42	23	22	23	20	24	Mansour et al.	2021	23
Palestine	Palestine	31.57	27	25	29	24	29	Abdallah et al.	2020	29
Egypt	Qena	26.90	23	23	24	20	25	Kassem	2020	27
Cyprus	Famagusta	35.60	28	28	29	27	31	Abdulsalam & Alibaba	2019	28

UK	Leeds	53.48	38	37	40	42	40	Dhimish et al.	2019	40
France	Bordeaux	44.50	34	34	36	40	37	Jacobson & Jadhav	2018	33
Germany	Munich	48.80	37	37	39	42	39			33
Kosovo	Pristina	42.39	33	33	35	37	35	Berisha et al.	2018	35
Morocco	Casablanca	33.34	28	28	29	25	31	Nfaoui & El-Hami	2018	30
USA	New York	40.42	32	31	33	35	34	Ajder et al.	2018	31
Romania	Craiova	44.19	35	34	36	40	37	Alboteanu et al.	2017	45
India	New Delhi	28.36	28	28	29	26	30	Markam & Sudhakar	2016	28
China	Shanghai	31.13	22	22	23	22	25	Zang et al.	2016	27
Jordan	Amman	31.57	27	27	28	24	28	Yasin et al.	2016	34
Spain	Madrid	40.25	31	31	32	35	33			39
Pakistan	Sindh	25.53	24	24	25	22	26	Khahro et al.	2015	23
Taiwan	Kaohsiung	22.37	19	19	20	18	21	Liu & Chang	2015	20
Japan	Niigata	37.55	26	25	27	30	29	Ramli & Walker	2015	34
Singapore	Singapore	1.21	0	0	1	0	3	Khoo et al.	2014	10
Lebanon	Bayreuth	33.53	27	27	27	25	29	Darhmaoui & Lahjouji	2013	32
Italy	Milano	45.27	32	31	33	38	33			43
UAE	Abu Dhabi	24.27	20	20	21	19	23	Jafarkazemi & Saadabadi	2013	22
Malaysia	K. Lumpur	3.70	2	2	2	2	4	Elhab et al.	2012	10
Canada	Winnipeg	49.53	43	43	45	46	44	Kemery et al.	2012	43
Slovenia	Kredarica	46.23	40	39	41	43	41	Rakovec et al.	2011	42
Nigeria	Benin	6.20	7	6	7	5	9	Okundamiya & Nzeako	2011	12
Ireland	Galway	53.16	39	38	41	44	41	Armstrong & Hurley	2010	44
Syria	Damascus	33.30	29	28	29	26	31	Skeiker	2009	31
Russia	Moscow	55.45	39	39	41	46	42	Qui & Riffat	2003	45
Brunei	Brunei	4.32	4	4	4	1	6	Yakop & Malik	2001	3

5.4. Results of Case Study (4): Maximization of TSR on Solar PV Surfaces in Antalya Province of Türkiye Based on LCOE

In this section, the proposed calculation model is applied to the Antalya province. The analyses, discussions, and findings on LCOE and payback and applying the calculation model to large-scope PV plants are presented. By using daily TSR values on a horizontal surface, climatic, and latitude data obtained from NASA-SSE for the districts of Antalya province, OPTAs of the PV surfaces, and maximal TSR gain have been calculated for a specific period. Results are presented in tabular and graphical forms. By using the calculation method, the tilt angle value where the predicted maximum TSR is determined as the OPTA. The PV surface azimuth angle is fixed to 0° for directly facing the equator. It can be used to calculate TSR intensity at any time of year for PV surfaces.

5.4.1. Solar PV plant cost analysis based on levelized cost of energy

The cost of solar energy continues to decrease thanks to increased module efficiency as well as lowered hardware and inverter costs in recent years despite the impact of the global pandemic and the disruptions caused by the spread of the COVID-19 virus (EIA, 2021). A significant portion of the cost declines over the past decade has been sourced from an 85% cost decline in solar module price (NREL, 2021). LCOE is a useful metric for detailed cost comparison, assessing economic potential including the payback period, and the most important criteria for the most large-scale solar PV plants (IFC, 2015). Solar engineers and investors aim to create solar PV plants to maximize financial returns by minimizing the LCOE.

5.4.1.1. Solar PV energy cost

LCOE is the product of all of the lifetime costs associated with the construction and operation of the solar PV plant divided by the energy produced during this lifetime. The value is ranged globally from under \$0.03/kWh to \$0.12/kWh. The LCOE in Türkiye almost halved between 2016 and 2021, reaching a value of \$0.064/kWh (IRENA, 2022). For this reason, there is no doubt that solar energy can be profitable in countries with high energy tariffs and high solar potential at the same time such as Türkiye.

5.4.1.2. Solar PV plant installation cost

Multiple unique factors go into the cost of PV surfaces, and the cost varies depending on different regions of the world. According to the Solar Energy Industries Association's average cost figures in 2021, utility-scale solar PV plant installation costs are typically between $0.89 to $1.01/Wdc (SEISA, 2021). It is assumed that the land is already owned to build the solar PV plant. Based on the U.S. Department of Energy's National Renewable Energy Laboratory, on average, complete solar PV plant costs are $2.65/Wdc for 7.2kW residential SFS, $1.56/Wdc for 200kW commercial SFS, $1.03/Wdc for 10MV large-scale SFS, and $1.13/Wdc for 10MV one-axis large-scale STS (NREL, 2021). These values represent the LCOE which is the average revenue per unit of energy generated that would be required to recover the costs of the solar PV plants over their life expectancy. The average cost of a solar PV plant for the last 5-years is presented in Figure 5.18, and the solar PV plant cost for a complete installation is shown in Table 5.27 provided by the NREL (2021).

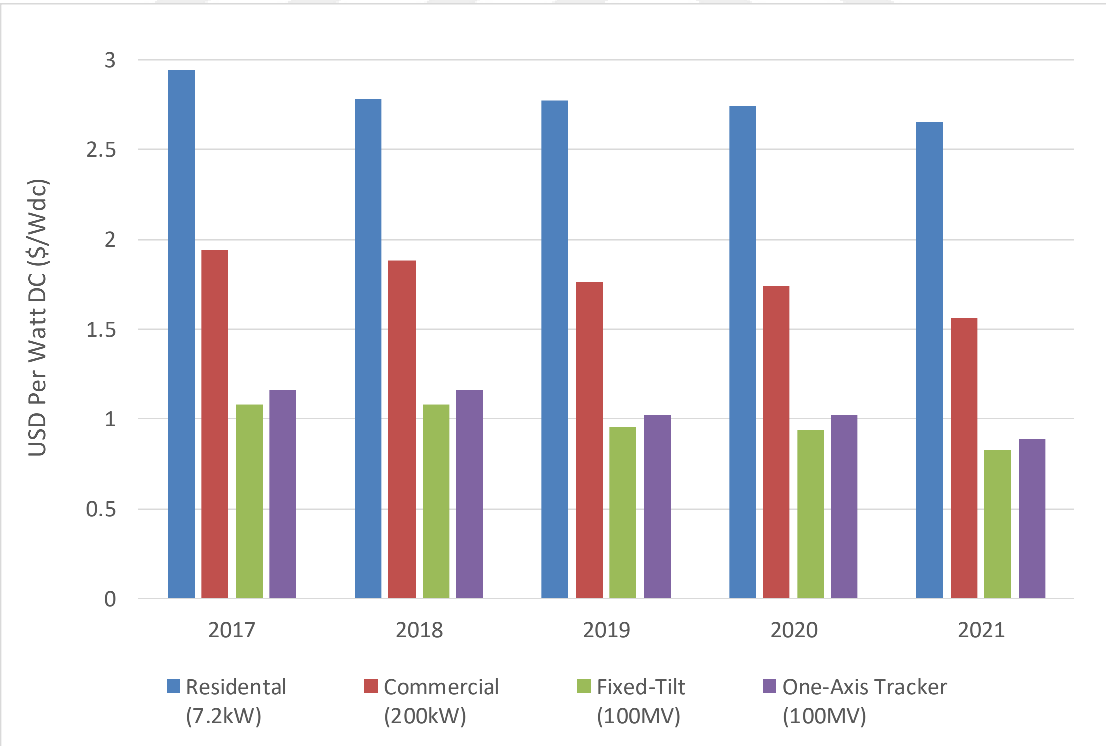

Figure 5.18. The average cost of a solar PV plant for the last 5-years [$/Wdc].

Compared to single-axis trackers, the initial cost of dual-axis trackers is higher, and both trackers require extra space to avoid shadowing effects from one PV surface to the next, thus, space may not be utilized as effectively as with SFSs. Oftentimes, solar trackers also require more maintenance. So, most solar engineers recommend buying additional PV surfaces instead of installing trackers. On the other hand, seasonal variations significantly affect the total energy provided by the PV surface. For a 1 kWp PV plant, the additional energy produced from the single-axis and double-axis STSs was found to be 33% and 37 % higher in comparison to the static systems (Vermaak, 2014). Also, one-axis STSs are the best option in all countries, reducing LCOE by more than 20% when compared to two-axis STSs (Laguna et al., 2021).

Table 5.27. The average cost of a solar PV plant for the year 2021 [$/Wdc].

Type	Capacity	Cost [$]	Type	Capacity	Cost [$]
Residential	7.5kWdc	2.65	Optimally Tilted SFS	10MV	1.03
	9kWdc	2.34		50MW	0.91
	11kWdc	2.14		100MV	0.83
Commercial	200kW	1.56	One-Axis STS	10MV	1.13
	500kW	1.46		50MW	0.98
	1MW	1.43		100MV	0.89

5.4.1.3. Solar PV plant installation cost factors

The cost of solar PV plant installation depends on location, energy needs, type of PV surfaces, inverter and equipment options, permits, inspection, tax credits, labor costs, etc. The cost factors are shown in Figure 5.19 as percentage values. Balance of System (BOS) includes structural, electrical, and installation components. Through the BOS components, cost control, efficiency, and modernization of systems are realized. Operational costs include supply chain, general overheads, tax, maintenance requirements, etc.

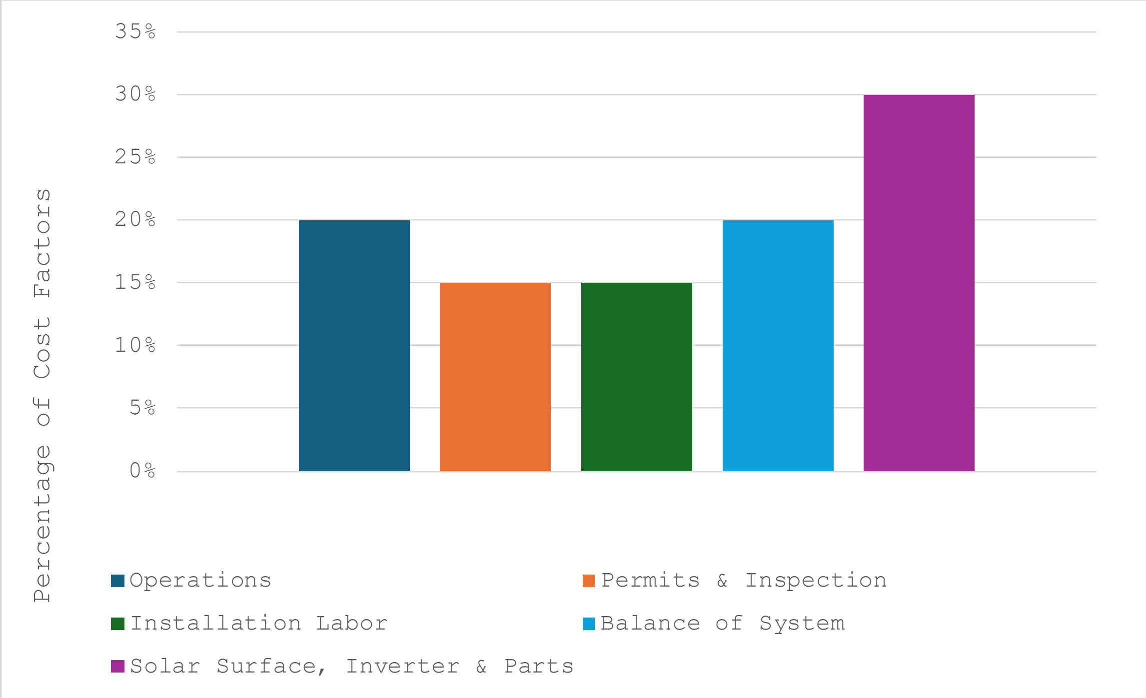

Figure 5.19. The average cost of a solar PV plant for the last 5-years [$/Wdc].

5.4.1.4. Payback period (recovery of investment)

A solar PV plant's cost recovery period can vary depending on the used technology, system type, region, and the cost of electricity. Payback periods could vary depending on different countries, and different regions even within one country. This period compares with the average solar PV plant lifetime of around 25-30 years (EIA, 2022). The average solar PV plant payback period is 7 to 12 years globally and most solar PV plants start generating a return on investment after 8-years. Economic analysis and payback period (recovery of investment) calculation studies have been conducted for various regions of Türkiye. It is found that the average solar PV plant payback period can vary depending on the region of the Türkiye (Dağtekin et al., 2014; ECA, 2018; Ozcan & Ersoz, 2019; Duman &Güler, 2020). The new incentives and tax breaks in Türkiye reduce average payback periods to under 7-years today and 2-years in 2030 (Flora et al. 2019; Acar et al. 2020) for residential systems.

5.4.2. GSR on horizontal surfaces

It is seen that from the horizontal GSR data depicted in Tab.4, the Manavgat district has the best GSR efficiency considering the monthly and annual values. The second-best productive district is Kaş. The elevation of Manavgat is higher than the others. Since the most important solar parameter is horizontal GSR distribution, Manavgat has advantageous productivity compared to other districts.

5.4.3. OPTA results on PV surfaces

OPTAs of the districts of Antalya province are calculated for solar PV plants, and the comparison of monthly OPTA values of the districts is shown in Fig. 6. Monthly OPTA values depending on the months are shown in the extreme points of the curves which represent the maximum values. It is understood from Figure 5.20 that there is an OPTA for each month of the year when TSR is at its highest. Taking the calculated OPTA values into account, GSR can be utilized to the maximum level. As seen from the monthly OPTAs graph (see Figure 5.20), the OPTAs reach their highest value in the winter season and go down to their lowest value in the summer season. While the highest OPTAs of all districts are seen in December, the lowest OPTA value for all districts is in June. This is because Türkiye is located in the northern hemisphere, the sun rays in the summer are steep compared to the winter months. The OPTA values for Antalya districts decrease from January to June and increase again from June to December. The biggest reason for these variations in the OPTAs during the year is that the declination angle (δ) increases until June and decreases after June. As the declination angle increases, the OPTA decreases or vice versa. The orientation (azimuth and tilt angles) of the PV surfaces can be adjusted when the supporting structure is designed accordingly.

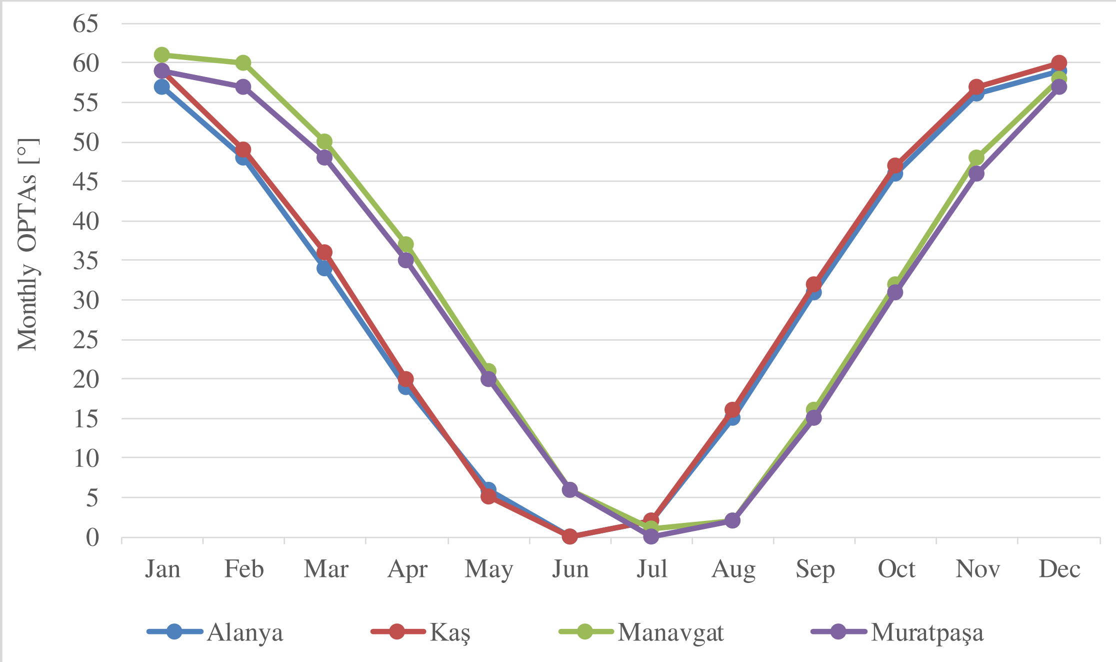

Figure 5.20. Monthly OPTA values obtained for districts of Antalya.

To find the OPTAs of surfaces and TSR collected by the tilted PV surface monthly, calculations are done for all tilt angles between 0° and 90°. For the districts of Antalya province, the monthly, seasonal, and annual OPTAs and the daily GSR gain at these OPTAs are presented in Table 5.28. The differences in the TSR gain as a result of the effect of the OPTA can be seen in Table 5.28. It is also seen that the OPTA values are determined between 0° (Jun) and 61° (Dec) throughout the year. The annual OPTA is determined to be between 28° and 30° for a PV surface that faces south throughout the year. It is determined that the lowest OPTA is between 0° (Jun) and 2° (Jul), and the highest TSR values are observed during the same months. The OPTA then rises during the winter months and reaches 61° in December. The OPTAs are determined for the winter season between 55°-57°, and the lowest TSR values are observed in December and January. The OPTAs determined for the summer season are between 4°-5°. In PV surfaces that do not have the STS, the tilt OPTAs can be varied seasonally to benefit from TSR more efficiently. However, when the OPTAs of the surfaces are not possible to set monthly or seasonally, the OPTAs of the PV surfaces can be set annually.

Table 5.28 a) OPTA values [°] and monthly TSR gains [kWh/m²/d] for Alanya District of Antalya.

Month	Monthly-Fixed		Seasonally-Fixed		Annually-Fixed	
	Tilt	Rad. Gain	Tilt	Rad. Gain	Tilt	Rad. Gain
12	59	3.05	55	3.04	28	2.70
1	57	3.41		3.41		3.06
2	48	3.84		3.81		3.67
3	34	4.60	19	4.47		4.57
4	19	5.26		5.26		5.22
5	6	6.39		6.30		6.12
6	0	7.45	5	7.44		6.89
7	2	7.45		7.45		7.00
8	15	6.79		6.7		6.68
9	31	6.10	43	6.0		6.09
10	46	5.10		5.1		4.90
11	56	3.87		3.79		3.51

Table 5.28. b) OPTA values [°] and monthly TSR gains [kWh/m²/d] for Kaş District of Antalya

Month	Monthly-Fixed		Seasonally-Fixed		Annually-Fixed	
	Tilt	Rad. Gain	Tilt	Rad. Gain	Tilt	Rad. Gain
12	60	3.59	56	3.59	29	3.17
1	59	4.15		4.15		3.70
2	49	4.58		4.55		4.36
3	36	5.43	21	5.28		5.40
4	20	5.98		5.98		5.93
5	5	6.99		6.85		6.65
6	0	8.06	4	8.05		7.37
7	2	7.94		7.94		7.39
8	16	7.28		7.14		7.14
9	32	6.70	44	6.59		6.69

10	47	5.65		5.64		5.43
11	57	4.41		4.31		3.99

Table 5.28. c) OPTA values [°] and monthly TSR gains [kWh/m²/d] for Manavgat District of Antalya.

Month	**Monthly-Fixed**		**Seasonally-Fixed**		**Annually-Fixed**	
	Tilt	Rad. Gain	Tilt	Rad. Gain	Tilt	Rad. Gain
12	61	3.70	57	3.69	30	3.25
1	60	4.20		4.20		3.75
2	50	4.76		4.73		4.52
3	37	5.64	21	5.46		5.60
4	21	6.08		6.08		6.03
5	6	7.07		6.93		6.71
6	1	8.06	5	8.05		7.35
7	2	7.98		7.99		7.42
8	16	7.41		7.30		7.26
9	32	6.87	45	6.74		6.86
10	48	5.78		5.77		5.55
11	58	4.53		4.44		4.10

Table 5.28. d) OPTA values [°] and monthly TSR gains [kWh/m²/d] for Muratpaşa District of Antalya.

Month	**Monthly-Fixed**		**Seasonally-Fixed**		**Annually-Fixed**	
	Tilt	Rad. Gain	Tilt	Rad. Gain	Tilt	Rad. Gain
12	59	3.04	55	3.03	29	2.71
1	57	3.29		3.29		2.98
2	48	3.86		3.84		3.7
3	35	4.77	20	4.65		4.75
4	20	5.36		5.36		5.31
5	6	6.16		6.06		5.88

6	0	7.17	5	7.16	6.62
7	2	7.19		7.19	6.73
8	15	6.49		6.41	6.37
9	31	5.97	44	5.86	5.96
10	46	5.02		5.01	4.83
11	57	4.09		4.01	3.71

5.4.4. Analyzing of OPTA values and average OPTA values

A comparison of the annual OPTA and the annual average OPTA is presented in Table 5.29. As can be seen in Tab 5.29, by taking the average of the monthly and seasonally determined OPTAs, the annual average OPTA values have been found. There are 2°-2.5° deviations between the annual average OPTA values and the annual OPTA values of the districts of Antalya province. This deviation is expected to increase further as move from the equator to the poles (especially at great latitudes) because the variations in the angle of incidence of the sun are greater or more frequent. This means the annual average OPTAs do not represent the annual OPTAs which is a separate concept. Optimal tilt degrees are reached when the maximum intensity of TSR falls on the tilted surface, using the mathematical model that takes into account the solar climate conditions. So, calculations made with this model show that monthly and seasonal average tilt angles are not an OPTA determination, it is an approximate estimation of tilt angles. It has been determined that average angles deviate from optimal angles.

Table 5.29. Comparison of the annual OPTA and annual average OPTA tilt [°].

Annual OPTA	**Alanya**	**Kaş**	**Manavgat**	**Muratpaşa**
Monthly AVG OPTA	31.08	31.92	32.67	31.33
Seasonally AVG OPTA	30.50	31.25	32	31
Fixed Annual OPTA	28	29	30	29

5.4.5. TSR collected by fixed solar PV surfaces

When the daily TSR values collected by PV surfaces with different OPTAs presented in Tab. 5 are analyzed comparatively. The TSR values are predicted between 2.70 kWh/m² (Dec) and 7.42 kWh/m² (Jul) in case the TSR reaches the PV surface with the annual OPTAs range. In the winter season (Dec-Jan-Feb), the OPTA values are determined between 55° and 58°, the daily TSR values are predicted between 3.04 kWh/m² and 4.76 kWh/m². In the spring season (Mar-Apr-May), the OPTA values are determined between 19° and 21°, the daily TSR values are predicted between 4.60 kWh/m² and 7.07 kWh/m². In the summer season (Jun-Jul-Aug), the OPTA values are determined between 4° and 5°, the daily TSR values are predicted between 6.49 kWh/m² and 8.06 kWh/m². In the autumn season (Sept-Oct-Nov), the OPTA values are determined between 43° and 45°, the daily TSR values are predicted between 3.87 kWh/m² and 7.87 kWh/m².

5.4.6. Analysis of TSR maximization results

The monthly TSR gain collected by the PV surfaces in case of using monthly, seasonal, and annual OPTAs for Antalya districts are listed in Table 5.29. Calculations have been performed to maximize TSR on the PV surfaces regarding each combination of a tilt and azimuth angle. The results are presented for all months of the year, it returns the best combination of both geometry parameters for calculated periods in terms of finding OPTA and maximizing TSR accordingly. Also, it can be observed that the increase or decrease of the collected TSR for any values of azimuth and tilt of PV surface in the chosen period. So, one of the important outcomes in this study is the graphs and tables displaying the change in tilt angle in terms of increase or decrease and the amount of collected TSR. It is seen that from Table 5.30, the monthly TSR values are predicted between 83.70 kWh/m² in December, and 230.02 kWh/m² in Jul in case of TSR reaches the PV surface with the annual OPTA. The conclusion to be drawn from the data in Table 5.29 is that TSR intensity can be captured as a maximal level if the OPTA is set for each month. As a result, surfaces should be set at OPTA to maximize the benefits of TSR.

Table 5.30. a) Monthly TSR gain [kWh/m²/d] in case of using OPTA [°] for Alanya District of Antalya.

Month	Monthly	Seasonally	Annually
1	105.71	105.71	94.86
2	107.52	106.68	102.76
3	142.60	138.57	141.67
4	157.80	157.80	156.60
5	198.09	195.30	189.72
6	223.50	223.20	206.70
7	230.95	230.95	217.00
8	210.49	207.70	207.08
9	183.00	180.00	182.70
10	158.10	158.10	151.90
11	116.10	113.70	105.30
12	94.55	94.24	83.70

Table 5.30. b) Monthly TSR gain [kWh/m²/d] in case of using OPTA [°] for Kaş District of Antalya

Month	Monthly	Seasonally	Annually
1	128.65	128.65	114.70
2	128.24	127.40	122.08
3	168.33	163.68	167.40
4	179.40	179.40	177.90
5	216.69	212.35	206.15
6	241.80	241.50	221.10
7	246.14	246.14	229.09
8	225.68	221.34	221.34
9	201.00	197.70	200.70
10	175.15	174.84	168.33
11	132.30	129.30	119.70
12	111.29	111.29	98.27

Table 5.30. c) Monthly TSR gain [kWh/m²/d] in case of using OPTA [°] for Manavgat District of Antalya.

Month	Monthly	Seasonally	Annually
1	130.20	130.20	116.25
2	133.28	132.44	126.56
3	174.84	169.26	173.60
4	182.40	182.40	180.90
5	219.17	214.83	208.01
6	241.80	241.50	220.50
7	247.38	247.69	230.02
8	229.71	226.30	225.06
9	206.10	202.20	205.80
10	179.18	178.87	172.05
11	135.90	133.20	123.00
12	114.70	114.39	100.75

Table 5.30. d) Monthly TSR gain [kWh/m²/d] in case of using OPTA [°] for Muratpaşa District of Antalya.

Month	Monthly	Seasonally	Annually
1	101.99	101.99	92.38
2	108.08	107.52	103.60
3	147.87	144.15	147.25
4	160.80	160.80	159.30
5	190.96	187.86	182.28
6	215.10	214.80	198.60
7	222.89	222.89	208.63
8	201.19	198.71	197.47
9	179.10	175.80	178.80
10	155.62	155.31	149.73
11	122.70	120.30	111.30
12	94.24	93.93	84.01

The annual TSR collected by the PV surfaces for the Antalya districts is presented in Table 5.30. Manavgat district has the best TSR efficiency considering the annual OPTA values in Tab 5.31. The maximal annual TSR values are predicted in Manavgat as 2,194.66 kWh/m² for monthly, 2,173.28 kWh/m² for seasonal, 2,082.50 kWh/m² for annual respectively with applying the OPTAs provided in this study. The high TSR intensity rates of districts are contributed significantly to the gain of more TSR on SFSs. It seems that the reason why Antalya province is preferred especially for the establishment of large-capacity solar PV plants is that it can be made a serious difference in energy production.

Table 5.31. Annual TSR gains [kWh/m²] in case of using OPTA [°].

Districts	Monthly	Seasonally	Annually
Alanya	1,928.41	1,911.95	1,839.99
Kaş	2,154.67	2,133.59	2,046.76
Manavgat	2,194.66	2,173.28	2,082.50
Muratpaşa	1,900.54	1,884.06	1,813.35

5.4.7. Analyzing TSR gain for STSs

STSs are effective tools to be used in solar PV plants where higher TSR efficiency is required. The monthly TSR on south-facing PV surfaces along the tilt angle gradient of 0° to 90° is calculated and presented in Tab. 9 for one-axis, and two-axis STSs of four districts of Antalya. It is understood that from Table 5.32, Manavgat and Kaş are the best productive districts for the TSR efficiency of the PV surfaces in the case using STSs. The maximal monthly TSR values are predicted in Manavgat as 326.12 kWh/m² for the one-axis, and 340.69 kWh/m² for the two-axis respectively. In cases where it is not applicable to set STSs, the monthly OPTA values presented in Figure 5.20 can be used for districts of Antalya province.

Table 5.32. a) Monthly TSR gain [kWh/m²-day] for STSs for Alanya and Kaş districts.

Month	**Alanya**		**Kaş**	
	One-Axis	Two-Axis	One-Axis	Two-Axis
1	114.70	122.14	141.05	150.97
2	122.36	125.44	148.68	152.60
3	175.15	175.15	214.21	214.52
4	191.10	192.30	223.80	225.30
5	249.86	257.61	280.55	290.16
6	281.10	294.90	310.80	327.30
7	298.22	310.31	323.64	340.38
8	285.51	289.54	313.10	317.75
9	237.90	237.90	266.40	266.40
10	197.16	200.88	222.27	225.99
11	128.40	135.90	147.90	156.60
12	100.44	107.88	119.66	128.96

Table 5.32. b) Monthly TSR gain [kWh/m²-day] for STSs for Manavgat and Muratpaşa districts.

Month	**Manavgat**		**Muratpaşa**	
	One-Axis	Two-Axis	One-Axis	Two-Axis
1	143.22	153.14	110.98	117.49
2	154.84	159.04	123.76	126.56
3	224.44	224.75	183.83	183.83
4	228.90	230.70	195.60	196.80
5	284.58	294.50	237.77	245.83
6	310.50	327.30	267.00	280.80
7	326.12	340.69	284.27	296.05
8	320.85	325.81	268.77	272.80
9	275.10	275.10	231.60	231.60
10	228.16	232.19	194.06	197.16

11	152.40	161.10	136.50	144.60
12	123.38	132.99	100.75	107.88

Maximal TSR gains for SFSs, and STSs are presented in Table 5.33. It is calculated that PV surfaces adjusted with OPTA achieve between 8.23% (Alanya) and 10.63% (Manavgat) more TSR annually compared to surfaces that are not angled at all for the SFS. It is also calculated that one-axis STSs harvest between 28.72% (Muratpaşa) and 33.17% (Manavgat) higher TSR, and two-axis STSs harvest between 32.19% (Kaş) and 37.49% (Manavgat) higher TSR than the SFSs in districts of Antalya. Considering an expected 25-year lifetime for the solar PV plants, optimal tilting of the surfaces should be taken seriously in solar PV plants. It is highly advised to utilize a one-axis STS in solar PV plants. However, STSs are high-cost to operate and maintain and are not always feasible because of the lack of free space. If changing the tilt angles of the PV surface is not possible, the annual OPTA values can be used for solar PV plants during the installation. In the light of the obtained results, it is calculated that if the OPTA is changed every month in the Antalya districts, an increase in the TSR values on the PV surfaces can be achieved between 4.87% (Kaş) and 5.28% (Manavgat) compared to annual OPTA. It is also calculated that if seasonally setting it between 3.80% (Alanya) and 4.32% (Manavgat) TSR gain compared to an annual SFS. Especially for large-scale solar PV systems, this difference will have a significant impact.

Table 5.33. Annual TSR gain percentages for SFSs and STSs [%].

Districts of Antalya	Annual Tilted SFS [%]	On-Axis STS [%]	Two-Axis STS [%]
Alanya	8.23	29.34	33.15
Kaş	9.62	32.19	36.09
Manavgat	10.63	33.17	37.49
Muratpaşa	9.03	28.72	32.59

Table 5.34 presents the annual TSR gain in the four investigated districts in case using the STSs. Manavgat district is the most productive district for the TSR efficiency of the PV surfaces. Total annual TSR values are predicted at 2,772.49 kWh/m² for the one-axis, and 2,857.31 kWh/m² for the two-axis respectively. It is also revealed that the

second-best productive district is Kaş in terms of TSR efficiency. Compared to annually, a considerable increase in TSR values is observed in the Antalya districts. For this reason, it is recommended to investors that the Manavgat and Kaş districts be preferred in the Antalya province. Especially for large-capacity solar PV plants, a two-axis STS can create a considerable impact and can contribute greatly to the business economy. However, two-axis systems are quite costly. In this context, to utilize a two-axis STS, cost and benefit analysis should be done first. It is strongly advised to utilize a one-axis STS in solar PV plants.

Table 5.34. Annual TSR gains [kWh/m²-day] for STSs.

District	Solar Tracker Type	TSR Gain
Alanya	One-Axis	2,381.90
	Two-Axis	2,449.95
Kaş	One-Axis	2,712.06
	Two-Axis	2,796.93
Manavgat	One-Axis	2,772.49
	Two-Axis	2,857.31
Muratpaşa	One-Axis	2,334.89
	Two-Axis	2,401.40

Figure 5.21 shows a comparison of TSR on SFS and STSs in the districts. The annual TSR values are calculated by changing the tilt of the south-oriented surfaces with steps between 0°-90°, curve graphs are drawn depending on TSR gain from the SFSs and STSs. It can be seen once again in Figure 5.21 that STSs make a serious contribution to energy efficiency. So, to maximize TSR efficiency, PV surfaces need to be structured so that the OPTA can be set effortlessly to use monthly or seasonal optimal tilt. At a minimum, surfaces should be set with an annual optimal tilt if the STS setup is not affordable financially.

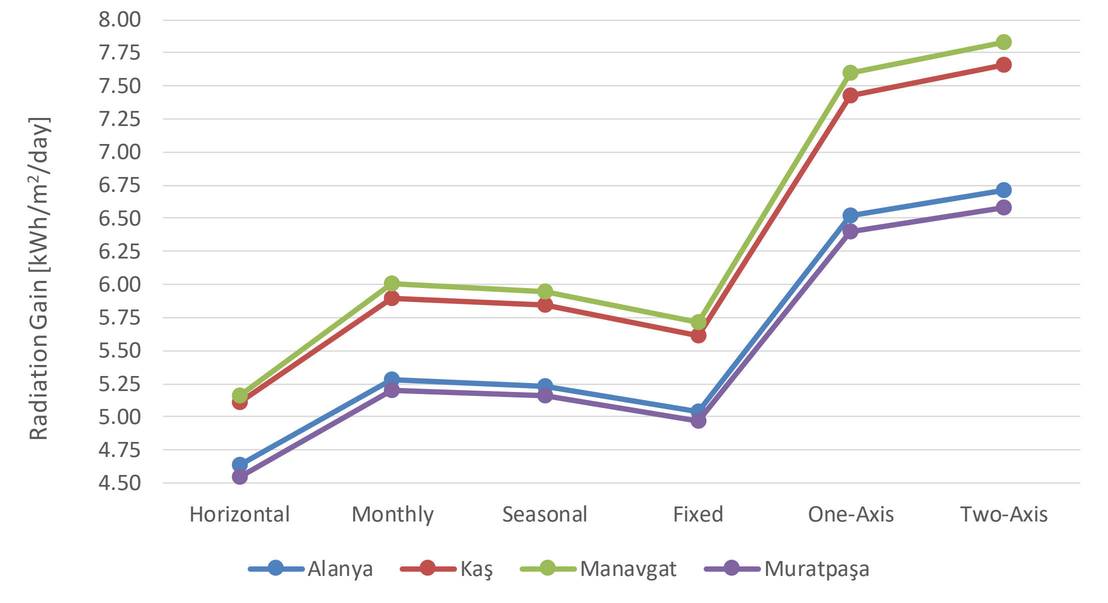

Figure 5.21. Annual average daily GSR and TSR on horizontal and tilted PV surfaces.

Figure 5.22 presents the annual TSR values of STSs and SFSs for evaluating the existence of solar potential in Antalya districts. It is understood that from Fig. 8, the variation of collected TSR values from the STSs and SFSs is the most essential parameter to the design and size of the large-capacity solar PV plants. It is also seen that STSs may significantly increase the collection of the TSR. Because of this, it is extremely important to use STSs to get high TSR efficiency.

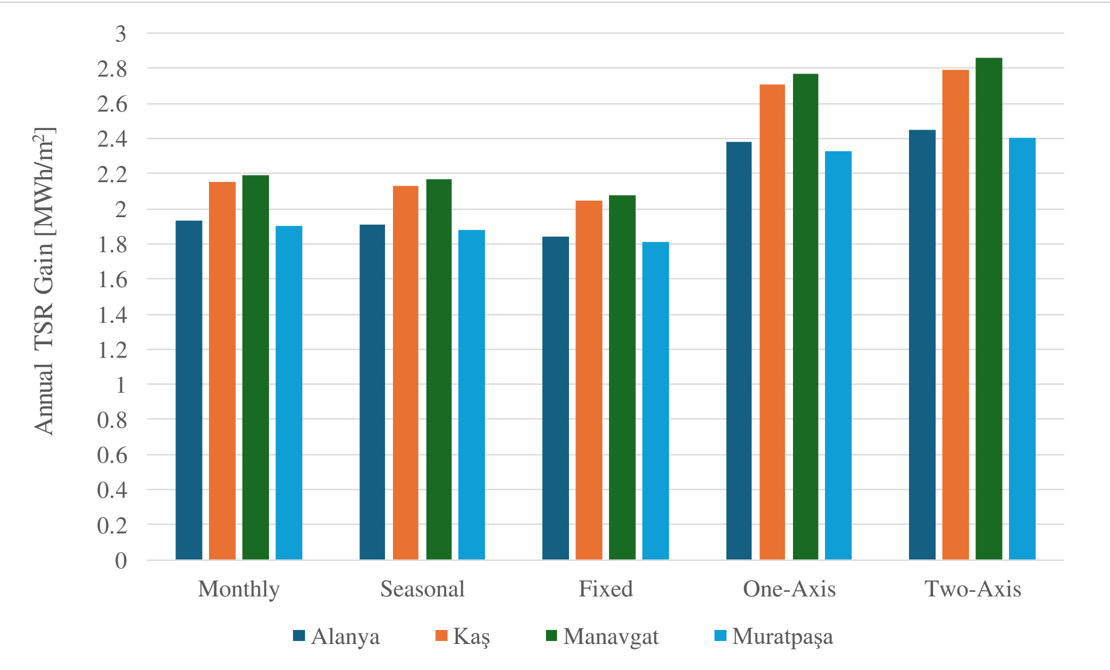

Figure 5.22. Average annual TSR intensity for the districts of Antalya.

5.4.8. Discussions on the cost analysis and payback period

As depicted in Figure 5.18, the cost of solar energy continues to decrease thanks to improved module efficiency as well as low hardware equipment costs in recent years. It is understood in Table 5.27, that large-scale solar PV plants are much cheaper to install and operate compared to residential and commercial solar PV plants. In other words, as the capacity of the solar PV plant grows, the system installation costs decrease or change the type of solar PV plant. Also, the cost increase in installing one-axis tracker structures in large-scale solar PV plants is less than expected. It is therefore highly suggested to install a one-axis tracker in such solar PV plants in terms of cost and economic efficiency. Figure 5.18 shows that between the last 2 years, there were 3.28% ($0.09/Wdc), 10.34% ($0.18/Wdc), 10.83% ($0.11/Wdc), and 12.74% ($0.13/Wdc) global reductions in the residential, commercial, large-scale SFS and one-axis STS cost respectively. The latest statistical data show that the solar energy in Türkiye cost has almost halved in the last 5 years. Hence, there is no doubt solar energy to support the economy in countries with high energy tariffs and at the same time high solar potential such as Türkiye. It is also seen that the average solar PV plant payback period is 7 to 12 years globally and most solar PV plants start generating a return on investment after 8 years comparing the 25 years lifespan of the system. The new incentives and tax breaks in Türkiye have reduced average payback periods to under 7 years. Due to the decrease in setup costs in the future, it is anticipated that the payback period will be a lot less than today's payback period.

5.4.9. Discussions on the proposed calculation model

Because tilting and tracking have significant effects on increasing incident TSR at all latitudes, the proposed model can be implemented in any location of interest to obtain specific estimates with a low computational cost. The proposed model can be used for evaluating the solar potential of a certain location before establishing a solar PV plant and can be also easily applied by researchers and technicians in the field to avoid energy yield losses and unnecessarily high LCOE. In addition, different desired periods can be obtained such as daily, weekly, monthly, seasonal, and yearly optimal tilt values or TSR values for solar PV plants by using the data set for each location of interest in Türkiye or the world. The model can be extended to other rural regions in developing countries.

5.5. Results of Case Study (5): Estimation of TSR Intensity and OPTAs for PV Surfaces in the Central Anatolia Region by Applying Transposition Models

In this section, results, and discussions on TSR intensity for one-axis and two-axis STS, as well as SFS, have been presented in the Central Anatolia region of Türkiye. Annual OPTA values and TSR gains have been predicted using the proposed transposition models, and the maximum amount of TSR that can be generated has been calculated for the provinces. The findings have been tabulated by using two independent models for cross-comparison purposes.

5.5.1. GSR intensity on horizontal surface

The annual GSR intensity on a horizontal surface for the provinces of the Central Anatolia region is presented in Figure 5.23. It is seen that the annual horizontal GSR intensity varies from 1,424 1966 kWh/m² to 1,966 kWh/m² over the provinces. Since the most important solar parameter is horizontal GSR intensity, Niğde province has the most advantageous energy productivity compared to other provinces, in line with the data received from Figure 5.23. Konya and Kayseri provinces have more advantages for energy productivity than others. The annual horizontal surface GSR value of the region provinces is 1663 kWh/m².

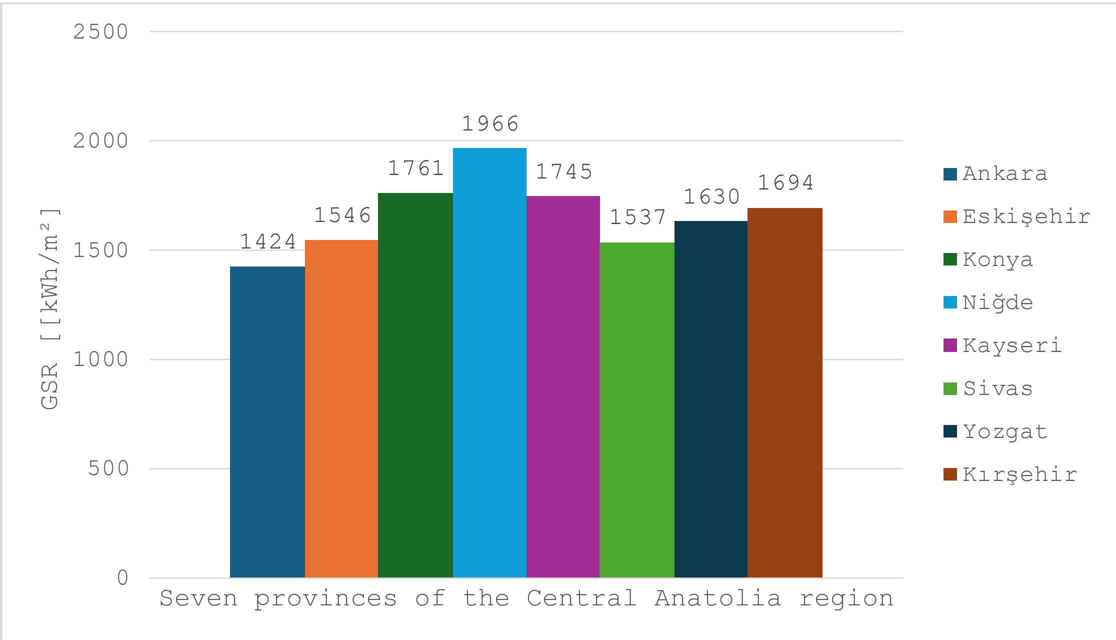

Figure 5.23. GSR on the horizontal surface of Central Anatolia.

5.5.2. TSR intensity and gain for SFSs

To receive maximal TSR, PV surfaces should be set at OPT values. Table 5.35 presents the annual OPTA values determined for the Liu-Jordan and Perez transposition models comparatively. The annual OPTA values are predicted to be 29°-30° by applying the Liu-Jordan model and 33°-35° by applying the Perez model for the provinces of the Central Anatolia region. It has been determined that anisotropic components in the Perez model calculate OPTAs 3°-4° higher than the Liu-Jordan model. The average OPTA of the Central Anatolia region is determined as 30° (Liu-Jordan) and 34° (Perez). The Perez model shows that by increasing the angulation by several degrees, more TSR can be collected, especially during the winter months. As depicted in Table 5.35, it is found that the OPTA values for the investigated provinces of the Central Anatolia region are below the latitude values. If the OPTA values of the PV surfaces are not possible to adjust monthly or seasonally, the OPTA values of the SFSs should be set as annually for better PV energy production.

Table 5.35. Determined annual OPTA values by using transposition models.

Province	Liu-Jordan [°]	Perez [°]
Ankara	29	33
Eskişehir	30	34
Konya	29	33
Niğde	31	35
Kayseri	30	34
Sivas	31	35
Yozgat	30	34
Kırşehir	30	34
AVG	30	34

The annual TSR intensity on the annual SFSs is predicted using the geo-referenced solar dataset (METEONORM). Calculations have been carried out with two separate transposition models, and the results are tabulated for the provinces of Central Anatolia. Annual TSR values obtained at OPTA values for the provinces of Central Anatolia are presented in Table 5.36. As inferred in Table 5.36, the annual TSR intensity on the SFSs varies from 1,456 kWh/m² (Ankara) to 2,085 kWh/m² (Niğde) over the provinces by applying the Liu-Jordon model, whereas it ranges from 1,525 kWh/m² (Ankara) to 2,186 kWh/m² (Niğde) by applying the Perez Model. Since the most important solar parameter is horizontal GSR intensity, Niğde province has the most advantageous energy productivity compared to other provinces, in line with the data received from Figure 5.35. Konya and Kayseri provinces have more advantages for energy productivity than others. The annual TSR intensity of the Central Anatolia region at OPTAs is predicted to be between 1,726 kWh/m² (Liu-Jordan) and 1,809 kWh/m² (Perez). The estimation difference between these two transposition models is 4.78% on average.

Table 5.36. Annual estimated TSR values obtained at OPTA for the provinces of Central Anatolia.

Province	Liu-Jordan [kWh/m²]	Perez [kWh/m²]	Difference [%]
Ankara	1456.9	1525.9	4.73
Eskişehir	1596.4	1674.7	4.90
Konya	1825.6	1911.2	4.68
Niğde	2085.2	2186.1	4.83
Kayseri	1814.4	1900.3	4.73
Sivas	1590.4	1667.3	4.83
Yozgat	1687.7	1769.7	4.85
Kırşehir	1758.4	1841.3	4.71
AVG	1726.9	1809.6	4.78

Table 5.37 presents annual TSR gain as a percentage obtained at OPTA values for the provinces of Central Anatolia. As inferred in Table 5.37, the gain in the amount of TSR because of the effect of the annual OPTA varies between 2.32% (Ankara) and 6.09% (Niğde) annual TSR gain by applying the Liu-Jordan model. By applying the Perez model, the gain varies between 7.17% (Ankara) and 11.22% (Niğde). The annual TSR gain of the Central Anatolia region at OPTAs is predicted to be between 3.75% (Liu-Jordan) and 8.72 (Perez). The annual OPTA can be set for the setup of SFSs throughout

Central Anatolia in the absence of an STS. Especially for large-capacity solar plants, this difference will have a significant impact on energy production.

Table 5.37. Annual TSR gain obtained at OPTA for the provinces of Central Anatolia.

Province	Liu-Jordan [%]	Perez [%]
Ankara	2.32	7.17
Eskişehir	3.23	8.29
Konya	3.66	8.52
Niğde	6.09	11.22
Kayseri	3.95	8.87
Sivas	3.48	8.49
Yozgat	3.53	8.57
Kırşehir	3.77	8.66
AVG	3.75	8.72

5.5.3. TSR intensity and gain for a one-axis STS

STS is costly to operate and maintain. Before the installation of one-axis and two-axis STSs in the provinces, benefit and cost analysis should be performed. Annual TSR intensity for a one-axis STS in the provinces of Central Anatolia is presented in Table 5.38. As depicted in Table 5.38, the annual TSR intensity on the one-axis STS varies from 1,748 kWh/m² to 2,586 kWh/m² over the provinces by applying the Liu-Jordon model, whereas it ranges from 1,905 kWh/m² to 2,798 kWh/m² by applying the Perez model. The annual TSR intensity of the Central Anatolia region for the one-axis STS is predicted to be between 2,107 kWh/m² (Liu-Jordan) and 2287 kWh/m² (Perez). The estimation difference between these two models is 8.55%.

Table 5.38. Annual TSR intensity for a one-axis STS in Central Anatolia.

Province	Liu-Jordan [kWh/m²]	Perez [kWh/m²]	Difference [%]
Ankara	1748.7	1905.2	8.94
Eskişehir	1922.7	2096.1	9.01
Konya	2238.6	2426.2	8.38
Niğde	2586.1	2798.9	8.22
Kayseri	2222.2	2408.5	8.38
Sivas	1918.9	2079.2	8.35
Yozgat	2061.1	2238.0	8.58
Kırşehir	2159.3	2343.6	8.53
AVG	2107.2	2287.0	8.55

Table 5.39 presents annual TSR gain as a percentage for a one-axis STS in the provinces of Central Anatolia. As depicted in Table 5.38, the gain in the TSR for the one-axis STS between 20.02% and 24.02% annual TSR is achieved by applying the Liu-Jordan model. By applying the Perez model, the gain is between 24.85% and 28.03%. The annual TSR gain of the Central Anatolia region for a one-axis STS is predicted to be between 21.89% (Liu-Jordan) and 26.27 (Perez).

Table 5.39. Annual TSR gain for a one-axis STS in Central Anatolia.

Province	Liu-Jordan [%]	Perez [%]
Ankara	20.02	24.85
Eskişehir	20.43	25.16
Konya	22.62	26.94
Niğde	24.02	28.03
Kayseri	22.47	26.74
Sivas	20.65	24.70
Yozgat	22.12	26.46
Kırşehir	22.79	27.27
AVG	21.89	26.27

5.5.4. TSR intensity and gain for two-axis STSs

The annual TSR intensity for q two-axis STS in the provinces of Central Anatolia is presented in Table 5.40. As inferred in Table 5.40, the annual TSR intensity on the two-axis STS varies from 1,875 kWh/m² to 2,811 kWh/m² over the provinces by applying the Liu-Jordon model, whereas it ranges from 2,075 kWh/m² to 3,080 kWh/m² by applying the Perez model. The annual TSR intensity of the Central Anatolia region for the two-axis STS is predicted to be between 2,277 kWh/m² (Liu-Jordan) and 2,507 kWh/m² (Perez). The difference in predicted values from these two transposition models is 10.14% on average.

Table 5.40. Annual TSR intensity for a two-axis STS in Central Anatolia.

Province	Liu-Jordan [kWh/m²]	Perez [kWh/m²]	Difference [%]
Ankara	1875.2	2075.0	10.65
Eskişehir	2056.1	2276.2	10.70
Konya	2411.3	2653.4	10.04
Niğde	2811.9	3080.7	9.55
Kayseri	2408.5	2649.1	9.98
Sivas	2080.3	2289.7	10.06
Yozgat	2236.6	2463.7	10.15
Kırşehir	2338.4	2572.7	10.01
AVG	2277.3	2507.6	10.14

Table 5.41 presents annual TSR gain as a percentage for a two-axis STS in the provinces of Central Anatolia. As depicted in Table 5.41, the gain in the amount of TSR for the one-axis STSs between 28.71% and 34.85% annual TSR gain is achieved by applying the Liu-Jordan model. By applying the Perez model, the gain is between 35.98% and 40.92%. The annual TSR gain of the Central Anatolia region for a two-axis STS is predicted to be between 31.68% (Liu-Jordan) and 38.41 (Perez).

Table 5.41. Annual TSR gain for a two-axis STS in Central Anatolia.

Province	Liu-Jordan [%]	Perez [%]
Ankara	28.71	35.98
Eskişehir	28.79	35.91
Konya	32.08	38.83
Niğde	34.85	40.92
Kayseri	32.74	39.40
Sivas	30.80	37.32
Yozgat	32.52	39.21
Kırşehir	32.98	39.72
AVG	31.68	38.41

5.5.5. Average TSR intensity and gain results for central Anatolia

Table 5.42 presents the annual TSR intensity for the Central Anatolia region and estimates differences in percentage between the two transposition models. Figure 5.24 shows the annual TSR intensity for the Central Anatolia region in a graphical form. The annual tilted TSR intensity for the SFS is compared to the horizontal GSR intensity for the Central Anatolia region. Similarly, the annual TSR intensity for a one-axis and a two-axis STS is compared to an SFS for the region. It is well understood from Table 5.42 and Figure 5.24 that the TSR collection of the STSs is always superior compared to the SFS. For the SFSs, the daily TSR intensity is predicted at a minimum of 1,726 $kWhm^2$ and a maximum of 1,809 $kWhm^2$. In the case of using the one-axis STS, the daily TSR intensity is predicted at a minimum of 2,107 $kWhm^2$ and a maximum of 2,287 $kWhm^2$. As for the two-axis STS, the annual TSR intensity is predicted at a minimum of 2,338 $kWhm^2$ and a maximum of 2,572 $kWhm^2$. The estimation differences between these two transposition models are 4.78% for the SFS, 8.55% for the one-axis STS, and 10.01% for the two-axis STS on average respectively.

Table 5.42. Annual average TSR intensity and percentage differences between the two models.

System Structure	Liu-Jordan [kWh/m²]	Perez [kWh/m²]	Difference [%]
Annual Tilted SFS	1726.9	1809.6	4.78
One-Axis STS	2107.2	2287.0	8.55
Two-Axis STS	2338.4	2572.7	10.01

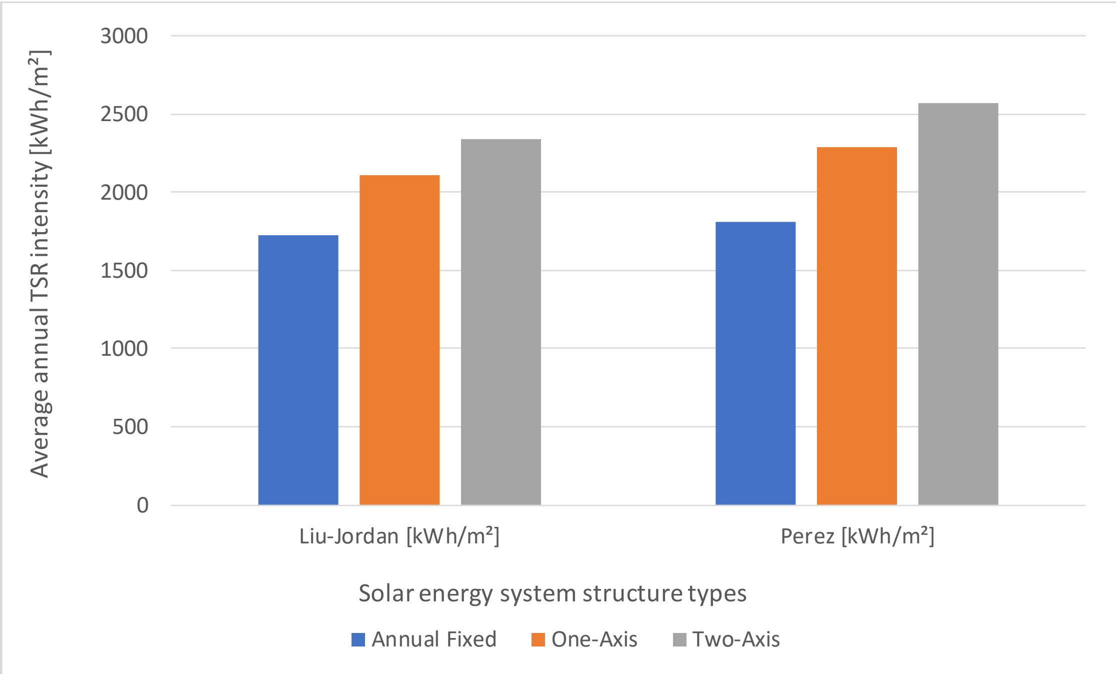

Figure 5.24 Annual average TSR intensity for Central Anatolia.

Table 5.43 and Figure 5.25 show the annual TSR gain as a percentage for the Central Anatolia region in tabular form and graphical form, respectively. It is well understood from Table 5.43 and Figure 5.25 that the annual optimally tilted TSR intensity is calculated at 3.75% for Liu-Jordan and 8.72% for Perez transposition models on average compared to a horizontal surface. For SFSs, the considerable disagreement rate between the two models is determined. Similarly, the annual TSR intensity for the one-axis STS is calculated at 21.89% for Liu-Jordan and 26.27% for Perez transposition models compared to the SFS. For one-axis STSs, the disagreement rate is %20.01 between the two models. It is also predicted that the annual TSR intensity for the two-axis STS is calculated at 31.68% for Liu-Jordan and 38.41% for Perez models compared to the SFS in Central Anatolia. For two-axis STSs, the disagreement rate is %21.24

between the two models. The Perez model shows that by increasing the angulation by several degrees, more TSR can be collected. This study reveals that some solar parameters involved in anisotropic models can contribute to the quality of the estimation results, especially during winter months. However, these theoretical results need to be confirmed with experimental data. Future works will focus on this issue. Taking into account the results of this study, it is strongly recommended to use an STS in the setting up of large-scale solar PV plants in Central Anatolia.

Table 5.43. Annual average TSR gains as a percentage for Central Anatolia.

System Structure	Liu-Jordan [%]	Perez [%]
Annual Fixed	3.75	8.72
One-Axis	21.89	26.27
Two-Axis	31.68	38.41

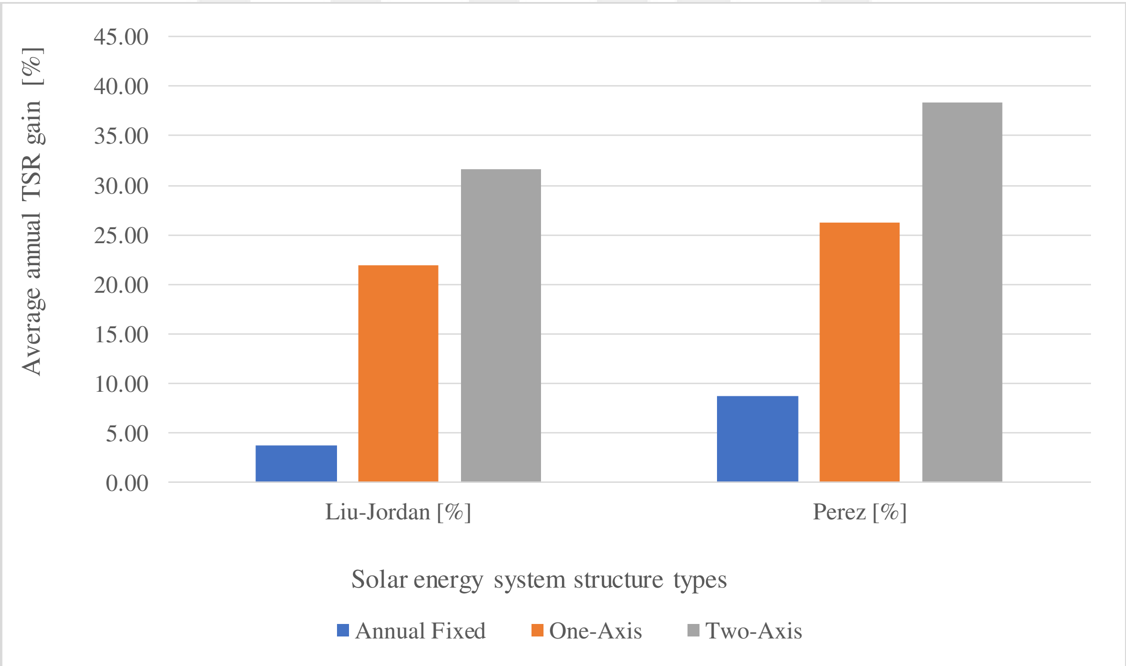

Figure 5.25. Annual average TSR gains as a percentage for Central Anatolia.

5.6. Results of Application Study (1): Transportable Solar Power Production for Rural Electricity Supply: An Application Study of Şanlıurfa

In this section, the findings for the developed microgrid regarding the essential parameters such as energy production, and ES performance are presented and discussed as long with the Matlab/Simulink DER and EU JRC PVGIS estimations specifically payback and lifespan of the microgrid under regional and solar climatic conditions. Furthermore, possible problems that may arise in terms of energy continuity and sustainability of the developed microgrid are evaluated, and possible solutions to take action are presented.

5.6.1. Results of regional analysis and simulation

PV energy production is influenced by environmental and regional conditions, aside from the technical structure of the microgrid. So, Solar climatic parameters greatly affect the TSR efficiency such as sunny days, cloudy days, sunshine, and GSR values. PV energy production, capacity, and sustainability of the developed microgrid should be analyzed under climatic conditions of the region where the PV plant will be installed for maximum efficiency. The climatic values of the region are summarized in Section 4.6.1. The predicted optimal tilt angles and daily TSR values are tabulated in Table 5.44 by applying the EU JRC PVGIS and PVGIS SARAH calculation method and solar data, respectively.

Table 5.44. OPTAs [°] and monthly average daily GSR gains [kWh/m²-day] of the region.

Month	GSR Horizontal	Monthly-Fixed		Annually-Fixed	
		Tilt	Rad. Gain	Tilt	Rad. Gain
1	2.37	59	3.94	33	3.63
2	3.36	50	4.75		4.57
3	4.52	37	5.33		5.32
4	5.49	21	5.77		5.68
5	6.60	7	6.64		6.21
6	7.73	1	7.73		6.94

7	7.75	4	7.76	7.09
8	6.66	17	6.85	6.64
9	5.35	32	6.04	6.04
10	3.69	46	4.86	4.76
11	2.70	58	4.39	4.05
12	2.10	62	3.71	3.33

The simulation also takes into account the impacts of ambient temperature, wind on the PV surface, and nominal operating cell temperature during the calculation of energy production. It is assumed that daily energy consumption is distributed over the hours of the day with most of the consumption during daylight hours. The predicted annual energy production capacity for an off-grid PV plant is shown in Figure 5.26. The ES performance of an off-grid PV plant is given in Figure 5.27 which tells the monthly statistics on how often the battery became full or empty during the day. Also, Figure 5.28 shows the probability of Battery Charge State (BCS) at the end of the day.

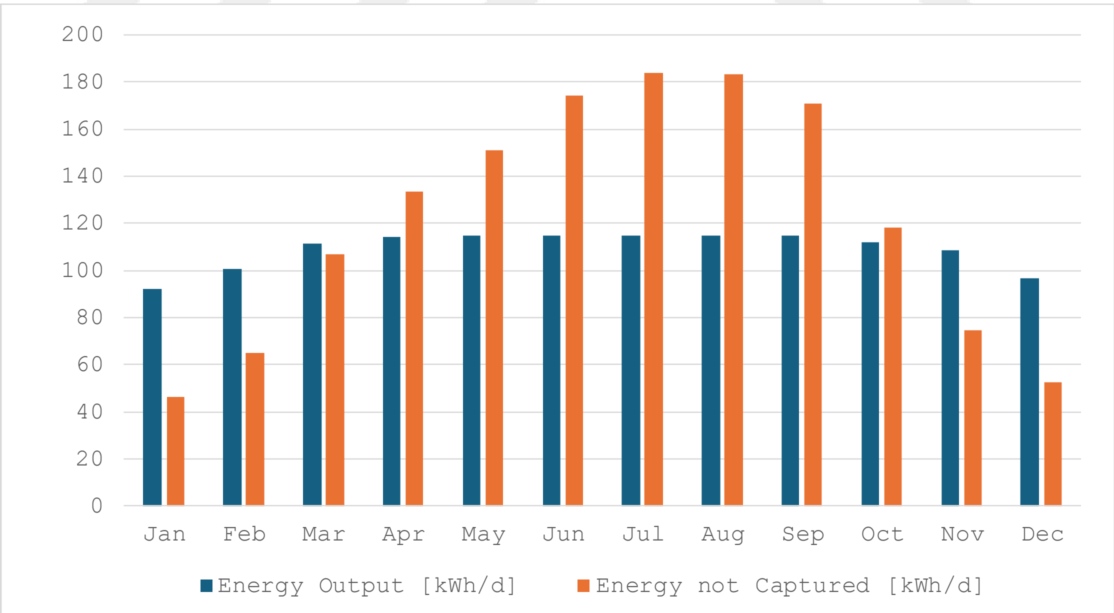

Figure 5.26. The energy production predicted for the microgrid.

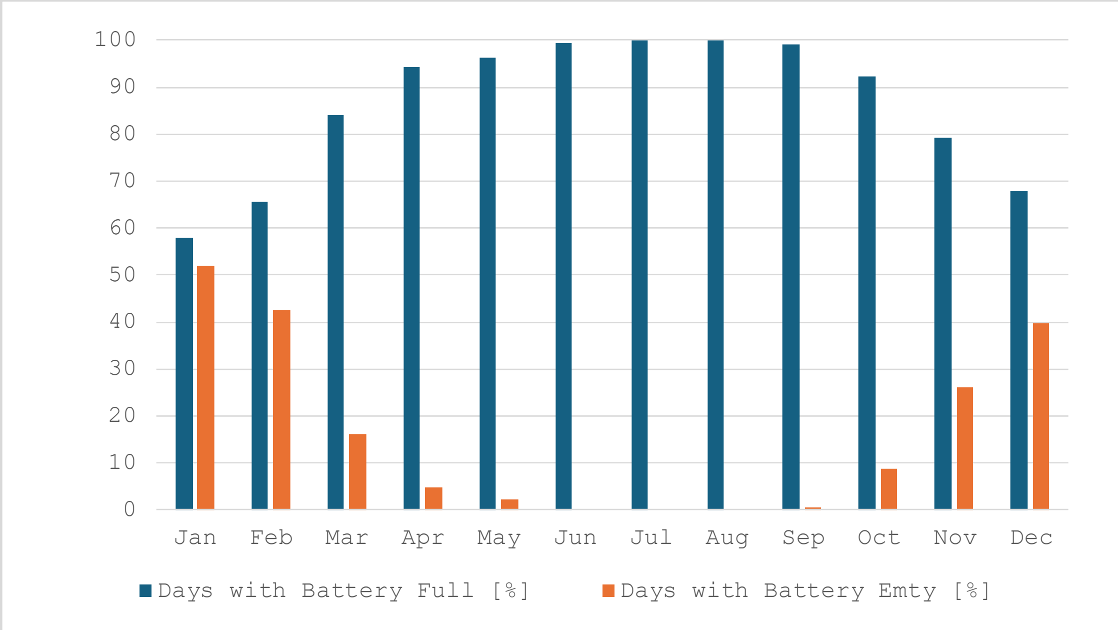

Figure 5.27. Predicted battery performance for the microgrid.

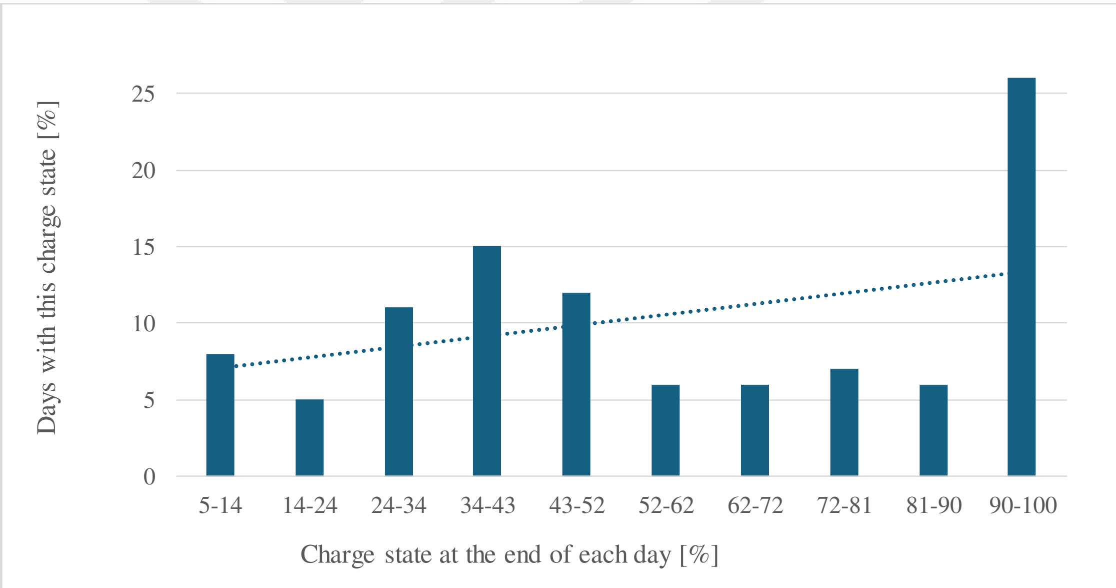

Figure 5.28. Probability of BCS at the end of the day.

Since the system is an isolated (off-grid) microgrid, the energy production plan should be determined according to the worst-case scenario at the location to be installed. The worst-case scenario plan is achieved by identifying the month with the least sunshine duration and calculating the daily Peak-Sun Hour (PSH) values in that month. It is understood that from Figures 5.26 and 5.27, the battery remains full in the summer and the charge status of the battery remains enough until the end of the day in other months. However, it is also observed that the battery capacity falls below 10% on some days during the winter months. It would be appropriate to increase the battery capacity accordingly so that the energy flow continues without interruption. According to the calculations, in 29% of the year, the battery charge status remains over 90% while in 15% of the year battery charge rate fluctuates between 34% and 43%.

5.6.2. Results of MATLAB simulation of the designed microgrid

This simulation in which DER and load flow are modeled allows us to observe the operations and behaviors of the microgrid's DER under varying circumstances. The results show some essential parameters such as the performance, efficiency, and sustainability of the DER in a 24-hour scenario. The simulation is based on the worst-case scenario. So, data from January, the month with the lowest PV energy production in winter are taken into account. Average load flow and DER for a clear day and a cloudy day in 24 hours are shown in Figures 5.29 and 5.30, respectively.

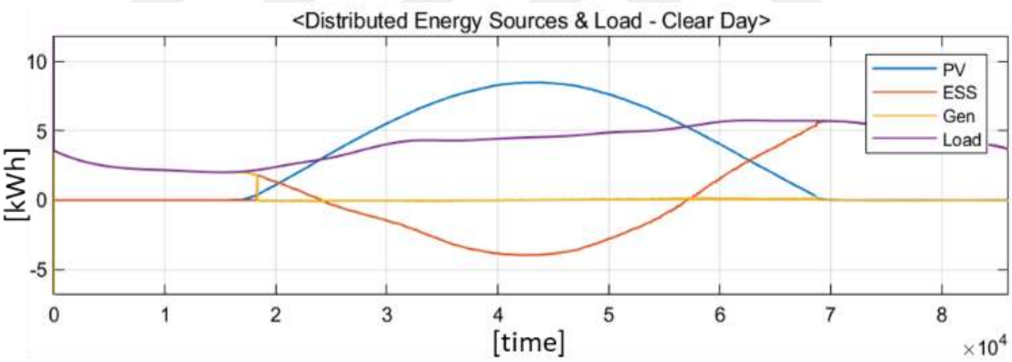

Figure 5.29. AVG load flow and DER for a clear day (24 hours).

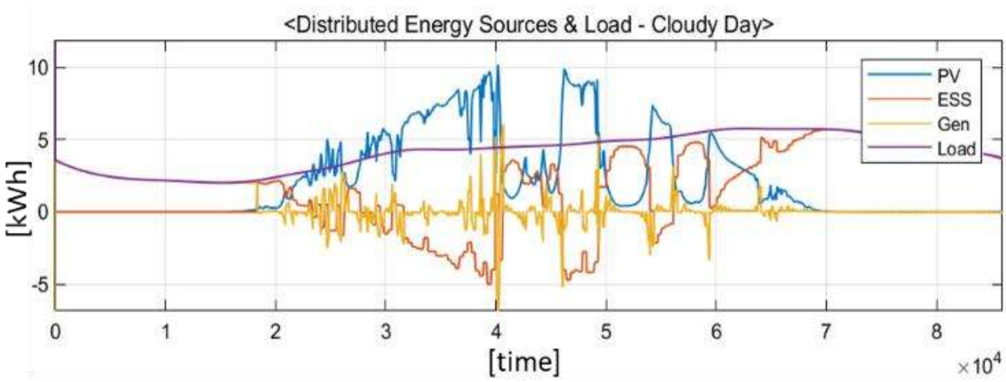

Figure 5.30. AVG load flow and DER for a cloudy day (24 hours).

The clear day simulation model in Figure 5.29 demonstrates the energy consumption is provided directly from the diesel generator first, and then alternately PV and ES meet the energy consumption needs. If one needs to evaluate the DER components separately, it is seen that after the PV energy production starts during the sunshine period, the generator is cut off, the energy consumption is provided directly from the PV, and the ES is charged at the same time. It is also understood that in line with the decrease in the sunshine duration, the ES comes into play and meets the energy consumption, and the microgrid performs well in terms of energy sustainability and continuity. It is understood from Figure 5.30 that the generator plays a more active role on cloudy days than on clear days, and the generator usage will be higher on some days in the winter months. It is seen that the technical simulation performed in MATLAB/Simulink supports the results in section 5.6.3.

5.6.3. Results of power and energy production

The simulation results for the location indicate that power production is extremely high during the summer months. In the simulation, the PV surface is considered as 60.75kWp, and the ES is considered as 105.98kWh ES. The predicted annual energy production capacity is shown in Figure 5.26. The monthly averages of daily energy production, as well as the monthly average of energy not captured because the battery became full, are shown in Figure 5.27. This data shows that annual energy production using annual OPTA is 39,828.80kWh. Also, 44,394.95kWh annual energy is not captured due to the ES limit. The annual electricity production and the life span of the microgrid are given in Table 5.45. It is observed that the certain times of the year including the winter months, the energy from PV surfaces is wasted regardless of the system load design (see Section 4.6.3) and day/night use. It is also seen that during some days in the winter months (Dec, Jan, and Feb), the ES and PV capacity can be increased to meet the determined daily electricity consumption, or the generator can be needed to run. However, making more use of daylight without increasing the microgrid power capacity is one of the important aims of this study. Therefore, especially during the winter months, the energy consumption should be planned based on the sunshine duration and hours, the high energy-consuming devices should be used during the sunshine period to ensure the continuous work of the system.

Table 5.45. Annual and life span electricity production.

Land requirement	760m2
Considered lifespan	25 years
Fuel cost	1.39 $/Lt
Annual electricity production (AVG)	39.83 MWh
Life span electricity production	995.75 MWh

5.6.4. Effect of OPTA values on energy production

The differences in the intensity of TSR gain as a result of the effect of the OPTA of the PV surfaces for the Şanlıurfa province are listed in Table 5.43. It is calculated that the OPTA values vary between 1° (June) and 62° (December) throughout the year. The annual OPTA is determined to be 33° for the region. For the PV surfaces that do not have an STS, the OPTAs can also be set monthly to benefit from TSR more efficiently (Akgül et al. 2022). It is calculated that monthly tilted PV surfaces achieve 16.25% more TSR throughout the year compared to the PV surfaces that are not angled. When the tilt angles of the PV surfaces are not possible to set monthly as in this study, the OPTAs can be set annually. It is calculated that annually tilted PV surfaces achieve 10.28% more TSR yearly compared to PV surfaces that are not angled.

5.6.5. Other optimization discussions

It is understood from the location results that it would be more beneficial to optimize the microgrid for the installation location. Tilt, azimuth, and orientation angles of the PV arrays are essential to provide better power production and they can vary from location to location. The OPTA should be set based on the maximum energy production in the winter months for off-grid PV plants. Besides, with more precise estimations, it is possible to change angles when surfaces are mounted on adjustable structures. Monthly or seasonally changing OPTAs four times a year further increases ES and PV module efficiency. Therefore, sensitive optimal tilt angles can be more helpful to fill up ES at a good level. In this section, the economic benefit is considered by keeping the surface structure unadjusted and simple, annual OPTA is determined, and all PV surfaces are set at this angle. section 5.6.3. The payback period is expected to be longer due to the cost of ES for the off-grid PV plants. The cost of ES can be higher than the cost of the PV. In this study, the payback period (depreciation time) of the microgrid to be installed in the desired location for the SFS is calculated as 10.67 years. The ability to reduce this period is necessary in terms of finances and continuity, and studies in this direction should be increased.

5.7. Results of Experimental Study (7): Optimization of OPTA and TSR on PV Surfaces: An Experimental Study in Malatya Province of Türkiye

This section addresses the data collection, analysis, and results of two different types of solar PV plants over two years in 2021 and 2002. One of the implementation types is 11.8 kWp horizontal one-axis N-S aligned STS, and the other is 11.8 kWp annual tilted SFS. So, this section presents the PV electricity production results of PV plants in both the SFS and STS. To compare the two PV systems (SFS and STS) at the same level, the systems have been configured with the same PV modules and installed powers. After relevant formulas are derived in Section 3, numerical estimations about TSR intensities have been presented. Then it showcases the results of a two-year-long experiment in which an annual tilted SFS and N-S aligned single-axis STS were implemented in Malatya, Türkiye. The performance results of the grid-connected SFS and STS have also been compared with the predicted results obtained by applying anisotropic transposition models.

5.7.1. Solar data and GSR intensity utilized in experimental study

The historical GSR values of the table are obtained by NASA-SSE. Accordingly, the monthly variations of GSR intensity, ambient temperature, Humidity, and wind speed are presented in Table 5.46. The annual horizontal GSR intensity is 1715.8 kWh/m². In July the GSR reaches its highest value of 238.1 kWh/m², and in December the GSR reduced its lowest value of 57.3 kWh/m². It is well-understood that geolocation receives an ample amount of GSR around the year. The PV electricity production depends heavily on GSR received by the geolocation. Since reasonable variations of GSR intensity throughout the year, the production from the solar plant fluctuates throughout the year.

Table 5.46. Monthly GSR intensity on the horizontal surfaces for the study geolocation.

Month	GSR [kWh/m²]	KT [ratio]	Temp-Amb. [°C]	Humidity [%]	Wind [m/s]
1	68.5	0.480	-1.89	73.9	2.0
2	85.1	0.503	-1.12	69.4	2.4
3	128.6	0.522	3.34	63.3	2.9
4	154.2	0.524	9.79	59.3	3.0
5	196.9	0.572	14.98	54.7	2.9
6	227.1	0.652	19.30	41.8	3.5
7	238.1	0.677	22.72	33.8	3.5
8	208.3	0.653	22.28	33.4	3.2
9	163.8	0.633	18.67	39.4	2.8
10	113.8	0.551	12.88	57.2	2.3
11	74.1	0.498	5.00	72.6	2.2
12	57.3	0.448	-0.37	76.4	1.9
Annual	1715.8	0.559	10.47	56.3	2.7

The ambient temperature at the proposed site varies between -1.89 °C and 22.72 °C. PV modules are temperature sensitive; the PV module efficiency is higher at low temperatures. As the PV module temperature increases, the energy production reduces. The annual average air temperature in the geolocation is 10.47 °C and is under the temperature value at standard test conditions (STC). According to the wind data in Table 5.46, the average wind speed in the geolocation has no significant variation throughout the year. The windier parts of the year are Jun and July months with an average wind speed of 3.50 m/s. From the favorable parameters such as GSR, ambient temperature, and wind speed, it can be concluded that the solar climatic conditions in Malatya province are suitable for the implementation of solar PV plants.

5.7.2. Actual (experimental) PV electricity production results of implemented solar PV plants

It is noted that the geolocation systems have been implemented side by side with the same type of components such as PV modules, inverter control parts, and so on. So most factors are the same such as GSR, ambient temperature, and climatic density. Monthly actual (experimental) PV electricity productions for the years 2021 and 2022 are presented in Tables 5.47 and 5.48. In addition, actual PV electricity productions are visually criticized in graphical form in Figures X and X. During the experimental period (24 full months of 2021 and 2022 years), the implemented one-axis STS produced a maximum PV energy of 3,417 kWh in July 2022. The implemented SFS adjusted at OPTA produced a maximum PV energy of 2,351 kWh in Jun 2021. These production values represent 45.34% more efficiency in July due to the occurrence of sunny days. It is seen that one-axis STS produces lower electrical energy compared to SFS In November, December, and January generally. It has been observed in the geolocation that the reduction in actual production efficiency was sourced by climatic variations such as snowy, rainy, cloudy, and partially cloudy days, especially in winter months. So, it is well-proven that the one-axis horizontal STS produces more energy than the SFS on sunny days. On the other hand, on snowy, rainy, cloudy, and partially cloudy days, the prediction efficiency is similar between the SFS and STS.

Table 5.47. Monthly actual PV electricity productions [kWh] of the SFS for years 2021 and 2022.

Month	Year 2021	Year 2022	AVG	Difference
1	579	832	706	43.7
2	1434	1279	1356	-10.8
3	1219	1559	1389	27.9
4	1801	1859	1830	3.2
5	2337	2034	2185	-12.9
6	2351	2268	2310	-3.5
7	2312	2316	2314	0.1
8	2165	2207	2186	2.0

9	2080	2027	2054	-2.6
10	1774	1704	1739	-4.0
11	1133	975	1054	-13.9
12	856	730	793	-14.7
Annual	20041	19791	19916	-1.2

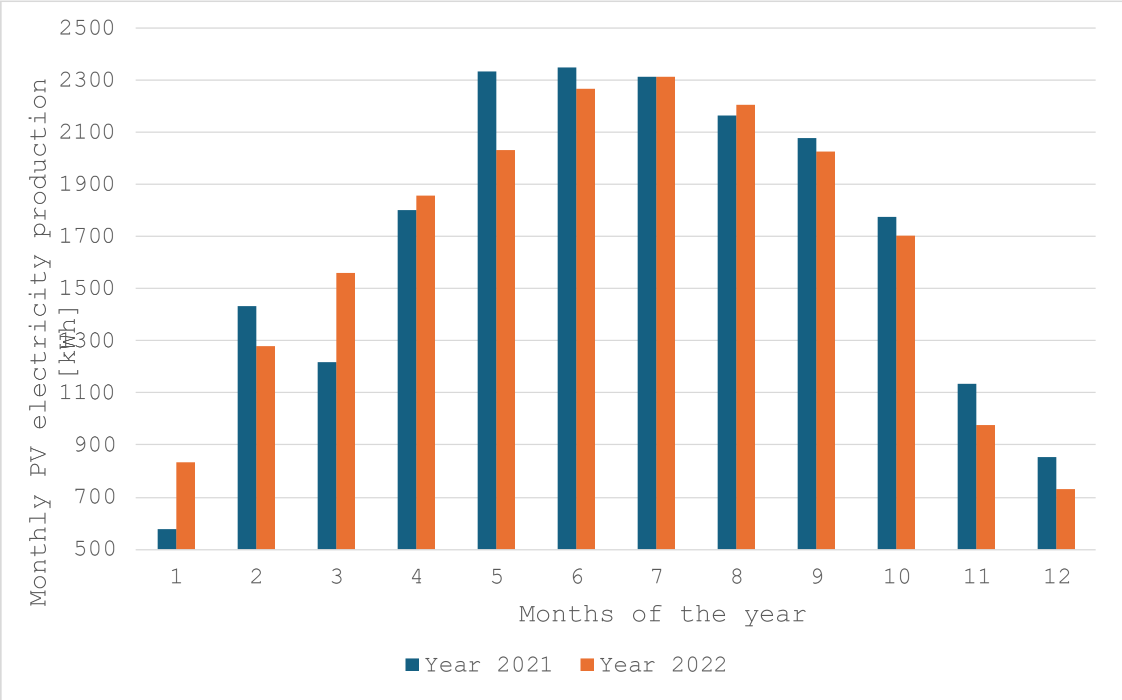

Figure 5.31. Monthly actual PV electricity productions in years 2021 and 2022 for SFS.

Table 5.48. Monthly actual PV electricity productions [kWh] of the STS for years 2021 and 2022.

Month	Year 2021	Year 2022	AVG	Difference
1	524	810	667	54.5
2	1490	1275	1382	-14.4
3	1235	1578	1406	27.8
4	2229	2315	2272	3.9
5	3204	2906	3055	-9.3
6	3414	3095	3254	-9.3
7	3250	3417	3334	5.1

8	2826	2956	2891	4.6
9	2560	2511	2536	-1.9
10	1933	1758	1846	-9.1
11	1084	932	1008	-14.0
12	786	647	717	-17.7
Annual	24535	24199	24367	-1.4

Actual yield parameters indicated that the maximum production values for both SFS and SFS PV plants were obtained in July. The lowest energy production occurs in January. This variation can be strongly attributed to the monthly GSR. For the SFS, the monthly average PV electricity production varies, with a minimum value of 706 kWh in January and a maximum of 2314 kWh in July. For the one-axis SFS, the monthly average PV electricity production varies, with a minimum value of 667 kWh in January and a maximum of 3334 kWh in July. So, monthly average energy gain varies throughout the year, depending mainly on the solar declination and GSR intensity. Adjusting the OPTA to the SFSs increases the energy gain for annual tilted SFS.

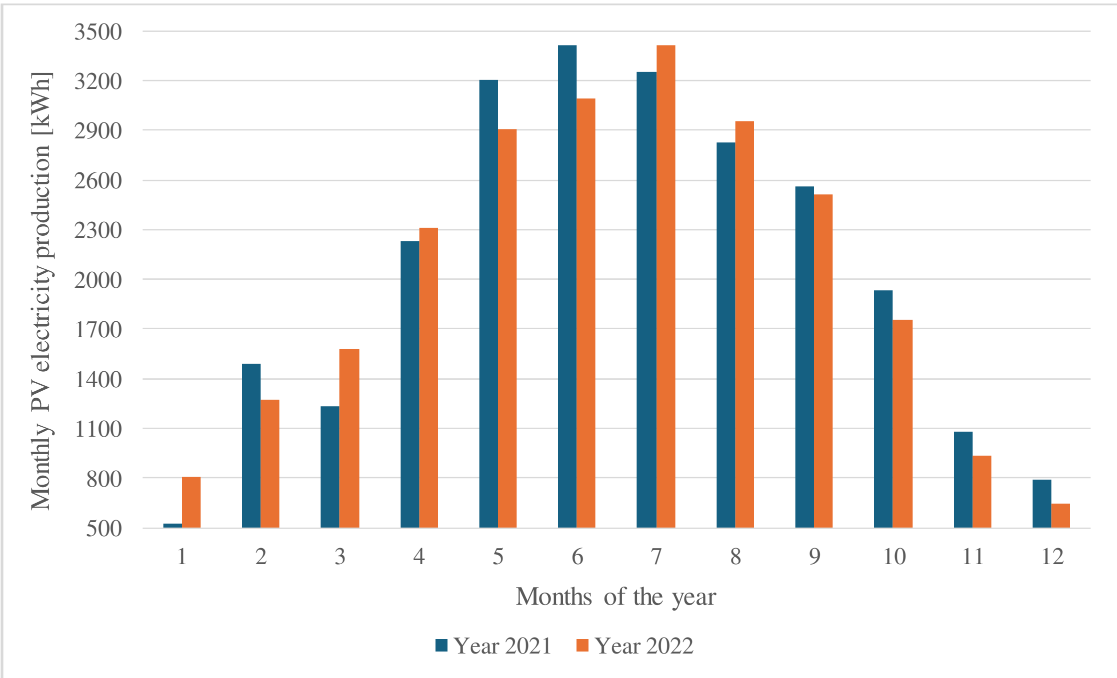

Figure 5.32. Monthly actual PV electricity productions in years 2021 and 2022 for one-axis STS.

Seasonal distributions of actual PV electricity productions for both SFS and one-axis STS have been presented in Tables 5.49 and 5.50, respectively. Moreover, the average comparative graph for seasonal distributions of actual PV electricity productions for both SFS and one-axis STS has also been presented in Figure 5.33. In the presented geolocation of Malatya province, the one-axis horizontal STS has produced PV electricity annual yield of 22.34% more than the SFS (average of 2021 and 2022 years). It is noted that OPTA cannot be adjusted for security and protection reasons for the horizontal one-axis STSs designed on a large scale as in this study. So, adjusting the OPTA constant at 0° is a result of the physical construction of the STS.

Table 4.49. Seasonal distribution of actual PV electricity productions for the SFS.

Season	**Month**	**Y-2021**	**Y-2022**	**AVG**	**Difference**
Spring	2 3 4	4454	4697	4575	-5.18
Summer	5 6 7	7000	6618	6809	5.77
Autumn	8 9 10	6019	5938	5979	1.37
Winter	11 12 1	2568	2538	2553	1.19
Annual		20041	19791	19916	0.79

The annual electricity production during the same periods was 24,367 kWh for one-axis horizontal STS, and 19,916 kWh for SFS adjusted at OPTA, according to the average of the two years. In contrast, on cloudy snowy, and rainy days the performance of both SFS and one-axis STS was reduced considerably. That is, it is determined that the meteorological conditions mentioned above affect the capture presence of GSR in solar PV plants, especially in the winter season. It is also seen that in the summer season, there is greater PV electricity production of both SFS and one-axis STS because there was a greater number of sunny days. The results show that the STS is more productive compared to FS. Because the STS constantly follows the path of the sun horizontally, STS receives the GSR intensity maximum level by utilizing the most appropriate tilt angle.

Table 5.50. Seasonal distribution of actual PV electricity productions for the horizontal one-axis STS.

Season	Month	Y-2021	Y-2022	AVG	Difference
Spring	2	4954	5167	5061	-4.12
	3				
	4				
Summer	5	9868	9419	9644	4.77
	6				
	7				
Autumn	8	7320	7225	7273	1.31
	9				
	10				
Winter	11	2394	2389	2392	0.21
	12				
	1				
Annual		24535	24199	24367	0.54

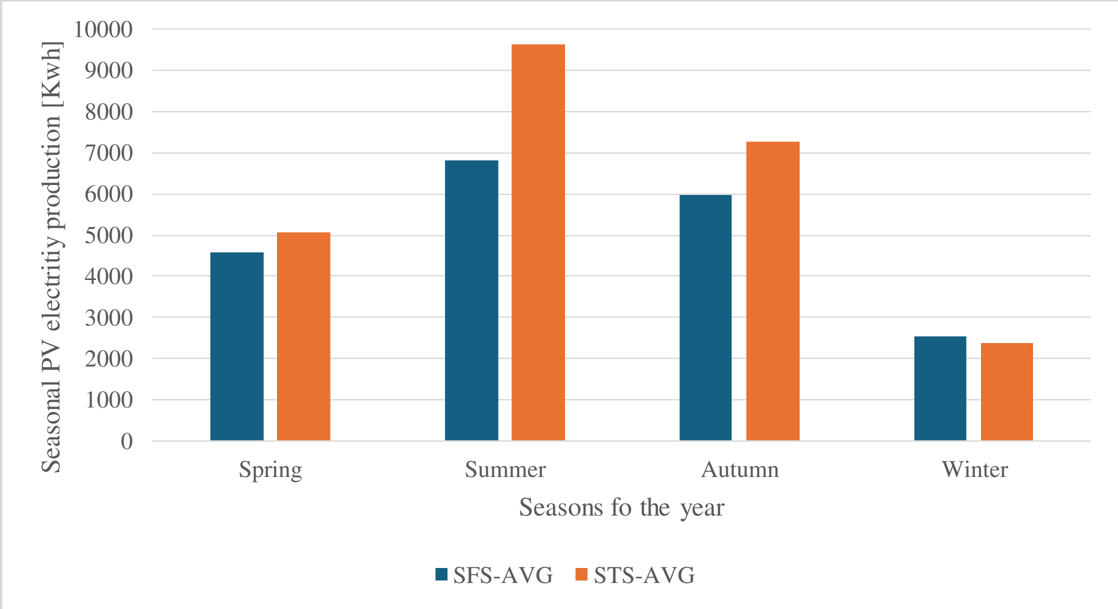

Figure 5.33. Comparison of seasonal PV electricity actual production average of 2021 and 2022 years.

5.7.3. Prediction results of the TSR intensity for implemented solar PV plants

Performance estimation is a key step in the process of implementing solar PV plants. The mayor's performance parameters are energy production, GSR-TSR, and system losses. Performance analysis helps to develop practical experiences for improving the operational performance of solar PV plants. Accordingly, the OPTA is predicted according to the geolocation of the solar PV systems by applying HAY and PERZ transposition models. To produce maximum PV electricity, the annual OPTA is determined as 33° of the SFS which is below the latitude of the location. Therefore, the predictions of TSR intensity by utilizing HAY and PEREZ transposition models for an SFS at OPTA=33° and the orientation angle is set 0° are presented in Tables 5.51 and 5.52, respectively. Moreover, the predictions of TSR intensity by utilizing HAY and PEREZ transposition models for a one-axis horizontal STS are presented in Tables 5.53 and 5.54, respectively. In general, PV electricity production depends on its efficiency rate, size, the intensity of GSR striking the surface, and so on. Therefore, small discrepancies and deviations between actual production and estimated production values can be considered normal. In addition, the prediction values provide very useful and beneficial solar data to see the big picture about the production capacity of the Solar PV Plant to be installed in the geolocation.

An important point for STSs is that the STSs rotate to maximize the cosine angle of GSR. This is achieved by matching the rotation of the STS to the sun's position. However, the STSs have a limited rotation range, which depends on the manufacturer but is around ±60° concerning the horizontal 0°, which is the value considered in this study. In theory, it is possible to increase this temperature up to ±90° degrees, but when the STS size, wind load, shading, and efficiency are calculated, manufacturers put locks after an average of ±60 for security reasons.

Table 5.51. Estimation of TSR intensity by utilizing the HAY model for an SFS [OPTA=33°].

Month	TSR [kWh/m²]	TSR-Eff [kWh/m²]	E-Array [kWh]	E-Grid [kWh]	PR [ratio]
1	114.5	113.2	1316	1290	0.948
2	122.7	121.3	1397	1368	0.938
3	156.9	154.7	1731	1694	0.909
4	161.4	158.7	1735	1696	0.885
5	186.2	182.6	1939	1894	0.856
6	204.2	200	2072	2021	0.833
7	219.1	214.8	2188	2134	0.820
8	211.8	208.3	2121	2070	0.823
9	194.4	191.6	1980	1933	0.837
10	157	155	1666	1629	0.873
11	118.9	117.4	1315	1285	0.910
12	98.7	97.4	1122	1097	0.935
Annual	1945.8	1915	20582	20111	0.881

Table 5.52. Estimation of TSR intensity by utilizing the PEREZ model for an SFS [OPTA=33°].

Month	TSR [kWh/m²]	TSR-Eff [kWh/m²]	E-Array [kWh]	E-Grid [kWh]	PR [ratio]
1	117.6	116.2	1351	1323	0.947
2	126.5	125	1438	1408	0.937
3	161.7	159.5	1780	1743	0.907

4	166.3	163.7	1785	1744	0.883
5	190.8	187.4	1985	1939	0.855
6	208.6	204.4	2114	2062	0.832
7	224.3	220	2236	2182	0.819
8	216.8	213.3	2167	2115	0.821
9	198.4	195.5	2017	1969	0.836
10	161	159	1706	1668	0.872
11	121.2	119.7	1339	1310	0.910
12	100.4	99.1	1140	1115	0.935
Annual	1993.6	1962.8	21058	20578	0.880

Table 5.53. Estimation of TSR intensity by utilizing the HAY model for a one-axis STS.

Month	TSR [kWh/m²]	TSR-Eff [kWh/m²]	E-Array [kWh]	E-Grid [kWh]	PR [ratio]
1	103.2	101.4	1198	1174	0.957
2	120.7	119.2	1389	1361	0.949
3	178.5	177	1993	1952	0.921
4	208.6	207.2	2258	2211	0.892
5	261.7	260.3	2731	2670	0.859
6	307.9	306.8	3121	3050	0.834
7	331.1	330.1	3312	3235	0.823
8	297.7	296.8	3005	2938	0.831
9	237.6	236.5	2445	2391	0.847
10	165	163.4	1779	1740	0.888
11	111.2	109.5	1246	1219	0.923
12	86.5	84.8	994	971	0.945
Annual	2409.7	2393.1	25471	24913	0.870

Table 5.54. Estimation of TSR intensity by utilizing the PEREZ model for a one-axis STS.

Month	TSR [kWh/m²]	TSR-Eff [kWh/m²]	E-Array [kWh]	E-Grid [kWh]	PR [ratio]
1	106.3	104.5	1233	1208	0.956
2	124.7	123.2	1434	1406	0.949
3	183.8	182.3	2049	2007	0.919
4	215.1	213.9	2326	2277	0.891
5	268.8	267.5	2802	2740	0.858
6	312.9	311.8	3168	3096	0.833
7	336.8	335.9	3364	3287	0.821
8	303.1	302.2	3055	2987	0.829
9	241.5	240.3	2483	2428	0.846
10	169.6	167.9	1826	1787	0.887
11	113.3	111.6	1269	1242	0.922
12	88.2	86.4	1013	990	0.945
Annual	2463.9	2447.5	26022	25454	0.870

5.7.4. Prediction of energy losses that may occur due to rotation limit for one-axis STS.

As informed earlier section, the STSs have a limited rotation range, which depends on the manufacturer but is around ±60° because of the device security. In this study, the ±60° rotation range is also considered. The issue that needs to be questioned at this stage is the ratio of the effects of STS rotation limits on PV production performance. In this context, the prediction of energy losses that may occur due to the rotation limit of one-axis STS is tabulated in Table 5.55. It is calculated from Table 5.55 that the increase in TSR intensity on one-axis horizontal STS is 0.63% in the case of the continued rotation from ±60° to ±90° (±30°). The increase in net PV electricity production is 1.36%. Another result emerging from the analysis is that between ±80 and ±90 degrees, there is no change (0%) in either the TSR intensity or the net PV electricity production.

Table 5.55. Prediction of energy losses that may occur due to the rotation limit of one-axis STS.

HAY Model			**PEREZ Model**		
STS Angle [°]	TSR [kWh/m²]	E-Grid [kWh]	STS Rotation Range [°]	TSR [kWh/m²]	E-Grid [kWh]
±60°	2409.7	24913	±60°	2447.5	25454
±70°	2422.4	25044	±70°	2461.9	25600
±80°	2424.9	25071	±80°	2481.0	25633
±90°	2424.9	25071	±90°	2481.0	25633

5.7.5. Losses predictions for implemented solar PV plants

Losses of DC energy include PV module and inverter mismatches, heat losses in power cables, interconnections, and losses due to dirt, snow, icing, soiling, etc. Losses of AC energy include inverter, AC cable, grid, etc. In this context, the predicted loss values are tabulated in Table 5.56 for implementing the SFS and STS. Annual energy losses for SFS are estimated at between 13.86 and 13.93. For one-axis horizontal STS, annual energy losses are estimated at between 13.95 and 14.06. System malfunctions and energy production losses can be detected based on the PR ratios. Lower PR is attributed to incorrect operation, PV module, or inverter malfunction. In the SFS estimations, the annual average value of PR ratios is found to be 0.881 for the HAY model and 0.880 for the PEREZ model. The highest value of PR ratios is found to be 0.947 and 0.948 in January, the lowest PR ratios are found to be 0.819 and 0.820 in July. Conversely, in the STS estimations, the annual average value of PR ratios is found to be 0.870 for both HAY and PEREZ models. The highest value of PR ratios is found to be 0.956 and 0.957 in January, the lowest PR ratios are found to be 0.821 and 0.823 in July. For example, as seen in Figure 5.36, the annual SFS production of the year 2021 with a deviation value of 0.36 means that the expected PR ratio value has almost been reached. Therefore, it shows that the predicted PR ratios are similar to the actual PR ratios but with small differences.

Table 5.56. Predicted loss values for Implemented Solar PV Plants.

PV Plant Losses	One-Axis STS [%]		OPTA [%]	
	HAY	PEREZ	HAY	PEREZ
IAM factor on global	0.69	0.67	1.58	1.55
PV loss due to radiation level	0.36	0.35	0.62	0.59
PV loss due to temperature	7.34	7.44	6.28	6.45
Mismatch loss, modules, and strings	2.10	2.10	2.10	2.10
Ohmic wiring loss	1.17	1.18	1.07	1.09
Inverter Loss during operation	2.09	2.09	2.15	2.13
Inverter Loss due to power threshold	0.01	0.01	0.03	0.03
Night consumption	0.10	0.09	0.12	0.12
Total predicted losses	13.86	13.93	13.95	14.06

5.7.6. Comparison of predicted production and actual production results

However, it can be emphasized that there is no transposition model largely better than another, whatever the statistical test chosen to determine the quality of the model (Notton et al. 2004). Therefore, it would be a more reasonable approach to analyze the accuracy of the anisotropic models by comparing them with actual (experimental) energy production results. The gain in PV electricity production is determined by the difference in the SFS and the STS. Actual and predicted results have been compared employing PV energy gain. Monthly energy gain varies throughout the year, depending mainly on the solar declination. Comparisons of predicted production and actual production results for both SFS and one-axis horizontal STS plants have been tabulated in Tables 5.57 and 5.58, respectively. On the other hand, Annual comparisons between predicted and produced PV electricity results for both SFS and one-axis horizontal STS plants have been presented in a graphical form in Figures 5.34 and 5.35, respectively. Moreover, the deviation rates of predicted production from actual production are plotted in Figure 5.36 according to yearly data.

It is understood that the correlation is inverse between solar declination and energy gain, both in the actual and predicted data. Considering annual predictions and actual productions. It can be noticed that there is considerable similarity in the trend of the theoretical and experimental results and a good fit of the simulation for both SFS and STS implementations. This result shows a clear validation of the presented transposition models and the numerical estimations. Apart from this, serious prediction discrepancies in December and January stand out.

Table 5.57. Comparison of estimated production and actual production for the SFS [OPTA=33°].

Month	Real Productions		Estimations		Deviations			
	Y-2021	Y-2022	Hay	Perez	HAY		Perez	
					Y-2021	Y-2022	Y-2021	Y-2022
1	579	832	1290	1323	122.79	54.99	128.49	58.96
2	1434	1279	1368	1408	-4.60	6.99	-1.81	10.12
3	1219	1559	1694	1743	39.01	8.67	43.03	11.81
4	1801	1859	1696	1744	-5.83	-8.79	-3.17	-6.21
5	2337	2034	1894	1939	-18.94	-6.90	-17.02	-4.69
6	2351	2268	2021	2062	-14.04	-10.90	-12.29	-9.09
7	2312	2316	2134	2182	-7.72	-7.85	-5.64	-5.78
8	2165	2207	2070	2115	-4.38	-6.22	-2.30	-4.18
9	2080	2027	1933	1969	-7.09	-4.63	-5.36	-2.85
10	1774	1704	1629	1668	-8.17	-4.40	-5.98	-2.11
11	1133	975	1285	1310	13.38	31.73	15.58	34.29
12	856	730	1097	1115	28.18	50.25	30.28	52.71
Annual	20041	19791	20111	20578	0.35	1.62	2.68	3.98

Table 5.58. Comparison of estimated production and actual production for the one-axis STSs.

Month	Real Productions		Estimations		Deviations			
	Y-2021	Y-2022	Hay	Perez	HAY		Perez	
					Y-2021	Y-2022	Y-2021	Y-2022
1	524	810	1174	1208	123.99	45.00	130.48	49.19
2	1490	1275	1361	1406	-8.65	6.77	-5.63	10.30

3	1235	1578	1952	2007	58.09	23.73	62.55	27.22
4	2229	2315	2211	2277	-0.80	-4.49	2.16	-1.64
5	3204	2906	2670	2740	-16.65	-8.13	-14.47	-5.72
6	3414	3095	3050	3096	-10.66	-1.46	-9.31	0.03
7	3250	3417	3235	3287	-0.47	-5.34	1.13	-3.81
8	2826	2956	2938	2987	3.95	-0.60	5.68	1.05
9	2560	2511	2391	2428	-6.60	-4.79	-5.16	-3.32
10	1933	1758	1740	1787	-10.00	-1.01	-7.57	1.66
11	1084	932	1219	1242	12.49	30.86	14.61	33.33
12	786	647	971	990	23.50	49.99	25.92	52.93
Annual	24535	24199	24913	25454	1.54	2.95	3.75	5.18

Many factors can cause a mismatch between predicted and produced PV electricity production. Possible major reasons for differences can be counted as cloud coverage, optical clutter, Shading, PV cell difference, tilt angle deviation, temperature, design, GSR modeling, etc. Isotropic theories assume a clear sky throughout the year. Prediction models consider equal and flawless PV surface conditions and ignore optical clutter like dirt and dust. Moreover, all losses are not considered in the prediction model, such as soiling, reflection, cable, and inverter losses. Also, the determination of OPTA error may cause a difference in energy predictions. Apart from this, temperature and humidity effects and construction design differences may result in different effects on heat dissipation, such as exposure to wind and airflow. The rates and modeling of diffuse and reflected radiation also affect the theoretical estimations.

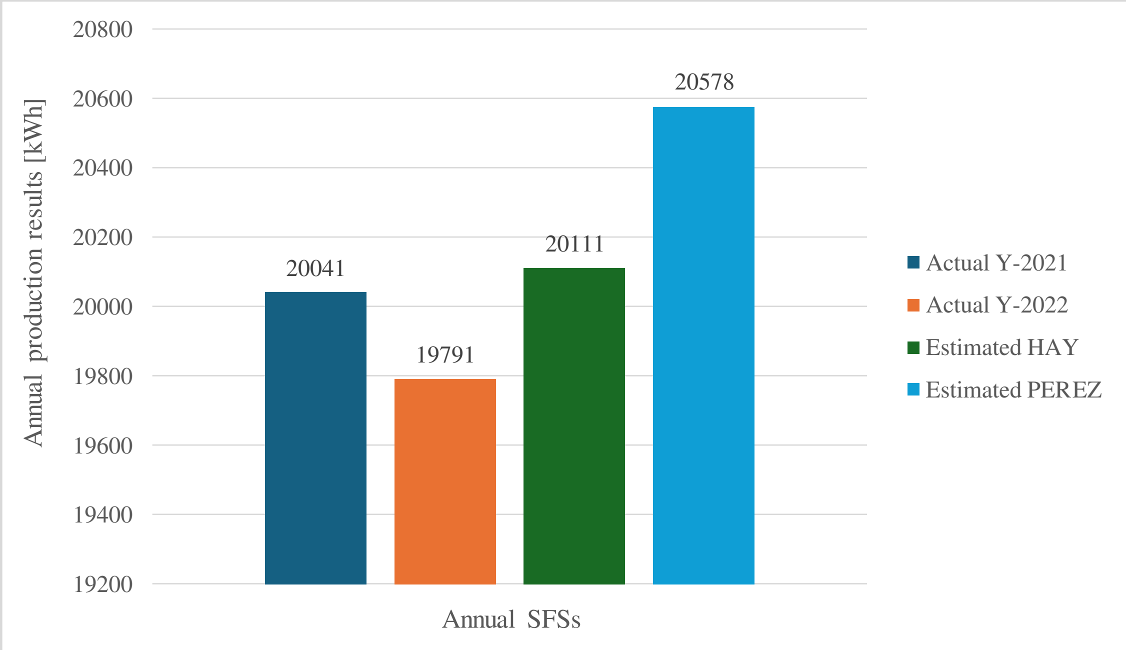

Figure 5.34. Annual comparisons of predicted and produced PV electricity results for the SFS.

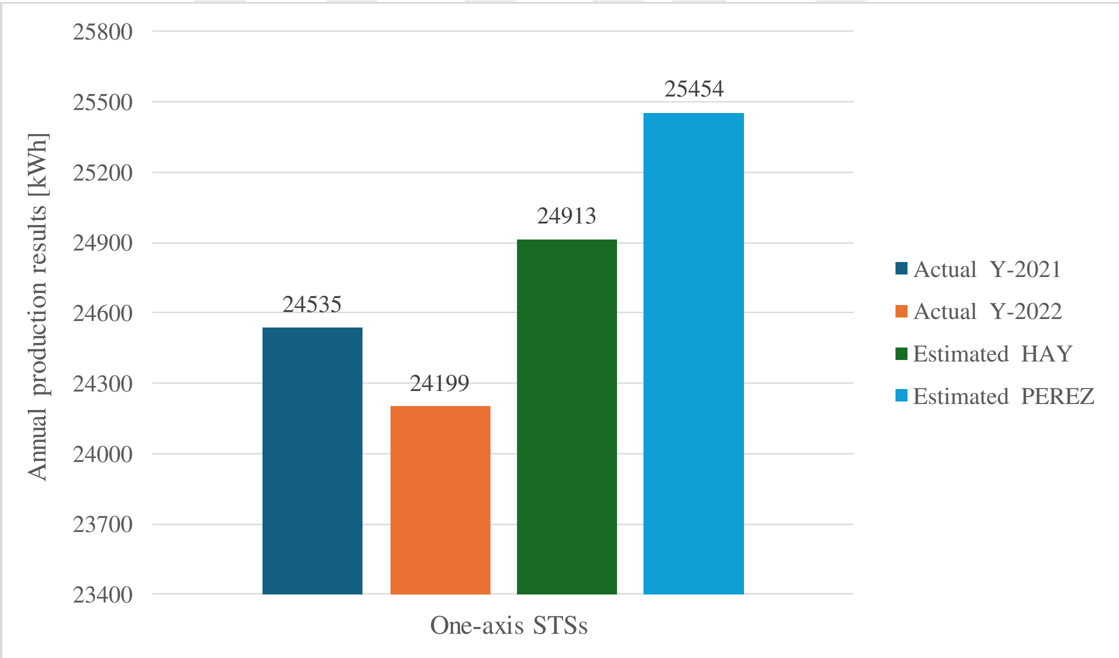

Figure 5.35. Annual comparisons of predicted and produced PV electricity results for the STS.

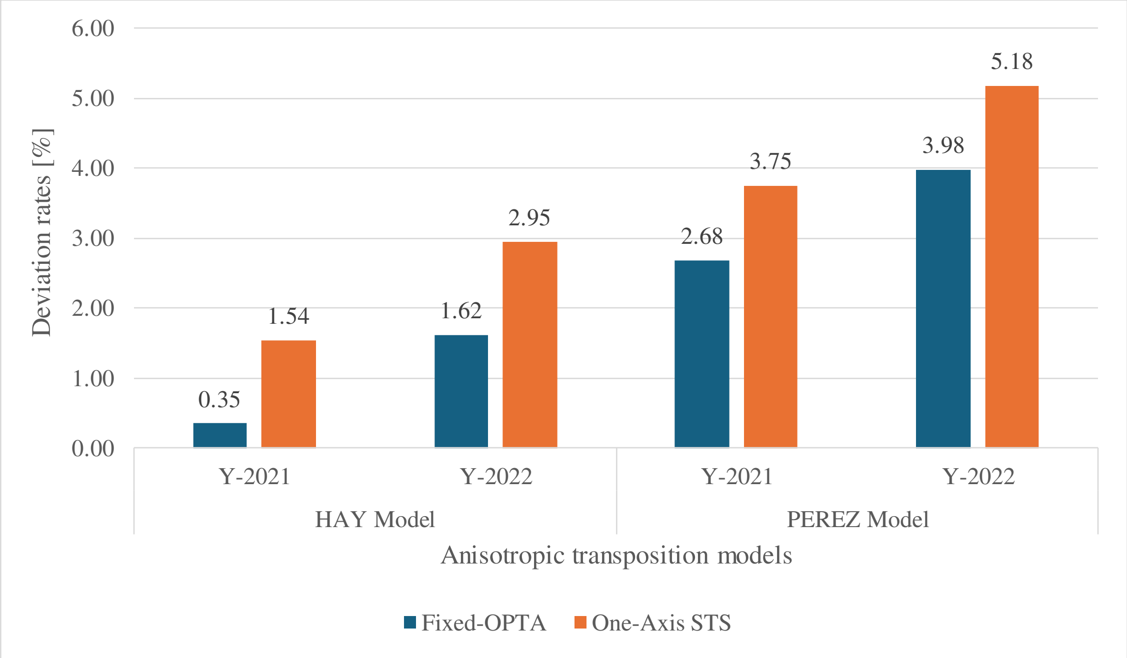

Figure 5.36. Deviation rates of predicted production from actual production.

Figures 5.34 and 5.35 prove that the TSR prediction models on PV surfaces are in good agreement with the field measurement. That is, the actual results confirm the trends of the transposition models in solar energy production estimations. Therefore, these validated transposition models in this implementation study can be securely applied to predict the performance of PV plants both one-axis STS, and annual tilted SFS with different OPTAs in different geolocations. It can be seen from Figure 5.36 that the biggest deviation occurred in the one-axis production predictions in the PEREZ model with 5.18% (The average of 2 years is 4.46% in STS). The minimum deviation was 0.35% in the HAY model SFS production predictions. (The average of 2 years is 0.98% in SFS). In comparison with actual production data, it can be seen that the prediction rates of the PEREZ model are generally higher than the HAY model in all categories. Additionally, it can be seen that the HAY model makes more robust production predictions than the PEREZ model in all categories. So, a reasonably small mismatch has been found between the theoretical predictions and the actual energy productions, which validates the proposed transposition models for predictions on PV electricity production. Another important point is that the predictions, it is used past NASA-SSE GSR data explained in Section 4.7.1 (averaged for Malatya over 20 years), which factor can lead to small differences between actual and theoretical PV production results. It is necessary to open a separate parenthesis here: In the study conducted with actual data, it has been determined that the accuracy of the satellite-based NASA-SSE monthly GSR data used in this study is quite high and that it can be used safely in solar plant projects. Considering that the HAY model is the simplest and the PEREZ model is the most complex anisotropic model, it is understood that very simple models as well as more complex models may yield good results.

It is expected that derived solar data and results provide insight into identifying the geolocation and suitable technologies and methodologies for the deployment of solar PV plants in the Malatya province of Türkiye. This derived data is useful in assessing the operational benefits of solar PV plants based on their actual PV electricity production. The produced data and implementing experience of solar PV plants, both SFS and STS, can be applied to future solar-based projects.

5.8. Assumptions, Constraints, and Uncertainties

As detailed in earlier sections, the PV energy production of a PV plant depends on many factors, such as GSR, power conversion efficiency, geolocation, PV surface angles, climatic conditions, physical aspects, etc. The most significant influence on PV electricity is GSR, including beam, diffuse, and reflected components. Among them, the beam component dominates PV energy production (Daut et al., 2011). The major constraints on the intensity of TSR estimation for tilted surfaces can be counted as physical, economic, and technical restrictions. Although the climatic conditions are highly suitable for solar energy utilization, the choice of appropriate land at an affordable price limits investment in some provinces of Türkiye. Large-scale solar PV plants need vast areas and should be far away from province centers without electric transportation lines. The investors must conduct sensitive cost-benefit analyses for some provinces because land prices are very expensive, especially in provinces with high populations. For the installation of a power system, the selection of land with infertile agricultural soil and the burden of agricultural production is the most critical issue. GSR and TSR estimations are also limited by computational complexity due to technical constraints, mainly due to the inclusion of parameters in the treatment model. Having limited coverage of GSR measuring networks, including ground and satellite stations, may affect the reliability of solar data used in estimating the solar TSR gain.

The major technical uncertainties of the solar TSR estimation on tilted surfaces can be calculated the TSR intensity availability, atmospheric conditions, electrical-thermal solar module characteristics, and long-term system output and performance (Nassar & Alsadi, 2019; Nassar et al., 2022). Uncertainties can also arise from the technical approaches involved in models. Because of the varying atmospheric conditions and complex characteristics of GSR, they are subject to some uncertainties in modeling. To present these complex characteristics of GSR and TSR, the assumption has been made that diffuse radiation has an isotropic distribution. The assumption of an isotropic model allows the beam and diffuse components on the horizontal surface to be corrected for TSR on the tilted surface by simple geometric relationships (Klucher, 1979). On the other hand, these asymmetric effects mentioned above are also limiting factors in obtaining accurate GSR estimation on tilted surfaces. At this point, the use of reliable solar data will increase the accuracy of the estimations. Considering these mentioned assumptions, some constraints and uncertainties in the isotropic or anisotropic transposition models researchers used for the estimation of TSR on tilted surfaces as in the present study. Despite all these uncertainties, these models still provide results with acceptable accuracy for predicted TSR. From an economic point of view, the cost of large-scale solar PV plant facilities is also considered a source of uncertainty, depending on the choice of installation equipment. It should be emphasized that the present study covers one year and all provinces of Türkiye.

The estimations' accuracy will increase with the use of reliable solar data. However, the complex and variable nature of diffuse solar irradiation requires some simplifications via assumptions to estimate TSR intensity on a tilted surface by utilizing empirical models (Hay & McKay, 1985). The limitations in the coverage of TSR measurements from ground and/or satellite stations can also influence the accuracy of solar data. Therefore, solar data itself might be one of the main sources of uncertainty (Nassar & Alsadi, 2019). Asymmetric effects such as varying atmospheric conditions and complex characteristics lead to some uncertainties in modeling as well (Nassar et al., 2022). TSR estimations for tilted surfaces are limited to the computational and technical complexity of the models, mostly as a result of the inclusion or exclusion of parameters in the transposition model. Another source of limitations is the technical assumptions that go into modeling. Most of the time, solar estimations are completely dependent on the transposition models and solar data utilized. Because of all these reasons, the anisotropic transposition models have specific assumptions, uncertainties, and constraints. So, choosing the best transposition model is essential since erroneous TSR estimates might cause both financial and technological problems, especially for large-scale solar investments. However, despite all these unfavorable situations, anisotropic transposition models still provide results with a reasonable level of precision for TSR estimation values. To ensure the reliability and accuracy of estimations, anisotropic models validated in various studies via statistical indicators and comparisons with actual data have been preferred in this study, also briefly discussed in the literature review section.

5.9. Validation of Correlation and Transposition Models

The accuracy of transposition models is highly dependent on the diffuse component and is usually evaluated using a model (Lui-Jordan or Erbs correlation). Using a measured diffuse component greatly improves the transposition's accuracy. The Erbs correlations is a simple fraction model that was suggested for the estimation of monthly average diffuse radiation on horizontal and tilted surfaces (Duffie & Beckman, 2013). Erbs correlations are also included as a reference model in some studies for performance assessments covering a wide range of latitudes, altitudes, and climates (Reindl et al., 1990; Ineichen, 2008; Benchrifa et al., 2021; Milosavljević et al., 2022). Based on the Orgill and Hollands correlations, the Erbs correlations were adapted to extend them to latitudes from 31°N to 42.5°N, including the entire land of Türkiye at 36°N to 42°N latitudes, and validated on data from the United States.

The Erbs correlations have also been validated by applying two widely used statistical indicators (mean bias and root mean square) to the isotropic, Hay, and Perez models (Feuermann & Zemel, 1992). It was found that despite the fact that some location and seasonal dependencies of the Erbs correlations exist, these effects are considered to be negligible to the correlations overall performance (Oliveira et al., 2002; Ineichen, 2008). It was also found that the developed correlations for different latitudes yield quite similar results to Erbs correlations (Ahwidea et al., 2013). Orgill & Hollands (1977) was used data obtained from Canadian stations, Erbs et al (1982) was used data from four U.S. and one Australian station, and Reindl et al (1990) was used an independent data set from the United States and Europe (Nassar et al., 2022). It was found that the results are essentially identical, although they were derived from three separate solar datasets (Duffie & Beckman, 2013). The Erbs et al. correlations have been widely used for practical purposes in Türkiye (Bilgili & Dağtekin, 2017; Beyazıt et al., 2017; Balo, 2018; Emeksiz, 2020). Recent studies have come to the conclusion that the Perez model is slightly better in terms of RMSD in any case, even with synthetic data (Ineichen, 2011). During the validations of Hay-Davies and Perez transposition models with the measured GSR data, the comparison of their mean errors (MBE) shows a systematic difference of 1.8 to 2.2%, depending on the geolocations (Pvsyst, 2024).

Lui and Jordan transposition model is the first isotropic sky model. Even though this is not the most accurate model available, it is still used today by many researchers and is also integrated into commercial software and database banks (Orgill & Hollands, 1977). Although many studies suggested the use of anisotropic models, the Liu & Jordan model has been commonly used to express the GSR and TSR data, determine the OPTA, and estimate the intensity of TSR in many scientific studies covering a wide range of locations and Türkiye provinces (Çelik, 2006; Bakırcı, 2012; Kaçan & Ulgen, 2012; Nassar & Samer, 2016; Alsadi & Nassar, 2017; Kallioğlu et al., 2019; Yıldırım & Aktacir, 2019; Mansour et al., 2021; Akgül et al., 2022; Nassar et al., 2022). Since one of the aims of this study is to accurately determine the intensity of GSR and the OPTA for the provinces of Türkiye, Liu & Jordan isotropic model, which has been validated in many scientific studies, is preferred.

Anisotropic models (Hay & Davies, 1978; Klucher, 1979; Perez et al., 1987; Reindl et al., 1990; Duffie & Beckman, 2006) presented in this study have been commonly used and validated recently to calculate the OPTA and predict TSR intensity across a broad latitude value in scientific research (Jakhrani et al., 2013; Shukla et al., 2015; Li et al., 2017; Nassar et al., 2020; Nassar et al., 2022). The Erbs correlation (1982) model used in this study was validated by using several independent solar data sets for geographically and climatologically diverse locations around the world (Reindl et al., 1990; Feuermann & Zemel, 1992; Notton et al., 2004) The Erbs model was referred to as a reference model for its performance in a number of research covering a broad spectrum of latitudes, altitudes, and climates (Feuermann & Zemel, 1992; Milosavljević et al., 2022). Although the Erbs correlations have some locational and seasonal dependencies, such dependencies are regarded as insignificant in the light of the overall performance of the correlations (Reindl et al., 1990; Oliveira et al., 2002). The results produced by the developed correlations at various latitudes are reasonably parallel to those obtained by the Erbs correlations (Ahwidea et al., 2013). In another study (Duffie & Beckman, 2006), despite deriving from three different solar datasets, the Erbs correlation outcomes were found to be almost identical. As stated above, in Türkiye, the Erbs correlations have also been frequently applied for pragmatic reasons (Beyazit et al., 2017; Bilgili & Dağtekin, 2017; Balo, 2018; Emeksiz, 2020). In the study (Beyazıt et al. 2017), it was determined that the Erbs correlation (1982) model was found to be the most appropriate model for Şanlıurfa after statistical evaluations of the results. It is well understood that the suggested correlation model is generic, meaning it may be used for various albedos, sky conditions, and locations. That is why, in this study, the Erbs correlation model is preferred since it is globally location-independent.

From the detailed investigation above, it becomes clear that the transposition models and methodologies proposed in this thesis have been validated in numerous ways. Hourly TSR calculations collected by the tilted surface for various tracking setups have been performed using weather data from a normal meteorological year as input, taking into account six major regions (Phoenix, Iqaluit, Toronto, Vancouver, Denver, and Singapore). Daily TSR values obtained from the hourly GSR data of the regions were compared with TSR values calculated by using the proposed algorithm. It is seen that the comparison between values obtained from hourly computations and values obtained with the proposed methodologies is in great agreement. Therefore, these methodologies have been proposed and employed to study the region of interest in this thesis.

6. CONCLUSIONS

In the last section of the thesis, the contributions and concluding remarks are highlighted for the geography of Türkiye and worldwide, where suggestions for improving the efficiency of solar PV plants are presented. To gain a different and broader perspective, the conclusions of the case, application and implementation studies have been presented separately, and general conclusions covering this thesis have been presented separately.

6.1. Conclusions of Case Study (1): Optimization of Tilt Angles and Solar Radiation Intensity for Fixed and Tracked Sout Facing Solar PV Surfaces in Provinces of Türkiye

This study estimates the annual OPTAs of PV surfaces for all provinces of Türkiye. It also estimates and provides a quantitative understanding of TSR intensity on both SFSs and STSs relative to horizontal surfaces across Türkiye. In this study, a detailed literature review has been conducted for Türkiye. It has been observed that the studies on Türkiye's use of its solar potential are not yet at a sufficient level. A numerical method is proposed to estimate the daily TSR on optimally tilted SFSs, and one-axis and two-axis STSs in 81 provinces and 7 geographical regions in Türkiye. Considering the climatic parameters and geographical positions, a map showing OPTAs of PV surfaces for all provinces has been created. This study particularly can be used as a guideline to determine the annual OPTAs for the SFSs across Türkiye.

Comprehensive solar data including the TSR values and percentage contributions that can be obtained in the case of installing SFSs and STSs in solar PV plants to be established in these regions and provinces contributes greatly to the literature. The proposed method may be applied to any province or particular region in Türkiye where the significance of solar plants is constantly increasing.

It is found that the OPTAs of all provinces and regions are below the latitude values of Türkiye. The OPTA value for a south-facing SFS is found between 28º to 36º across the year. The necessity of set OPTA and orientation is also demonstrated in this study. It can be inferred that annual OPTA can be used in a variety of solar applications to reduce PV surface installation costs. In circumstances when changing the tilt angles of

PV surfaces isn't possible, the annual OPTAs can be set for Türkiye's provinces to gain the best TSR efficiency.

It has been found that the topographic diversity and climatic characteristics in Türkiye significantly affect the intensity of TSR on the PV surfaces. It is also shown that the intensity of TSR collected by the PV surfaces can be varied noticeably according to the geographical locations of Türkiye. Even over small distances or close latitude values in Türkiye, climate variation has a considerable impact on annual TSR intensity.

The obtained TSR values for one-axis and two-axis STSs are compared to TSR values for annual tilted SFS, it is found that such STSs are more efficient than the annual tilted SFSs as expected. Findings show that STSs yield significant solar energy gains. Considering the cost of two-axis STSs, it is strongly advised to use one-axis STSs in the setup of large-scale solar plants in Türkiye.

It is well understood from the analysis of the effect of the OPTA on the daily TSR gain that the reduction in daily TSR does not exceed 0.5% due to the offset of tilt angle from the OPTA in the case of applying isotropic transposition model for all the provinces of Türkiye.

The study shows that Türkiye has substantial solar potential and has an advantageous geographical location for the plant of solar-based systems. It is believed that the findings of this study will support the solar data literature for all provinces of Türkiye and will provide useful knowledge for researchers, investors, designers, and engineers dealing with solar PV plants. The proposed methodology can be implemented for determining the solar potential in a certain location of Türkiye and extended to any place in the world by using iterative algorithms thanks to the low computational cost.

6.2. Conclusions of Case Study (2): Estimation of OPTAs and Solar Radiation Collected by Fixed and Tracking PV surfaces in the Mediterranean Region, Türkiye

This study presents the determination of the OPTA, and the calculation of maximal TSR collected by tilted PV surfaces, both of which are highly important criteria affecting the efficiency of solar PV plants. Maximizing TSR gain on PV surfaces can be improved by setting the surfaces to the OPTA for the entire year or by installing solar trackers. Theoretically calculated results for the maximal TSR collected at annual tilted SFS and STS in the Mediterranean provinces are analyzed and presented in detail.

It is shown that the Mediterranean Region provinces have a large potential for solar plants. It is also found that Antalya is among the most advantageous provinces in terms of solar energy potential. Along with this study, the results provide technical inputs to guide the solar industry for planting cost-effective solar PV plants in the Mediterranean region of Türkiye. This study may also contribute to the sizing of solar PV plants for specified locations thanks to determining the OPTA based on maximizing the TSR on tilted PV surfaces. It is hoped that the values presented in this study will support the solar data in the literature and also investors, researchers, and solar engineers dealing with solar PV plants specifically any possible establishment in the Mediterranean Region.

In this study, a strong numerical method is proposed to estimate the TSR collected by SFS and STS by using GSR data depending on solar parameters such as location, clearness index, and declination in the Mediterranean region for specific periods. Low computing effort is required by the utilized RETScreen method. The proposed method can be used to figure out the amount of maximal TSR collected by surfaces and to determine the OPTA of surfaces at any time of the year for a specific geographic coordinate. This study can be beneficial in solar energy projects during the determination of accurate OPTA, the calculation of maximal TSR and the analysis of the performance of solar PV plants.

The results have revealed that the proposed method seems to be highly acceptable for calculating TSR and OPTA. It is found that the annual OPTA range of 29°-33° for south-facing PV surfaces and optimally tilted surfaces achieve between 9.34% and 12.91% more daily TSR gain compared to surfaces that are not tilted in the Mediterranean provinces. Under the same conditions, it is also found that a one-axis STS harvests between 28.49% and 33.10%, and a two-axis STS harvests between 32.42% and 37.13% more daily TSR gain in comparison to the SFS.

The cost of an STS should be analyzed and evaluated according to the location. The addition of PV surfaces to solar PV plants instead of installation costs for trackers can further increase power production yield. The results of this study are shown that one-axis STS is the best preference in terms of collecting more TSR when the cost-benefit balance is considered. It is highly advised to utilize a one-axis STS in solar PV plants in the provinces of the Mediterranean region because of the cost of installation and maintenance of two-axis STSs. If adjustment of the tilt angles of the PV surface is not possible, an annual OPTA can be utilized in PV surfaces in order to avoid the installation costs of STSs. The latitude-based approximate tilt angle used by solar PV plants cannot be suitable for all locations, depending on the geographical location of the world. It is understood that tilt calculations that do not rely on maximizing TSR intensity can only remain as an approximately estimations.

As a result of this study, it is found that tilting and tracking are significant factors to increase intensity of TSR at all latitudes, so that the proposed model can be implemented in any location of Türkiye and extended to any place in the world to obtain specific estimates with a little computational expense. Türkiye is among the leading countries in Europe in terms of GSR distribution. Therefore, this study can be extended further out to all provinces of the Anatolia region as a future work. The annual OPTAs of the provinces can be determined. In addition, the TSR efficiency of the provinces in Türkiye can be predicted for solar PV plants. Studies can be carried out to create a reference for investors and researchers by presenting Türkiye's OPTA and maximal TSR in a table.

6.3. Conclusions of Case Study (3): Investigation of Anisotropic Models in Estimating TSR Intensity on Solar PV Surfaces, A Case Study for the Southeastern of Türkiye

In light of the present investigation, the following conclusions are reached based on the comparative analysis of anisotropic transposition models to investigate solar potential and the estimation of TSR intensity on SFS and STS in the Şanlıurfa province, which is geolocated in the Southeastern Anatolia region of Türkiye.

The annual OPTA for a south-facing PV surface is determined to be 30°-31° in the Şanlıurfa province, the value of the OPTA is close to the latitude but lower than the latitude (6°-7°) of the relevant geolocation. The monthly OPTA values all through the year range from 3° in July to 64° in December. The seasonal OPTA values all year long are between the lowest value of 8° in summer and the highest value of 59° in winter.

It is found that the monthly TSR for an annual SFS is predicted between 100.4 kWh/m² (December) and 229.3 kWh/m² (July) throughout the year. It is also found that the HDKR model predicted the highest amount of TSR on an optimally tilted PV surface over the entire year conversely the Reindl model predicted the lowest value compared to all other investigated models. These values are 1,968.2 kWh/m² and 1,921.3 kWh/m², respectively. It is noticed that the variation of annual TSR values for a single axis tracker is predicted between 2,401.8 kWh/m² (Klucher) and 2,478.9 kWh/m² (HDKR), for a dual axis tracker between 2,596.7 kWh/m² (Klucher) and 2,698.6 kWh/m² (HDKR) entire the year. It is also found that the gain in annual TSR for an optimally SFS (30°) when compared to a horizontal surface (0°) is predicted between 6.06% (Hay-Davies) and 8.63% (HKDR). It is revealed that the gain in annual TSR for a single-axis tracker is predicted between 22.04% (Klucher) and 25.95% (HDKR) and, for a dual-axis tracker between 31.50% (Klucher) and 37.12% (HDKR) in the Şanlıurfa province.

Compared to a horizontal surface, the averages of results obtained from the investigated anisotropic models imply that monthly, seasonal, and annual OPTA adjustments of PV surfaces can yield 13.41%, 12.32%, and 7.44% extra energy, respectively. Once compared to the annual OPTA, monthly adjustments may generate an average of 6.37% extra energy, whereas seasonal adjustments can generate an average of 5.45% extra energy. Furthermore, there is a decline of approximately 1% in solar energy on a seasonally tilted surface compared to a monthly tilted surface. In addition, compared to an annually tilted surface, single-axis and dual-axis trackers may yield an average of 24.99% and 36.02% extra energy, respectively. It is inferred that the dual-axis STS can boost the harvested energy by 8.85% versus the single-axis STS for the Şanlıurfa province.

It is found that the loss in annual TSR does not vary more than 0.5% due to the 5° offset of tilt angle from the OPTA of the PV surfaces in the case of utilizing anisotropic models for Şanlıurfa This result is also expected to be valid for close latitude values in the world. The present investigation has shown that the Şanlıurfa province has a significant potential for solar energy availability. The results obviously indicate that Şanlıurfa has superior year-round access to horizontal TSR. This potential can be further increased by implementing annual optimal SFSs or STSs. The present research emphasizes that the TSR intensity on a tilted surface might be particularly improved by setting the tilt of a PV surface. Therefore, the annual OPTA can be utilized for PV surfaces where setting the OPTA is not possible monthly or seasonally. The improvement in the gain of such solar investment helps to lower the time of recovery. The results confirm that STS is needed to optimize PV surfaces and increase TSR intensity. This inference is consistent with similar studies in literature. When possible, the PV surface should be installed with trackers for better utilization of solar energy. However, since solar trackers are not always economical, a separate cost-benefit analysis should also be done before taking any action.

The present study demonstrates that the anisotropic transposition models involve some solar parameters, and there are differences in the integration of these parameters in the models. The precision of these parameters has an impact on the models' performance and the reliability of the outputs. It is understood that the predicted OPTA values should be considered as an initial part of the effective implementation of a PV plant. The presented anisotropic transposition models can be safely and successfully utilized for estimating TSR intensity on tilted and tracked PV surfaces in any province of Türkiye, as well as other latitudes around the world.

In this study, it is pointed out that the values of variabilities in outputs and disagreements between the models are in a relative cross-comparison rather than identifying the best model. It is understood that for a more robust estimation of TSR intensity on tilted and tracked surfaces, different anisotropic models should be tested and validated for the location of interest. It is also discussed that the latitude-based general rules available in the literature may not give accurate results since the rules do not consider the solar climatic parameters that affect TSR yields on PV plants.

This study demonstrated the high potential of the utilized models to provide reliable data to be used in optimum engineering design, eco-energetic analysis, and implementation processes in the absence of measured GSR data. So, it is expected that the findings of this study will be beneficial for solar PV investors and researchers to determine the most effective system installation and transposition models for estimation of TSR intensity, respectively.

6.4. Conclusions of Case Study (4): Maximization of Solar Radiation on Fixed and Tracking Surfaces in Antalya Province of Türkiye Based on Levelized Cost of Energy

This study contributes in-depth to determining the OPTA of the PV surfaces and measuring TSR intensity on the tilted surface monthly, seasonal, and annually in Antalya districts within the proposed calculation model. The study also highly contributes to the estimation of TSR values collected by the surfaces in case using STSs for evaluating the existence of solar potential in Antalya districts.

The daily TSR values are calculated using the proposed model by changing the tilt of the south-oriented surface with steps between 0° and 90°. It is observed that the OPTAs during the year are varied between 0° and 61°. The annual OPTA is determined to be between 28° and 30° for a south-facing PV surface throughout the year. So, it has been determined that there is a ±1 or ±2 OPTA difference between the four districts.

The daily TSR values are predicted between 2.70kWh/m² and 7.42kWh/m² in case of TSR reaches the PV surface with the optimal annual OPTA in the districts. The maximal total TSR values are predicted 2,194.66kWh/m² for monthly, 2,173.28kWh/m² for seasonal, 2,082.50kWh/m² for annual respectively with applying the OPTAs. The maximal TSR values are predicted 326.12kWh/m² for the one-axis, and 340.69kWh/m² for the two-axis respectively. It is calculated that PV surfaces adjusted at OPTA achieve between 8.23% and 10.63% more TSR annually compared to surfaces that are not angled at all for the SFS. It is also calculated that one-axis STSs harvest between 28.72% and 33.17% higher TSR, two-axis STSs harvest between 32.19% and 37.49% higher TSR than SFSs in districts of Antalya.

For the districts of Antalya, it is calculated that the monthly optimal tilt setting contributes between 4.87 and 5.28% TSR gain compared to an annual SFS. It is also calculated that a seasonal setting contributes between 3.80 and 4.32% TSR gain compared to an annual SFS. These results demonstrate that monthly, seasonal, and annual positioning of the PV surfaces at the OPTAs provides significant TSR efficiency. It is found that, under the same conditions, the STSs harvest great TSR efficiency compared to the SFSs.

It is understood that the period, latitude, climatic characteristics, and geographical location are the most important parameters affecting the OPTA and TSR efficiency. It is also seen that Antalya has a perfect location for the installation of solar PV plants. The proposed calculation method can be applied to specific locations in Turkiye where the importance of solar PV plants is constantly increasing. It is thought that this study can help solar engineers and designers to improve the efficiency of PV surfaces, properly set OPTAs, and choose the right methodology for installing solar PV plants in the districts of Antalya province.

When the findings of this study are compared to those of other studies in the literature, it is discovered that as consistent with the findings of similar studies. This study shows the importance of accurate OPTA and orientation. It is thought that the study can contribute to the solar data literature of Antalya province. The proposed calculation model can be implemented at any location in Türkiye and the world.

Recent research studies show that the solar energy cost and solar PV plant installation cost continued to decrease thanks to increased surface efficiency and decreased hardware costs globally. It is believed that LCOE based analysis presented in this study can guide engineers and investors to create solar PV plants and maximize financial returns by minimizing the costs in Antalya province. It is expected that solar energy will support the economy in countries with high energy tariffs and at the same time, high solar potential such as Türkiye since the solar energy cost is almost halved last 5-years. Because of the global reduction in large-scale one-axis solar PV plant costs for the last 2-years 12.74%, it is highly recommended to install one-axis tracker systems in terms of not only economic potential but also energy efficiency.

It is also shown that in Türkiye, most solar PV plants start generating a return on investment after 8-years comparing the 25 years lifespan, the new incentives, tax breaks, existing solar potential, and continued declines in installation costs reduced average payback periods to under 7-years today.

6.5. Conclusions of Case Study (5): Estimation of the Solar Radiation Intensity and OPTAs of PV Surfaces in the Central Anatolia Region of Türkiye Applying Transposition Models

The following conclusions have been drawn within the scope of this study.

Annual OPTA values for seven provinces Central Anatolia Region of Türkiye are predicted for SFSs. Transposition models are proposed to estimate the annual TSR intensity in seven provinces of the Central Anatolia Region of Türkiye. This study can be used as a guideline to set the OPTA values and total TSR intensity for the SFSs and STSs in Central Anatolia.

The annual OPTA values are predicted to be 29°–30° by applying the Liu-Jordan model and 33°–35° by applying the Perez model for the provinces of the Central Anatolia region. It has been determined that anisotropic components in the Perez model calculate OPTAs 3°-4° higher than the Liu-Jordan model. The average OPTA of the Central Anatolia region is determined as 30° (Liu-Jordan) and 34° (Perez). It is found that the OPTA values are below the latitude values of the investigated provinces. TSR intensity for the annual optimally tilted PV surface is calculated at 3.75% for Liu-Jordan and 8.72% for Perez transposition models on average compared to a horizontal surface.

The annual TSR intensity for the one-axis STS is calculated at 21.89% for Liu-Jordan and 26.27% for Perez transposition models compared to the SFS. It is also predicted that the annual TSR intensity for the two-axis STS is calculated at 31.68% for Liu-Jordan and 38.41% for Perez transposition models compared to the SFS. It has been found that an STS is more efficient than a SFS as expected. It is understood that highly possible that the generated solar energy in the Central Anatolia region can be significantly enhanced by installing the STS under the findings of this study.

The Perez model shows that by increasing the angulation by several degrees, more TSR can be collected, especially during winter months. This study reveals that some solar parameters involved in anisotropic models can contribute to the quality of the estimation results. The estimation differences between Liu-Jordan isotropic and Perez anisotropic transposition models are determined as 4.78% for a SFS, 8.55% for a one-axis STS, and 10.01% for a two-axis STS on average respectively.

It has been found that the geographic positions and climatic characteristics in Central Anatolia significantly affect the amount of TSR collected by the PV surfaces. It is believed that the comprehensive solar data presented in this study, including the TSR intensity and percentage gains, contributes to the literature. Thanks to the low computational cost, the transposition models presented in this study can be used to accurately estimate TSR intensity on PV plants for any geographical location in Türkiye and around the world.

6.6. Conclusions of Application Study (1): Analysis of Transportable Off-Grid Solar Power Production for Rural Electricity Supply: An Application Study of Şanlıurfa, Türkiye

In this study, a transportable isolated (off-grid) microgrid is developed based on PV energy production to meet electricity to serve in various fields by providing technical, regional, climatic, and cost analysis as well as numerical modeling for specifically Şanlıurfa region of Türkiye. So, this work proposes practical, effective, and reliable solutions that can be used for various applications for rural areas and humanitarian services. It is anticipated that this microgrid can be installed in refugee camps and rural areas with no electricity in the region, and the microgrid can be transported between the locations in line if needed.

The study is completed with 60.75kWp PV capacity, and 105.98kWh ES energy capacity for the Şanlıurfa province in Türkiye. Energy production efficiency, capacity, and sustainability of the region have been evaluated under climatic and regional conditions. Şanlıurfa has the highest solar potential in Southeastern Anatolia. It is confirmed that the energy production is extremely high during the summer months in the region. The daily energy not captured due to the ES limit is considerably high. So, the ES and the PV power capacity can also be increased in case of any need to resize the load capacity in the future.

A strong PV energy production system is developed with a minimal size of the battery to ensure production, transmission, distribution, and continuity of power. In order to provide energy flow regularly, to keep energy enough level, and to make a stable energy balance, the ES is optimized to provide a strong solution. A diesel generator is integrated into microgrid to balance the power and provide the startup power.

A considerable effort is also put into the system performance and dynamic behavior investigation of the microgrid by modeling DER and load flow on MATLAB/Simulink in a 24-hours scenario. The findings taken from the simulations show that the designed microgrid is reliable and stable.

In comparison to similar installations in industrialized countries, the payback period is found to be rather long, which shows that the cost of power system equipment like ES and PV module in the Türkiye is still at high levels. It is highly recommended that the next studies should investigate the possibility of establishing an isolated PV plant with a lower cost and larger capacity to decrease the payback period. Existing PV technologies should be analyzed and compared to determine the most suitable technology with a lower cost.

System performance results show that the annual energy production using a yearly OPTA is 39.83MWh. Considering the average life span of the system as 25 years, the total amount of energy to be produced is 995.75MW. In 29% of the year, the battery charge status remains over 90% while in 15% of the year battery charge rate fluctuates between 34% and 43%. It is calculated that monthly optimal tilted PV surfaces achieve 16.20% more TSR and annually optimal tilted PV surfaces achieve 10.18% more TSR compared to PV surfaces that are not angled. The payback period of the microgrid is calculated as 10.67 years.

It is also expected that this kind of study can contribute to increased energy security and sustainability in the region and facilitate the transportation and installation of such systems to the required regions. This study's data and findings can be used in similar applications and can shed light to future studies. It can also be served as a foundation study for off-grid PV installations in the region. The findings of the study can be considered an asset to support further studies and investigations in this region.

6.7. Conclusions of Experimental Study (1): Optimization of OPTA and TSR on PV Surfaces: An Experimental Study in Malatya Province of Türkiye

This implementation study investigates solar PV plant performances in Malatya of Turkey, by using yearlong recorded production data from the PV plant geolocation. The OPTA is predicted as 33° of the SFS PV system by applying HAY and PERZ transposition model which is below the latitude of the location. It is understood that the correlation is inverse between solar declination and energy gain, both in the actual and predicted data. In the study conducted with actual data, it has been determined that the accuracy of the satellite-based NASA-SSE monthly GSR data is quite high and that it can be used safely in solar plant projects.

It is seen that the HAY model makes more robust production predictions than the PEREZ model in all categories. On the other hand, reasonably small mismatches have been found between the theoretical predictions and the actual energy productions, which validates the proposed transposition models for prediction. It is well-proven that the TSR prediction models on PV surfaces are in good agreement with the field measurement. That is, the actual results confirm the trends of the transposition models in solar energy production estimations. Therefore, these validated transposition models in this implementation study can be securely applied to predict the performance of PV plants both one-axis STS, and annual tilted SFS with different OPTAs in different geolocations. So, this result shows a clear validation of the presented transposition models and the numerical predictions.

It has been observed in the geolocation that the reduction in actual production efficiency was sourced by climatic variations. The one-axis horizontal STS have produced PV electricity annual yield of 22.34% more than the SFS (average of 2021 and 2022 years). The annual electricity production during the same period was 19,916 kWh for one-axis horizontal STS, and 24,367 for SFS adjusted at OPTA, according to the average of the two years.

It is seen that the biggest deviation occurred in the one-axis production predictions in the PEREZ model with 5.18% (The average of 2 years is 4.46% in STS). The minimum deviation was 0.35% in the HAY model SFS production predictions. (The average of 2 years is 0.98% in SFS). In comparison with actual production data, it is seen that the prediction rates of the PEREZ model are generally higher than the HAY model in all categories. Additionally, it is seen that the HAY model makes more robust production predictions than the PEREZ model in all categories. Considering that the HAY model is the simplest and the PEREZ model is the most complex anisotropic model, it can be concluded that very simple models as well as more complex models may yield good results.

The annual energy loss for the implemented one-axis STS is estimated to be 13.89% on average, and for SFS it is estimated to be 14.00% on average. It is found that the increase in TSR intensity on one-axis horizontal STS is 0.63% in the case of the continued rotation from ±60° to ±90° (±30°). The increase in net PV electricity production is 1.36%.

It is expected that derived solar data provides an insight into identifying the geolocation and suitable technologies and methodologies for the deployment of solar PV plants in the Malatya province of Türkiye. This derived data is useful in assessing the operational benefits of solar PV plants based on their actual PV electricity production. The produced data and implementing experience of solar PV plants, both SFS and STS, can be applied to future solar-based projects. Therefore, this implementation study will not only provide invaluable information and tools for Turkish PV industries and researchers but also offer helpful prediction methodologies for PV implementations in other countries.

6.8. General Conclusions

In light of the present thesis covering the case, application and experimental studies, the following conclusions have been reached for Türkiye geolocations and provinces.

Solar energy production efficiency, capacity, and sustainability have been studied in Türkiye under climatic and regional conditions. It is clearly understood that the Türkiye provinces have a large solar potential, and Türkiye is among the leading countries in Europe in terms of GSR distribution and solar energy availability. It is revealed that from the conducted literature review, the studies on Türkiye's utilizing of its solar potential are not yet at a sufficient level. It is found that the topographic diversity and climatic characteristics in Türkiye significantly affect the of TSR intensity on the PV surfaces. It is also revealed that climate variation has a considerable impact to TSR intensity on PV surfaces, even over small distances or close latitude values in Türkiye. It is believed that the comprehensive and comparative findings of this thesis will contribute greatly to the solar data literature for all provinces of Türkiye.

The TSR intensity on PV surfaces is estimated for different geolocations in Türkiye based on transposition models, from the simplest one to the most complex one. So, empirical transposition models are applied to estimate the TSR on PV surfaces in 81 provinces and 7 geographical regions in Türkiye by utilizing GSR data. Considering the climatic parameters and geographical positions, an OPTA map for all provinces is created. It is found that the OPTAs of all provinces and regions are close to latitude but lower than the latitude values of Türkiye. The OPTAs for south-facing SFSs are found between 28º to 36º across the year. This thesis particularly can be used as a guideline to predict the annual OPTAs and TSR intensity for the SFSs across Türkiye.

The present thesis emphasizes that the TSR intensity can be particularly improved by setting the OPTA of a PV surface. Therefore, the annual OPTA can be adjusted for PV surfaces where setting the OPTA is not possible monthly or seasonally. It is understood that the determination of OPTA values should be considered as an initial part of the effective implementation of a solar PV plant.

It is understood that OPTA calculations that are not based on maximizing TSR intensity on PV surfaces can only remain as an approximately estimations. Therefore, the latitude-based approximate OPTA utilized by solar PV plants cannot be suitable for all geolocations of the world. Therefore, it is concluded that the latitude-based general rules available in the literature may not give accurate results since the rules do not consider the solar climatic parameters that affect TSR yields on solar PV plants. On the other hand, from the analysis of the effect of OPTA on TSR gain in Türkiye, it is well understood that the reduction in TSR intensity on the PV surface is not greater than 0.5% due to the 5° deviation of the tilt angle from the OPTA. This result is expected to be valid for close latitude values in the world. Therefore, this result, which may seem small but will lead to significant energy loss, should be taken into consideration, especially in large-scale PV plant configurations.

Most of the PV plant implementations have not been done with the STSs in Türkiye territories so far. Keeping that point in mind, it is discussed the benefits of STSs by theoretically and experimentally analyzing the possible PV plant implementations for the future in Türkiye. It is found that tilting and tracking of PV surfaces are significant affects to yield of TSR intensity of at all latitudes. It is seen that STSs are more efficient than the SFSs as expected. Results showed that STSs yield significant solar energy gains. Because of the global reduction in large-scale one-axis solar PV plant costs in recent years, it is strongly recommended to install one-axis tracker systems in terms of not only economic potential but also energy efficiency.

This thesis does not identify the best anisotropic model, but with a relative cross-comparison, it points out the values of high variability in outputs and disagreements between different models. The present thesis demonstrates that the transposition models involve some solar parameters, and there are differences in the integration of these parameters in the models. The precision of these parameters has an impact on the models' performance and the reliability of the outputs. So, this thesis reveals that solar parameters involved in anisotropic models can contribute to the quality of the estimation results. It is understood that multiple transposition models should be applied in the interested geolocation for a more robust estimation of TSR intensity on tilted and tracked surfaces. It is demonstrated that the utilized transposition models have high potential to be used in optimal engineering design, eco-energetic analysis, and implementation processes in the absence of measured GSR data.

It is well emphasized that the precision of the models strongly depends on the GSR input data. It is concluded that there is no model to be ranked as the best for all sets of GSR input data; very simple models as well as more complex models may yield good results. That is, no model can be safely and successfully declared to be the best for every collection of GSR input data; both extremely simple and more complex estimation models can produce good results. The proposed transposition models can be applied to accurately estimate TSR intensity on PV plants for any province or particular region in Türkiye and extended to any place in the world by using iterative algorithms, thanks to their low computational cost, where the significance of solar PV plants is constantly increasing.

It has been observed in geolocation that the reduction in actual production efficiency is sourced by climatic variations. It is found that, under the same conditions, the one-axis horizontal STS have produced PV electricity annual yield of 22.34% more than the SFS. It is understood from the actual and estimated data that the production of solar PV energy in Anatolia region can be significantly enhanced by installing the STS according to the results of this thesis. It is seen that the average 4.46% deviation occurred in the one-axis STS for PV production predictions in transposition models. The average deviation is 0.98% in the SFS for PV production predictions. The annual energy loss for the implemented one-axis STS is estimated to be 13.89% on average, and for SFS it is estimated to be 14.00% on average. It is found that the increase in TSR intensity on one-axis horizontal STS is 0.63% in the case of the continued rotation from ±60° to ±90° (±30°). The increase in net PV electricity production is 1.36%.

It is understood from the implementation studies that the correlation is inverse between solar declination and energy gain, both in the actual and predicted data. Conducted with actual (experimental) data, it is determined that the accuracy of the satellite-based NASA-SSE monthly GSR data is quite high and that it can be used safely in solar plant projects in Türkiye. On the other hand, reasonably small mismatches have been found between the theoretical predictions and the actual energy productions. It is well-proven that the TSR prediction models on PV surfaces are in good agreement with the field measurement which clearly validates the proposed transposition models and utilized solar data for PV production estimations. Therefore, these validated transposition models in this implementation study can be securely applied to predict the performance of PV plants both one-axis STS, and annual tilted SFS with different OPTAs in different geolocations.

The LCOE of an SFS and STS should be analyzed according to the specific geolocation. It is highly recommended that solar PV plants should be constructed with STSs for better utilization of solar energy. The addition of PV surfaces to solar PV plants instead of installation costs for SFS can further increase PV power production yield. Therefore, since STSs are not always economical, a separate LCOE analysis should also be performed. It is believed that the LCOE-based analysis presented in this thesis can guide engineers to create solar PV plants by maximizing financial returns and minimizing costs in Türkiye.

A considerable effort is also put into the system performance and dynamic behavior investigation of the solar PV plant by modeling DER and load flow on

MATLAB/Simulink in a 24-hours scenario to particularly improve of the system performance. It is anticipated that the designed transportable isolated (off-grid) microgrid will propose practical, effective, and reliable solutions that can be used for various applications in rural areas, refugee camps, and humanitarian services.

The findings of this thesis are compared with other studies in the literature and is found to be consistent with the findings of similar studies in terms the properly determination of OPTA, validation of transposition models, and accurately prediction of TSR intensity on PV surfaces.

It is expected that derived solar data will provide insight into identifying the suitable technologies and methodologies for the deployment of solar PV plants in Türkiye, and the derived data in this thesis will shed light on future assessments of the operational benefits of solar PV plants. It is also expected that this thesis will also be contributed for choosing the right methodologies and improve the energy security, sustainability and PV system performance. The produced data and implementing experience of solar PV plants, both SFS and STS, can be applied to future solar-based projects. Along with this thesis, the results provide technical inputs to guide the PV industry in planting cost-effective solar PV plants in Türkiye. Therefore, this thesis will not only provide invaluable solar data for investors and researchers but also offer helpful prediction methodologies and useful knowledge for solar PV plant implementations in other countries.

7. FUTURE WORKS

Experimental measurements and statistical processing should be conducted to pinpoint the discrepancies between the theoretically estimated values from different models. However, it can be emphasized that there is no transposition model largely better than another, whatever the statistical test chosen to determine the quality of the model (Notton et al. 2004). Therefore, it would be a more reasonable approach to analyze the accuracy of the anisotropic models by comparing them with actual (experimental) energy production results. In other words, In order to identify the most accurate models, a more realistic approach would be to compare the production results predicted by transposition models with the actual production results, determine the resulting deviations, and make more accurate analyzes accordingly. It is believed that the results obtained from the actual solar data will guide the determination of the disagreement between the produced and estimated values of the TSR. Thus, in the future study, the experimental data of monthly TSR will be measured in Gaziantep province, and the transposition models presented in this study will be analyzed along with the actual data indicators. The long-term and short-term performances of the transposition models, the linear relationship between the obtained and estimated TSR values, absolute percentage deviations, and overall accuracy of the estimated TSR values will be assessed. In this respect, a one-axis solar horizontal STS with a capacity of 6.3 kWp has been installed at Gaziantep University in Türkiye to obtain experimental data for further studies. This STS contains ES and developed web monitoring. An overview of the designed STS and its core components is shown in Figure 5.37. Another point is that the STS is installed not only for the purpose of collecting experimental data but also for the electricity generation and transmission of the innovation center of Gaziantep University. Therefore, GSR inputs, TSR outputs, electrical power outputs, and produced PV energy will be measured continuously for the whole year by using an installed STS. This understructure will allow the analysis of the deviation between theoretically estimated and experimentally measured TSR intensity under the solar climatic conditions of Gaziantep province.

a) b) c)

Figure 7.1. The one-axis solar tracking system is implemented at Gaziantep University of Turkiye.

a) Solar PV modules, b) Tracking engine and electronics components, c) Transmission, distribution, and monitoring system

REFERENCES

Abdallah, R., Juaidi, A., Abdel-Fattah, S., & Manzano-Agugliaro, F., Estimating the optimum tilt angles for south-facing surfaces in Palestine. *Energies, 13*(3), 1-29. https://doi.org/10.3390/en13030623

Abdallah, S., & Nijmeh, S. (2004). Two-Axes Sun STS with PLC Control. *Energy Conversion and Man., 45*(11-12), 1931-1939. https://doi.org/10.1016/j.enconman.2003.10.007

Abdulsalam, H. S., & Alibaba, H. Z. (2019). Optimum tilt angle for photovoltaic surfaces in Famagusta, Cyprus. *International Journal of Social Science and Humanities Research, 7*(1), 29-35.

Abdulwahab, S. M., Nassar, Y. F., El-Khozondar, H. J., Khaleel, M., Ahmed, A. A., & Alsharif, A. (2023). Meeting solar energy demands: significance of transposition models for solar irradiance. *International Journal of Electrical Engineering and Sustainability, 1*(3), 90-105.

Acakpovi, A., Asabere, N. Y., & Sunny, D. B. (2015). Low-Cost Two-Axis Automatic Solar Tracking System. Communications on Applied Electronics, 3(8), 46-53. https://doi.org/10.5120/cae2015652015

Acar, A., Sarı, A. C., & Taranto, Y. (2020). Rooftop solar energy potential in buildings, financing models and policies for the deployment of rooftop solar PV energy systems in Türkiye. *SHURA Energy Transition Center,* 1-57.

Afgan, N. H., & Carvalho, M. G. (2008). Sustainability Assessment of a Hybrid PV energy system. *International Journal of Hydrogen Energy, 29*(3). 2903-2910. https://doi.org/10.1016/j.ijhydene.2004.01.005

Agbo, E. P., Nkajoe, U., Okono, M. A., Inyang, E. P., & Edet, C. O. (2023). Temperature and solar radiation interactions in all six zones of Nigeria. *Indian Journal of Physics, 97*(1), 655-669. https://doi.org/10.1007/s12648-022-02429-6

Ağbulut, Ü., Gürel, A. E., & Biçen, Y. (2021). Prediction of Daily GSR Using Different Machine Learning Algorithms: Evaluation and Comparison. *Renewable and Sustainable Energy Reviews, 135(1), ID:110114,* 1-14.

Aghajani, G., & Ghadimi, N. (2018). Multi-objective Energy Management in a Microgrid. *Elsevier Energy,* *4*(1), 218-225. https://doi.org/10.1016/j.egyr.2017.10.002

Aghamohammadi, A., & Foulaadvand, M. E. (2023). Efficiency comparison between tracking and optimally fixed flat solar collectors. *Scientific Reports 13*(1), ID: 12712. https://doi.org/10.1038/s41598-023-39892-y

Ahangharnejhad, R. H., Phillips, A. B., Song, Z., & Celik, I. (2022). Impact of Lifetime on the Levelized Cost of Electricity from Perovskite Single Junction and Tandem Solar Cells. *Royal Society of Chemistry,* *6*(1), 2718-2726. https://doi.org/10.1039/D2SE00029F

Ahwidea, F., Spenab, A., & El-Kafrawyc, A. (2013). Correlation for the Average Daily Diffuse Fraction with Clearness Index and Estimation of Beam Solar Radiation and Possible Sunshine Hours Fraction in Sabha, Ghdames and Tripoli – Libya. *APCBEE Procedia, 5*(1), 208-220. https://doi.org/10.1016/j.apcbee.2013.05.037

Ajder, A., & Durusu, I. (2018). Nakir, Impact of climatic conditions on PV array's optimum tilt angle. *European Journal of Science and Technology, 13*(1), 84-90. https://doi.org/10.31590/ejosat.418559

Akgül, B. A., & Özyazici, M. S. (2022). Obtaining Maximum Radiation by Determining Optimum Tilt Angles in Large-Scale Grid-Connected PV Plants, Efficiency Analysis of STSs: A Case Study for Şanlıurfa, Türkiye. *ISER International Conference, 1*(1), 21-24. Los Angeles, USA.

Akgül, B. A., & Yeğingil, İ. (2021). Design and Modeling an Off-Grid Photovoltaic System to Meet the Electrical Energy Requirement of a House in Gaziantep Region, Performing Technical Analysis and Basic Simulation. Euroasia Journal, 8(14), 145-159, https://doi.org/10.38065/euroasiaorg.456

Akgül, B. A., Alisinanoğlu F., & Özyazıcı, M. S. (2022). Optimization of Tilt Angle and Maximization of Solar Radiation for Fixed and Tracking Surfaces: A Case Study for Gaziantep, Türkiye. *Proceedings of the 2022 International Symposium on Energy Management and Sustainability*. 187-195. https://doi.org/10.1007/978-3-031-30171-1_21

Akgül, B. A., Alisinanoglu, F., & Ozyazici, M. S. (2022). Obtaining maximum radiation by determining optimum tilt angles in large-scale grid-connected PV plants, efficiency analysis of STSs: a case study for Şanlıurfa, Türkiye. *Int. Journal of Industrial Electronics and Electrical Engineering, 10*(7), 25-28.

Akgül, B. A., Alisinanoglu, F., Ozyazici, S., Hasoglu, M. F., & Haznedar, B. (2023). Analysis of transportable off-grid solar power production for rural electricity supply: an application study of Şanlıurfa, Türkiye. *Pamukkale University Journal of Engineering Sciences, 29*(5), 458-467. https://doi.org/10.5505/pajes.2022.87894

Akgül, B. A., Alisinanoğlu. F., Hasoğlu, M. F., & Özyazıcı, M. S. (2022). Maximization of Solar Radiation for Fixed and Tracking Surfaces in Antalya Province of Türkiye. *TEHNIČKI GLASNIK, 17*(3), 47-58. https://doi.org/10.31803/tg-20220426082153

Akgül, B. A., Ozyazici, M. S. & Hasoglu, M. F. (2024). Estimation of OPTAs and solar radiation collected by fixed and tracking PV surfaces for the Mediterranean region Türkiye Indian Journal of Physical, 98(1), 1187-1200. https://doi.org/10.1007/s12648-023-02894-7

Akgül, B. A., Ozyazici, M. S., Hasoglu, M. F., & Haznedar, B. (2024). Investigation and determination of OPTAs and solar radiation gains for fixed and tracked south-facing solar photovoltaic surfaces in provinces of Türkiye. Environmental Modeling & Assessment, 29(1), 101-123. https://doi.org/10.1007/s10666-023-09933-x

Akinyele, D. O. (2017). Environmental Performance Evaluation of a Grid-Independent Solar Photovoltaic Power Production (SPPG) Plant. *Energy, 130*(1), 515-529. https://doi.org/10.1016/j.energy.2017.04.126

Akkılıç, K., Ocak, Y. S., & Yılmaz, M. (2015). Analysing Enhancement of Electricity Generating Capacity with STS of the Most Sunning Region of Türkiye. *International Journal of Clean Energy Technologies, 3*(4), 291-295. https://doi.org/10.7763/JOCET.2015.V3.211

Aksoy, M. H., İspir, M., & Yesil, E. (2023). Impact of tilt angle on the performance of the photovoltaic systems for different row spacing. *Journal of Polytechnic, 26*(4), 1573-1585. https://doi.org/10.2339/politeknik.1260228

Aksungur, S., & Koca, T. (2018). Solar tracking system with PID control of solar energy panels using servo motor. *International Journal of Energy Applications and Technologies, 5*(3), 127-130. https://doi.org/10.31593/ijeat.450834

Aktacir, M. N., Yildirim, E., Isiker, Y. (2020). A Detailed analysis of daily, seasonal, and yearly performance values of photovoltaic modules using a simplified method. *European Mechanical Science, 4*(4), 142-151. https://doi.org/10.26701/ems.763303

Akyürek, Z., Akyüz, A. Ö., & Güngör, A. (2019). Optimizing the Tilt Angle of PV Surfaces to Reduce Carbon Footprint: Case for the West Mediterranean Region of Türkiye. *Int. Journal of Engineering, Design, and Technology, 1*(1), 10-15.

Al-Karaghouli, A., & Kazmerski, L. L. (2010). Optimization and Life-Cycle Cost of Health Clinic PV plant for a Rural Area in Southern Iraq Using HOMER. *Solar Energy, 84*(4), 710-714, https://doi.org/10.1016/j.solener.2010.01.024

Al-Naima, F. M., Ali, S. R., & Abid, A. J. (2013). Solar Tracking System Design based on GPS and Astronomical Equations. *International Journal of Information Technology and Web Engineering, 9*(1), 1-19. https://doi.org/10.4018/ijitwe.2014010102

Al-Rawahi N. Z., & Al-Azri, N. Z. (2019). Effect of latitude and sky clearance factor on the effectiveness of solar tracking strategies. Cogent Engineering, 6(1), 1-16. https://doi.org/10.1080/23311916.2019.1609387

Alawadhi, W., & Phelan, E. P. (2022). Review of residential air conditioning systems operating under high ambient temperatures. *Energies, 15*(8), 1-46. https://doi.org/10.3390/en15082880

Alberto, A. D. B., & Simao, A. (2013). Iterative Minimization of Partial Finite State Machines. *Central European Journal of Computer Science, 3*(2), 91-103. https://doi.org/10.2478/s13537-013-0106-0

Alboteanu, I. L., Bulucea, C. A, & Degeratu, S. (2015). Estimating Solar Irradiation Absorbed by Photovoltaic Surfaces with Low Concentration Located in Craiova. *Romania. Sustainability, 7*(3), 2644-2661. https://doi.org/10.3390/su7032644

Alboteanu, I. L., Bulucea, C. A., Bulucea, C. A., & Degeratu, D. (2017). Determining the solar radiation absorbed by the photovoltaic surfaces located in Craiova province, Romania, to estimate optimal energy production. *Int. Journal of Energy and Environment, 11*(1), 153-159.

Alfa Solar Energy Türkiye, 72 Cell Polycrystalline 330Wp PV Module, A3S72P. https://www.alfasolarenerji.com/

Alkaff, S. A., Shamdasania, N. H., Go, Y. L., & Venkiteswaran, V. K. (2019). A Study on the implementation of PV tracking for sites proximate and away from the Equator. *Integration and Optimization Sustainability, 3*(1), 375-382. https://doi.org/10.1007/s41660-019-00086-7

Alsadi, S. Y., & Nassar, Y. F. (2017). Estimation of Solar Irradiance on Solar Fields: An Analytical Approach and Experimental Results. *IEEE Transactions on Sustainable Energy, 8*(4), 1601-1608. https://doi.org/10.1109/TSTE.2017.2697913

Alsafadi, M., & Başaran Filik, Ü. (2020). Hourly GSR Estimation Based on Machine Learning Methods in Eskişehir. Eskisehir Technical Unv. *Journal of Science and Technology, A- Applied Sciences and Eng. (21)*2, 294-313. https://doi.org/10.18038/estubtda.650497

Amadi, H. N. (2018). Design and Performance Evaluation of a Dual-Axis Solar Tracking System for Rural Applications. *Journal of Electrical & Electronic Systems, 7*(4), 1-5. https://doi.org/10.4172/2332-0796.1000275

Ambient Conditions: A Case Study for Burdur, Türkiye. *Journal of Solar Energy Engineering, 139*(4), 1-32. https://doi.org/10.1115/1.4036412

Anoune, K., Bouya, M., & Abdellah, A. B. (2015). New Design and Architecture of a Smart Tracker: Flexible and Scalable for PV and CSP Systems. *Journal of Energy and Power Engineering 9*(1), 252-258. https://doi.org/10.17265/1934-8975/2015.03.003

ANSI/ASHRAE Standard. (2021). Climatic Data for Building Design Standards. *American Society of Heating, Refrigerating, and Air-Conditioning Engineers, 169*(1), Atlanta GA USA, https://www.ashrae.org/

Arçelik, A. Ş. (2022). Arçelik 144HC-450W PV surface. https://www.arcelikkurumsalcozumler.com/solar-surface/

Arıkan, O., İşen, E., & Kekezoğlu, B. (2019). Performance analysis of stand-alone hybrid (wind-photovoltaic) PV energy system. *Pamukkale University Journal of Engineering Sciences, 25*(5), 571-576. https://doi.org/10.5505/pajes.2018.98958

Armstrong, S., & Hurley, W. G. (2010). A new methodology to optimize solar energy extraction under cloudy conditions. *Renewable Energy, 35(4)*, 780-787. https://doi.org/10.1016/j.renene.2009.10.018

Arslan, G., & Bayhan, B. (2016). Solar Energy Potential in Mersin and a Smile Model to Predict Daily Solar Radiation. *Mugla Journal of Science and Technology, 1*(1), 1-4.

Arslan, G., Bayhan, B., & Yaman, K. (2019). Estimation of Measured GSR by Artificial Neural Networks for Mersin / Türkiye and Comparison with Common Solar Radiation Models. *Gazi Unv. Journal of Science Part C: Design and Technology, 7*(1), 80-96. https://doi.org/10.29109/gujsc.419473

Arslanoglu, N. (2016). Empirical modeling of solar radiation exergy for Türkiye, Applied Thermal Engineering, 108(2016), 1033-1040. http://dx.doi.org/10.1016/j.applthermaleng.2016.08.002

Arslanoglu, N. (2016). Optimization of Tilt Angle for Solar Collectors: A Case Study for Bursa, Türkiye. *International Journal of Energy and Power Engineering,* 10(5), 590-593.

Ayaz, R., Durusu, A., & AKCA, H. (2017). Determination of Optimum Tilt Angle for Different Photovoltaic Technologies Considering Ambient Conditions: A Case Study for Burdur, Türkiye. *Journal of Solar Energy Engineering, 139*(4), 139-145. https://doi.org/10.1115/1.4036412

Aydemir, E.,& Toslak, F. (2019). Efficiency Comparison of The Fixed Axis System with Double Axis Movement STS. *4th Eurasian Conference on Civil and Environmental Engineering,* 170-1174.

Ayvazogluyuksel, O., & Filik, U. B. (2017). Estimation of monthly average hourly GSR from the daily value in Canakkale Türkiye. *Clean Energy Technologies, 5*(5), 389-393. https://doi.org/10.18178/jocet.2017.5.5.403

Badescu, V. (2002). 3-D isotropic approximation for solar diffuse irradiance on tilted surfaces. *Renewable Energy 26*(2), 221-223. https://doi.org/10.1016/S0960-1481(01)00123-9

Badescu, V., Gueymard, C. A., Cheval, S., Oprea, C., Baciu, M., & Dumitrescu, A. (2012). Computing global and diffuse solar hourly radiation on a clear sky. Review and testing of 54 models. *Renewable and Sustainable Energy Reviews, 16*(3), 1636-1656, https://doi.org/10.1016/j.rser.2011.12.010

Bahrami, A., Okoye, C. O., & Atikol, U. (2016). The effect of latitude on the performance of different solar trackers in Europe and Africa. *International Journal of Applied Energy, 177*(C), 896–906. https://doi.org/10.1016/J.APENERGY.2016.05.103

Bahramia, A., Okoye, C. O., & Atikol, U. (2017). Technical and Economic Assessment of Fixed, Single and Dual-Axis Tracking PV Surfaces in Low Latitude Countries. *Renewable Energy, 113*(1), 563-579. https://doi.org/10.1016/j.renene.2017.05.095

Bakirci, K. (2012). General models for optimum tilt angles of PV surfaces: Türkiye case study. *Renewable and Sustainable Energy Reviews, 16*(8), 6149-6159. http://dx.doi.org/10.1016/j.rser.2012.07.009

Bakırcı, K. (2006). Variation of Optimum Collector Inclination Angle According to Months. *Journal of Engineer and Machine, 47*(562), 26-30.

Bakırcı, K. (2017). Investigation of Solar Energy Potential to Inclined Surfaces. Env. Progress & Sustainable Energy, 37(1), 524-532. https://doi.org/10.1002/ep.12680

Bakırcı, K., & Kaltakkıran, G. (2018). Determination of Tilt Angles of PV surfaces: A Study on Gaziantep. *3rd International Energy & Eng. Congress Proceedings Book,* 393-401.

Balabel, A., Mahfouz, A. A., & Salem, F. A. (2013). Design and Performance of Solar Tracking Photo-Voltaic System; Research and Education. *International Journal of Control Automation Systems, 1*(2), 49-55.

Balli, O., Aras, H., Aras, N., & Hepbasli, A. (2007). Estimating and Statistically Analyzing the GSR Potential Over Big Cities in Türkiye. *Energy Exploration & Exploitation, 25*(4), 301-311. https://doi.org/10.1260/014459807783129895

Balo, F. (2018). Investigation of solar energy potential for Çanakkale province with data analysis model. *DUMF Journal of Engineering, 9* (1), 143-152.

Banguero, E., Arias, H. D. A., Cardona, A. J. A., & Barragánd, D. H. O. (2019). Renewable microgrid operational results and economic evaluation using RETScreen.

International Journal of Electrical and Computer Engineering, 9(2), 723-731. https://doi.org/10.11591/ijece.v9i2.pp723-731

Bawazir, R. O., Chakchak, J., Çetin, N. S., & Ulgen, K. (2016). Investigating the Optimum Tilt Angle for Solar Receiver in Izmir. *3rd Int. Symposium on Env. and Morality*, 809-817.

Benchrifa, M., Tadili, R., Idrissi, A., Essalhi, H., & Mechaqrane, A. (2021). Development of New Models for the Estimation of Hourly Components of Solar Radiation: Te STS, Comparisons, and Application for the Production of a Solar Database in Morocco. *International Journal of Photoenergy, ID 8897818,* 1-16.

Benghanem, M. (2011). Optimization of Tilt Angle for PV surface: A Case Study for Madinah, Saudi Arabia. *Applied Energy, 88*(4), 1427-1433. https://doi.org/10.1016/j.apenergy.2010.10.001

Berisha, X., Zeqiri, A., & Meha, D. (2018). Determining the optimum tilt angles to maximize the incident solar radiation - case of study Pristina. *Journal of Renewable Energy Development, 7*(2), 123-130. https://doi.org/10.14710/ijred.7.2.123-130

Beyazit, N. I., Unal, F., & Bulut, H. (2020). Modeling of the Horizontal Solar Diffuse Radiation in Şanlıurfa, Türkiye. *Thermal Science, 24*(2A), 939-950. https://doi.org/10.2298/TSCI190223274B

Beyazit, N. I., Unal, F., & Bulut, H. (2020). Modeling of the hourly horizontal solar diffuse radiation in Şanlıurfa, Türkiye. *THERMAL SCIENCE, 24(2A),* 939-950.

Beyazit, N., Bulut, H., & Demirtaş, Y. (2017) Analysis of Diffuse Radiation Models for Horizontal Surface According to Measurement Results. *Journal of Polytechnic, 20*(3), 557-563.

Bilen, K., Ozyurt O., Bakırcı, K., Karslı S., Erdogan, S., & Yılmaz, M. (2008). Energy production, consumption, and environmental pollution for sustainable development: a case study in Türkiye. *Renewable Sustain Energy 12*(6), 1529-1561, https://doi.org/10.1016/j.rser.2007.03.003

Bilgili, M. E. & Dağtekin, M. (2017). Determination of appropriate slope angle and yearly energy difference in electricity production with photovoltaic battery. *Gaziosmanpasa Journal of Scientific Research, 6*(SI), 156-167.

Bingöl, O., Altıntaş, A., & Öner, Y. (2006). Microcontroller Based Solar Tracking System and Its Implementation. *Pamukkale University, Journal of Engineering Science, 12*(2), 243-248.

Blanco-Muriel, M. (2001). Computing the Solar Vector. *Solar Energy, 70*(5), 431-441. https://doi.org/10.1016/S0038-092X(00)00156-0

Braun, J. E. &b Mitchell, J. C. (1983). Solar geometry for fixed and tracking surfaces. *Solar Energy, 31*(5), 439-444. https://doi.org/10.1016/0038-092X(83)90046-4

Breyer, C., & Schmid, J. (2010). Population Density and Area Weighted Solar Irradiation: Global Overview on Solar Resource Conditions for Fixed Tilted, One-Axis and Two-Axes PV Plants. *25th PVSEC,* 4692-4709. https://doi.org/10.4229/25thEUPVSEC2010-4BV.1.91

Breyer, C., Bogdanov, D., Gulagi, A., Aghahosseini, A., Barbosa, L., Koskinen, O., Barasa, M., Caldera, U., Afanasyeva, S., Child, M., Farfan, J., & Vainikka, P. (2017). On the Role of Solar Photovoltaics in Global Energy Transition Scenarios. *Progress in Photovoltaics, 25*(8), 727-745. https://doi.org/10.1002/pip.2885

Brisha, A. M. (2019). Enhancement of Power Generation for PV Systems Using Dynamic Tracking System. International Journal of Electrical Components and Energy Conversion. 5(1), 1-9. https://doi.org/10.11648/j.ijecec.20190501.11

Brownson, J. R. S., (2014). Solar Energy Conversion Systems. *1st Edition, Academic Press*, Boston, USA.

Bugler, J. (1977). The determination of hourly insolation on an inclined plane using a diffuse irradiance model based on hourly measured global horizontal insolation. *Solar Energy, 19*(5), 477-491, https://doi.org/10.1016/0038-092X(77)90103-7

Bulut, H., Büyükalaca, O., & Yilmaz, A. (2009). Production of Typical Solar Radiation Year for Mediterranean Region of Türkiye. *International Journal of Green Energy, 6*(1), 173-183. https://10.1080/15435070902784970

Çağlar, A. (2017). Determination of Optimum Tilt Angle for Cities in Different Degree-Day Regions. Süleyman Demirel University. *Journal of Natural and Applied Sciences, 22*(2), 849-854. https://doi.org/10.19113/sdufbed.94899

Calabrò. E. (2013). An Algorithm to Determine the Optimum Tilt Angle of a PV surface from Global Horizontal Solar Radiation. *Journal of Renewable Energy, ID:307547,* 1-12. http://dx.doi.org/10.1155/2013/307547

Canada, S., Moore, L., Post, H., & Strachan, J. (2005). Operation and Maintenance Field Experience for Off-grid Residential Photovoltaic Systems. *Progress in PV Research and Applications, 13*(1), 67-74. https://doi.org/10.1002/pip.573

Cano, D., Monget, J. M., Albuisson, M., Guillard, H., Regas, N., & Wald, L. (1986). A method for the determination of GSR from meteorological satellite data. *Solar Energy, 37*(1), 31-39. https://doi.org/10.1016/0038-092X(86)90104-0

Caspary, G. (2009). Gauging the Future Competitiveness of Renewable Energy in Colombia. *Elsevier Energy, 31*(3). 445-450. https://doi.org/10.1016/j.eneco.2008.12.007

Çelik, A. N. (2006). Analysis of Ankara's Exposure to Solar Radiation: Evaluation of Distributional Parameters Using Long-Term Hourly Measured GSR Data. *TUBITAK Turkish J. Eng. Env. Sci. 30*(1), 115-126.

Cengiz, M. S., Mamiş, M. S., & Yurci, Y. (2016). Cost Comparison of Constant and Tracking System PV Panels with Stirling Motor-Operated Systems. *Bitlis Eren University Science & Technology Journal, 6*(1), 26-28. https://doi.org/10.17678/beujst.92728

Chandel, S. S. & Aggarwal, R. K. (2011). Estimation of Hourly Solar Radiation on Horizontal and Inclined Surfaces in Western Himalayas. *Smart Grid and Renewable Energy, 2*(1), 45-55. https://doi.org/10.4236/sgre.2011.21006

Chandel, S. S., Aggarwal, R. K., & Pandey, A. N. (2005). New correlation to estimate GSR on horizontal surfaces using sunshine hour and temperature data for Indian sites. *Journal of Solar Energy Engineering, 127*(1), 417-420, https://doi.org/10.1115/1.1877512

Chang, T. P. (2009). The Sun's Apparent Position and the Optimum Tilt Angle of a Solar Collector in the Northern Hemisphere. *International Journal of Solar Energy, 83*(8), 1274-1284, https://doi.org/10.1016/j.solener.2009.02.009

Chinnery, D. N. W. (1967). Solar water heating in South Africa. *CSIR Report, Council for Scientific and Industrial Research, 44*(1), 76.79.

Chowdhury, M. E. H., Khandakar, A., Hossain, B., & Abouhasera, R. (2019). A Low-Cost Closed-Loop Solar Tracking System Based on the Sun Position Algorithm. *Journal of Sensors, ID: 3681031,* 1-12. https://doi.org/10.1155/2019/3681031

Chudinzow, D., Klenk, M., & Eltrop, L. (2020). Impact of Field Design and Location on the Techno-Economic Performance of Fixed-Tilt and Single-Axis Tracked Bifacial Photovoltaic Power Plants. Solar Energy, 207(1), 564-578. https://doi.org/10.1016/j.solener.2020.06.096

Collares-Pereira, M. & Rabl, A. (1979). Average distribution of radiation correlations between diffuse and hemispherical insolation values. *Solar Energy, 22*(2), 155-164. https://doi.org/10.1016/0038-092X(79)90100-2

Cooper, P. I. (1969). The Absorption of Solar Radiation in Solar Stills. *Solar Energy, 12*(3), 333-346. https://doi.org/10.1016/0038-092X(69)90047-4

Cuong, D. M., & Ancheta, A. C. (2018). Energy Yields of a GPS-based Dual-Axis Solar Tracker and a Fixed Mount PV Panel Operating in Different Weather Conditions. *Journal of Science, Engineering, and Technology, 6*(1), 43-56.

Dağtekin, M., Kaya, D., Öztürk H. H., & Kiliç, F. Ç. (2014). A Study of Techno-Economic Feasibility Analysis of Solar Photovoltaic (PV) Power Gen. in the Province of Adana in Türkiye. *Energy Exploration & Exploitation, 32*(4), 719-735. https://doi.org/10.1260/0144-5987.32.4.719

Dal, A. R. (2021). Investigation of the Effect of Optimum Tilt Angle on Yield in Solar Energy Pane. *BSEU Journal of Science, 8*(1), 241-250. https://doi.org/10.35193/bseufbd.878795

Darhmaoui, H., & Lahjouji, D. (2013). Latitude-based model for tilt angle optimization for solar collectors in the Mediterranean region. *Energy Procedia, 42*(1), 426-435. https://doi.org/10.1016/j.egypro.2013.11.043

Daut, I., Irwanto, M., Irwan, Y. M., Gomesh, N., & Ahmad, N. S. (2011). Clear sky global solar irradiance on tilt angles of photovoltaic module in Perlis, Northern Malaysia. International Conference on Electrical, Control and Computer Engineering, 1(1), 445-450. https://doi.org/10.1109/INECCE.2011.5953923

Demain, C., Journée, M., Bertrand, C. (2017). Corrigendum to “Evaluation of different models to estimate the GSR on inclined surfaces. *Renewable Energy, 101*(1), 1401-1403. https://doi.org/10.1016/j.renene.2016.07.041

Dhimish, Mather, P., Holmes, V., & Sibley, M. (2019) CDF modeling for the optimum tilt and azimuth angle for PV installations: a case study based on 26 different locations in the region of the Yorkshire UK. *IET Renewable Power Production, 13*(3), 399-408, https://doi.org/10.1049/iet-rpg.2018.5301

Diken, B., & Kayişoğlu, B. (2022). Feasibility Study of Photovoltaic System that Can Be Applied to Tekirdağ Namık Kemal

Dincer, S. K., Kaymil (2017). Potential and utilization of wind and solar energy in Türkiye. *Journal of Engineering Research and Applied Science 6*(1) 599-604.

Dirlik, E. E., Gezegini C., & Mohammadi, S. A. D. (2023). Comparison of PVsyst, PVSOL, and HOMER Simulation Software Results with Real Production Data of Solar Power Plants in Different Provinces of Turkey. Journal of Engineering Research and Applied Science, 12 (2), 2357-2364.

Duffie, J. A., & Beckman, W. A. (2013). Solar Engineering of Thermal Processes. *Part I, Fundamentals 1, 4th Edition,* New York, Wiley and Sons, USA.

Duman, A. C., & Güler, Ö. (2020). Economic Analysis of Grid-Connected Residential Rooftop PV Plants in Türkiye. *Renewable Energy, 148*(1), 697-711. https://doi.org/10.1016/j.renene.2019.10.157

Dunlop, E., Halton, D., & Ossenbrink, H. (2005). 20 Years of Life and More: Where is the End of Life of a PV Module? *IEEE Xplore Photovoltaic Specialists Conference, 1*(1), 1593-1596. https://doi.org/10.1109/PVSC.2005.1488449

Đurić, M. B., & Đurišić, Z. R. (2005). Combined Fourier and Zero Crossing Technique for Frequency Measurement in Power Networks in the Presence of Harmonics. RE&PQJ, pp. 463-469. https://doi.org/10.24084/repqj03.330

Eke, R., & Şentürk, A. (2012). Comparison of a Double-Axis Sun-Tracking Versus Fixed PV Plant. *Solar Energy, 86*(1):2665-2672. https://doi.org/10.1016/j.solener.2012.06.006

Eke, R., Özden, S., Şentürk, A., Fleck, O., & Oktik, Ş. (2011). The Largest Double-Axis Sun Tracking PV plants with Electronic Control and Photosensors in Türkiye. *25th European Photovoltaic Solar Energy Conf. and Exhibition*, 4744-4747.

El-Borie, M. A., Thabet, A. A., El-Mallah, E. S., Abd El-Zaher, M., & Bishara, A. A. (2020). The response of the atmosphere to solar variations. *Indian Journal of Physics, 94*(1), 737-752. https://doi.org/10.1007/s12648-019-01502-x

El-Hammoumi, A., Motahhir, S., & El-Ghzizal, A. (2018). A simple and low-cost active dual-axis solar tracker. Energy Science & Engineering, 6(1), 607-620. https://doi.org/10.1002/ese3.236

El-Sebaii, A. A., Al-Hazmi, F. S., Al-Ghamdi, A. A. & Yaghmour, S. J. (2010). Global, direct, and diffuse solar radiation on horizontal and tilted surfaces in Jeddah, Saudi Arabia. *Applied Energy 87*(2), 568-576. https://doi.org/10.1016/j.apenergy.2009.06.032

Eldin, S. A. S., Abd-Elhady, M. S., & Kandil, H. A. (2016). Feasibility of STSs for PV surfaces in Hot and Cold Regions. *International Journal of Renewable Energy, 85*(1),228-233. https://doi.org/10.1016/j.renene.2015.06.051

Elhab, B. R., Sopian, K., Mat, S., Lim, C., Sulaiman, M. Y., Ruslan, M. H., & Saadatian, O. (2012). Optimizing tilt angles and orientations of PV surfaces for Kuala Lumpur, Malaysia. *Scientific Research and Essays, 7*(42), 3758-3765. https://doi.org/10.5897/SRE12.241

Elminir, H. K., Ghitas, A. E., El-Hussainy, F., Hamid, R., Beheary, M. M., & Abdel-Moneim, K. M. (2006). Optimum solar flat-plate collector slope: a case study for Helwan, Egypt. *Energy Convers Management, 47*(5), 624-637. https://doi.org/10.1016/j.enconman.2005.05.015

Emeksiz, C. (2020). The estimation of diffuse solar radiation on tilted surfaces using created new approaches with rational function modeling. *Indian Journal of Physics, 94*(1), 1311-1322. https://doi.org/10.1007/s12648-019-01573-w

Emikonel, S., & Bilhan, A. K. (2022). Analysis of Türkiye's solar energy potential in different regions. *OKU Journal of The Institute of Science and Technology, 5*(SI), 170-184, https://doi.org/10.47495/okufbed.1034175

Energy and Extractives Global Practice Group Europe and Central Asia Region. (2018). Türkiye: Rooftop Solar Market Assessment Summary Note. *World Bank Group ECA,* 1-14.

Energy Sector Management Assistance program. (2020). Global Photovoltaic Power Potential by Country. *ESMAP-World Bank,* 1-48.

Er, Z. (2018). Dual axis solar angle tracking system without any sensor. Journal of Energy Systems, 2(3), 130-139. https://doi.org/10.30521/jes.456606

Er, Z. & I.B. Turna, I. B. (2018). Solar radiation evaluation by t statistical analysis method for south and north regions of Türkiye. Arabian Journal of Geosciences, 11(1), 1-6. https://doi.org/10.1007/s12517-018-3603-6

Erbs, D. G., Klein, S. A., & Duffie, J. A. (1982). Estimation of the Diffuse Radiation Fraction for Hourly, Daily, and Monthly-Average Global Radiation. *Solar Energy, 28(4)*, 293-302. https://doi.org/10.1016/0038-092X(82)90302-4

Erdem, Z. B. (2010). The contribution of renewable resources in meeting Türkiye's energy-related challenges. *Renewable and Sustainable Energy Reviews, 14*(9), 2710-2722, http://dx.doi.org/10.1016/j.rser.2010.07.003

Ertekin, C., Evrendilek, & F., Kulcu, R. (2008). Modeling Spatio-Temporal Dynamics of Optimum Tilt Angles for Solar Collectors in Türkiye. *International Journal of Sensors, 8*(1), 2913-2931. https://doi.org/10.3390/s8052913

European Commission (2022). Photovoltaic Geographical Information System for Solar Photovoltaic Systems. https://ec.europa.eu/jrc/en/pvgis

Evans, D. L. (1981). Simplified Method for Predicting Photovoltaic Array Output. *Solar Energy, 27*(6), 555-560. https://doi.org/10.1016/0038-092X(81)90051-7

Evseev, E. G., & Kudish, A. I. (2009). Assessment of different models to predict the GSR on a surface tilted to the south. *Solar Energy 83*(1), 377-388, https://doi.org/10.1016/j.solener.2008.08.010

Faccio, M., Gamberi, M., Bortolini, M., & Nedaei, M. (2018). State-of-art review of the Optimization Methods to Design the Configuration of Hybrid Renewable PV energy systems. *Frontiers in Energy, 12*(1), 591-622. https://doi.org/10.1007/s11708-018-0567-x

Feng-Jiao, L., & Tian-Pau, C., Optimizing the tilt angle of solar collector under clear sky by particle swarm 0ptimization method. *Journal of Applied Science and Engineering, 18*(2), 167-172. https://doi.org/10.6180/jase.2015.18.2.09

Feuermann, D., & Zemel, A. (1992). Validation of Models for Global Irradiance on Inclined Planes. *Solar Energy, 48*(1), 59-66. https://doi.org/10.1016/0038-092X(92)90177-C

Filik, T., & Filik, Ü. B. (2017). Efficiency analysis of the Solar Tracking PV plants in Eskisehir Region. *Anadolu University Journal of Science and Technology A- Applied Sciences and Engineering, 18*(1), 209-217. https://doi.org/10.18038/aubtda.267116

Flora, A., Özenç, B., & Wynn, G. (2019). New Incentives Brighten Türkiye's Rooftop Solar Sector. *Institute for Energy Economics and Financial Analysis (IEEFA),* 1-11.

Franceschi, J., Rothkop, J., & Miller G. (2014). Off-grid solar PV power for Humanitarian Action: from Emergency Communications to Refugee Camp Microgrids, Humanitarian Technology: Science, Systems and Global Impact. *Procedia Engineering, 78*(1), 229-235, https://doi.org/10.1016/j.proeng.2014.07.061

Frydrychowicz-Jastrzebska, G., & Bugala, A. (2021). Solar Tracking System with New Hybrid Control in Energy Production Optimization from Photovoltaic Conversion for Polish Climatic Conditions. *Energies, 14*(1), 1-26. https://doi.org/10.3390/en14102938

Gabbar, H.A., El-Hendawi, M., El-Saady, & G., El-Nobi AI. (2016). Supervisory Controller for Power Management of AC/DC Microgrid. *IEEE Int. Conference on Smart Energy Grid Engineering, 1*(1), 147-152. https://doi.org/10.1109/SEGE.2016.7589516

Garg, H. P. (1982). Treatise on solar energy, fundamentals of solar energy. *John Wiley & Sons,* New York, USA.

Gebremedhen, Y. B. (2014). Determination of Optimum Fixed and Adjustable Tilt Angles for Solar Collectors by Using Typical Meteorological Year data for Türkiye. *International Journal of Renewable Energy Research, 4*(4), 924-928.

Geliş, K., Akyürek, E. F., & Yoladı, M. (2020). Effect Of Surface Position and Angle on Photovoltaic Surface Characteristics. *Journal of the Institute of Science and Tech., 10*(3), 1899-1908. https://doi.org/10.21597/jist.686478

Ghosh, H. R., Bhowmik, N. C., & Hussain, M. (2010). Determining seasonal optimum tilt angles, and solar radiations on variously oriented, single, and double-axis tracking surfaces at Dhaka. *Renewable Energy* *35*(6), 1292-1297. https://doi.org/10.1016/j.renene.2009.11.041

Gonul, O., Duman, A. C., Barutcu, & B., Guler, O. (2022). Techno-economic analysis of PV plants with manually adjustable tilt mechanisms. *Engineering Science and Technology, an International Journal,* *35*(1), 1-13. https://doi.org/10.1016/j.jestch.2022.101116

Gueymard, C. (1986). Mean daily averages of beam radiation received by tilted surfaces as affected by the atmosphere. *Solar Energy, 37*(4), 261-267. https://doi.org/10.1016/0038-092X(86)90043-5

Gueymard, C. (2000). Prediction and performance assessment of mean hourly global radiation. *Solar Energy, 68*(3), 285-303, https://doi.org/10.1016/S0038-092X(99)00070-5

Gümuş, B., & Kilic, H. (2018). Time-dependent prediction of monthly GSR and sunshine duration using an exponentially weighted moving average in southeastern Türkiye. *Thermal Science, 22*(2), 943-95., https://doi.org/10.2298/TSCI160107228K

Gündoğdu, K., Kabadayı, H. S. & Öztürk, A. (2016). Photovoltaic PV surfaces for You Follow A Simple And Economic System Design. *Duzce University Journal of Science and Technology, 4*(1), 634-639.

Gunerhan, H., & Hepbasli, A. (2007). Determination of the optimum tilt angle of solar collectors for building applications. *Building and Environment, 42*(2), 779-783. https://doi.org/10.1016/j.buildenv.2005.09.012

Gurlek, C., & Sahin, M. (2018). Estimation of the GSR with the Artificial Neural Networks for the Province of Sivas. *European Mechanical Science, 2*(2), 46-51. https://doi.org/10.26701/ems.359681

Hafez, A. Z., Solimana, A., El-Metwallya, K. A., & Ismaila, I. M. (2017). Tilt and azimuth angles in solar energy applications, A review. *Renewable and Sustainable Energy Reviews, 77*(1), 147-168. http://dx.doi.org/10.1016/j.rser.2017.03.131

Hafez, A. Z., Yousef, A. M., & Harag, N. M. (2018). STSs: Technologies and trackers drive types – A review. *Renewable and Sustainable Energy Reviews, 91*(1), 754-782. https://doi.org/10.1016/j.rser.2018.03.094

Hailu, H., & Fung, A. S. (2019). Optimum Tilt Angle and Orientation of Photovoltaic Thermal System for Application in Greater Toronto Area, Canada. *Sustainability, 11*(22), 1-21. https://doi.org/10.3390/su11226443

Hasan, R., & Abubakar, B. (2020). Intelligent Arduino-Based Automatic Solar Tracking System Using Light Dependent Resistors (LDRs) and Servo Motor. *Optics, 9*(2), 13-18. https://doi.org/10.11648/j.optics.20200902.11

Hay, J. E., & Davies, J. A. (1978). Calculations of the solar radiation incident on an inclined surface. *Proceedings of first Canadian solar radiation data workshop, Canadian Atmospheric Environment Service,* 59-72, April 17-19, Ontario, Canada.

Hay, J. E., & McKay, D. C. (1985). Estimating solar irradiance on inclined surfaces: a review and assessment of methodologies. *International Journal of Solar Energy, 3*(4-5), 203-240. https://doi.org/10.1080/01425918508914395

Heywood, H. (1971). Operating experiences with solar water heating. *Journal IHVE, 39*(1), 63-69.

Hofmann, M., & Seckmeyer, G. (2017). A new model for estimating the diffuse fraction of solar radiation for photovoltaic system simulations. *Energies, 10*(2), 1-21, https://doi.org/10.3390/en10020248

Hoque, M. E., Rashid, F., Shahriar, S., & Islam, M. K. (2018). An Automatic Solar Tracking System Using Programmable Logic Controller. *Int. Conference on Mechanical, Industrial and Energy Engineering,* 23-24 December, Bangladesh.

Hu, L., Shan, Z., Zhen-Biao, W., & Feng-Ju, G. (2010). A New Solar Tracking System of HCPV Based on Zigbee. International Conference on Computer and Electrical Engineering, 53(2), 1-6. https://doi.org/10.7763/IPCSIT.2012.V53.No.2.27

Hua, Z., Ma, C., Lian, J., Pang, X., & Yang, W. (2019). Optimum Capacity Allocation of Multiple Solar Trackers and Storage Capacity for Utility-Scale Photovoltaic Plants Considering Output Characteristics and Complementary Demand. *International Journal of Applied Energy*, *238*(1), 721-733. https://doi.org/10.1016/j.apenergy.2019.01.099

Igawa, N., Koga, Y., Matsuzawa, T., & Nakamura, H., Models of sky radiance distribution and sky luminance distribution. *Solar Energy, 77*(2), (2004) 137-157, https://doi.org/10.1016/j.solener.2004.04.016

Ihya, B., Mechaqrane, A., Tadili, R., & Bargach, M. N. (2014). OPTAs for solar collectors facing south at Fez province (Morocco). Journal of Natural Sciences Research 4(10), 120-127.

Ineichen, P. (2008). Comparison and validation of three global-to-beam irradiance models against ground measurements. Solar *Energy, 82*(1), 501-512. https://doi.org/10.1016/j.solener.2007.12.006

Ineichen, P. (2011). Global irradiance on tilted and oriented planes: model validations. *University of Geneva, 1*(1), 1-23.

International Finance Corporation. (2015). Utility-Scale Solar Photovoltaic Power Plants: A Project Developer's Guide. *IFC,* 1-206.

International Renewable Energy Agency. (2022). Renewable Power Production CoSTS in 2021. *IRENA,* 1-202

International Standard of Organization. (1987). 54Bases for design of structures, Actions due to the self-weight of structures, non-structural elements and stored materials. *ISO/TC 98/SC 3, 1*(1), 1-10.

Iqbal, M. (1979). Average Diffuse and Beam Radiation with Hours of Bright Sunshine. *Int. Journal of Solar Energy, 23*(2), 169-173. https://doi.org/10.1016/0038-092X(79)90118-X

Iqbal, M. (1980). Prediction of hourly diffuse solar radiation from measured hourly global radiation on a horizontal surface. Solar Energy, 24(5), 491-503. https://doi.org/10.1016/0038-092X(80)90317-5

Işık, S. K., & Çulun, P. (2023). Experimental Investigation of Photovoltaic Surface Performance in Bingöl Province for Different Parameters. *Turkish Journal of Nature and Science, 12*(2), 568-75. https://doi.org/10.46810/tdfd.1256109

Jacobson, M. Z., & Jadhav, V. (2018) World estimates of PV OPTAs and ratios of sunlight incident upon tilted and tracked PV surfaces relative to horizontal. *Solar Energy, 169(1)*, 55-66. https://doi.org/10.1016/j.solener.2018.04.030

Jafarkazemi, F. & Saadabadi, S. A. (2013). Optimum tilt angle and orientation of PV surfaces in Abu Dhabi, UAE. *Renewable Energy, 56*(1). 44-49, https://doi.org/10.1016/j.renene.2012.10.036

Jakhrani, A. Q., Othman, A., Rigit, A. R. H., Samo, S. R., & Kamboh, S. A. (2012). Estimation of Incident Solar Radiation on Tilted Surface by Different Empirical Models. *International Journal of Scientific and Research Publications, 2*(12), 1-6.

Jakhrani, A. Q., Samo, S. R., Rigit, A. R. H., & Shakeel, S. A. (2013). Selection of Models for Calculation of Incident Solar Radiation on Tilted Surfaces. *World Applied Sciences, 22*(9), 1334-1343. https://doi.org/10.5829/idosi.wasj.2013.22.09.316

Jamroen, C., Komkum, P., Kohsri, S., Himananto, Panupintu, S., & Unkat, S. (2020). A low-cost dual-axis solar tracking system based on digital logic design: Design and implementation. *Sustainable Energy Technologies and Assessments, 37*(1), 1-14. https://doi.org/10.1016/j.seta.2019.100618

Kaçan, E., & Ülgen, K. (2012). Effect of Collector Slope and Orientation on Solar Energy Utilization. *Journal of the Faculty of Eng. and Architecture of Gazi University, 27*(4), 837-846.

Kaçıra, M., Şimşek, M., Babür, Y., & Demirkol, S. (2004). Determining Optimum Tilt Angles and Orientations of PV surfaces in Şanlıurfa, Türkiye. *Renewable Energy, 29*(8), 1265-1275. https://doi.org/10.1016/j.renene.2003.12.014

Kaldellis, J., & Zafirakis, D. (2012). Experimental investigation of the optimum photovoltaic surfaces' tilt angle during the summer period. *Energy, 38*(1), 305-314. https://doi.org/10.1016/j.energy.2011.11.058

Kallioğlu, M. A., Durmuş, A., Karakaya, & H., Yılmaz, A. (2019). Empirical Calculation of the Optimum Tilt Angle for Solar Collectors in the Northern Hemisphere. *Journal of Energy Sources, Part A: Recovery and Environmental Effects, 42*(11), 1335-1358. https://doi.org/10.1080/15567036.2019.1663315

Kallioğlu, M. A., Durmuş, A., Karakaya, H., & Yılmaz, A. (2020). Empirical calculation of the OPTA for solar collectors in northern hemisphere. *Energy Sources Recovery Utilization and Environmental Effects, 42*(11), 1335-1358. https://doi.org/10.1080/15567036.2019.1663315

Kallioğlu, M. A., Ercan, U., Avcı, S. A., & Karakaya, H. (2017). Optimization of Tit Angle for PV surface. *2nd International Energy & Engineering Conference,* 180-186.

Kallioğlu, M. A., Genç, O., Ercan, U., & Karakaya, H. (2018). Creating the Optimum Surface Inclination Angles of the Southern Aegean Region. *International Journal of Advances in Science Engineering and Technology, 6*(2), 58-62.

Kamali, G. A., Moradi, I, & Khalili, A. (2006). Estimating solar radiation on tilted surfaces with various orientations: a study case in Karaj (Iran). *Theoretical and Applied Climatology, 84*(1), 235-241. https://doi.org/10.1007/s00704-005-0171-y

Kambezidis, H. D., & Psiloglou, B. E. (2021). Estimation of the optimum energy received by solar energy flat-plate convertors in Greece using typical meteorological years. *Part I: south-oriented tilt angles, Applied Sciences, 11*(4), 1-26. https://doi.org/10.3390/app11041547

Kamil, B., Varınca, M., & Gonüllü, T. (2006). A Study on Solar Energy Potential in Türkiye and Its Use Degree Method and Prevalence. *I. National Solar and Hydrogen Energy Congress,* 270-275.

Kapoor, M., & Garg, R. D. (2021). Evaluation of optimum PV tilt angle with generated and predicted solar electric data using geospatial open-source software in a cloud environment. *Sadhana, 46*(108). 1-14, https://doi.org/10.1007/s12046-021-01621-4

Karafil, A., Özbay H., Kesler, M., & Parmaksız, H. (2016). Calculation of Optimum Fixed Tilt Angle of PV surfaces Depending on Solar Angles and Comparison of the Results with Experimental Study Conducted in Bilecik, Türkiye. *9th Int. Conference on Electrical and Electronics Eng. IEEE Xplore*, 971-976. https://doi.org/10.1109/ELECO.2015.7394517

Karakaya, H., Avci, A. S., Ercan, U., & Kallioglu, M. A. (2019). Modeling of instantaneous GSR coming to the horizontal surface in Şanlıurfa province. *DUMF J. of Engineering, 10*(1), 147-155. https://doi.org/10.24012/dumf.430522

Karakaya, H., Kallioğlu, M. A., Durmuş, A., & Yılmaz, A. (2020). Empirical Calculation of the OPTA for Solar Collectors in the Northern Hemisphere. *Energy Sources, Part A: Recovery, Utilization, Env. Effects, 42*(11), 1335-1358. https://doi.org/10.1080/15567036.2019.1663315

KARJEN Karadeniz Generator. (2022). Diesel Generator Sets KJPT/16 Diesel Generator. https://karjen.com/

Kassem, K. O. (2020). TSR and Ideal Incline Angles of a South-Facing PV surface in Qena/Egypt. *Resources and Environment, 10*(1), 10-17. https://doi.org/10.5923/j.re.20201001.03

Kaygusuz, K. (2020). Calculation of Solar Radiation Data on Horizontal and Tilted Surfaces for Trabzon, Türkiye. *Journal of Engineering Research and Applied Science, 9*(2), 1471-1476.

Kaygusuz, K., & Sarı, A. (2003). Renewable Energy Potential and Utilization in Türkiye. *Energy Conversion and Management, 44*(3), 459-478. https://doi.org/10.1016/S0196-8904(02)00061-4

Kemery, B. P., Beausoleil-Morrison, I., & Rowlands, I. H. (2012). Optimal PV orientation and geographic dispersion: a study of 10 Canadian cities and 16 Ontario locations. *The Canadian Conference on Building Simulation, Halifax Nova Scotia,* May 1-4, 136-149.

Kentli, F. & Yılmaz, M. (2015). Mathematical Modelling of Two-axis Photovoltaic System with Improved Efficiency. *ELEKTRONIKA IR ELEKTROTECHNIKA, 21*(4), 1392-1215. https://dx.doi.org/10.5755/j01.eee.21.4.12780

Kentli, F., & Yilmaz, M. (2017). Improving the tracking efficiency of dual-axis sun STSs. *Energy Harvesting and Energy Efficiency Lecture Notes in Energy, 37*(1), 179–203. https://doi.org/10.1007/978-3-319-49875-1_7

Kern, J., & I. Harris, I. (1975). On the optimum tilt of a solar collector. *Solar Energy, 17*(2), 97-102. https://doi.org/10.1016/0038-092X(75)90064-X

Khahro, S. F., Tabbassum, K., Talpur, S., Alvi, M. B., Liao, X., & Dong, L. (2015). Evaluation of solar energy resources by establishing empirical models for diffuse solar radiation on a tilted surface and analysis for optimum tilt angle for a prospective location in the southern region of Sindh, Pakistan. *International Journal of Electrical Power & PV energy systems, 64*(1), 1073-1080. https://doi.org/10.1016/j.ijepes.2014.09.001

Khan, M. S., Ramli, M. A. M., Sindi, H. F., Houssem T. H., and Bouchekara, R. E. H. (2022). Estimation of Solar Radiation on a PV Surface with an OPTA Using Electric

Charged Particles Optimization. *Electronics,* 11(13), 1-29. https://doi.org/10.3390/electronics11132056

Khan, T. M. Y., Elahi, M., Soudagar, M., Kanchan, M., Afzal, A., Banapurmath, N. R., Akram, N., Mane, S. D., & Shahapurkar, K. (2020). Optimum location and influence of tilt angle on performance of solar PV surfaces. *Journal of Thermal Analysis and Calorimetry, 141*(1), 511-532.

Khoo, Y. S. & Nobre, A., Malhotra, R., & Yang, D. (2014). Optimal orientation and tilt angle for maximizing in-plane solar irradiation for PV applications in Singapore. *IEEE Journal of Photovoltaics, 4*(2), 647-653. https://doi.org/10.1109/JPHOTOV.2013.2292743

Khorramdel, H., Aghaei, J., Khorramdel, B., & Siano, P. (2016). Optimal Battery Sizing in Microgrids Using Probabilistic Unit Commitment. *IEEE Trans. Industrial Informatics, 12*(2), 35-845. https://doi.org/10.1109/TII.2015.2509424

Khosravi, A., Rodriguez, O. R. S., Talebjedi, B., Laukkanen, T., Pabon, J. J. G., & Assad, M. E. H. (2020). New correlations for determination of optimum slope angle of solar collectors. *Energy Engineering, 117(5),* 249-265. https://doi.org/10.32604/EE.2020.011024

Kırbaş, İ., Çifci, A., & İşyarlar, B. (2013). Sunbathing Rate and Solar Energy Potential of Burdur, Türkiye. Mehmet Akif Ersoy Unv. *Institute of Science and Technology, 4*(2), 20-23.

Kıvrak, S., Gündüzalp, M., & Dinçer, F. (2012). Theoretical and Experimental Performance Investigation of a Two-Axis Solar Tracker Under the Climatic Condition of Denizli, Türkiye. *Journal of Przeglad Elektrotechniczny (Electrical Review), 88* (2), 332-336.

Kıyak, E., & Göl, G. (2016). A comparison of fuzzy logic and PID controller for a single-axis solar tracking system. *Renewables, 3*(7), 1-14. https://doi.org/10.1186/s40807-016-0023-7

Klein, S. A. (1977). Calculation of monthly average insolation on the tilted surface. *Solar Energy, 19*(4), 325-329, https://doi.org/10.1016/0038-092X(77)90001-9

Klein, S. A., & Beckman, W. A. (1987). Loss-of-load Probabilities for Stand-Alone Photovoltaic Systems. *Solar Energy, 39*(6), 499-512. https://doi.org/10.1016/0038-092X(87)90057-0

Klein, S. A., & Theilacker, J. C. (1981). An Algorithm for Calculating Monthly-Average Radiation on Inclined Surfaces. *International Journal of Solar Energy Engineering, 103*(1), 29-33. https://doi.org/10.1115/1.3266201

Klucher, T. M. (1979). Evaluation of Models to Predict Insolation on Tilted Surfaces. *Int. Journal of Solar Energy, 23*(2), 111-114. https://doi.org/10.1016/0038-092X(79)90110-5

Koçer, A., Şevik, S., & Güngör, A. (2016). Determination of Solar Collector Optimum Tilt Angle for Ankara and Districts. *Uludağ Univ. Journal of Engineering Faculty, 21*(1), 63-78. https://doi.org/10.17482/uujfe.80088

Koçer, A., Yaka, I. F., Sardogan, G. T., & Gungor, A. (2015). Effects of Tilt Angle on Flat-Plate Solar Thermal Collector Systems. *British J. of Applied Science & Tech., 9*(1), 77-85. https://doi.org/10.9734/BJAST/2015/17576

Kok, M. V. (2015). Renewable energy sources: current perspectives and prospects in Türkiye. *Energy Sources, Part A: Recovery, Utilization, and Environmental Effects 37*(1) 1-10, http://dx.doi.org/10.1080/15567036.2014.947447

Kondili, E. (2010). Design and performance optimization of stand-alone and hybrid wind PV energy systems. *Stand-Alone and Hybrid Wind PV energy systems, 1*(1), 81-101. https://doi.org/10.1533/9781845699628.1.81

Koronakis, P. S. (1986). On the Choice of the Angle of Tilt for South-Facing Solar Collectors in the Athens Basin Area. *Solar Energy, 36*(3), 217-225. https://doi.org/10.1016/0038-092X(86)90137-4

Koussa, M., Cheknane, A., Hadji, S., Haddadi, M., & Noureddine, S. (2011). Measured and Modelled Improvement in Solar Energy Yield from Flat Plate Photovoltaic Systems Utilizing Different STSs and Under a Range of Environmental Conditions. *International Journal of Applied Energy, 88*(5), 1756-1771. https://doi.org/10.1016/j.apenergy.2010.12.002

Kulcu, R. (2015). Modeling of solar radiation reaching the earth for Isparta province. *Süleyman Demirel University, Journal of The Faculty of Agriculture, 10*(1), 19-26.

Kulcu, R., & Ersan, R. (2021). Empirical modeling of GSR in Hatay (Türkiye) province. *Journal of Tekirdag Agricultural Faculty, 18*(3), 446-456. https://doi.org/10.33462/jotaf.828187

Kulcu, R., Suslu, A., Cihanalp, C., & Yilmaz, D. (2017). Modelling of GSR on Horizontal Surfaces for Mersin Province. *Journal of Clean Energy Technologies, 5*(1), 77-80. https://doi.org/10.18178/jocet.2017.5.1.348

Kumar, B. S., & Sudhakar, K. (2015). Performance Evaluation of MW Grid Connected Solar Photovoltaic Power Plant in India. *Energy Reports, 1*(1), 184-192. https://doi.org/10.1016/j.egyr.2015.10.001

Kumar, K., Kiran, S. R., Ramji, T., Saravanan, S., Pandiyan, P., & Prabaharan, N. (2020). Performance Evaluation of Photo Voltaic System with Quadratic Boost Converter Employing MPPT Control Algorithms. *Int. Journal of Renewable Energy Research, 10*(3), 1083-1091.

Kuttybay, N., Saymbetov, A., Mekhilef, S., Nurgaliyev, M., Tukymbekov, D., Dosymbetova, G., Meiirkhanov, A., & Svanbayev, Y. (2020). Optimized Single-Axis Schedule Solar Tracker in Different Weather Conditions. *Energies, 13*(1), 1-18. https://doi.org/10.3390/en13195226

Laguna, D. L., Vargas, A. A., & Hernandez, F. N. (2021). A European Assessment of the Solar Energy Cost: Key Factors and Optimal Technology. *Sustainability 13*(6), 1-21. https://doi.org/10.3390/su13063238

Lalita, V. P., Saibabu, C., & Prasad, S. G. R. K. D. (2013). Energy and Comfort Management in Energy Efficient Buildings Using RETSCREEN Software-A Case Study Analysis. *International Journal of Engineering Research and Applications, 3*(6), 378-381.

Larico, E. R. A., & Gutierrez, A. C. (2022). STS with photovoltaic cells: experimental analysis at high altitudes, *Int. Journal Renewable Energy Development, 11*(3), 630-639. https://doi.org/10.14710/ijred.2022.43572

Laseinde, T., & Ramere, D. (2019). Low-cost automatic multi-axis solar tracking system for performance improvement in

Lave M., & Kleissl, J. (2011). Optimum fixed orientations and benefits of tracking for capturing solar radiation in the continental United States. *Renewable Energy, 36*(3), 1145-1152. https://doi.org/10.1016/j.renene.2010.07.032

Li, Z., Xing, H., Zeng, S., Zhao, J., & Wang, T. (2017). Comparison of anisotropic radiance models for radiation estimation on building facades. *Procedia Engineering, 205*(1), 779-786, https://doi.org/10.1016/j.proeng.2017.10.010

Liu B. Y. H. & Jordan, R. C. (1963). The long-term average performance of flat-plate solar-energy collectors: With design data for the U.S., its outlying possessions, and Canada. *Solar Energy, 7*(2), 53-74. https://doi.org/10.1016/0038-092X(63)90006-9

Liu, B. Y. H. & Jordan, R. C. (1960). The interrelationship and characteristic distribution of direct, diffuse, and TSR. *Solar Energy, 4*(3), 1-19. https://doi.org/10.1016/0038-092X(60)90062-1

Liu, B. Y. H., & Jordan, R. C. (1961). Daily insolation on surfaces tilted towards the equator. *ASHRAE Journal 10*(1), 526-541.

Löf, G. O., & Tybout, R. A. (1973). Cost of house heating with solar energy. *Solar Energy, 14*(3), 253-278. https://doi.org/10.1016/0038-092X(73)90094-7

Louis, L., & Bucciarelli, J. R. (1986). The Effect of Day-to-Day Correlation in Solar Radiation on the Probability of Loss-of-Power in a Stand-alone Photovoltaic PV energy system. *Solar Energy, 36*(1), 11-14, https://doi.org/10.1016/0038-092X(86)90054-X

Lubitz, W. D. (2011). Effect of manual tilt adjustments on incident irradiance on fixed and tracking PV surfaces. *Applied Energy, 88*(5), 1710-1719. https://doi.org/10.1016/j.apenergy.2010.11.008

Lunde, P. J. (1980). Solar thermal engineering: space heating and hot water systems. *John Wiley & Sons,* New York, USA.

Maatallah, T., El-Alimi, S. & Nassrallah, S. B. (2011). Performance modeling and investigation of fixed, single and dual-axis tracking photovoltaic surface in Monastir province, Tunisia. *Renewable and Sustainable Energy Reviews, 15*(8), 4053-4066.

Mah, A. X. Y., Ho, W. S., Hassim, M. H., & Hashim, H. (2021). Optimization of Photovoltaic Array Orientation and Performance Evaluation of STSs. *Chemical Engineering Transactions, 83*(1), 109-114. https://doi.org/10.3303/CET2183019

Mansour, R. B., Khan, M. A. M., & Alsulaiman, F. A. (2021). Optimizing the solar PV tilt angle to maximize the power output: A case study for Saudi Arabia. *IEEE Access, 9*(1), 15914-15928, https://doi.org/10.1109/ACCESS.2021.3052933

Mansour, R. B., Mam, K. Alsulaiman, F. A., & Mansour, R. B. (2021). Optimizing the Solar PV Tilt Angle to Maximize the Power Output: A Case Study for Saudi Arabia. *IEEE Access, 9*(1), 15914-15928. https://doi.org/10.1109/ACCESS.2021.3052933

Mansouri, E., Pirsalami, M., Nasiri, N., Farrizi, M., Hashemizadeh M., & Alihosseini H. (2016). Optimum Tilt Angle for Fixed-Array PV surfaces at a Constant Latitude of 29° to Receive the Maximum Sunlight. *Bulletin of Environment Pharmacology and Life Sciences, 1*(SI), 1 26. http://doi-ds.org/doilink/05.2016-13212626/

Manzoor, T., & Singh, P. (2021). Optimization and Techno-Economic Analysis of a Microgrid for an Industry with Intermittent Grid Service using HOMER Software: A Case Study in Ladakh, India. *International Journal of Scientific and Research Publications, 11*(6), 460-462. http://dx.doi.org/10.29322/IJSRP.11.06.2021.p11461

Markam, K. & Sudhakar, K. (2016). Estimation of OPTA for solar photovoltaic installations in India. *International Research Journal of Engineering and Technology, 3*(5), 2735-2741.

Masili, M., & Ventura, L. (2019). Local Tilt Optimization of Photovoltaic PV surfaces for Maximum Radiation Absorption. *Journal of Photoenergy, ID:3254780,* 1-10. https://doi.org/10.1155/2019/3254780

Matius, M. E., Ismail, M. A., Farm, Y. Y., Amaludin, A. E., Radzali, M. A., Fazlizan, A., & Muzammil, W. K. (2021). On the OPTA and orientation of an on-site solar photovoltaic energy production system for Sabah's rural electrification. *Sustainability, 13*(10), https://doi.org/10.3390/su13105730

Maxwell, E. L. (1987). A quasi-physical model for converting hourly global horizontal to direct normal insolation report SERI/TR-215-3087. U.S. Department of Energy, *Solar Energy Research Institute*, Golden, Colorado.

McKeon, B. B., Furukawa, J., & Fenstermacher, S. (2014). Advanced Lead–Lead-acid batteries and the Development of Grid-Scale Energy Storage Systems. *Proceedings of the IEEE, 102*(6), 951-963. https://doi.org/10.1109/JPROC.2014.2316823

Mehler, E. D., Zervas, P. L., Sarimveis, H., Palyvos, J. A., & Markatos, N. C. (2010). Determination of the OPTA and orientation for solar Photovoltaic arrays. *Renewable Energy, 35*(11), 2468-2475. https://doi.org/10.1016/j.renene.2010.03.006

Mengi, O. O., & Altas, I. H. (2015). A New Energy Management Technique for PV/Wind/Grid Renewable PV energy system. *Int. Journal of Photoenergy, ID:356930,* 1-19. https://doi.org/10.1155/2015/356930

Meteotest. (2023). *METEONORM Irradiation data for every place on Earth.* Switzerland, https://METEONORM.com/en/

Michalsky, J. J. (1988). The Astronomical Almanac's algorithm for the approximate solar position (1950–2050). Solar Energy, Volume 40(3), 227-235. https://doi.org/10.1016/0038-092X(88)90045-X

Miguel, H., Gomes, L. C., Campos, C. T., & Muniz, P. R. (2021). Estimation of Daily Energy Gain of Solar Tracking Surfaces Based on geographic Position. *Journal of Revista Lfes Ciencia, 7*(1), 1-14. https://doi.org/10.36524/ric.v7i1.940

Milosavljević, D.D., Kevkić, T. S., & Jovanović, S. J. (2022). Review and validation of photovoltaic solar simulation tools/software based on case study. *Open Physics, 20*(1), 431-451. https://doi.org/10.1515/phys-2022-0042

Modiri-Delshad, M., Kaboli, S. H. A., Renani, E., & Rahim, N. A. (2016). Backtracking Search Algorithm for Solving Economic Dispatch Problems with Valve-Point Effects and Multiple Fuel Options. *Energy, 116*(1), 637-649. https://doi.org/10.1016/j.energy.2016.09.140

Moghadam, H., Tabrizi, F. F., & Sharak, A. Z. (2011). Optimization of solar flat collector inclination. *International Journal of Desalination, 265*(1-3), 107-111. https://doi.org/10.1016/j.desal.2010.07.039

Motahhir, S., El-Hammoumi, A., & El-Ghzizal, A. (2019). The Most Used MPPT Algorithms: Review and the Suitable Low-cost Embedded Board for Each Algorithm. *Journal of Cleaner Production, 246*(1), 1-35. https://doi.org/10.1016/j.jclepro.2019.118983

Mubarak, R., Hofmann, M., Riechelmann, S., & Seckmeyer, G. (2017). Comparison of modeled and measured tilted solar radiation for PV applications. *Energies, 10*(11), 1-18, https://doi.org/10.3390/en10111688

Muneer, T. (1990). Solar radiation model for Europe, *Building Services Engineering Research and Technology* *11*(4), 153-163, https://doi.org/10.1177/014362449001100405

Muneer, T., Fairooz, F., & Zhang, X. (2003) Sky luminance and radiance distributions: a comparison based on data from Bahrain, Israel, Japan, and Europe. *Lighting Research Technology, 35*(1), 11-17. https://doi.org/10.1191/1477153503li078oa

Nassar, Y. F. (2006). Solar energy engineering, Active applications. *Sebha University Publications,* 528 pages. Libya.

Nassar, Y. F. & Alsadi, S. Y. (2019). Assessment of solar energy potential in Gaza Strip-Palestine. *Sustainable Energy Technologies and Assessments, 31*(1), 318-328. https://doi.org/10.1016/j.seta.2018.12.010

Nassar, Y. F. & Hafez, A. A., Belhaj, S., Alsadi, S. Y., Abdunnabi, M. J., Belgasim, B., & Sbeta, M. N. (2022). A generic model for optimum tilt angle of flat-plate solar harvesters for Middle East and North Africa Region. *Applied Solar Energy, 58*(1), 800-812. https://doi.org/10.3103/S0003701X22060135

Nassar, Y. F., & Alsadi, S. Y., El-Khozondar, H. J., Ismail, M. S., Al-Maghalseh, M., Khatib, T., Sa'ed, J. A., Mushtaha, M. H., & Djerafi T. (2022). Design of an isolated renewable hybrid PV energy system: a case study. *Mater Renew Sustain Energy, 11*(1), 225-240. https://doi.org/10.1007/s40243-022-00216-1

Nassar, Y. F., & Samer, A. (2016). View Factors of Flat Solar Collectors Array in Flat, Inclined, and Step-Like Solar Fields. *Journal of Solar Energy Engineering, 138*(6), 1-8. https://doi.org/10.1115/1.4034549

Nassar, Y. F., Abuhamoud, N. M., Miskeen, G. M., El-Khozondar, H. J., Alsadi, S. Y., & Ahwidi, O. M. (2022). Investigating the applicability of horizontal to tilted sky-diffuse solar irradiation transposition models for key Libyan cities. *IEEE 2nd International Maghreb Meeting of the Conference on Sciences and Techniques of Automatic Control and Computer Engineering,* 23-25 May, https://doi.org/10.1109/MI-STA54861.2022.9837500

Nassar, Y. F., Aissa K. R., & Alsadi, S. Y. (2018). Air Pollution Sources in Libya. *Research & Reviews: Journal of Ecology and Environmental Sciences* 6(1), 63-79.

Nassar, Y. F., Alsadi, S. Y., El-Khozondar, H. J., & Refaat, S. S. (2022). Determination of the most accurate horizontal to tilted sky-diffuse solar irradiation transposition model for the capital cities in MENA region. *International Conference on Smart Grid and Renewable Energy,* 20-22 March, 1-6, https://doi.org/10.1109/SGRE53517.2022.9774146

Nassar, Y. F., Alsadi, S. Y., El-Khozondar, H. J., Ismail, M. S., Al-Maghalseh, Khatib, M. T., Saed, J. A., Mushtaha, M. H., & Djerafi, T. (2022). Design of an isolated renewable hybrid PV energy system: a case study. *Materials for Renewable and Sustainable Energy, 11*(1), 225–240. https://doi.org/10.1007/s40243-022-00216-1

Nassar, Y. F., Belhaj, S., Alsadi, S. Y., & El-Khozondar, H. J. (2022). Analysis of the View Factors in Rooftop PV Solar. *3rd International Conference on Smart Grid and Renewable Energy (SGRE),* https://doi.org/10.1109/SGRE53517.2022.9774104

Nassar, Y. F., Hafez, A. A. & Alsadi, S. Y. (2020). Multi-Factorial comparison for 24 distinct transposition models for inclined surface solar irradiance computation in the State of Palestine: A case study. *Frontiers in Energy Research, 7*(1), https://.doi.org/10.3389/fenrg.2019.00163

Nassar, Y. F., Khozondar, H. J. E., Abouhmod, N. M., Abubaker, A.A., Ahmed, A. A., Alsharif, A., Khaleel, M. M., Elnaggar, M., & Khozondar, R. J. E. (2023). Regression model for optimum solar collectors' tilt angles in Libya. *International Engineering Conference on Renewable Energy & Sustainability,* May 08-09, https://doi.org/10.1109/ieCRES57315.2023.10209547

National Aeronautics and Space Administration-NASA, Atmospheric Science Data Center-ASDC. (2024). https://asdc.larc.nasa.gov/project/SSE

National Renewable Energy Laboratory. (2021). Documenting a Decade of Cost Declines for PV plants. *NREL.* https://www.nrel.gov/news/program/2021/documenting-a-decade-of-cost-declines-for-pv-systems.html

Nfaoui, N., & Hami, K. E. (2018) Extracting the maximum energy from PV surfaces. *Energy Reports, 4*(1), 536-545. https://doi.org/10.1016/j.egyr.2018.05.002

Noorian, A. M., Moradi, I., & G.A. Kamali, G. A. (2008). Evaluation of 12 models to estimate hourly diffuse irradiation on inclined surfaces. *Renewable Energy 33*(1), 1406-1412, https://doi.org/10.1016/j.renene.2007.06.027

Notton, G., Cristofari, C., Muselli, M., & Poggi, P. (2004). Calculation on an hourly basis of solar diffuse irradiations from global data for horizontal surfaces in Ajaccio. *Energy Conversion and Management* *45*(18-19) 2849-2866. https://doi.org/10.1016/j.enconman.2004.01.003

Obiwulu, A. U., Erusiafe, N., Olopade, M. A., & Nwokolo, S. C. (2022). Modeling and estimation of the OPTA, maximum incident solar radiation, and global radiation index of the photovoltaic system. *Heliyon,* *8*(6), 1-27. https://doi.org/10.1016/j.heliyon.2022.e09598

Oclon, P., Cisek, P., Kozak-Jagiela, E., Taler, J., Taler, D., Skrzyniowska, D. & Fedorczak-Cisak, M. (2020). Modeling and experimental validation and thermal performance assessment of a sun-tracked and cooled PVT system under low solar irradiation. *Energy Conversion and Management,* *222*(1), 1-23. https://doi.org/10.1016/j.enconman.2020.113289

Oğulata, R. T., & Oğulata, S. N. (2002). Solar radiation on Adana, Türkiye. *Applied Energy, 71*(4), 351-358. https://doi.org/10.1016/S0306-2619(01)00050-2

Okhaifoh, J. E., Uzedhe, G., & Odigwe, I. A. (2021). Hybrid PV energy systems: Optimal Resource Determination and Cost Evaluation Using Homer Grid Software. *Equity Journal of Science and Technology,* *8*(1), 33-39. https://dx.doi.org/10.4314/equijost.v8i1.5

Okundamiya, M. S., & Nzeako, A. N. (2011). Influence of orientation on the performance of a Photovoltaic conversion system in Nigeria. *Research Journal of Applied Sciences Engineering and Technology, 3*(12), 1384-1390.

Oliveira, A. P., Escobedo, J. F., Machado, A. J., & Soares, J. (2002). Correlation models of diffuse solar radiation applied to the province of Sao Paulo, Brazil. *Applied Energy, 71*(1), 59-73. https://doi.org/10.1016/S0306-2619(01)00040-X

Olomiyesan, B. M., Oyedum, O. D., Ugwuoke, P. E., & Abolarin, M. S. (2017). Evaluation of some GSR models in selected locations in Northwest, Nigeria. *MOJ Solar and PhotoPV energy systems* *1*(1), 1-6, https://doi.org/10.15406/mojsp.2017.01.00001

Önler, E., & Kayışoğlu, B. (2023). Estimation of Monthly, Seasonal and Annual Total Solar Radiation on the Tilted Surface at Optimum Tilt Angles in Two Provinces, Turkiye. *Journal of Tekirdag Agricultural Faculty, 20*(3), 712-722. https://doi.org/10.33462/jotaf.1268745

Orgill, J. F., & Hollands, K .G. T. (1977). Correlation equation for hourly diffuse radiation on a horizontal surface. *Solar Energy, 19*(4), 357-359. https://doi.org/10.1016/0038-092X(77)90006-8

Othman, A. B., Belkilani, K., & Besbes, M. (2018). GSR on tilted surfaces in Tunisia: Measurement, estimation and gained energy assessments. *Energy Reports, 4*(1), 101-109. https://doi.org/10.1016/j.egyr.2017.10.003

Oumarou, M. B., Toyin, A. A., & Oluwole, F. A. (2015). Design Optimization and Performance Evaluation of a Single Axis Solar Tracker. *Sustainable Energy, 3*(1), 9-13. https://doi.org/10.12691/rse-3-1-2

Özbay, H., Karafil, A., Onal, Y., Kesler, M., & Parmaksız, H. (2017). The Monitoring of Monthly, Seasonal, and Yearly Optimum Tilt Angles by Raspberry Pi Card for Bilecik province, Türkiye. Energy Procedia *Int. Scientific Conference on Environmental and Climate Technologies, 113*(1), 311-318.

Özcan, G Ö., Gunerhan, H., Yildirim, N., & Hepbasli, A. (2019). A comprehensive evaluation of PV electricity production methods and life cycle energy-cost assessment of a particular system. *Journal of Cleaner Production, 238*(1), 1-13. https://doi.org/10.1016/j.jclepro.2019.117883

Özcan, O., & Ersoz, F. (2019). Project and cost-based evaluation of solar energy performance in three different geographical regions of Türkiye: Investment analysis application. *Engineering Science and Technology, 22*(4), 1098-1106. https://doi.org/10.1016/j.jestch.2019.04.001

Özer, T., Kelek, M. K., Oğuz, Y., Kıvrak, S., & Şahin, M. (2018). Double Axis Solar Tracking System Design and Implementation. *International Journal of Scientific & Engineering Research, 9*(8), 66-71.

Özerdem, O. C., &Shahin, A. (2014). A PV solar Tracking System Controlled By Arduino/MATLAB/Simulink. *International Journal on Technical and Physical Problems of Engineering. 6*(4), 5-10.

Öztürk, A., Alkan, S., Hasırcı, U., & Tosun, S. (2016). Experimental Performance Comparison of a 2-Axis Sun STS with a SFS Under the Climatic Conditions of

Düzce, Türkiye. *TUBITAK Turkish Electrical Engineering and Computer Sciences, 24*(1), 4383-4390. https://doi.org/:10.3906/elk-1404-344

Öztürk, M., & Kayabaşı, R. (2023). Usability and system analysis of solar energy in the Central Anatolia region. *Niğde Ömer Halisdemir University Journal of Engineering Sciences, 12*(4), 1351-1359. https://doi.org/10.28948/ngmuh.1310627

Öztürk, M., Çirak, B. B., & Özek, N. (2012). Life Cycle Cost Analysis of Domestic Photovoltaic System. *Pamukkale University Journal of Engineering Sciences, 18*(1), 1-11. https://doi.org/10.5505/pajes.2012.76486

Parhizi, S., Lotfi, H., Khodaei, A., & Bahramirad, S. (2015). State -of-Art in Research on Microgrids: A review. *IEEE Access, 3*(1), 890-925. https://doi.org/10.1109/ACCESS.2015.2443119

Patil, V. R., Biradar, V. I., Shreyas, R., Garg, P., Orosz, M. S., & Thirumalai, N. C. (2017). Techno-Economic Comparison of Solar Organic Rankine Cycle (ORC) and Photovoltaic (PV) Systems with Energy Storage. *Renewable Energy, 113*(1), 1250-1260. https://doi.org/10.1016/j.renene.2017.06.107

Pavlović, T., Pavlović, Z., Pantić, L., & Kostić, L. (2010). Determining Optimum Tilt Angles and Orientations of Photovoltaic Surfaces in Nis, Serbia. *Contemporary Materials, 1*(1), 151-156.

Perez, R., Ineichen, P., Maxwell, E., Seals, R., & Zelenka, A. (1992). Dynamic global to direct irradiance conversion models. *ASHRAE Transactions 98*(1), 354-369.

Perez, R., Ineichen, P., Seals, R., Michalsky, J., Stewart, R. (1990). Modeling Daylight Availability and Irradiance Components from Direct and Global Irradiance. *Solar Energy, 44*(5), 271-289. https://doi.org/10.1016/0038-092X(90)90055-H

Perez, R., Seals, R., Ineichen, P., Stewart, R., & Menicucci, D. (1987) A simplified version of the Perez diffuse radiation model for tilted surfaces. *Solar Energy, 39*(3), 221-231, https://doi.org/10.1016/S0038-092X(87)80031-2

Perez, R., Stewart, C. Arbogast, Seals, R., & Scott, J. (1986). An anisotropic hourly diffuse radiation model for sloping surfaces: description. performance validation, and site dependency evaluation. *Solar Energy, 36*(6), 481-497. https://doi.org/10.1016/0038-092X(86)90013-7

Praliyev, N., Zhunis, K., Kalel, Y., Dikhanbayeva, D., & Rojas-Solórzano, L. (2020). Impact of both One- and Two-axis Solar Tracking on the Techno- Economic Viability of On-Grid PV plants: Case of the Burnoye-1 Power Plant, Kazakhstan. *Int. J. of Sustainable Energy Planning and Management,* *29*(1), 79-90. https://doi.org/10.5278/ijsepm.3665

Pvsyst, Photovoltaic System Study Software. (2024). Satigny, Switzerland. https://www.pvsyst.com/

Qiu, G., & Riffat, S. B. (2003). The optimum tilt angle of solar collectors and its impact on performance. *International Journal of Ambient Energy, 24*(1), 13-20. https://doi.org/10.1080/01430750.2003.9674898

Quaschning, V. (1996). Contributions to solar research solar radiation, solar energy photovoltaics: simulation of shading losses in solar electric systems. *1st edition, 6*(1), 205 pages Berlin.

Raji, L., Zhigilla, Y. I., Wadai, J. (2021). Using Homer Software for Cost Analysis of Stand-Alone Power Generation for Small Scale Industry in Nigeria: A Case Study Lumatec Aluminum Products. *International Journal of Applied Technology Research, 2*(2), 90-102.

Rakovec, J., Zakšek, K., Brecl, K., Kastelec, D., & Topic, M. (2011). Orientation and tilt dependence of a fixed PV array energy yield based on measurements of solar energy and ground albedo: a case study of Slovenia. *Energy Management Systems, 65*(1), 145-160. https://doi.org/10.5772/18386

Ramasamy, V., Feldman, D., Desai, J., & Margolis, R. (2021). U.S. Solar Photovoltaic System and Energy Storage Cost Benchmarks: Q1 2021 Technical Report. *National Renewable Energy Laboratory (NREL),* 1-76.

Ramli, N., & Walker, S., (2015). Pan-global, annualized determination of solar collector optimum tilt angle. *7th Int. Conference on Modelling, Identification and Control IEEE,* December 18-20, https://doi.org/10.1109/ICMIC.2015.7409455

Reda, I., & Andreas, A. (2008). Solar Position Algorithm for Solar Radiation Applications. National Renewable Energy Laboratory, 1(1), 1-16.

Reindl, D. T., Beckman, W. A. & Duffie, J. A. (1990). Diffuse fraction correlations. *Solar Energy, 45*(1), 1-7. https://doi.org/10.1016/0038-092X(90)90060-P

Reindl, D. T., Beckman, W. A., & Duffie, J. A, (1990). Evaluation of Hourly Tilted Surface Radiation Models. *Solar Energy, 45*(1), 9-17. https://doi.org/10.1016/0038-092X(90)90061-G

Republic of Türkiye Ministry of Energy and Natural Resources (2022). Solar Potential Atlas (GEPA), Global Radiation and Sunshine Duration Values of Türkiye Provinces. https://gepa.enerji.gov.tr/MyCalculator/

RETScreen International (2005). Clean Energy Project Analysis, Photovoltaic Project Analysis Chapter. *Engineering & Cases Textbook,* 5-45, Third Edition, Canada.

Romana, A., Setiawan, E. A., & Joyonegoro, K. (2018). Comparison of Two Calculation Methods for Designing the Solar Electric Power System for Small Islands. *E3S Web of Conferences, 67*(1), 1-6, https://doi.org/10.1051/e3sconf/20186702052

Rowlands, I. H., Kemery, B. P., & Beausoleil-Morrison, I. (2011). Optimal solar-PV tilt angle and azimuth: an Ontario (Canada) case study. *Energy Policy, 39*(3), 1397-1409. https://doi.org/10.1016/j.enpol.2010.12.012

Ruelas, J., Munoz, F., Lucero, B., & Palomares, J. (2019). PV Tracking Design Methodology Based on an Orientation Efficiency Chart. *Applied Sciences, 9*(5), 1-15. https://doi.org/10.3390/app9050894

Runsheng, T., & Tong, W. (2004). Optimal tilt-angles for solar collectors used in China. *Applied Energy, 79*(3), 239-248. https://doi.org/10.1016/j.apenergy.2004.01.003

Ruşen, S. (2018). Performance Evaluation of a Coupled Method for the Estimation of Daily GSR on a Horizontal Surface. *Atmósfera 31*(4), 347-354. https://doi.org/10.20937/ATM.2018.31.04.03

Rustemli, S., Dincadam, F., & Demirtas, M. (2010). Performance Comparison of the Sun STS and SFS in the Application of Heating and Lightning. *The Arabian Journal for Science and Engineering, 35*(2B), 171-183.

Safaraliev, M. K., Odinaev, I. N., Ahyoev, J. S., Rasulzoda K. N. & Otashbekov R. A. (2020). Energy Potential Estimation of the Region's Solar Radiation Using a Solar Tracker. *Applied Solar Energy, 56*(1), 270-275. https://doi.org/10.3103/S0003701X20040118

Sahin, M., Kaya, Y., & Uyar, M. Comparison of ANN and MLR models for estimating solar radiation in Türkiye using NOAA/AVHRR data. *Advances in Space Research, 51*(5), 891-904. http://dx.doi.org/10.1016/j.asr.2012.10.010

Samadi, S., & Sing, C. (2014). Reliability Evaluation of Production Systems with Solar Power. *International Conference on Probabilistic Methods Applied to Power Systems,* 07-10 July, UK. https://doi.org/10.1109/PMAPS.2014.6960580

Sarkın, A. S., & Dindar, T. (2017). The Effect of Latitude Differences, Sunshine Periods, Solar Radiation Quantities and Air Temperatures on Electricity Production. *Int. J. of Transactions on Smart Grid and Sustainable Energy, 1*(1), 20-23.

Sawyer, R. L., Anderson, J. M., Foulks, E. L., Troxler J.O., & Cox, R. W. (2009). Creating Low-Cost Energy-Management Systems for Homes Using Non-Intrusive Energy Monitoring Devices. *IEEE Energy Conversion Congress and Exposition,* https://doi.org/10.1109/ECCE.2009.5316132

Selbaş, R., Yakut, A. K., & Şencan, A. (2003). An Application for Electricity Production with Solar Tower Model. *Pamukkale University Journal of Engineering Sciences, 9*(2), 179-184.

Seme, S., Srpcic, G., Kavsek, D., Bozicnik, S., Letnik, T., Praunseis, Z., Stumberger, B., & Hadziselimovic, M. (2017). Dual-Axis Photovoltaic STS - Design and Experimental Investigation. *Energy, 139*(1), 1267-1274. https://doi.org/10.1016/j.energy.2017.05.153

Şenkal, O. (2016). Solar Radiation Modeling for Türkiye Using Atmospheric Parameters with Artificial Neural Networks. *Çukurova University Journal of the Faculty of Engineering and Architecture, 31*(2), 179-185.

Şenpınar, A., & Cebeci, M. (2012). Evaluation of Power Output for Fixed and Two-Axis Tracking PV Arrays. *Applied Energy, 92*(1), 677-685. https://doi.org/10.1016/j.apenergy.2011.07.043

Şevik, S., Kocer, A., Ince, H., & Tombus, F. E. (2021). Determination of the optimum tilt angle of the solar collector and evaluation of the position of the existing buildings in terms of solar potential. *Architectural Engineering and Design Management, 18*(6), 812-828. https://doi.org/10.1080/17452007.2021.1926899

Shariah, A., Al-Akhras, M. A., & Al-Omari, A. I. (2002). Optimizing the tilt angle of solar collectors. *Renewable Energy, 26*(4), 587-598. https://doi.org/10.1016/S0960-1481(01)00106-9

Sharma, D. K., Verma, V., & Singh, A. P. (2014). Review and Analysis of Solar Photovoltaic Software. *International Journal of Current Engineering and Technology 4*(2), 725-731.

Sharma, K. R., Palit, D., & Krithika, P. R. (2015). Economics and Management of Off-Grid Solar PV plant. *Green Energy and Technology, 1*(1), 137-164. https://doi.org/10.1007/978-3-319-14663-8_6

Shayeghi, H., Shahryari, E., Moradzadeh, M., & Siano, P. (2019). A Survey on Microgrid Energy Management Considering Flexible Energy Sources. *Energies, 12*(11), 1-26. https://doi.org/10.3390/en12112156

Shingleton, J. (2008). One-axis trackers, improved reliability, durability, performance, and cost reduction. Final subcontract technical status report, NREL/SR-520-42769, 1-56.

Shukla, K. N., Rangnekar, S., & Sudhakar, K. (2015). Comparative study of isotropic and anisotropic sky models to estimate solar radiation incident on a tilted surface: A case study for Bhopal, India. *Energy Reports, 1*(1), 96-103, https://doi.org/10.1016/j.egyr.2015.03.003

Sidek, M. H. M., Azis, N., Hasan, W. Z. W., Kadir, M. Z. A., Shafie, S., & Radzi, M. A. M. (2017). Automated positioning dual-axis solar STS with precision elevation and azimuth angle control. *Energy, 124*(1), 160-170. https://doi.org/10.1016/j.energy.2017.02.001

Sinjari, A. M., & Shareef, S. J. M. (2016). Dual Axis Solar Tracking System Using PLC. *International Conference on Engineering and Innovative Technology,* April 12-14, Iraq.

Siraki, A. G., Pillay, P. (2012). Study of optimum tilt angles for PV surfaces in different latitudes for urban applications. *Solar Energy, 86*(6), 1920-1928. https://doi.org/10.1016/j.solener.2012.02.030

Skartveit, A., & Olseth, A. J. (1986). Modeling Slope Irradiance at High Latitudes. *Journal of Solar Energy,* 36(4), 333-344. https://doi.org/10.1016/0038-092X(86)90151-9

Skartveit, A., Olseth, J. A., & Tuft, M. E. (1988). An hourly diffuse fraction model with correction for variability and surface albedo. *Solar Energy, 63*(1), 173-183. https://doi.org/10.1016/S0038-092X(98)00067-X

Skeiker, K. (2009). Optimum tilt angle and orientation for solar collectors in Syria. *Energy Conversion and Management, 50*(9), 2439-2448. https://doi.org/10.1016/j.enconman.2009.05.031

Skoczek, A., Sample, T., & Dunlop, E. D. (2009). The Results of Performance Measurements of Field-aged Crystalline Silicon Photovoltaic Modules. *Progress in Photovoltaics Research, 17*(1), 227-240. https://doi.org/10.1002/pip.874

Solanki, C. S., & Sangani, C. S. (2008). Estimation of monthly average direct normal solar radiation using elevation angle for any location. *Solar Energy Materials Cells, 92*(1), 38-44. https://doi.org/10.1016/j.solmat.2007.08.006

Solar Energy Industries Association. (2021). Solar Market Insight Report 2021 Q4. *SEISA.* https://www.seia.org/research-resources/solar-market-insight-report-2021-q4

Solar Energy Potential Map of Türkiye. (2023). Ministry of Energy and Natural Resources, https://gepa.enerji.gov.tr/MyCalculator/pages/63.aspx

Solmaz, O., & Ozgoren, M. (2012). Prediction of hourly solar radiation in six provinces in Türkiye by artificial neural networks. *Journal of Energy Engineering, 138*(4), 194-204. https://doi.org/10.1061/(ASCE)EY.1943-7897.0000080

Soulayman, S., Hamoud, M., Hababa, M., & Sabbagh, W. (2021). Feasibility of Solar STS for PV Panel in Sunbelt Region. *Journal of Modern Power Systems and Clean Energy, 9*(2), 395-403. https://doi.org/10.35833/MPCE.2018.000658

Stanciu, C., & Stanciu, D. (2014). Optimum tilt angle for flat plate collectors all over the World declination dependence formula and comparisons of three solar radiation models. *Energy Conversion and Management, 81*(2014), 133-143. https://doi.org/10.1016/j.enconman.2014.02.016

Stanton, K. N., Giri, J. C., & Bose, A. (2017). Systems, Controls, Embedded Systems. Energy and Machines. *CRC Press, 1*(1), 1-672. https://doi.org/10.1201/9781420037043

Steffen, B., Beuse, M., Tautorat, P., & Schmidt, T. S. (2020). Experience Curves for Operations and Maintenance CoSTS of Renewable Energy Technologies. *Joule CelPress, 4*(2), 359 -375. https://doi.org/10.1016/j.joule.2019.11.012

Suchitra, D., Jegatheesan, R., Subramaniyan, V., & Venkatesam, R. S. (2017). Energy Management of a Microgrid Using Multi-Objective Genetic Algorithm. *African Journal of Basic & Applied Sciences, 9*(3), 105-111. https://doi.org/10.5829/idosi.ajbas.2017.105.111

Sudhakar, K., Srivastava, T., Satpathy, G., & Premalatha, M. (2013). Modeling and Estimation of Photosynthetically Active Incident Radiation Based on Global Irradiance in Indian Latitudes. *Int. Journal of Energy and Environmental Eng., 4*(21), 1-19. https://doi.org/10.1186/2251-6832-4-21

Sufyan, M., Rahim, A. R., Tan, C., Azam, M., & Rohani, S. (2019). Optimal Sizing and Energy Scheduling of Isolated Microgrids Considering the Battery Lifetime. *PLOS ONE, 14*(2): 1-28. https://doi.org/10.1371/journal.pone.0211642

Sulukan, E. (2020). Techno-economic and environmental analysis of a photovoltaic system in İstanbul. *Pamukkale University Journal of Engineering Sciences, 26*(1), 127-132, https://doi.org/10.5505/pajes.2019.24022

Sümer, Y., & Güngör, A. (2023). Carbon Footprint Reduction Potential of Solar Thermal Heating Technologies for Antalya Province. *Journal of Bilim Armonisi, 6*(2), 52-58. https://doi.org/10.37215/bilar.1290260

Sungur, C. (2009). Multi-Axes Sun-STS with the PLC Control for Photovoltaic Surfaces in Türkiye. *International Journal of Renewable Energy, 34*(4), 1119-1125. https://doi.org/10.1016/j.renene.2008.06.020

Talebizadeh, P., Mehrabian, M. A., & Abdolzadeh, M. (2011). Determination of Optimum Slope Angles of Solar Collectors Based on New Correlations. *International Journal of Energy, Sources Part A: Utilization, and Env. Effects, 33*(17), 1567-1580. https://doi.org/10.1080/15567036.2010.551253

Tang, R., & Wu, T. (2004). Optimal tilt-angles for solar collectors used in China. *Applied Energy 79*(3), 239-248. https://doi.org/10.1016/j.apenergy.2004.01.003

Taşkın, O., & Korucu, T. (2014). Solar Energy Potential and Facilities of Use in Kahramanmaras Province. *KSU Journal of Natural Sciences,* 17(4), 12-16.

Tchakounté, H., Fapi, C. B. N., Kamta, M., Djalo H., & Woafo P. (2021). Design, Experimental Implementation, and Performance Comparison of Two Solar Tracking Approaches. *Applied Solar Energy, 57*(1), 44–58. https://doi.org/10.3103/S0003701X21010102

The Republic of Türkiye. (2024). Ministry of Energy and Natural Resources, Renewable Energy Potential, https://enerji.gov.tr/eigm-resources-en

Tian, Y. Q., Davies-Colley, R. J., Gong, P., & Thorrold, B. W. (2001). Estimating solar radiation on slopes of arbitrary aspect. *Agricultural and Forest Meteorology, 109*(1), 67-74, https://doi.org/10.1016/S0168-1923(01)00245-3

Tırmıkcı, C. A., & Yavuz, C. (2018). Establishing New Regression Equations for Obtaining the Diffuse Solar Radiation in Sakarya. *Tehnički Vjesnik, 25*(2), 503-508. https://doi.org/10.17559/TV-20170202131249

Tırmıkcı, C., & Yavuz, C. (2018). Determining Optimum Tilt Angles of PV surfaces in Sakarya, Türkiye. *Theoretical and Applied Climatology, 133*(2), 15-22. https://doi.org/10.1007/s00704-017-2174-x

Topal, A., Ozoglu, B., & Eksioglu, D. (2021). The evaluation of factors in utilizing the potential of solar energy: the case of Türkiye. *Environmental Research and Technology 4*(3), 266-276, https://doi.org/10.35208/ert.972541

Torreglosa, J. P., Garcia, P., Fernandez, L. M., & Jurado. F. (2014). Predictive Control for the Energy Management of a Fuel-Cell–Battery–Supercapacitor Tramway. *IEEE Transactions on Industrial Informatics, 10*(1), 276-285. https://doi.org/10.1109/TII.2013.2245140

Toylan, H. (2017). Performance of Dual Axis Solar STS Using Fuzzy Logic Control: A Case Study in Pinarhisar, Türkiye. *European Journal of Engineering and Natural Sciences, 2*(1), 130-136.

Tuama, S. A., & Razzaq, O. A., Abdulridha, S. K., & Faiq, N. (2021). Investigating the Impact of Tilt Angle, Orientation, and Configuration on PV plant Performance Using

PVSyst Software. *Applied Sciences and Nanotechnology 1*(3), 73-85. https://doi.org/10.53293/jasn.2021.3916.1059

Turkish Standards Institution. (2024). Calculation Values of Loads to be Taken in Dimensioning of Building Elements and Design Loads for Buildings. *ICS 91.040, 1*(1), 1-21.

Turkish State Meteorological Service. (2024). https://www.mgm.gov.tr/kurumici/radyasyon_iller.aspx

U.S. Energy Information Administration. (2021). Average Construction CoSTS for Solar Photovoltaic Systems. *Independent Statistics & Analysis (EIA).* https://www.eia.gov/todayinenergy/detail.php?id=48736

U.S. Energy Information Administration. (2022). Levelized CoSTS of New Production Resources in the Annual Energy Outlook 2022. *EIA,* 1-26.

Uba, F. A. & Sarsah, E. A. (2013). Optimization of tilt angle for solar collectors in WA, Ghana. *Advances in Applied Science Research, 4*(4), 108-114.

Üçgül, I., & Şenol, R. (2016). PV and Solar-STS for Meteorology Station in Isparta/Türkiye. *Journal of Phoenix, 1*(1), 1-7.

Uçkan, İ. (2018). Analysis of Solar Radiation Data in Van, Türkiye. *Celal Bayar University Journal of Science, 14*(1), 421-427. https://doi.org/10.18466/cbayarfbe.434552

Udoakah, Y. N., & Okpura, I. (2015). Determination of OPTA for maximum solar insolation for PV plants in Enugu-Southern Nigeria. *Nigerian Journal of Technology, 34*(4), 838-843. https://doi.org/10.4314/njt.v34i4.24

Ülgen, K. (2007). Optimum Tilt Angle for Solar Collectors. *International Journal of Energy Sources Part A: Recovery Utilization and Environmental Effects, 28*(13), 1171-1180. https://doi.org/10.1080/00908310600584524

University Ziraatbiyotek Building using RetScreen Program. *Journal of Tekirdağ Agricultural Faculty, 19*(3), 656-667. https://doi.org/10.33462/jotaf.1058491

Uyan, M., & Doğmuş, O. L. (2023) An Integrated GIS-Based ANP Analysis for Selecting Solar Farm Installation Locations: Case Study in Cumra Region, Türkiye.

Environmental Modeling & Assessment volume 28(1), 105–119. https://doi.org/10.1007/s10666-022-09870-1

Valentin Software. (2023). PVSOL Calculation-Irradiation-Tracking. *User Manuel,* https://help.valentin-software.com/pvsol/en/calculation/irradiation/tracking/

Vartiainen, E., Masson, G., Breyer, C., Moser, D., & Medina, E. R. (2019). Impact of Weighted Average Cost of Capital, Capital Expenditure, and Other Parameters on Future Utility-Scale PV Levelized Cost of Electricity. *Prog Photovoltaic Res Appl., 28*(1), 439–453. https://doi.org/10.1002/pip.3189

Vera, Y. E. G., Dufo-López, R., & Bernal-Agustín, J. L. (2019). Energy Management in Microgrids with Renewable Energy Sources: A Literature Review. *Applied Sciences, 9*(18), 1-28. https://doi.org/10.3390/app9183854

Vermaak, H. J. (2014). Techno-economic Analysis of STSs in South Africa. *Energy Procedia, 61*(1), 2435-2438. https://doi.org/10.1016/j.egypro.2014.12.018

vertical support solar panels using Arduino board. *International Journal of Low-Carbon Technologies, 14*(1), 76–82. https://doi.org/doi:10.1093/ijlct/cty058

Windarta, J., Handoko, S., Sukmadi, T., Nafadinanto, K., Muqtasida, S., & Halim, C. (2022). Design of a solar power plant system for micro, small, and medium enterprises using PVSyst 7.1 as a renewable energy alternative source in remote areas. IOP Conf. Series: *Earth and Environmental Science, 969*(1), 1-12. https://doi.org/10.1088/1755-1315/969/1/012029

Xiaoqiang, D., Yuechan, L., Pengcheng, W., Zenghong, M., Dangwei, L., & Chuanyu, W. (2021). Design and optimization of the solar tracker with U-PRU-PUS parallel mechanism. *Mechanism and Machine Theory, 155*(1), 1-17. https://doi.org/10.1016/j.mechmachtheory.2020.104107

Yadav, A. K., & Chandel, S. S. (2013). Tilt angle optimization to maximize incident solar radiation. *Renewable and Sustainable Energy Reviews, 23*(1), 503-513. https://doi.org/10.1016/j.rser.2013.02.027

Yağlı, H., & Koç, Y. (2020). Determination of Optimum Inclination Angles of Surfaces to be Installed in Solar Production for Gaziantep Region. *European Science and Technology 19*(1), 475-483. https://doi.org/10.31590/ejosat.733530

Yakup, M. A. M., & Malik, A. O. (2001). Optimum tilt angle and orientation for solar collector in Brunei Darussalam. *Renewable Energy, 24*(2), 223-234. https://doi.org/10.1016/S0960-1481(00)00168-3

Yalçın, C., & Yüce, M. (2019). Evaluation of the Spatial Suitability of Solar Power Plants (SPP) in Burdur Province, Türkiye. *Journal of Natural & Applied Sciences of Mehmet Akif Ersoy University, 10*(2), 132-140. https://doi.org/10.29048/makufebed.562722

Yan, R., Saha, T. K., Meredith, P., & Goodwin, S. (2013). Analysis of the Year-Long Performance of Differently Tilted Photovoltaic Systems in Brisbane, Australia. *Energy Conversion, 74*(1), 102-108. https://doi.org/10.1016/j.enconman.2013.05.007

Yang H., & Lu, L. (2007). The Optimum Tilt Angles and Orientations of PV Claddings for Building-Integrated Photovoltaic (BIPV) Applications. *Journal of Solar Energy Engineering, 129*(2), 253-255. https://doi.org/10.1115/1.2212439

Yaniktepe, B., Kara, O., & Ozalp, C. (2017). Estimation of the Solar Radiation Model Using Measured Data of Osmaniye, Türkiye. *RAD Conference Proceedings, 2*(1), 195-197.

Yanıktepe, B., & Genç, Y. A. (2015). Establishing a new model for predicting GSR on horizontal surfaces. *International Journal of Hydrogen Energy, 40*(44). 15278-15283. https://doi.org/10.1016/j.ijhydene.2015.02.064

Yao, W., Li, Z., Wang, Y., Jiang, F., & Hu, L. (2014). Evaluation of GSR models for Shanghai, China. *Energy Conversion Management 84*(1) 597-612, https://doi.org/10.1016/j.enconman.2014.04.017

Yasin, A. S., Fathi, N. Y., & Ali, A. K. (2016). General Polynomial for Optimizing the Tilt Angle of Flat Solar Energy Harvesters Based on ASHRAE Clear Sky Model in Mid and High Latitudes. *Energy and Power, 6*(2), 29-38. https://doi.org/10.5923/j.ep.20160602.01

Yellott, J. (1973). Utilization of sun and sky radiation for heating and cooling of buildings. *ASHRAE Jornal, 15*(12), 31-42.

Yigit, A., & Arslanoglu, N. (2021). Investigation of optimum PV surface efficiency power depends on instant solar radiation and environmental factors. *Uludağ*

University Faculty of Engineering Journal, 26(1), 301-314. https://doi.org/10.17482/uumfd.824582

Yıldırım, E., & Aktacir, M. A. (2019). Investigation of Azimuth and Tilt Angle Effects on Building Integrated Photovoltaic Systems. *International Journal of the Faculty of Engineering and Architecture of Gazi University, 34*(2), 609-619. https://doi.org/10.17341/gazimmfd.416413

Yıldırım, E., Aktacir, M. A. (2021). Determination of rooftop PV electricity production potential: the case of Şanlıurfa. *Dicle University Journal of Engineering, 12*(1), 69-77. https://doi.org/10.24012/dumf.860242

Yıldırım, H. B., Çelik, Ö., Teke, A., & Barutçu, B. (2018). Estimating daily GSR with a graphical user interface in the Eastern Mediterranean region of Türkiye. *Renewable and Sustainable Energy Reviews, 82*(1), 1528-1537. https://doi.org/10.1016/j.rser.2017.06.030

Yılmaz, A., & Şimşek, C. (2022). Calculation of the Optimum PV Surface Incline Angle for Mediterranean Climate. *European Journal of Science and Technology, 35*(1), 322-329. https://doi.org/10.31590/ejosat.1082398

Yılmaz, A., Kocer, A., Yaka, F. I., & Güngör, A. (2016). Determination of Optimum Tilt Angle on Solar Thermal Collectors for Batman Province of Türkiye. *Solar Conference & Exhibition*, 674-678.

Yılmaz, M. (2017). Improving Tracking Efficiency of Two-Axis STSs. *Batman University Journal of Life Sciences, 7*(1/2), 56-62.

Yılmaz, M., & Kentli, F. (2015). Increasing Electrical Energy with STS at the Region which Has Türkiye's Most Solar Energy Potential. *Journal of Clean Energy Technologies, 3*(4), 287-290. https://doi.org/10.7763/JOCET.2015.V3.210

Yolcan, O. O., & Köse, R. (2020). Finding Optimum Tilt Angles of Photovoltaic Surfaces: Kütahya Case Study. *International Journal of Energy Studies, 5*(2), 89-105.

Zang, H., Guo, M., Wei, Z. & Sun, G. (2016). Determination of the OPTA of Solar Collectors for Different Climates of China. *Sustainability, 8*(7), 1-16. https://doi.org/10.3390/su8070654

Zhejiang Sandi Electric Co., Ltd. (2022). 100kWh PV Energy Storage Lithium Battery System with BMS System Off-Grid Inverter All in One. http://www.cnsandi.cn/sdp/911164/4/main-4781195/0/Home.html

Zhu, Y., Liu, J., & Yang, X. (2020). Design and performance analysis of an STS with a novel single-axis tracking structure to maximize energy collection. *Applied Energy, 264*(1), 1-7. https://doi.org/10.1016/j.apenergy.2020.114647

Zlateva, M. (2020). Assessment of the Annual Performance of Solar Collectors Employing the Utilizability Method. *E3S Web of Conference, 207*(1), 1-10, https://doi.org/10.1051/e3sconf/202020702007

CURRICULUM VITAE

PERSONAL DETAILS

Name Surname	: Batur Alp AKGÜL
Nationality	: Republic of Turkey
Date & Place of Birth	: 10.11.1979, Ankara

EDUCATIONAL BACKGROUND

Ph.D.	: Hasan Kalyoncu University,	Electrical-Electronics Eng.	2024
M.Sc.	: Hasan Kalyoncu University,	Electronics-Computer Eng.	2018
A.Sc.	: Kırıkkale University,	Control and Automation	2015
A.Sc.	: Ahmet Yesevi University,	Computer Programming	2011
M.Sc.	: Ahmet Yesevi University,	Information Systems	2007
B.Sc.	: Anadolu University,	Public Administration	2004

PROFESSIONAL EXPERIENCE

2015 – Present	: ICT Department of UN-IOM, ICT Officer.
2013 – 2015	: IT Department of Turkish Aviation (THK), IT Officer.
2004 – 2013	: IT Department of Çağdan A.Ş., IT Officer.
1996 – 2004	: IT Department of Bartek Technologies, IT Associate.

TRAINING

2003 – 2006	Microsoft MCP Certification Trainings and Exams.
2006 – 2009	Public Accountancy-Finance Course by TURMOB.
2009 – 2013	License, Union of Chambers of Certified Public Accountants of Türkiye.

FOREIGN LANGUAGE

English, Professional Level.

INTERNATIONAL PUBLICATIONS

Akgul, B. A., Ozyazici, M. S., Hasoğlu, M. F. & Haznedar, B. (2024). Investigation and Determination of Optimal Tilt Angles and Solar Radiation Gains for Fixed and Tracked South-Facing Solar Photovoltaic Surfaces in Provinces of Türkiye. *Environmental Modeling & Assessment, 29*(1), 101-123. DOI:10.1007/s10666-023-09933-x

Akgul, B. A., Ozyazici, M. S., & Hasoğlu, M. F. (2024). Estimation of optimal tilt angles and solar radiation collected by fixed and tracking solar panels for the Mediterranean region, Turkey. *Indian Journal of Physics, 98*(1), 1187-1200. DOI:10.1007/s12648-023-02894-7

Akgul, B. A., Ozyazici, M. S., Hasoğlu, M. F. & Alisinanoglu, F. (2023). Maximization of Solar Radiation for Fixed and Tracking Surfaces in Antalya Province of Türkiye. *Tehnički Glasnik, 17*(3), 47-58. DOI:10.31803/tg-20220426082153

Akgul, B. A., Ozyazici, M. S., Hasoğlu, M. F., Alisinanoglu, F., & Haznedar, B. (2023). Analysis of transportable off-grid solar power generation for rural electricity supply: an application study of Sanliurfa, Turkey. *Pamukkale University Journal of Engineering Sciences, 29*(5), 458-467. DOI:10.5505/pajes.2022.87894

Akgul, B. A., Ozyazici, M. S., & Alisinanoglu, F. (2022). Obtaining Maximum Radiation by Determining Optimum Tilt Angles in Large-Scale Grid-Connected PV Plants, Efficiency Analysis of Solar Tracking Systems: A Case Study for Sanliurfa, Turkey. *International Journal of Industrial Electronics and Electrical Engineering, 10*(7), 25-28.

Akgul, B. A., Ozyazici, M. S., Alisinanoglu, F., & Bayram, K. S. (2022). Development of Real-Time Traffic Sign Recognition with Convolutional Neural Network Using Deep Learning Techniques. *Int. Journal on Mathematic, Engineering and Natural Sciences, 22*(6), 366-377.

Akgul, B. A., Hasoğlu, M. F., Alisinanoglu, F., & Haznedar, B. (2021). Development of A Real-Time Traffic Sign Recognition System Based on Deep Learning Approach with Convolutional Neural Networks and Integrating to the Embedded Systems. Euroasia Int. Journal of Mathematics and Engineering, 8(14), 46-64. DOI:10.38065/euroasiaorg.481

Akgul, B. A., & Karapinar, E. (2021). Investigation and Evaluation of Thermal Analysis for Different Wall Structures with Finite Element Method, Simulation of Temperature Distribution and Reaction in the Wall Types. *Euroasia Int. Journal of Mathematics and Engineering, 8*(14), 132-144. DOI:10.38065/euroasiaorg.452

Akgul, B. A., & Yegingil, I. (2021). Design and Modeling an Off-Grid Photovoltaic System to Meet the Electrical Energy Requirement of a House in Gaziantep Region, Performing Technical Analysis and Basic Simulation. *Euroasia Int. Journal of Mathematics and Engineering, 8*(14), 145-159. DOI:10.38065/euroasiaorg.456

Akgul, B. A., Yasar, A., & Haznedar, B. (2021). Indoor Position Routing (IPR) and Data Monitor Using Bluetooth Low Energy Technology (iBeacon-BLE): An Implementation Study. *ICONTECH International Journal of Surveys, Engineering, Technology, 5*(1), 38-61. DOI:10.46291/ICONTECHvol5iss1pp38-61

Akgul, B. A., & Karapinar, E. (2020). Investigation, Modeling, and Simulation of Radiofrequency Ablation Systems with Finite Element Method for Varicose Vein Treatment. Int. Journal on Mathematic and Engineering, 16(4), 817-825. DOI:10.38063/ejons.333

Bayraktar, R., Akgul, B. A., & Bayram, K. S. (2020). Color Recognition Using Color Histogram Feature Extraction and K-Nearest Neighbor Classifier. *New Trends and Issues Proceedings on Advances in Pure and Applied Sciences, 12*(1), 08-14. DOI:10.18844/gjpaas.v0i12.4981

Akgul, B. A., Hasoğlu, M. F., & Haznedar, B. (2019). PIC-Based Solar Energy Harvesting Module Design for Wireless Sensor Networks. *Harran University, Journal of Engineering, 4*(1), 69-80.

Akgul, B. A., Hasoğlu, M. F., & Haznedar, B. (2018). Investigation and Implementation Ultra-Low Power PIC-Based Sensor Node with Renewable Energy Source and Decision-Making Unit, *Journal Of Wireless Sensor Network, 10*(1), 41-58. DOI:10.4236/wsn.2018.102002